JOURNAL OF LIQUID CHROMATOGRAPHY

VOLUME 17 NUMBER 3 1994

JOURNAL OF LIQUID CHROMATOGRAPHY

February 1994

Aims and Scope. The journal publishes papers involving the applications of liquid chromatography to the solution of problems in all areas of science and technology, both analytical and preparative, as well as papers that deal specifically with liquid chromatography as a science within itself. Included will be thin-layer chromatography and all models of liquid chromatography.

Identification Statement. *Journal of Liquid Chromatography* (ISSN: 0148-3919) is published semimonthly except monthly in May, July, October, and December for the institutional rate of $1,350.00 and the individual rate of $675.00 by Marcel Dekker, Inc., P.O. Box 5005, Monticello, NY 12701-5185. Second Class postage paid at Monticello, NY. POSTMASTER: Send address changes to *Journal of Liquid Chromatography*, P.O. Box 5005, Monticello, NY 12701-5185.

Volume	Issues	Institutional Rate	Individual Professionals and Student Rate	Foreign Postage		
				Surface	Airmail to Europe	Airmail to Asia
17	20	$1,350.00	$675.00	$75.00	$110.00	$130.00

Your order must be prepaid by personal check or may be charged to MasterCard, VISA, or American Express. Please mail payment with your order to: Marcel Dekker Journals, P.O. Box 5017, Monticello, New York 12701-5176.

CODEN: JLCHD8 17(3) i-viii, 483-730 (1994)
ISSN: 0148-3919

Printed in the U.S.A.

JOURNAL OF LIQUID CHROMATOGRAPHY

JOURNAL OF LIQUID CHROMATOGRAPHY

Indexing and Abstracting Services. Articles published in *Journal of Liquid Chromatography* are selectively indexed or abstracted in:

■ Analytical Abstracts ■ ASCA ■ Berichte Pathologie ■ BioSciences Information Service of Biological Abstracts (BIOSIS) ■ Cambridge Scientific Abstracts ■ Chemical Abstracts ■ Chemical Reactions Documentation Service ■ Current Awareness in Biological Sciences ■ Current Contents/Life Sciences ■ Current Contents/Physical and Chemical Sciences ■ Engineering Index ■ Excerpta Medica ■ Journal of Abstracts of the All-Union Institute of Scientific and Technical Information of the USSR ■ Physikalische Berichte ■ Reference Update ■ Saltykov-Shchedrin State Public Library ■ Science Citation Index

Manuscript Preparation and Submission. See end of issue.

This journal is also available on CD-ROM through ADONIS™ beginning with the 1991 volume year. For information contact: ADONIS, Marketing Services, P.O. Box 839, Molenwerf 1, 1000 AV Amsterdam, The Netherlands, Tel: +31-20-6842206, Fax: +31-20-6880241.

The Journals of Marcel Dekker, Inc. are available in microform form: RESEARCH PUBLICATIONS, 12 Lunar Drive, Drawer AB, Woodbridge, Connecticut, 06525, (203) 397-2600 or Toll Free 1-800-REACH-RP(732-2477). Outside North and South America: P.O. Box 45, Reading, RG1 8HF, England, 0734-583247.

Contributions to this journal are published free of charge.

Effective with Volume 6, Number 11, this journal is printed on acid-free paper.

JOURNAL OF LIQUID CHROMATOGRAPHY

Volume 17, Number 3, 1994

CONTENTS

JOURNAL OF LIQUID CHROMATOGRAPHY, 17(3), 483-497 (1994)

HPLC ENANTIOSEPARATION OF DI- AND TRIPEPTIDES ON CYCLODEXTRIN BONDED STATIONARY PHASES AFTER DERIVATIZATION WITH 6-AMINOQUINOLYL-N-HYDROXYSUCCINIMIDYL CARBAMATE (AQC)

SHUSHI CHEN, MARIA PAWLOWSKA, AND DANIEL W. ARMSTRONG*
Department of Chemistry
University of Missouri-Rolla
Rolla, Missouri 65401

ABSTRACT

Enantiomeric separations were performed on a number of di- and tripeptides after their pre-column derivatization with the fluorescence derizatizing agent 6-aminoquinolyl-N-hydroxysuccinimidyl carbamate (AQC). It has been demonstrated that the choice of a suitable cyclodextrin bonded phase in conjunction with nonaqueous polar mobile phases offers an effective means to resolve chiral peptides. It was found that the strength of interaction between the cyclodextrin and the solute, and therefore the retention and stereoselectivity, is extremely sensitive to small structural variations of the analyte.

---

*To whom correspondence should be sent.

INTRODUCTION

6-Aminoquinolyl-N-hydroxysuccinimidyl carbamate (AQC) was recently developed as a new pre-column derivatizing agent for primary and secondary amine containing compounds [1,2]. We reported the first enantiomeric separations of AQC-primary and secondary amino acids on cyclodextrin bonded columns [3]. The derivatization reaction is fast, proceeds without any detectable racemization and provides stable and highly fluorescent derivatives suitable for efficient and sensitive HPLC analysis. The use of nonaqueous systems e.g., different cyclodextrin bonded phases in conjunction with polar organic mobile phases, offered a wide range of possibilities to optimize enantioselectivity. It has been postulated that the enantioseparation has been achieved via external complex formation between the solute and the cyclodextrin molecule. In the case of native cyclodextrin bonded phases the chiral recognition arises from stereoselective hydrogen bonding between donor and acceptor sites of the analyte with the secondary hydroxyl groups at the mouth of the cyclodextrin. The discrimination of enantiomers on derivatized bonded cyclodextrin phases may arise from stereoselective hydrogen bond formation between the solute and the residual secondary hydroxyl groups as well as other polar moieties at the mouth of the cyclodextrin. It has been postulated that the 6-aminoquinolyl moiety provides not only high absorptivity for easy photometric and/or fluorescence detection but also contributes to the overall stereorecognition. It has been found that mobile phase composition controls both retention and enantioselectivity. The addition of methanol can be used to decrease retention while small amounts of triethylamino and glacial acetic acid have been used to optimize selectivity and retention parameters. The addition of water decreases dramatically the retardation and selectivity. In this paper we extend the use

of AQC to the analysis of di- and tripeptides. Also we discuss the effect of solute structure on retention in terms of the overall mechanism. Comparisons with other fluorescent "tagging" agents are beyond the scope of the present paper, but are being made. This information will be reported in a latter work.

EXPERIMENTAL

Chemicals. All peptides and boric acid used in this work were purchased from Sigma (St. Louis, MO). The derivatizing reagent (AQC, Acc Q-Fluor Reagent) was obtained from Waters (Milford , MA). Calcium sodium EDTA was purchased from Aldrich (Milwaukee, WI). All HPLC grade solvents including acetonitrile, methanol, triethylamine and acetic acid were obtained from Fisher Scientific (Pittsburgh, PA).

Methods

Derivatization procedures. The AQC derivatized peptides were obtained according to references 1-3 by dissolving 500 pmol of each compound in 35 µl of sodium borate buffer (0.2 M, pH 8.8) in a vial; vortex several seconds and then add 10 µl of AQC solution to it (3 mg per 1 ml of acetonitrile). The vial was heated in an oven for 10 minutes of 50°C. The resulting solution was injected into a column without further purification. The FMOC-Gly derivatization of Phe and Leu was performed as reported previously in reference 4.

Chromatographic experiments. Separations were performed at ambient temperature with a Waters dual pump solvent delivery module Model 590. The spectrophotometric detector (Waters, Model 440) with UV wavelength of 254 nm or fluorescence scanning detector (Waters,

Model 470) was used for monitoring the effluent. The excitation and emission wavelengths were 250 nm and 395 nm, respectively. The flow rate in all cases was 1 ml/min. All columns used in this work were obtained from Advanced Separation Technologies (Whippany, NJ). The mobile phases were mixtures of acetonitrile, methanol, triethylamine and acetic acid. The volume ratios of each solvent is reported in the appropriate tables and figures.

RESULTS AND DISCUSSION

Table I shows the chromatographic data for a number of AQC functionalized di- and tripeptides with one chiral center, e.g. containing at least one achiral glycine or β-alanine moiety, obtained under optimal experimental conditions. Table II gives the retention parameters for AQC-di- and tripeptides with two chiral centers. As can be seen from the data presented the chiral recognition of AQC derivatized solutes occurs on native as well as derivatized cyclodextrin bonded phases operated with polar organic solvents. The enantioseparation of the analytes studied can be achieved in some cases also in the reversed phase mode as presented in Figure 1B. However, compared with the nonaqueous system (Figure 1A) the selectivity obtained in a water-rich system is rather poor. The change of the mobile phase composition also changed the elution order of the enantiomers, which is not surprising since the chiral recognition mechanism involved is different for each mode [3,4].

It has been found that cyclodextrin bonded phase columns operated with nonaqueous eluents exhibit enantioselectivity towards AQC functionalized di- and tripeptides which results in baseline resolution for many solutes studied (see Figure 2 and Table I). Obviously enantioseparation depends very strongly on the type of the chiral stationary

TABLE I CHROMATOGRAPHIC DATA FOR SEPARATION OF RACEMIC AQC-DIPEPTIDES AND TRIPEPTIDES WITH ONE CHIRAL CENTER ON CYCLODEXTRIN BONDED PHASES USING NONAQUEOUS POLAR MOBILE PHASES

Compound	k'[a]	Config.	α	R_s	Mobile Phase[b]	Column[c]
AQC-Gly-Leu	4.70	D	1.33	2.97	450/50/4/6	RN
	8.98	D	1.15	1.82	450/50/2/6	SN
AQC-Leu-Gly	3.71		1.29	2.44	450/50/4/6	RN
	5.03		1.24	2.31	450/50/3/6	SN
AQC-Gly-α amino n-butyric acid	3.55	D	1.08	1.01	475/25/4/6	γ
	3.47		1.09	1.01	450/50/4/6	RN
AQC-Gly-Nleu	4.69		1.30	3.00	450/50/4/6	RN
AQC-Gly-Val	3.49	D	1.24	2.29	450/50/4/6	RN
AQC-Gly-Nval	3.66		1.14	1.53	450/50/4/6	RN
AQC-Gly-Met	4.75	L	1.15	1.34	470/30/4/6	AC
	5.05	D	1.27	2.70	450/50/4/6	RN
AQC-Gly-Ser	5.45		1.04	0.55	450/50/3/6	SN
AQC-Gly-Asn	1.83		1.05	0.70	450/50/3/6	SN
AQC-Gly-Asp	7.67	D	1.18	2.81	450/50/4/6	AC
AQC-Gly-Phe	6.85	L	1.12	1.24	450/50/4/6	RN
	10.03	L	1.11	1.37	450/50/3/6	SN
AQC-β-Ala-Leu	8.25		1.12	1.90	460/40/4/6	β
	4.09		1.14	1.71	475/25/3/6	RSP
	5.72		1.36	2.68	460/40/5/3	RN
	5.00		1.21	2.23	450/50/3/6	SN
AQC-β-Ala-Val	3.62		1.10	1.17	475/25/3/6	RSP
AQC-Gly-Gly-Leu	7.48		1.12	1.74	450/50/3/6	γ
	6.71		1.25	2.14	450/50/4/6	RN
AQC-Ala-Gly-Gly	8.65	D	1.12	1.23	450/50/3/6	SN

[a] k' is the capacity factor for the first eluted enantiomer.

[b] Mobile phases are mixtures of acetonitrile/methanol/acetic acid/triethylamine by volume(v/v)

[c] Columns β, γ, RSP, AC, SN, RN stand for , β–, γ–, R,S-2-hydroxypropyl, acetylated β–, S-naphthylethyl-carbamate, R-naphthylethylcarbamate, cyclodextrin bonded stationary phases.

TABLE II CHROMATOGRAPHIC DATA FOR SEPARATION OF RACEMIC AQC-DIPEPTIDES AND TRIPEPTIDES WITH TWO CHIRAL CENTERS ON CYCLODEXTRIN BONDED PHASES USING NONAQUEOUS POLAR MOBILE PHASES

Compound	k'^{b}_{DD}	k'_{LL}	$k'_{DL,LD}$	$k'_{LD,DL}$	Mobile Phase[a]	Column[c]
AQC-Ala-Ala[d]	6.92	7.32	7.72	7.72	450/50/3/5	β
AQC-Ala-Val[d]	4.96	5.38	5.57	5.98	460/40/4/6	β
	2.95	3.73	3.14	3.60	450/50/2.5/5	RN
AQC-Ala-Ser[d]	4.42	4.68	6.08	6.08	490/10/2/6	AC
	4.72	4.72	5.57	6.22	460/40/2/6	SN
AQC-Leu-Ala[d]	3.90	4.05	4.56	4.76	485/15/6/6	AC
	4.22	6.70	5.28	6.43	460/40/2/6	RN
	4.36	5.64	3.52	5.29	450/50/2/6	SN
AQC-Leu-Val[d]	4.02	4.31	5.29	5.63	450/50/3/6	β
	3.54	5.41	4.78	5.14	450/50/3/6	SN
AQC-Leu-Phe[d]	11.13	7.12	8.44	9.56	450/50/3/6	α
AQC-Ala-Phe[d]	11.12	10.09	8.48	9.67	450/50/5/3	β
	15.97	14.65	11.89	12.76	465/35/5/2	AC
	8.27	5.25	4.34	4.68	450/50/4/6	RN
	13.68	10.13	7.28	7.45	450/50/2/6	SN
AQC-Ala-Leu[e]	9.03	10.26	9.29	8.76	460/40/2/6	β
	5.96	8.14	6.89	5.49	460/40/5/3	RN
AQC-Leu-Leu[e]	3.97	7.08	4.97	5.45	450/50/2/6	SN
AQC-Leu-Tyr[e]	10.56	9.17	11.78	12.78	460/40/4/6	β
	5.70	4.84	6.60	7.05	450/50/3/6	γ
AQC-Ala-Met[f]		7.26	5.72	6.02	460/40/2/6	RN
		6.10	4.76	5.04	450/50/2/6	SN
AQC-Leu-Gly-Phe[f]	5.50	6.14	6.54	7.67	450/50/4/6	RN
AQC-Ala-Leu-Gly[f]	7.02	7.34	7.77	8.80	450/50/4/6	β
	4.57	4.95	5.28	5.81	470/30/4/6	AC
	3.58	4.26	4.41	7.02	450/50/4/6	RN
AQC-Gly-Leu-Ala[f]	9.53	9.70	12.53	13.26	490/10/2/6	γ

Mobile phases are mixtures of acetonitrile/methanol/AA/TEA by volume(v/v)

The capacity factor, k', is equal to t_r-t_0 / t_0

Columns α, β, γ, RSP, AC, SN, RN stand for α–, β–, γ–, R,S-2-hydroxypropyl, acetylated β–, S-naphthylethyl-carbamate, R-naphthylethylcarbamate, cyclodextrin bonded stationary phases.

The retention order for the DD and LL enantiomers are known and are correct as shown in this table. However, the retention order for the DL and LD enantiomers is unknown since standards were not available.

The retention order for these peptides is k'_1=DD, k'_2=DL, k'_3=LD, k'_4=LL.

No standards were available for these compounds. Consequently in those cases the retention order for the stereoisomers is listed from lowest to highest (left to right) and the stereochemical designation at the top of each column may not be correct.

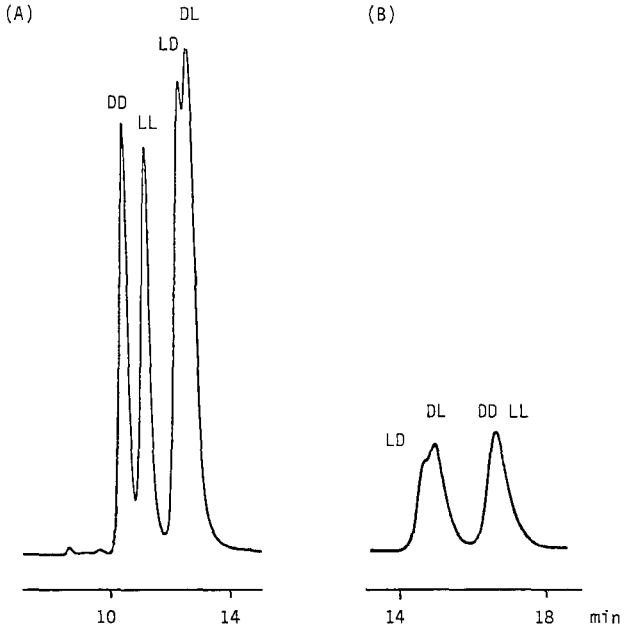

Figure 1. Enantiomeric resolution of AQC-Leu-Leu obtained on (R,S)-hydroxypropyl derivatized β-CD using; a) nonaqueous mobile phase: 475 acetonitrile + 25 methanol + 3 acetic acid + 6 triethylamine (v/v/v/v), b) reversed phase mode with a mobile phase consisting of 5% acetonitrile in 95% triethylammonium acetate buffer (1 % pH = 7.1). Fluorescence detection (λex = 250 nm, λem = 395 nm) was used.

phase used as well as the structure of the analyte. Generally the carbamate derivatives of β-cyclodextrin, where several types of adsorption (binding) sites are available, were found to have the broadest enantioselectivity. The chiral recognition may arise from stereoselective hydrogen bonding between donor and acceptor sites of the analyte with the residual secondary

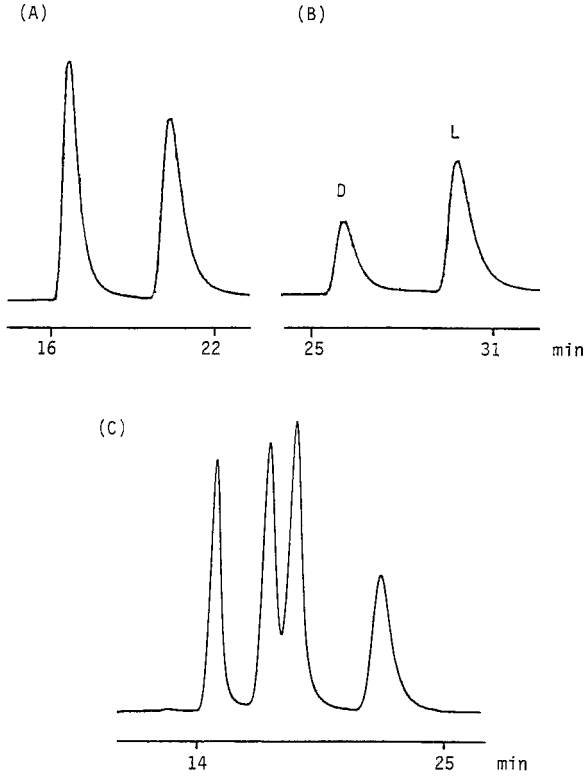

Figure 2. Enantioseparation of selected AQC-dipeptides under optimal chromatographic conditions. a) test compound: AQC-Gly-Nle; column: RN-β-CD; eluent: 450 acetonitrile + 50 methanol + 4 acetic acid + 6 triethylamine (v/v/v/v), b) test compound: AQC-Gly-Asp; column: AC-β-CD; eluent: 450 acetonitrile + 50 methanol + 4 acetic acid + 6 triethylamine (v/v/v/v), c) test compound: AQC-Leu-Leu; column: SN-β-CD; eluent: 450 acetonitrile + 50 methanol + 2 acetic acid + 6 triethylamine (v/v/v/v). Fluorescence detection (λex = 250 nm, λem = 395 nm) was used.

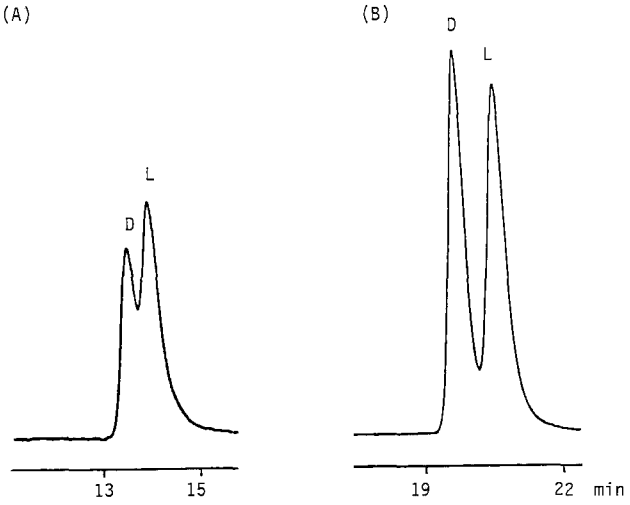

Figure 3. Enantioseparation of AQC-Val (A) and AQC-Gly-Val (B) obtained on a SN-β-CD column with a mobile phase consisting of: 450 acetonitrile + 50 methanol + 3 acetic acid + 6 triethylamine (v/v/v/v). Fluorescence detection (λex = 250 nm, λem = 395 nm) was used.

hydroxyl groups as well as the polar moieties of the chiral naphthylethylcarbamate substituent. Also, π-π interactions between the aromatic substituents at the mouth of the cyclodextrin cavity and the aromatic part of the analytes are possible. All these factors lead to the unique selectivities observed.

Figures 3-5 show the change in the enantioseparation of different AQC derivatives caused by the introduction of a glycine moiety. It was found in all instances that extending the peptide chain length and introducing new hydrogen bonding groups resulted in increased retention.

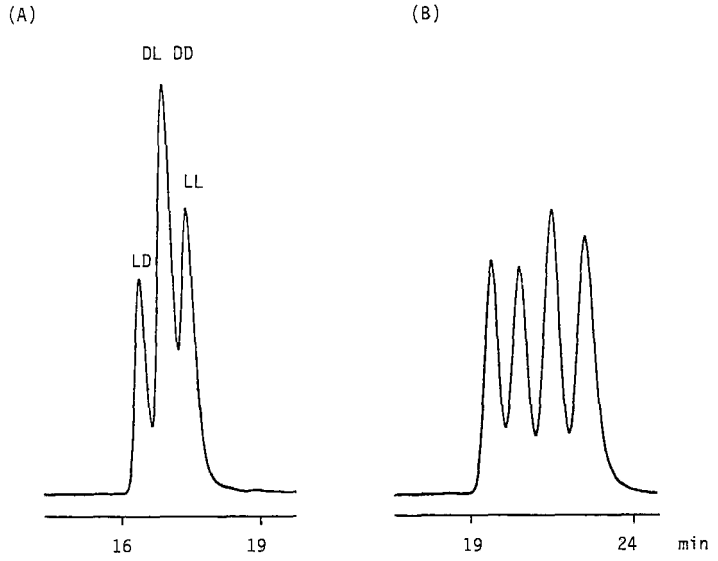

Figure 4. Enantioseparation of AQC-Ala-Leu (A) and AQC-Ala-Leu-Gly (B) on an AC-β-CD column using a mobile phase of 470 acetonitrile + 30 methanol + 2 acetic acid + 6 triethylamine (v/v/v/v). Fluorescence detection (λex = 250 nm, λem = 395 nm) was used.

As can be seen in Figure 3 and Figure 4 for AQC-Val and AQC-Ala-Leu the additional glycine moiety also causes an enhancement in enantioselectivity. Figure 5 shows the interesting case of AQC-Met. Introduction of glycine resulted in a reversal in the retention order. This shows that the enantioselectivity exhibited by the stationary phase is highly sensitive to changes in the molecular structure of the analyte that are not necessarily near the chiral center. The effects of the structural features of the solute on retention also are shown in Figure 6 and Figure 7. In

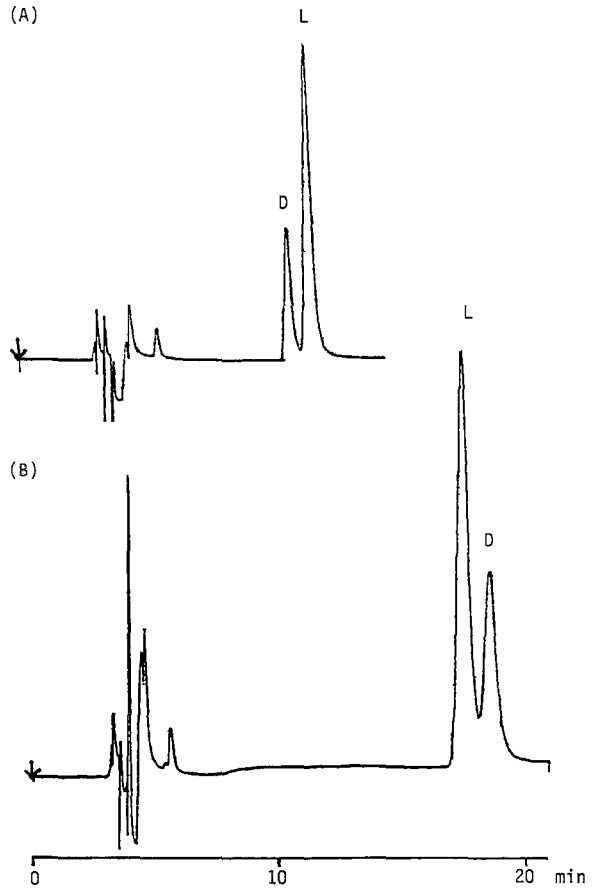

Figure 5. Enantioseparation of AQC-Met (A) and AQC-Gly-Met (B) using a mobile phase of 475 acetonitrile + 25 methanol + 3 acetic acid + 6 triethylamine (v/v/v/v) and an AC-β-CD column. UV detection was used at 254 nm. Both racemic mixtures were spiked with L-enantiomers. Note that elution order has been reversed.

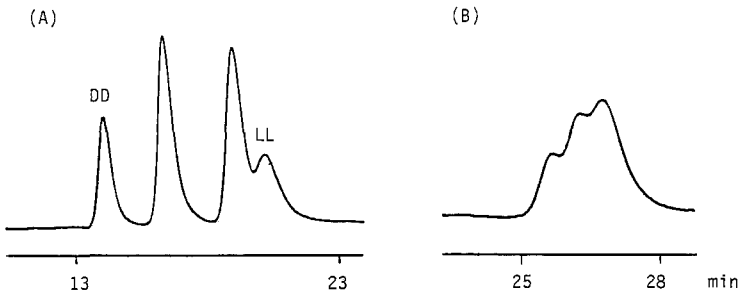

Figure 6. Enantioseparation of AQC-Leu-Ala (A) AQC-Gly-Leu-Ala (B) on a SN-β-CD bonded stationary phase with a mobile phase of 450 acetonitrile + 50 methanol + 1.8 acetic acid + 6 triethylamine (v/v/v/v). Fluorescence detection (λex = 250 nm, λem = 395 nm) was used.

contrast to the results presented above in Figures 3 and 4, the addition of a glycine moiety to the AQC-Leu-Ala resulted in decreased selectivity toward the enantiomers of the resulting tripeptide (Fig. 6). A similar effect is demonstrated in Figure 7. The best enantioseparation is achieved for AQC-Leu. The AQC-based separations are somewhat different from those that use FMOC, in that an added glycine moiety always enhanced the resolution of primary FMOC tagged amino acids [4]. However, in the AQC-case an added glycine can either enhance, decrease or not affect the enantiomeric separation. Currently there is no way to predict which will occur. The retention of the solute always increases with the number of polar groups capable of hydrogen bond formation, however magnitude of this effect depends on the analyte structure. As shown in Fig. 7B and Fig. 7D the retardation of AQC-Gly-Leu and AQC-Leu-Gly (which have the same amino acid residues but in a different order) are significantly different.

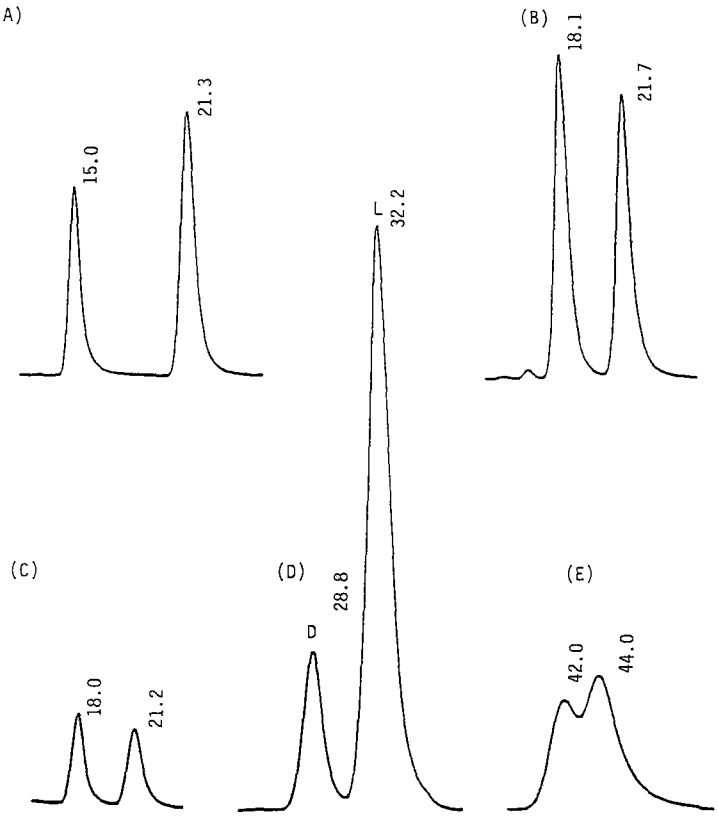

Figure 7. Chromatograms for AQC-Leu (A), AQC-Leu-Gly (B), AQC-β-Ala-Leu, (C) AQC-Gly-Leu (D) and AQC-Gly-Gly-Leu (E) obtained on a SN-β-CD column with a mobile phase of 450 acetonitrile + 5 methanol + 3 acetic acid + 6 triethylamine (v/v/v/v). In the (A) and (D) chromatograms, the L enantiomers have been spiked. Fluorescence detection (λex = 250 nm, λem = 395 nm) was used.

It has been postulated previously from the comparison of retention data obtained for AQC [3] and FMOC derivatives [4] that the 6-aminoquinolyl substituent does not sterically interfere with the chiral recognition process. In fact, it may enhance chiral recognition in some cases. This supposition is confirmed in this study. The elution of AQC derivatized amino acids [1] as well as di- and tripeptides from the cyclodextrin columns requires the addition of methanol to the mobile phase (in some cases as much as 20% which usually was not necessary for FMOC derivatives [4]). It is likely that both the 6-aminoquinolyl moiety containing two nitrogen atoms capable of hydrogen bond formation and the polar amino acids (or their peptide bonds) are closely associated with the cyclodextrin, which results in strong retardations and affects the stereorecognition as well. Addition of too much methanol to the mobile phase usually destroys enantioselectivity.

CONCLUSION

The data presented in this study provide support for the noninclusion model of chiral discrimination on cyclodextrin bonded stationary phases in nonaqueous systems as proposed previously [3,4]. It is demonstrated that the enantiomer separation is extremely sensitive to relatively small structural variations. The strength of the interactions between the cyclodextrin stationary phase and the solutes and therefore the retention and the stereoselectivity are determined both by the structure of the analyte and competitive interaction of the mobile phase components.

ACKNOWLEDGEMENT

Support of this work by the National Institute of General Medical Science (BMT 1R02 GM36292-04) is gratefully acknowledged.

LITERATURE

1. S. A. Cohen and D. M. Michaud, *Anal. Biochem.* **211**: 279 (1993).
2. S. A. Cohen, K. De Antonis and D. M. Michaud, in Techniques in Protein Chemistry IV, R. H. Angeletti (ed.), Academic Press, San Diego, 1993, pp 289-298.
3. M. Pawlowska, S. Chen and D. W. Armstrong, *J. Chromatogr.* **641**: 257 (1993).
4. J. Zukowski, M. Pawlowska and D. W. Armstrong, *J. Chromatogr.* **623**: 33 (1992).

Received: September 12, 1993
Accepted: October 8, 1993

JOURNAL OF LIQUID CHROMATOGRAPHY, 17(3), 499-520 (1994)

THERMO-OPTICAL SPECTROSCOPY: NEW AND SENSITIVE SCHEMES FOR DETECTION IN CAPILLARY SEPARATION TECHNIQUES

J. M. SAZ[1]* AND J. C. DÍEZ-MASA[2]
[1]*Department of Analytical Chemistry*
Faculty of Science
Alcalá de Henares University
28801 Alcalá de Henares, Madrid, Spain
[2]*Institute of Organic Chemistry*
C.S.I.C.
Juan de la Cierva, 3
28006 Madrid, Spain

ABSTRACT

Detection is a major problem in the application of Open-Tubular Capillary Liquid Chromatography (OTCLC) and Capillary Electrophoresis (CE) for analyzing very dilute samples, for instance in trace analysis. Thermo-optical Spectroscopy is a new branch of Spectroscopy which allows the detection of samples with low light absorbances (10^{-8} - 10^{-9} AU) using a few picoliters sample cell. A few attomoles of analyte can be detected in OTCLC or in CE with these techniques. These results are similar to those achieved by Laser-Induced Fluorescence detection in open-tubular capillary tubings. However, many organic substances present a high absorption coefficient and only a few of them provide good quantum yields. The principles of Thermo-optical Spectroscopy are presented in this work. The main thermo-optical methods and their application in OTCLC and CE are also reviewed.

**Temporarily assigned to Institute of Organic Chemistry (C.S.I.C.).*

INTRODUCTION

In recent years, capillaries whose internal diameter is increasingly smaller are being employed in Open-Tubular Capillary Liquid Chromatography (OTCLC) and Capillary Electrophoresis (CE) to contain the separation media (stationary phase, mobile phase or separation buffer). Capillary columns of a few micrometers of i.d. (5-10 μm) have been developed to be used as open-tubular capillary columns in HPLC. These columns allow the achievement of large efficiencies and short analysis time. Capillary tubes of 25 μm i.d. or smaller are being more frequently used in CE because of their excellent heat dissipation. However, such a reduction in i.d. requires the use of a very small volume (nL-pL) and mass (in the range of pg) of sample. Otherwise, efficiency loss and/or column overloading might occur. The use of such small samples is very demanding for other system components (injector, connexions, and detector) and prevent the analytical use of these techniques in trace analysis (ng/mL-pg/mL) due to detection limitations.

To illustrate the above detection problems using these capillary separation techniques in trace analysis, let's consider a sample volume of 1 nL (this is usually the maximum volume allowed in OTCLC and CE) with a trace level concentration of the solutes (1 ng/mL - 1 pg/mL) injected into the column. If we assume that the sample dilution is negligible during separation and consider that the volume of the detector cell should be around 1/10 of the peak volume to avoid efficiency losses, the detection limit for an analyte having a molecular weight of 100 a.m.u. should be 10^{-18}-10^{-21} moles. For a conventional UV-Vis detector (1 cm path length) and an analyte with an absorption coefficient $\approx 10^3$ AU $\times$ cm^{-1} $\times$ M^{-1}, this detection limit is equivalent to 10^{-5} AU. However, detection in OTCLC and CE must be on-column to prevent efficiency losses, which involves a great reduction in the optical path (capillary i.d. usually ranges from 5 to 100 μm in these separation techniques). This means that to use OTCLC and CE in trace analysis using conventional UV-Vis detection, a detection limit in the range of 1×10^{-7}-0.5×10^{-9} AU is required. At the present time, the best commercial UV-Vis detectors for

these capillary separation techniques have detection limits approximately 10^{-4}-10^{-5} AU.

There are only a few major possibilities to overcome the detection problem in trace analysis using capillary separation techniques: i) the use of sample preconcentration, particularly on-line techniques (1-4), ii) the pre-, on- or post-column sample derivatization (5), and iii) the use of high-sensitivity detection techniques. The on-line preconcentration can involve sample and efficiency losses and the hardship of finding a stationary phase to retain the analytes concerned. The sample derivatization can also involve efficiency losses (in post-column methodologies), and, in pre- and on-column derivatization, the appearance of some extra-peaks (derivatization agent, system peaks, etc) which make the analysis more complicated . The use of high-sensitivity detectors does not require sample manipulation, avoiding the above-mentioned problems. Since at the present time, spectroscopic methods present less problems for on-column detection, detection schemes employing this methodology are the most used in OTCLC and CE. From this viewpoint, those spectroscopic detection techniques whose response is proportional to the illuminating power (UV-Vis, Fluorescence, Phosphorescence, Photoionization, Photoconductivity, Thermo-optic and Thermo-acoustic techniques, etc) are especially appealing. The use of high illuminating power sources (e.g., laser radiation) in such detection techniques significantly improves their detection limits. Other spectroscopic methods whose response does not depend on the optical path (e.g., some thermo-optical methods) could be very interesting too for on-column detection in capillary separation techniques. Finally, detection schemes involving large optical paths which do not affect in a substantial manner the separation efficiency (e.g., UV-Vis Axial Detection (6)) could also be used in capillary separations.

The aim of this paper is to review the possibilities of the thermo-optical methods for detection in OTCLC and CE. In general terms, these methods can detect a very small sample absorbance (10^{-8}-10^{-9} AU) in only a few picoliters of sample using an optical path in the range of micrometers. A few attomoles injected

into the capillary (7) could be monitored using these detectors, allowing the use of the OTCLC and CE in trace analysis. This sensitivity is similar to that obtained with Laser-Induced Fluorescence, but thermo-optical methods have a wider range of application because many substances absorb UV-Vis radiation and only a few present native fluorescence.

LASER PROPERTIES

The development of thermo-optical methods is associated to the laser unique properties, particularly its intensity (power per area unit) and coherence. Laser intensity is generally much larger than that of any other light source. This is very important in thermo-optical methods since there is a direct relationship between the illuminating power and the response obtained. However, due to the solvent absorbance, sample flow, and thermic effects, the noise also increases with the illuminating power and, hence, the signal/noise ratio increases up to a certain value and then remains constant.

The spatial and temporal coherence are related to the degree of correlation between the phases of any two points in the beam and the temporal variation of this correlation. Laser coherence is also higher than that of conventional illuminating sources. This feature allows focusing the beam within a very small spot size (a few micrometers radius), letting the design of detectors with very small sample cells (a few picoliters) and increasing detector response.

THE THERMO-OPTICAL EFFECT

All thermo-optical methods are based on the same principle: the Thermo-optical Effect. When a radiation beam with sufficient illuminating power (e.g., a laser) passes through a sample, it causes a temperature rise in the illuminated zone. This temperature rise is due to the light absorption of the analytes and the subsequent non-radiant relaxation of the originated species so that the temperature

increase is proportional to the sample absorbance. Such temperature rise causes a change in the refractive index of the sample transforming the illuminated zone in an optical element (a lens, a prism or a diffraction grating, depending on the beam transversal energy distribution). The characteristics of the thermo-optical elements are very sensitive to small absorbance changes and, therefore, thermo-optical methods can be used as high-sensitivity analytical techniques. Since there is a relationship between the thermo-optical element characteristics and the sample radiation absorbance, these thermo-optical elements can be used for detection in separation techniques and for quantitation purposes.

The response of thermo-optical methods depends on the thermo-optic effect intensity which, in turn, considerably depends on the solvent properties, particularly on the refractive index change with temperature (dn/dT) and thermic conductivity (k). The larger dn/dT and the smaller k, the larger the refractive index gradient is, the longer this gradient remains, and thus, the larger the thermo-optical response will be. Table 1 presents the dn/dT and k values for some solvents. It shows that non-polar solvents like Cl_4C are good solvents for thermo-optical techniques. Polar solvents (e.g., water) are the least appropriate for thermo-optical purposes due to their high k (however, if water is mixed with organic solvents as methanol or acetone its thermo-optical properties improve). Fluids at supercritical state like CO_2 (at 34 °C and 77 atm) are ideal solvents for thermo-optical techniques due to their large dn/dT.

In the following sections, the main thermo-optical methods, their principles, applications on OTCLC and CE detection, and detection limits will be described.

LASER-INDUCED INTERFEROMETRY

When a laser beam traverses a sample which absorbs the laser radiation, it causes a temperature rise and a concomitant refractive index decrease in the illuminated sample zone. The refractive index variation originates a phase change in the beam, and hence a change in the intensity of the interference beam obtained

TABLE 1

Thermo-optical properties of some solvents[a].

solvent	k (mW × cm^{-1} × K^{-1})	dn/dT × 10^4 (K^{-1})
CO_2 (34 °C y 77 atm)	0.95	-910
Cl_4C	1.03	-5.9
cyclohexane	1.24	-5.4
n-heptane	1.26	-5.0
acetone	1.60	-5.4
dioxane	1.39	-4.6
isobutyl alcohol	1.52	-3.9
methanol	2.02	-4.2
water	6.11	-0.8

[a] Data from (41) and (42).

when recombined with another. The change in the interference beam intensity can be related to the sample absorbance.

The thermo-optical effect was first reported by Gordon et al (8), who described the relationship between the temperature increase $\Delta T(r,t)$ caused by a gaussian laser beam (as a function of the distance from the center of the irradiated zone r, and the irradiation time t) and the sample absorption coefficient (ε):

$$\Delta T(r,t) = \frac{\epsilon P}{16.8\pi k}\left[\ln(1+8Dt/\omega^2) - \frac{1}{(1+\omega^2/8Dt)}\frac{2r^2}{\omega^2}\right] \quad (1)$$

(see Glossary for symbols).

The temperature increase is related to the refractive index variation (Δn) by:

$$\Delta n = \frac{\partial n}{\partial T} \Delta T \qquad (2)$$

In turn, the refractive index change is related to the phase beam change ($\Delta\phi$) by:

$$\Delta\phi = 2\pi \frac{l}{\lambda} \Delta n \qquad (3)$$

Finally, the phase change is related to the interference beam intensity (I_s):

$$I_s = \frac{1}{2} I_{max} (1 + \cos\Delta\phi) \qquad (4)$$

Equations 1 to 4 show a relationship between laser properties (P, λ and ω), sample characteristics (dn/dT, k and l), and signal produced (I_s). High power and short wavelength lasers tightly focused within the sample increase the signal. Samples with large temperature dependence of refractive index, small thermal conductivity, and long optical path also do.

Figure 1 shows a laser interferometer. The radiation from a He-Ne laser goes through an uncoated optical flat splitting the laser radiation in two beams (M and m) with different energy (M has much more energy than m). Both beams pass through the sample. M heats the sample producing a refractive index variation which causes a phase shift. The phase shift in m is negligible because it has low energy and almost no refractive index variation is originated in the sample region traversed by this beam. After passing across the sample, M goes through another uncoated optical flat and it is again divided in two beams (MM and Mm). Mm interferes with m producing an interference beam (mMm) whose intensity is related to the sample absorbance. MM is sent to a photodiode as reference signal.

Several laser-induced interferometry schemes have been described to determine small absorbance in static samples (9-12). Sample cells with several centimeters of optical path have been used in these schemes. To compare detection

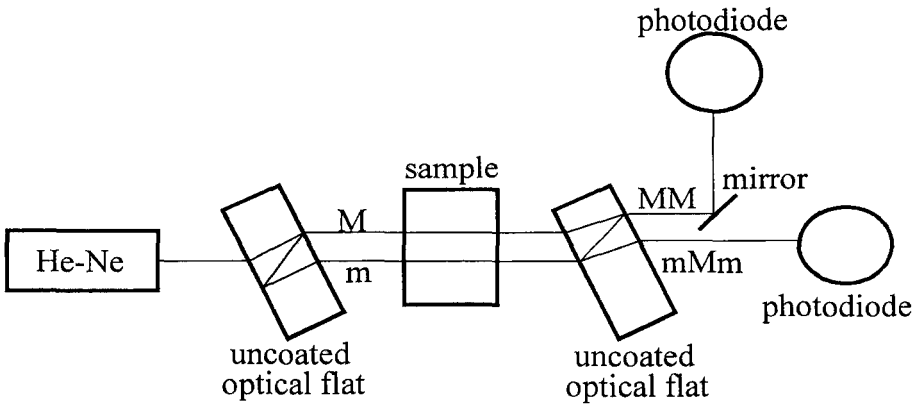

FIGURE 1. Jamin-laser interferometer. The laser beam from a He-Ne laser is splitted in two beams (*M* and *m*) with different energy (*M* has much more energy than *m*). Both of them go through the sample causing a different heating and refractive index change in the region traversed producing a phase shift between them. *M* is again splitted in two beams (*MM* and *Mm*), *MM* goes to the photodiode and is used as reference, and *Mm* is superimposed to *m* producing an interference signal that goes to another photodiode.

limits achieved with different cells, the sensitivity should be expressed as the εC product (absorbance per optical path unit). Detection limits in the range of 10^{-5} - 10^{-6} AU × cm^{-1} were obtained (13).

These laser-based interferometers have also been used as detectors in liquid chromatography (packed, 4.6 mm i.d. columns). Employing 1 cm path length sample cells, a detection limit of 2.6×10^{-6} AU was obtained (14).

LASER-INDUCED THERMAL LENS SPECTROSCOPY

When a laser beam with sufficient power and a gaussian distribution of energy (TEM_{oo}) traverses a sample region, it generates a gaussian temperature distribution and, therefore, a gaussian refractive index distribution in the region

illuminated. Since the temperature value in the center of the illuminated zone is the highest, the refractive index value at the center of this zone is the lowest and this value increases radially along the sample. Consequently, the illuminated zone behaves as a divergent lens for any beam which traverses it. The focal distance (f) of such a lens is related to the sample absorbance (A) (15) according to the equation:

$$\frac{1}{f} = \frac{2.03P(dn/dT)A}{\pi k \omega^2} \qquad (5)$$

The divergence originated by the thermal lens produces an increase in the section area of the beam and, because the total beam energy is constant, it causes a drop in the illuminating intensity at the beam center. Therefore, the intensity change at the beam center can be related to the sample absorbance. When the sample is placed at the position $\sqrt{3}z_c$ behind the beam waist, the equation proposed by Carter and Harris (15) relates the intensity change to the sample absorbance:

$$\frac{I_o - I}{I_o} = 2.303EA + \frac{(2.303EA)^2}{2} \qquad (6)$$

Where E is defined as:

$$E = -\frac{P(dn/dT)}{1.91\lambda k} \qquad (7)$$

Equations 6 and 7 show that the signal originated by the thermal lens is proportional to the sample absorbance and the E factor. The E factor can be considered as an increment factor of the thermal lens signal when compared to conventional UV-Vis spectroscopy signal (A). This increment depends on the laser power (P), laser wavelength (λ), the variation of the sample refractive index with temperature (dn/dT), and sample thermal conductivity (k). An increase in the intensity change (I_o-I/I_o) can be achieved for the same sample by increasing the laser power (P).

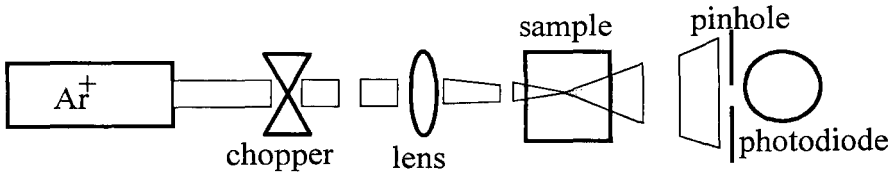

FIGURE 2. Single-beam thermal lens spectrophotometer. The laser beam from a laser source with sufficient power to produce the thermo-optical effect (e.g., a Ar^+ laser) is modulated by a chopper and focused by a lens within the sample producing a divergent thermal lens which increases the beam section and decreases its intensity at the center, being detected by a photodiode through a pinhole.

Several thermal lens spectroscopy schemes have been described. Figure 2 shows the simplest arrangement based on a single laser beam with sufficient power to produce the thermal lens effect. The beam is modulated with a chopper so that the thermal lens is intermittently formed and dissipated. Data on the beam center intensity is periodically obtained before and after lens formation.

The noise decreases and, therefore, detection limit improves by using two lasers (16) (Figure 3). A pump laser (e.g., Ar^+), with high power and low stability to produce the thermal lens effect and a probe laser (e.g., He-Ne), with low power and larger stability (whose intensity change are measured after passing through the thermal lens), are used in this technique. The pump laser is modulated with a chopper. Using a mirror and a beam splitter, the pump and probe beams are superimposed; a filter before the photodiode blocks the pump beam radiation.

The detection limits achieved using thermal lens spectroscopy in static samples (detection cells with 1 cm or more optical paths) are in the range of 10^{-7}-10^{-8} AU $\times$ cm^{-1} (17). Thermal lens spectroscopy has also been used for detection in liquid chromatography with packed columns (1 mm and 4.6 mm i.d.) (18-20) as well as in open-tubular capillaries (20 μm i.d.) (21). The detection limit obtained in liquid chromatography using 20 μm i.d. capillaries has been 9×10^{-5} AU ($\varepsilon C \simeq 9\times10^{-3}$ AU $\times$ cm^{-1}) (21).

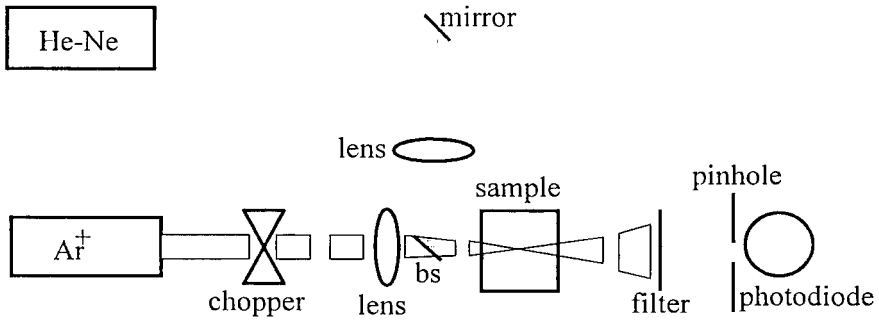

FIGURE 3. Coaxial-beam thermal lens spectrophotometer. The laser beams from two laser sources illuminate coaxially the sample. One of the lasers is modulated and has sufficient power to produce the thermal lens effect (Ar^+ laser), the other has high stability to decrease the noise (He-Ne laser) and probes the thermal lens undergoing a section increase and an intensity drop at its central point, which can be detected by a photodiode. The filter blocks the Ar^+ laser beam radiation.

Another thermal lens setup uses two orthogonally crossed beams instead of coaxial beams (Figure 4). The thermo-optical element behaves as a cylindrical lens which produces a beam divergence related to the sample absorbance. Since the true optical path is reduced to the crossing volume of the pump and probe beams, a high spatial resolution (small illuminated volume) in the sub-picoliter range (22) and a signal not depending on the virtual optical path (sample cell thickness) have been obtained. These features make the crossed-beam thermal lens spectroscopy suitable as a detection system in capillary separation techniques.

The mathematical model for crossed-beam thermal lens spectroscopy has been developed (23) for a pulsed pump laser, but it can be easily adapted to a continuous or modulated pump laser. This model relates the change in relative intensity at the probe beam center (I_t-I_o/I_o) to the sample absorption coefficient (ε) and sample concentration (C):

$$\frac{I_t - I_o}{I_o} = \frac{\theta E_e / t_c}{(1 + 2t/t_c)^{3/2}} \qquad (8)$$

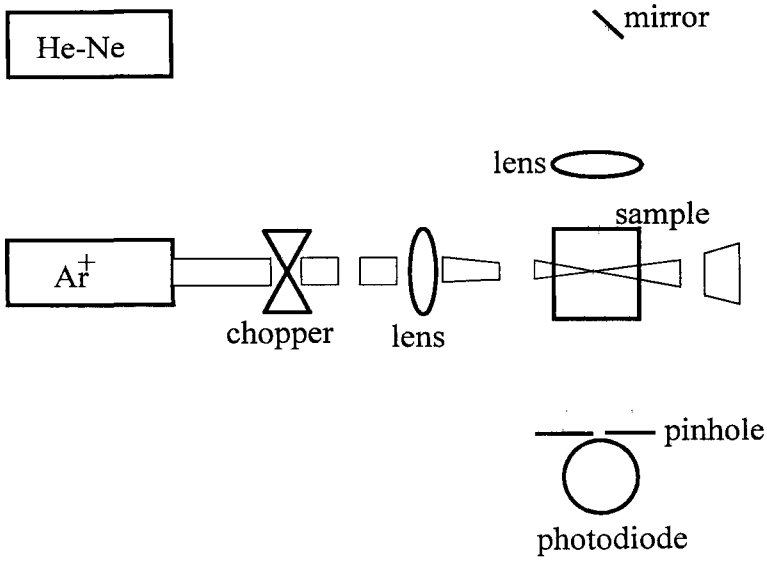

FIGURE 4. Crossed-beam thermal lens spectrophotometer. The thermo-optical element produced by a modulated Ar^+ laser beam behaves as a cylindrical lens generating a divergence in the He-Ne laser beam detected by the photodiode.

Where:

$$\theta=\frac{4.606\epsilon C(dn/dT)z_1}{(2\pi)^{1/2}\omega_e k} \qquad (9)$$

and t_c is a constant related to thermo-optical element relaxation time, defined as:

$$t_c=\frac{\omega_e C}{4k\rho} \qquad (10)$$

Using orthogonally crossed-beam techniques, the detection limits obtained in static samples are ~10^{-9} AU with optical paths of ~3 μm (24). This means a detection limit of 1-2 orders of magnitude smaller than those obtained using coaxial beams thermal lens arrangements (10^{-7} -10^{-8} AU), with a detection volume in the sub-picoliter range.

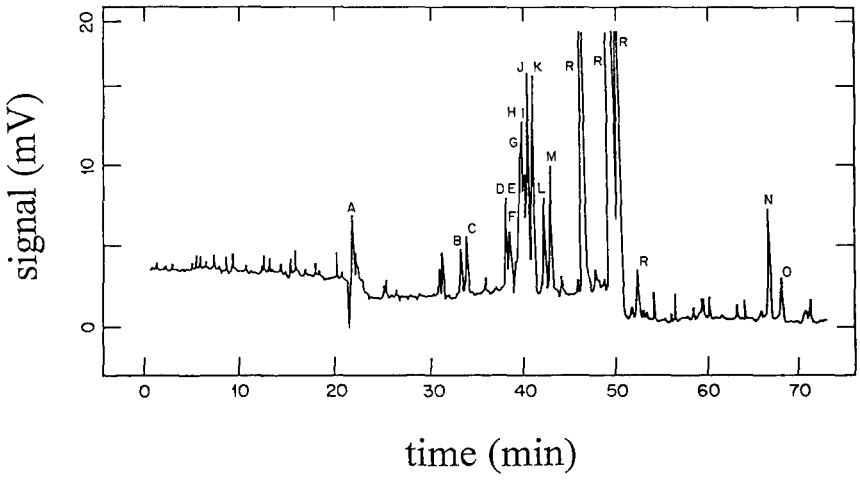

FIGURE 5. Electropherogram of DABSYL-amino acids using crossed-beam thermal lens detection. 2.5×10^{-6} M solution injected, at 5 kV for 5 s, corresponding to 0.7 nL and 1.7 fmol of each amino acid approximately. A, arginine; B, histidine; C, lysine; D, cysteine and tyrosine; E, tryptophan; F, proline; G, phenylalanine; H, leucine; I, methionine; J, isoleucine and valine; K, tyrosine and serine; L, alanine; M, glycine; R, reagent peaks; N, glutamic acid; O, aspartic acid. Reproduced from reference (7) with permission of the American Chemical Society.

Crossed-beam thermal lens spectroscopy has been applied to detection in separation techniques using microbore columns (0.25 - 1 mm i.d.) (25-27), and capillary columns (50 - 200 μm i.d.) (7,28). The detection limit obtained in all cases was in the range of 10^{-7} AU despite the cell thickness was different in each case. Detection limits of 37 attomoles injected into a capillary electrophoresis column have been obtained using 4-(dimethylamino)azobenzene-4'-sulfonyl chloride derivatized amino acids (DABSYL-amino acids) (7). This result is similar to the best results obtained in fluorescent detection using derivatized amino acids (29-30). Figure 5 shows an electropherogram of several DABSYL-amino acids separated by capillary electrophoresis (50 μm i.d.) using crossed-beam thermal lens spectroscopy detection.

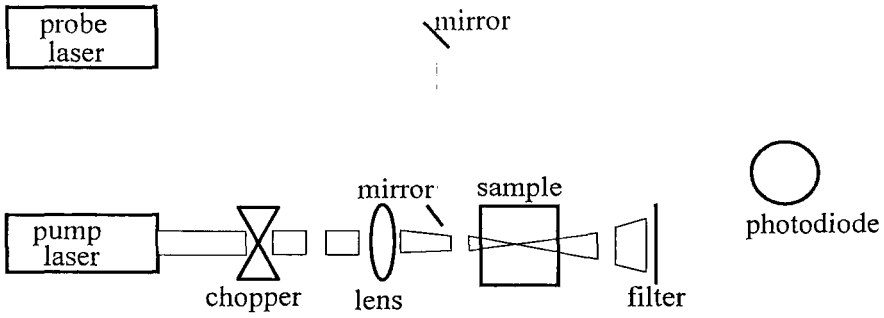

FIGURE 6. Thermal prism spectrophotometer. A modulated pump beam produces a thermal lens within the sample, and a probe laser traverses it close to the thermal lens border originating a beam deflection detected by a position-sensitive photodiode.

LASER-INDUCED THERMAL PRISM SPECTROSCOPY

In this thermo-optical technique, a laser beam with a gaussian energy distribution illuminates the sample, but the probe beam passes through a region close to the thermal lens border instead of through its center as in thermal lens techniques. In this way, the thermal element behaves as an optical prism deflecting the beam (Figure 6). Although the deflection amplitude is very small (10^{-8} - 10^{-9} rad), it can be measured and related to the sample absorbance (31).

The theoretical model proposed by Boccara et al (31) is based on the assumption that the sample behaves as an optical prism. The equations of this model relate the beam deflection (ψ) to the sample absorption coefficient (ε). If the thermic gradient radius in the sample is smaller than the pump beam radius (e.g., using high modulation frequencies in the pump beam or pulsed pump lasers), then:

$$\psi = \frac{P_e(dn/dT)}{v\rho c\pi^2\omega_e^2}\,[1-\exp(-\epsilon l)]\,\left[-\frac{2x_o}{\omega_e}\exp\left(-\frac{x_o^2}{\omega_e^2}\right)\right] \qquad (11)$$

But if the sample thermal diffusion is larger than the pump beam radius, then:

$$\psi = \frac{P_e (dn/dT)}{k\pi^2 x_o} [1 - \exp(-\epsilon l)] [1 - \exp(-\frac{x_o^2}{\omega_e^2})] \qquad (12)$$

According to these equations, the response of this technique (ψ) depends on the pump laser power (P_e) and radius (ω_e), the sample thermo-optical properties (dn/dT and k), and the distance (x_o) between pump and probe beam centers.

The detection limits obtained in static samples using detection cells of 100 μm thickness are around 10^{-8} AU (32). The thermal prism spectroscopy has also been used for liquid chromatography detection using microbore columns (1 mm i.d.). In this case, a detection limit of 3×10^{-8} AU was achieved (33).

LASER-INDUCED THERMAL DIFFRACTION GRATING SPECTROSCOPY

If a laser beam is splitted in two beams which are subsequently crossed with a given angle within the sample, it causes a fringe interference pattern and, therefore, a similar fringe pattern in the sample refractive index (Figure 7). In this case, the illuminated zone generates a diffraction grating. The fringe spacing (d) depends on the laser wavelength (λ_e) and the crossing angle (θ_e) (referred to the bisectrix of both beams) according to Bragg's law:

$$d = \frac{\lambda_e}{2 \sin \theta_e} \qquad (13)$$

Equation 13 shows that the fringe spacing can be modified by changing the beams' crossing angle. When this spacing is much smaller than the fringe thickness, the thermo-optical element behaves as a Bragg diffraction grating. If a probe beam intersects this grating at Bragg's angle ($\theta_b = 2\sin^{-1}(\lambda_p/2d)$), the intensity of the diffracted radiation (I_d) is related to the sample absorption

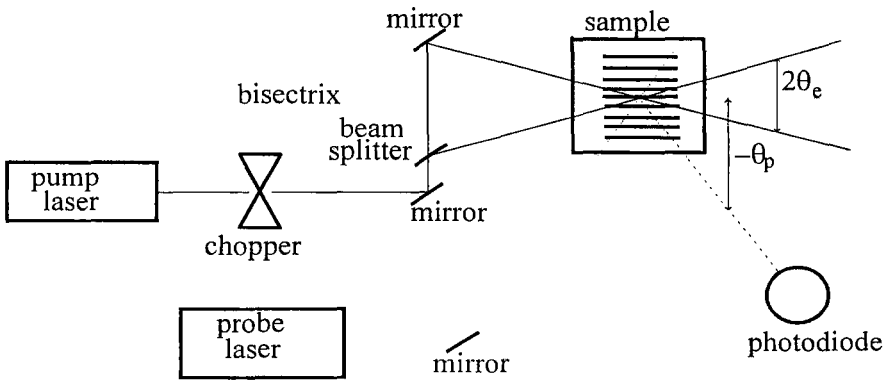

FIGURE 7. Thermal diffraction grating spectrophotometer. The laser beam from a modulated pump laser is splitted in two beams which are crossed within the sample causing a fringe interference pattern on the sample refractive index. This thermo-optical element diffracts the probe beam behaving as a diffracted grating. The intensity of the diffracted beam is measured by a photodiode.

coefficient (ε) and sample concentration (*C*) by:

$$\frac{I_d}{I_o} = \frac{8\pi}{3^{1/2}} \left[\frac{2.303 E_e (dn/dT) \epsilon C}{\rho c \omega_e \lambda_p \sin(2\theta_b)} \right]^2 \qquad (14)$$

The sample volume is defined by the pump and probe beams intersection like in crossed-beam thermal lenses. Hence, this volume can be very small and, consequently, the signal is independent of the real sample cell size. Equation 14 also shows an inverse and quadratic relationship between the true optical path (ω_e) and the interference signal. It also shows a quadratic relationship between the signal and pump beam energy (E_e) and the sample concentration (*C*), demonstrating the potential that thermal grating has as a high-sensitivity detection technique.

A minimum number of fringes (10 to 20) is necessary to obtain a signal intense enough. In practice, this makes sample volumes in thermal gratings (nL)

not as small as in crossed-beam thermal lens spectroscopy (pL). The instrumentation alignment in a thermal grating setup is more strict than in the other thermo-optical methods. Small alignment changes (in the order of one thousandth of degree) produce large signal variations.

The detection limits for this technique in static samples are in the range of 10^{-7} AU (34). However, to the best of our knowledge, this technique has not been applied in OTCLC or CE detection yet.

POTENTIALS AND LIMITATIONS OF THERMO-OPTICAL METHODS APPLIED TO OTCLC AND CE DETECTION

One of the thermo-optical detection problems limiting the technique sensitivity is the noise. The instability of the laser intensity (for continuous pump lasers normally used in Thermo-optical Spectroscopy approximately 1%) is the primary cause of this noise. This instability is two orders of magnitude larger than that of a good conventional (non-coherent) light source. The use of laser stabilizers reduces the laser noise up to 0.1 %. The two laser arrangements (for pumping and probing the sample) (16), and/or the use of reference channels to compensate the source fluctuations (35) can also reduce the noise.

The thermo-optical element dissipation due to the mobile phase flow which decreases the signal amplitude is another problem. The use of pulsed lasers (36,37), continuous lasers with high modulation frequencies (38), and focusing of the probe beam slightly down the pump beam (39), decrease the dissipation effect caused by the flow rate producing more intense signals .

A further limitation for using thermo-optical methods as routine detection in capillary separation techniques is associated with the small internal diameter of the capillaries used (40). This effect can originate a beam section deformation when it passes through the capillary, a beam deflection when it is not symmetrically focused on the capillary axis, and a complicated interference patterns if the beam size and the capillary i.d. are similar.

On the other hand, Thermo-optical Spectroscopy is a promising technique for OTCLC and CE detection despite only a few applications have been described in this field to date. Crossed-beam thermo-optical techniques are particularly promising for their high sensitivity (detection limit in the range of 10^{-9} AU), small probing volume (in the sub-picoliter range), and virtual non-path length dependence of the response. The sensitivity obtained by some thermo-optical techniques could allow the use of OTCLC and CE in trace analysis. However, thermo-optical methods are not yet being used on a routine basis for detection in capillary separation techniques. The pump lasers' high cost, the lack of tunable lasers in most of the UV range, and the skill required to design good thermo-optical setups, may be some of the reasons for the restricted use of these techniques. The progress in laser technologies nowadays (tunable lasers, diode lasers, etc.) will allow a more routinary use of thermo-optical methods as detection techniques in OTCLC and CE in a near future.

ACKNOWLEDGEMENTS

The authors thank DGICYT for granting project PB-88-034 on Capillary Electrophoresis Detection which has made this work possible.

GLOSSARY

A: sample absorbance.
C: analyte sample concentration.
c: sample specific heat capacity.
D: analyte diffusion coefficient.
d: fringe spacing in thermal grating spectroscopy.
E: response increment factor in thermal lens spectroscopy.
E_e: pump beam energy.
f: thermal lens focal distance.
I: probe beam intensity after passing through the thermo-optical element.
I_d: diffracted probe beam intensity in thermal grating spectroscopy.
I_{max}: signal maximum intensity in laser interferometry.
I_o: probe beam intensity prior to thermo-optical element formation.
I_s: signal intensity in laser interferometry.
I_t: probe beam intensity after passing through the thermo-optical element at

a given time t.
k: sample thermic conductivity.
l: sample cell thickness.
n: sample refractive index.
Δn: sample refractive index change.
P: laser beam power.
P_e: pump beam power.
r: position of any point anywhere in the beam referred to section center.
T: sample temperature.
ΔT: change in sample temperature.
t: time.
t_c: constant related to the thermo-optical element relaxation time.
x_o: distance between the pump and probe beam centers in thermal prism spectroscopy.
z_c: confocal distance; distance between the beam waist and the point for what beam section is double than beam waist section.
z_1: distance between the probe beam waist and beams' crossing point in crossed-beam thermal lens spectroscopy.
ε: sample absorption coefficient.
θ_b: Bragg's angle.
θ_e: angle between pump beams and their bisectrix in thermal grating spectroscopy.
θ_p: angle between probe beam and pump beams bisectrix in thermal grating spectroscopy.
λ: laser beam wavelength.
λ_e: pump beam wavelength.
λ_p: probe beam wavelength.
ν: pump beam modulation frequency.
ρ: sample density.
$\Delta\phi$: change in the probe beam phase in laser interferometry.
ψ: probe beam deflection in thermal prism spectroscopy.
ω: laser beam radius in the sample.
ω_e: pump beam radius in the sample.

REFERENCES

(1) M. Goto, T. Takeuchi and D. Ishii, Adv. Chromatogr., 30: 167 (1989).

(2) F. Foret, E. Szoko and B.L. Karger, J. Chromatogr., 608: 3 (1992).

(3) M. Merion, R.H. Aebersold and M. Fuchs, 3rd Int. Symp. on High Performance Capillary Electrophoresis, San Diego, 1991.

(4) R.L. Chien and D.S. Burgi, Anal. Chem., 64: 489A (1992).

(5) D.F. Swaile and M.J. Sepaniak, J. Liq. Chromatogr., 14: 869 (1991).

(6) E.S. Yeung, J. Chin. Chem. Soc., 38: 307 (1991).

(7) M. Yu and N.J. Dovichi, Anal. Chem., 61: 37 (1989).

(8) J.P. Gordon, R.C.C. Leite, R.S. Moore, S.P.S. Porto and J.R. Whinnery, J. Appl. Phys., 36: 3 (1965).

(9) J. Stone, J. Opt. Soc. Am., 62: 327 (1972).

(10) J. Stone, Appl. Opt., 12: 1828(1973).

(11) L. Skolnik, A. Hordvik and A. Kahan, Appl. Phys. Lett., 23: 477 (1973).

(12) A. Hordvik, Appl. Opt., 16: 2827 (1977).

(13) D.A. Cremers and R.A. Keller, Appl. Opt., 21: 1654 (1982).

(14) S.D. Woodruff and E.S. Yeung, Anal. Chem., 54: 1174 (1982).

(15) C.A. Carter and J.M. Harris, Anal. Chem., 56: 922 (1984).

(16) M.E. Long, R.L. Swofford and A.C. Albrecht, Science, 191: 183 (1976).

(17) N.J. Dovichi and J.M. Harris, Anal. Chem., 53: 106 (1981).

(18) R.A. Leach and J.M. Harris, J. Chromatogr., 218: 15 (1981).

(19) C.E. Buffett and M.D. Morris, Anal. Chem., 54: 1824 (1982).

(20) C.E. Buffett and M.D. Morris, Anal. Chem., 55: 378 (1983).

(21) M.J. Sepaniak, J.D. Vargo, C.N. Kettler and M.P. Maskarinec, Anal. Chem., 56: 1252 (1984).

(22) T. G. Nolan, W.A. Weimer and N.J. Dovichi, Anal. Chem., 56: 1704 (1984).

(23) N. J. Dovichi, T.G. Nolan and W.A. Weimer, Anal. Chem., 56: 1700 (1984).

(24) T. G. Nolan and N.J. Dovichi, IEEE Circuits Devices Mag., 2: 54 (1986).

(25) T.G. Nolan, B.K. Hart and N.J. Dovichi, Anal. Chem., 57: 2703 (1985).

(26) T.G. Nolan, D.J. Bornhop and N.J. Dovichi, J. Chromatogr., 384: 189 (1987).

(27) T.G. Nolan and N.J. Dovichi, Anal. Chem., 59: 2803 (1987).

(28) C.N. Kettler and M.J. Sepaniak, Anal. Chem., 59: 1733 (1987).

(29) S. Einarsson, S. Folestad, B. Josefsson and S. Lagerkvist, Anal. Chem., 58: 1638 (1986).

(30) P. Gozel, E. Gassmann, H. Michelsen and R.N. Zare, Anal. Chem., 59: 44 (1987).

(31) A.C. Boccara, D. Fournier, W.J. Jackson and N.M. Amer, Opt. Lett., 5: 377 (1980).

(32) W.B. Jackson, N.M. Amer, A.C. Boccara and D. Fournier, Appl. Opt., 20: 1333 (1981).

(33) T.W. Collette, N.J. Parekh, J.H. Griffin, L.A. Carreira and L.B. Rogers, Appl. Spectrosc., 40: 164 (1986).

(34) D.J. McGraw and J.M. Harris, J. Opt. Soc. Am., B 2: 1471 (1985).

(35) N.J. Dovichi and J.M. Harris, Anal. Chem., 51: 728 (1979).

(36) S.L. Nickolaisen and S.E. Bialkowski, Anal. Chem., 57: 758 (1985).

(37) S.L. Nickolaisen and S.E. Bialkowski, Anal. Chem., 58: 215 (1986).

(38) K.J. Skogerboe and E.S. Yeung, Anal. Chem., 58: 1014 (1986).

(39) W.A. Weimer and N.J. Dovichi, Anal. Chem., 57: 2436 (1985).

(40) A.E. Bruno, A. Paulus and J. Bornhop, Appl. Spectrosc., 45: 462 (1991).

(41) J.M. Harris, Optics News, oct: 8 (1986).

(42) B.G. Belenkii, J. Chromatogr., 434: 337 (1988).

Received: April 10, 1993
Accepted: August 2, 1993

JOURNAL OF LIQUID CHROMATOGRAPHY, 17(3), 521-532 (1994)

RAPID ASSAY FOR THE DETERMINATION OF TWO PHOTOACTIVATIBLE KAINIC ACID ANALOGUES BY HIGH-PERFORMANCE LIQUID CHROMATOGRAPHY

NIKOS K. KARAMANOS[1], EMMANUEL SIVVAS[2], AND DIONISSIOS PAPAIOANNOU[1]

[1]*Section of Organic Chemistry, Biochemistry, and Natural Products*
Department of Chemistry
[2]*Laboratory of Physiology*
Department of Medicine
University of Patras
26110 Patras, Greece

ABSTRACT

An anion-exchange isocratic high-performance liquid chromatographic method for the separation and determination of two kainic acid analogues, namely (2*S*,3*S*,4*S*)-4-[1-(4'-azidobenzoyl)aminomethylethenyl]-2-carboxy-3-pyrrolidineacetic acid and (2*S*,3*S*,4*S*)-4-[1-(4'-azidophenyl)thioureylenemethylethenyl]-2-carboxy-3-pyrrolidineacetic acid is described. These kainic acid analogues were obtained by coupling dimethyl (2*S*,3*S*,4*S*)-4-(1-aminomethylethenyl)-2-carboxy-1-(9-fluorenylmethoxycarbonyl)-3-pyrrolidineacetic acid with N-hydroxysuccinimidyl 4-azidobenzoate and 4-azidophenyl isothiocyanate respectively, followed by saponification. The thus obtained products were purified by reversed phase flash column chromatography and separated on Econosphere $-NH_2$, using 5% (v/v) acetonitrile in 50 mM acetate buffer pH 5.5, at a flow rate of 1.5 ml/min. The effect of mobile phase pH, and of the acetonitrile concentration on the

resolution between kainic acid and its analogues was also studied. Kainic acid was determined by using either low ultraviolet detection (190 nm) or the ninhydrin reaction. Detection of the eluted kainic acid analogues was performed at 215 nm. The detection limit is approximately 1.5 pmol for both kainic acid analogues and the calibration graphs were linear up to 100 nmol (approximately 50-μg).

INTRODUCTION

(−)-α-Kainic acid (KA, Figure 1), a natural product isolated from the marine alga *Digenea simplex*, exhibits powerful neuroexcitatory activity which is attributed to its interaction with specific populations of receptors of the major excitatory neurotransmitters of the mammalian central nervous system, glutamic and aspartic acids [1]. Despite considerable research efforts our knowledge on the molecular properties of these receptors is still far from complete. Since significant progress in the purification and characterization of receptors has been recently achieved using the technique of photoaffinity cross-linking [2], we synthesized KA analogues bearing photolabile moities in different positions of the parent molecule. The most promising of such analogues was found to be the [(2*S*,3*S*,4*S*)-4-[1-(4'-azidobenzoyl)aminomethyl-ethenyl]-2-carboxy-3-pyrrolidineacetic acid, abbreviated here as ABCPA [3]. Using the same methodology (2*S*,3*S*,4*S*)-4-[1-(4'-azidophenyl)thioureylenemethylethenyl]-2-carboxy-3-pyrrolidineacetic acid, abbreviated as ATCPA,

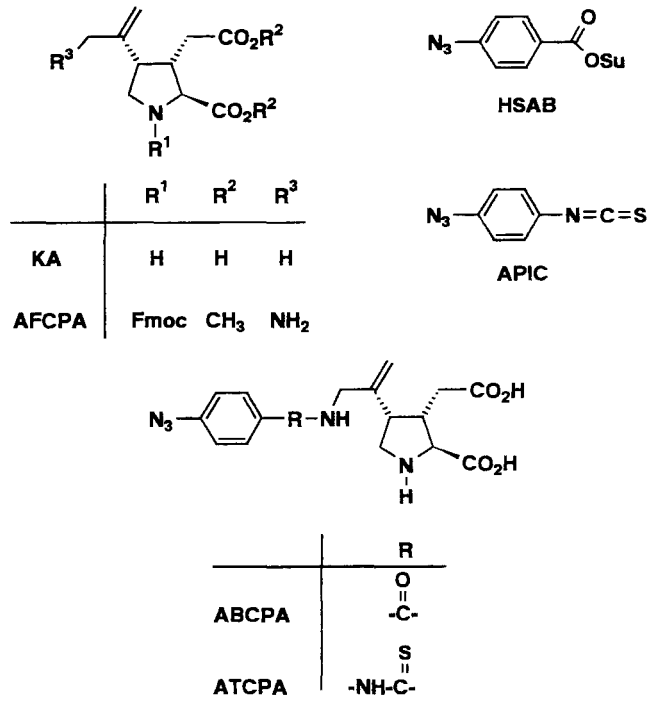

FIGURE 1. Structures of compounds encountered in this report.

was quite recently obtained as briefly described in the experimental part of the present report. Because both analogues showed a significant, but lower than KA itself, specificity for the afore mentioned receptors we decided to study the chromatographical behaviour of these analogues by HPLC against an authentic sample of KA in order to secure that their biological activity was not

simply due to the presence of free KA contaminating the synthesized samples.

In this paper we report an isocratic highly sensitive HPLC method in which both KA analogues ABCPA and ATCPA are completely separated from each other as well as from KA.

EXPERIMENTAL

Apparatus and Chemicals

For the determination of KA and its analogues a LDC system with an LDC III pump, a UV-vis detector LDC 1204A set at 215 or 190 nm with 8-µl flow cell and with a 20-µl loop injector was used. The analytical column is a Econosphere $-NH_2$ 5U, 5-µm, 250 x 4.6 mm I.D., stainless steel (Alltech, Deerfield, IL) equipped with an amino guard column, 30 x 4.6 mm I.D. (Brownlee Labs., Santa Clara, CA, U.S.A.).

KA, N-hydroxysuccinimidyl 4-azidobenzoate (HSAB), and 4-azidophenyl isothiocyanate (APIC) were obtained from Sigma Chemical Co. The KA analogues ABCPA and ATCPA were obtained by coupling KA derivative AFCPA (Figure 1) with HSAB and APIC respectively, followed by saponification which resulted in complete deprotection. AFCPA, bearing at nitrogen the commonly used in peptide synthesis 9-fluorenylmethoxycarbonyl (Fmoc) group, was obtained from KA by a multistep reaction sequence [3] involving as a

key-step, palladium mediated allylic amination [5]. The thus obtained KA analogues ABCPA and ATCPA were finally purified by reversed phase flash column chromatography [4] on RP-silica octadecyl silane (ODS) which was eluted with distilled water. Full experimental details for the preparation of ATCPA will be published elsewhere. Eluant components were HPLC-grade acetonitrile, obtained from Merck (Darmstadt, Germany) and glass-distilled water. All other chemicals used were of analytical reagent grade.

Chromatographic Conditions

The mobile phase used for the separation of KA analogues ABCPA and ATCPA was 5% (v/v) acetonitrile in 50 mM acetate buffer, pH 5.5. The flow rate was 1.5 ml/min and the pressure 1100 psi. The detection of both KA analogues was performed at 215 nm, whereas for KA at 190 nm. KA was also detected by post-column derivatization using the ninhydrin reaction. The separation was performed at room temperature. The eluent used was degassed by vacuum filtration through a 0.2-μm memrane filter followed by aggitation in an ultrasonic bath.

System Suitability

The column was equilibrated with mobile phase at flow rate of 1.5 ml/min. After a stable baseline was obtained, the standard solutions were injected into the column and the peaks appeared over the increased

TABLE 1

High-Performance Liquid Chromatographic Characteristics for the Determination of Kainic Acid and Photoactivatible Kainic Acid Analogues.

Compound	Retention Time/min (t_R)	Resolution (R_s)
KA	8.5	-
ABCPA	11.0	1.43
ATCPA	13.0	2.57 (1.22)

The resolution between ABCPA and ATCPA is given in parenthesis

retention time. The resolution factors, R_s, were calculated between the chromatographic peak of KA and each individual peak of the KA analogues from the equation $R_s = 2\ (t_2-t_1)/(W_1+W_2)$, where t_2 and t_1 are the retention times of the two peaks and W_1, W_2 are the peak widths at the base of the respective peaks. The resolution factors, R_s, were more than 1.2 indicating complete separation between KA and its analogues as well as between KA analogue ABCPA and ATCPA. This is illustrated in Table 1.

Selectivity

Chromatography of the samples of ABCPA and ATCPA, as obtained by their multistep synthesis from KA, showed no endogeneous interferences at the retention times of KA as

well as the respective times of analogues. This indicated that the proposed method could be used in the determination of both KA and its photoactivable analogues without the use of internal standard.

Detection Limit

The detection limits for the KA analogues were estimated as the quantity of these substances producing a signal of the peak height twice the baseline noice. The minimum detectable amount in pmol injected into the column was estimated to be 1.5 pmol (0.75 ng).

Standard Calibration Graphs

Both KA analogues tested were accurately weighed and dissolved in water to give stock solutions of 25 ng/µl each. Standard solutions of 1.0, 5.0, 12.5 and 10.0 ng/µl were prepared by serially diluting the stock solutions. Aliquots of 10-µl were taken for HPLC analysis. The calibration curves were constructed by plotting the peak heights of KA analogues against their concentrations.

RESULTS AND DISCUSSION

The retention times of KA and its analogues ABCPA and ATCPA were reproducible under the chromatographic conditions used with a relative standard deviation of less than 0.5%. The mobile phase used enabled a good column performance for long period of time. On the other

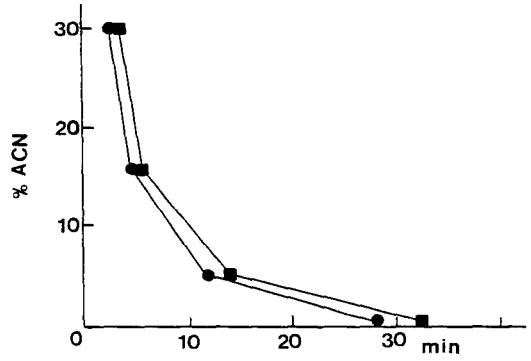

FIGURE 2. Influence of acetonitrile concentration on the retention times of KA analogues ABCPA (●) and ATCPA (■).

hand the KA analogues used were stable at least for several months when kept at 4^0C, under exclusion of light.

The presence of the organic modifier, acetonitrile, in mobile phase gave rise to heigher and more reproducible peaks than the aqueous phase alone thus improving the sensitivity and the accuracy of the described method [6]. As it is shown in Figure 2 the best resolution between the two KA analogues was obtained in concentrations of acetonitrile lower than 5% (v/v), whereas in higher acetonitrile concentrations both KA analogues were coeluted with KA. However, when the peak height were measured in the presence of acetonitrile, it was found that concentrations of more than 5% (v/v) gave heigher

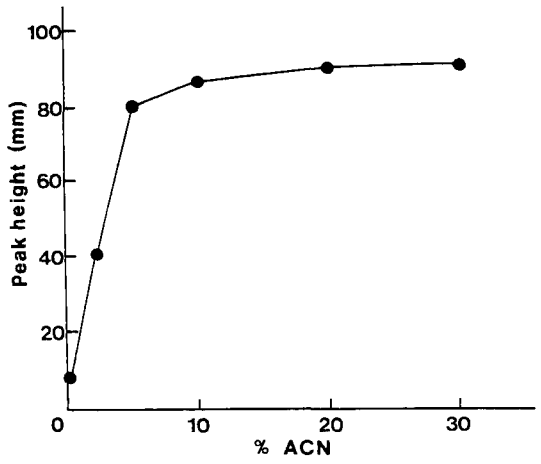

FIGURE 3. Influence of acetonitrile concentration on the peak heights of KA analogue ABCPA (●). The same curve was obtained for KA analogue ATCPA.

peaks (Figure 3). These results indicated that the optimum acetonitrile concentration to use for the separation of KA analogues was 5% (v/v). When pH of the aqueous mobile phase was ranged from 3 to 6 it was found that for pH values 3, 4 and 5 no resolution was obtained, whereas in pH 5.5 and 6 the resolution was complete (Figure 4). However, pH 5.5 was selected for the separation, because it gave the same resolution with pH 6.0 and moreover lower retention times.

Under these conditions, KA as well as its analogues ABCPA and ATCPA gave rise to single peaks (Figure 5A, B

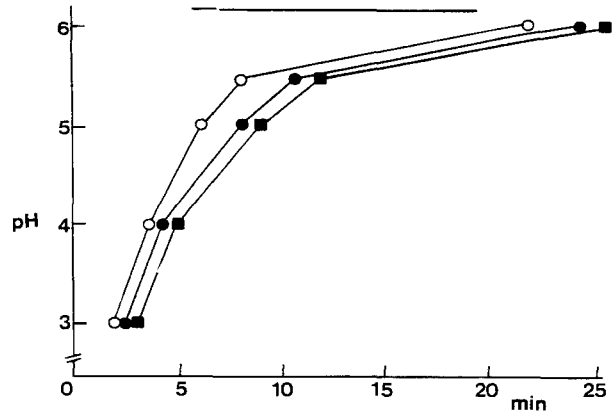

FIGURE 4. Effect of pH of the mobile phase on the retention times of KA (o), ABCPA (●) and ATCPA (■).

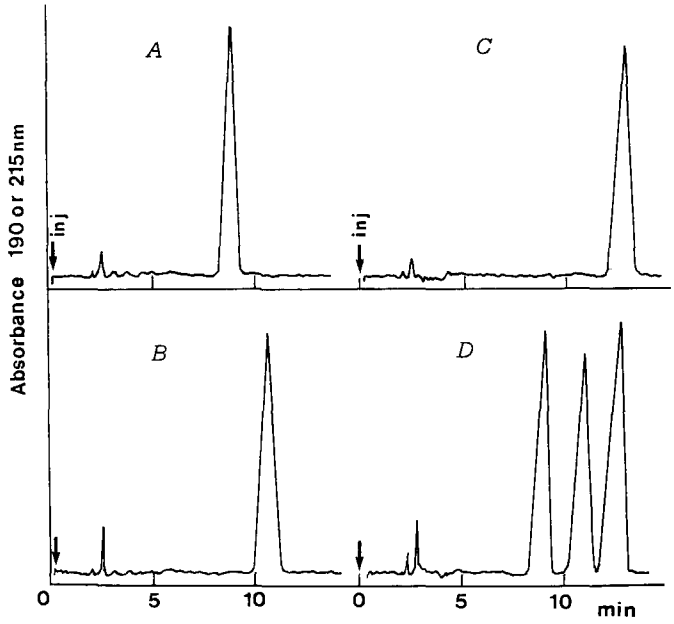

FIGURE 5. Typical HPLC chromatograms of KA (A), ABCPA (B), ATCPA (C) and a mixture of these three compounds (D). KA was detected at 190 nm or with the ninhydrin reaction, whereas the KA analogues were detected at 215 nm.

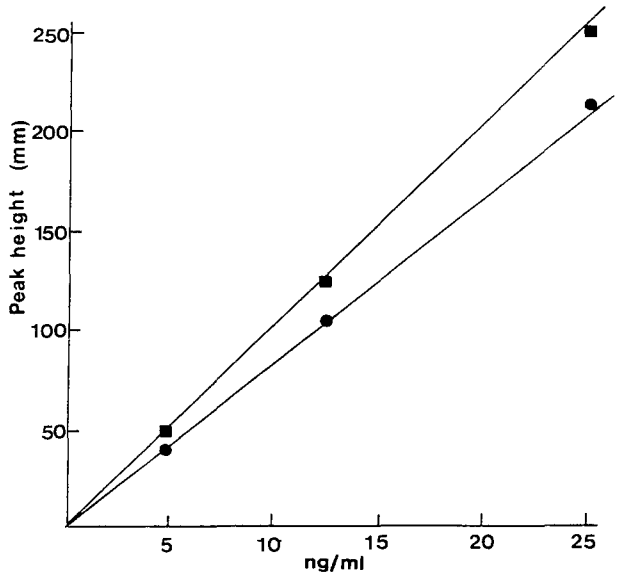

FIGURE 6. Calibration graphs obtained by injecting various amounts of ABCPA (●) and ATCPA (■).

and C). KA was widely separated from the two KA analogues (Figure 5D) in the $-NH_2$ column. Separate chromatographies of KA analogues ABCPA and ATCPA showed the absence of any KA contaminant (Figure 5B and 5C). The front peaks eluted before the compounts of interest were due to the buffer used for column elution (Figure 5).

The sensitivity and the linearity of the method were tested with the use of standard mixtures of various concentrations (Figure 6). The obtained peak heights for the compounds of interest were found to be linear related

to the concentration, up to 100 nmol, *i.e.*, when approximately 50-μg of each derivative injected into the column. The precision of the method was determined by six repeated determinations of each derivative. When 15 nmol of each KA derivative were measured, the relative standard deviation was 2.0% for ABCPA and 2.4% for ATCPA, and with 5 nmol the corresponding values were 2.6% and 3.1%, respectively.

REFERENCES

1.A. C. Foster, G. E. Fagg, Brain Research Reviews, 7: 103-164 (1984).

2. P. F. Pilch, M. P. Czech,"Affinity Cross-Linking of Peptide Hormones and thier Receptorsin in Receptor Biochemistry and Methodology: , J. C. Venter and L. C. Harrison eds., Allan R. Riss, New York, 1984, Vol. 1, pp 161-175.

3.E. Sivvas, G. Voukelatou, E. D. Kouvelas, W. G. Francis, D. W. Aksnes, D. Papaioannou, Acta Chem. Scand. Ser B, submitted for publication.

4.I. A. O'Neil, Synlett, 661-662 (1991).

5.B.M. Trost, Acc. Chem. Res. 13: 385-393 (1980).

6. N. K. Karamanos, Pharmakeftiki 5: 128-141 (1992).

Received: June 18, 1993
Accepted: June 30, 1993

JOURNAL OF LIQUID CHROMATOGRAPHY, 17(3), 533-548 (1994)

THE DETERMINATION OF CHARGE OF CATIONIC ^{99m}Tc-RADIOPHARMACEUTICALS

A. L. M. RILEY AND D. P. NOWOTNIK#
Amersham International plc
White Lion Road
Amersham, Bucks HP7 9LL, United Kingdom

ABSTRACT

Cation exchange HPLC methods for the determination of charge of cationic ^{99m}Tc-complexes were developed, based on a method described previously for anions. Non-specific retention of lipophilic complexes was reduced by the addition of acetonitrile. The method was validated using a number of metal salts, and was used to confirm the charges on several lipophilic technetium cationic complexes.

INTRODUCTION

The discovery that cationic, lipophilic ^{99m}Tc complexes demonstrate perfusion-dominated heart uptake in several species [1] has prompted extensive research into related compounds with properties suitable for planar and SPECT myocardial perfusion imaging in man [2]. Attempts have been made to develop structure-distribution relationships (SDRs) in order to identify compounds with optimum properties in a series [3], with the primary properties studied being lipophilicity and molecular weight. The

Author for correspondence. Present address: Bristol-Myers Squibb Pharmaceutical Research Institute, P.O. 4000, Princeton, NJ 08543-4000, U.S.A.

absolute charges of complexes will also have a profound influence on their biodistribution, but this has not been the subject of a systematic study

The majority of cationic technetium complexes prepared and studied as potential myocardial perfusion tracers belong to the group termed "technetium-essential" [4]. For these complexes, the overall charge results from the difference between the oxidation state of technetium and the number of negative charges generated on the ligand(s) as a result of metal complexation. As technetium has a wide variety of available oxidation states and coordination numbers/geometries [5,6], it is often difficult to predict the net charge of a complex from knowledge of its ligand structure. As most ^{99m}Tc preparations are at concentrations of $10^{-6}M$, or less, the charge of a ^{99m}Tc complex is usually assigned from knowledge of the structure of its ^{99}Tc counterpart [7]. Ideally, the charge on ^{99m}Tc complexes should be determined directly from measurements of these complexes, as the chemistry of ^{99m}Tc complexes cannot be predicted with certainty from knowledge of the ^{99}Tc chemistry [5,6].

We recently described an HPLC method for the determination of charge of anionic complexes [8], which was based upon methods described previously [9-11]. The method involved anion exchange chromatography, and the net charge of an anionic complex was determined from a relationship which links retention time with the aqueous eluent competing ion activity. In this procedure, the observed retention time had to be corrected for the system dead-time (R_0) and for any retention of the complex due to mechanisms other than ion-exchange (R_C).

We now report on studies to adapt the method for anion charge determination for the determination of charge of cationic complexes. Several cation-exchange columns were examined for this purpose, and the Partisil and TSK SCX columns were selected for further study. Using these columns, the charge determination method was validated by the determination of charges of uncomplexed metal ions, and the HPLC systems are used to determine the charges on previously reported technetium DMPE [12] and TBI [13,14] complexes. The charges on several new technetium complexes were also determined.

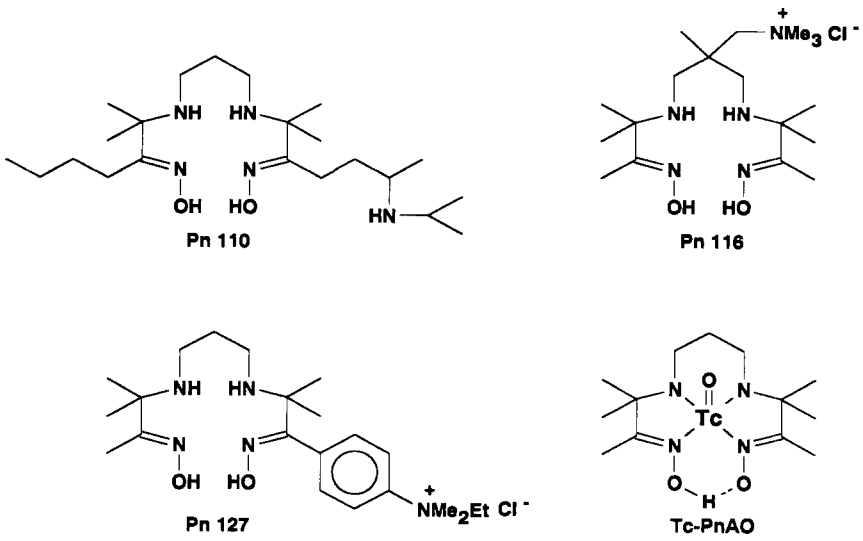

a. Structures of the PnAO ligands and Tc-PnAO

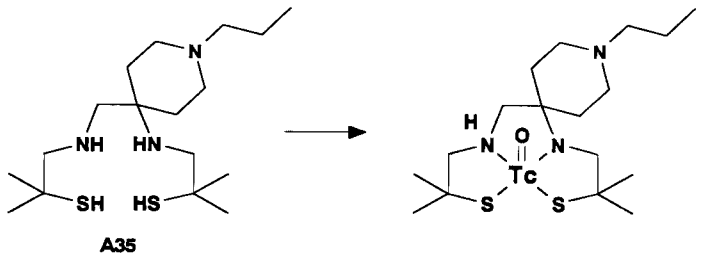

b. Structure of the ligand A35, and its technetium complex

Figure 1. Structures of the PnAO and DADT ligands, and their ^{99m}Tc complexes.

These were based on the ligands PnAO [15] and DADT [16] (which form neutral technetium complexes) in which the ligand is derivatized with a cationic group. The structures of these ligands are shown in figure 1.

EXPERIMENTAL

Theory

In our studies on the chromatographic determination of the charge of anions [8] by anion exchange HPLC, the following relationship was used

$$\log (R_i) = \text{constant} - \frac{m}{a} \log (A) \qquad \text{---------- (1)}$$

where R_i is the corrected retention time ($R_i = R_t - (R_o + R_c)$; R_t is the observed retention time, and R_c and R_o are as described, above) and A is the activity of the competing ion, m is the charge of the test compound, and a is the charge of the competing ion in the mobile phase. The charge on the test compound was determined by plotting log (R_i) against log (A) by measuring R_t over a range of competing ion concentrations, and applying corrections for R_o and R_c. The slope of this linear plot equals the ratio of charges carried by the test compound and the eluate competing ion. The relationship in equation 1 is also valid for the behaviour of cations in cation exchange chromatograqphy. In this study, a variety of cation exchange column/competing ion combinations were examined for the determination of the charge of cations. R_o was determined by using a non-retained marker, while R_c was minimised by the addition of an organic modifier to the eluent.

Materials

A preliminary investigation was conducted using a number of cation exchange columns, as summarised in table 1.

Table 1. Preliminary evaluation of candidate Strong cation exchange (SCX) columns

Column	Retention mechanisms*	Base	Solvent compatability	Comments
TSK SCX	Strong hydrophobic	copolymer	Wide tolerance to buffer types, pH, and organic solvents	Only useful with an organic modifier. Its high hydrophobicity limits compounds to low (<2) log P values
TSK SP5PW	Moderately hydrophobic	polymer	- ditto -	- ditto -
MONO-S	Moderately hydrophobic	Hydrophilic polymer	- ditto -	- ditto -
Waters ion column	very high hydrophobic	polymer	- ditto -	Hydrophobicity gives excessive R_f values.
AMINEX	Strong hydrophobic	polmer	High back pressure	Unpredicatable performance
Partisil	Low hydrophobicity. Possible interference from free silanols	silica	Best competing ion is NH_4^+. pH 2.5-8.0. Good tolerance to organic modifiers	Organic modifier required for lipophilic cations, but R_f can be reduced to negligible values by using a modifier.

Aqueous solutions containing K^+ and NH_4^+ as competing ions were prepared as the mobile phases for the validation of the method using metal cations. Ammonium hydroxide or potassium hydroxide was dissolved in HPLC grade water, and the pH was adjusted to pH 7.4 with glacial acetic acid. The solution was then diluted to the required maximum competing ion strength. For the studies involving aqueous acetonitrile HPLC mobile phases, solutions were prepared as described above, using a mixture of either 30:70 or 70:30 acetonitrile/water. Solvents were degassed and filtered prior to use.

Solutions of the radioactive metal cations (^{201}Tl(I), ^{24}Na(I), ^{54}Mn(II)), used to validate the HPLC systems, were obtained from Amersham International plc.

Dimethylphosphinoethane (DMPE) was obtained from Lancaster Synthesis. t-Butylisonitrile (TBI) was synthesized in-house by the reported method [14]. The ligands Pn110, Pn 116, Pn 127 and HM-PAO were synthesized in-house, using methods

based on those described elsewhere [17-20]. Formation of the ^{99m}Tc-complexes of these ligands follows the procedures described previously for the formation of ^{99m}Tc-PnAO complexes [15,21]. The ^{99}Tc(I)(DMPE)$_3$, $^{99/99m}$Tc(III)(DMPE)$_2$Cl$_2$ and $^{99/99m}$Tc(V)O$_2$(DMPE)$_2$ complexes were prepared by methods similar to those described previously [22-24]. The synthesis and technetium labeling of the ligand A35 were described elsewhere [25].

Chromatographic Procedure

A two-pump Gilson system (controlled by an Apple IIe with Gilson 702/3 software) was used in conjunction with a Rikadenki chart recorder, Gilson 802 manometric module and an Anachem mixer. A Gilson Holochrome UV/visible detector was fitted for detection of Co(II) (540nm) and ^{99}Tc samples (280 nm), while a radioisotope detection system (Mini-instrument gamma scintilation detector and ESI 5140 ratemeter) was used for the detection of all other radioactive samples. A third pump was used for automatic sample injection. Peripheral equipment were automated with the aid of a Gilson 501 contact module plus AC accessory, controlled by the 702/3 software. Sample retention times were provided by the system software.

The determination of system dead times (R_0) and estimation of R_C

The system dead-times (R_0) of the TSK and Partisil SAX columns were determined using nitrate. As the main contributor to R_C (the portion of substrate retention by mechanisms other than ion exchange) on the polymer column is likely to be hydrophobic, the retention of a series of neutral, lipophilic compounds (benzyl alcohol, benzaldehyde, nitrobenzene, benzene) were determined. The lipophilicities (Log P values) of these compounds were obtained from the MedChem database [26].

Procedures for charge determination

As the majority of cations examined were radioactive, standard procedures and precautions were used for the safely handling of these materials. Solutions (2-10mL) containing the radioactive cations were contained in a sealed 10mL vial, encased within a lead container. Vials were stoppered with a rubber septum, and sealed with a metal fitting. The vial was vented with a hypodermic needle, and connected via a six inch length of narrow bore PTFE tubing, pushed through a pucture in the septum, to the injection pump of the HPLC system. Automatic sample injection was controlled by the system software.

Either a TSK or Partisil SCX column was used with a mobile phase containing either K^+ or NH_4^+ as the competing ion. A mobile phase containing no organic modifier was used with metal ions to validate the system. The use of an organic modifier (to reduce non-specific retention) was validated by the determination of charge of ^{201}Tl using mobile phases composed of 30:70 and 70:30 acetonitrile: water. The charges on several $^{99m/99}$Tc-complexes were determined using a mobile phase based on 30:70 acetonitrile: water. An appropriate maximum competing ion concentration for a given test compound was selected by some preliminary studies, and this was selected as solvent 'A' for the HPLC system. Solvent 'B' was either water (for the 100% aqueous system) or the same acetonitrile/water mixture as used for solvent 'A'. All measurements of solute retention time were conducted with isocratic elution using predetermined proportions of solvents 'A' and 'B', at a flow rate of 1 mL/min, unless stated otherwise. Columns were equilibrated with the desired mobile phase prior to the start of the determination. Details of the column and mobile phase used with individual test compounds are given in the results section.

Observed retentions times were corrected for system dead time. The competing ion activities were determined from published data [27,28], shown in table 2. Using these

Table 2. Cation activities for the mobile phases used in this study

	Cation activities				
% A	KOAc 1M	NH_4OAc 0.1M	KOAc 1.1M	KOAc 0.07M	NH_4OAc 0.07M
100	0.7810	0.0800	0.8690	0.0700	0.0581
75	0.5700	0.0619	0.6353	0.0525	0.0444
50	0.3750	0.0425	0.4136	0.0350	0.0305
25	0.1886	0.0221	0.2076	0.0175	0.0158
10	0.0800	0.0092	0.0869	0.0070	0.0065

data, linear regression analyses were performed using a programmed Casio FX 300 calculator of $\log_{10}$ (activity) vs $\log_{10}$ (corrected retention volume), from which the charges of the test substrates were determined using equation 1.

RESULTS AND DISCUSSION

Preliminary evaluation of columns and competing ions

The basis for the HPLC method reported previously [8] for the determination of charge of anions was that retention due to mechanisms other than ion-exchange (R_c) and the system dead-time (R_o) should remain constant in determinations involving only a change in competing ion activity (A). Therefore, from equation 1, the relationship between log (R_t) and log (A) will be curvilinear, but it will convert to a linear relationship by subtracting a value from all observed R_ts which equals R_c and R_o. An iterative method was used to obtain the optimum linear relationship between $\log(R_t - x)$ vs log(A). The slope of this plot provided the charge of the anion.

While equation 1 will be applicable to the determination of charge of cations by cation exchange HPLC, the method developed previously for anion charge determination may not be suitable (when converted to an analogous cation exchange system) for the

highly lipophilic cations which have been studied as myocardial perfusion tracers. By using a purely aqueous eluent (as was the case in the anion charge method [8]), there is the possibility that $R_C >> R_i$ (particularly at low competing ion concentrations) for the more lipophilic compounds in this study. High R_C values reduce the precision in charge determination, as was indicated by the determination of charge of the moderately lipophilic Tc-EHIDA complex [8]) and observed by others [29]. Therefore, we decided to employ an alternative strategy. This relied upon the addition of an organic modifier to the eluent in sufficient quantities to minimise the contribution of hydrophobic interactions to R_C. We did not conduct a systematic study to select the most appropriate organic modifier; acetonitrile was selected as it appeared to have little effect on the activity coefficient of the chosen competing ion and it had previously been used successfully as the organic modifier in an HPLC method for the determination of pK_a of technetium chelates [30]. The column dead-time (R_O) was determined using a non-retained marker (nitrate). Thus, R_i could be determined directly from measurements of retention time.

While there are many possible choices for competing ion, K^+ or NH_4^+ were favoured as they have moderate-to-good solubility with common anions, and activity coefficients were known (table 2). Preliminary studies demonstrated that they generally provided a suitable range of retention times with test cations. In addition, the NH_4^+ competing ion suppresed tailing in amine-containing ligands on the silica-based columns.

The summary of the preliminary evaluation of columns for charge determination are shown in table 1. The columns evaluated were restricted to the strong cation exchange (SCX) type, based on sulphonic acids, as the weak exchange systems are generally based on carboxylic acids, a functional group which might give rise to metal retention through coordination. The primary variable in this evaluation is the column base, and columns with polymer, resin, and silica bases were included in the study. Our intial preference was the polymer base. Underivatised polymer-based columns have been

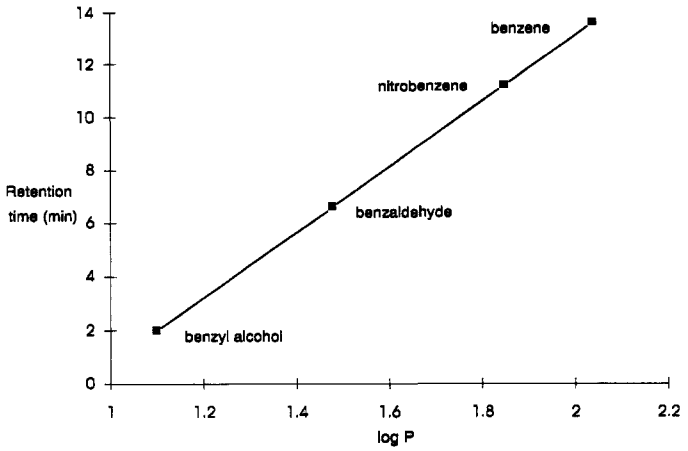

Conditions: TSK SCX (15 x 0.5 cm) column, eluted with 0.1M NH_4OAc in acetonitrile-water (30:70) at 1 mL/min, ambient temperature.

Figure 2. The retention on the TSK SCX column of neutral, lipophilic compounds.

used, for example, for the determination of lipophilicity, as their mode of retention is almost exclusively hydrophobic [31,32]. Thus, we felt that an SCX column with a polmer base will have hydrophobicity as the sole contributor to R_C, which might be eliminated through the use of a organic modifier. However, we found that for the polymer and resin SCX columns hydrophobic interactions remain a problem. Figure 2 shows the relationship between retention times and lipophilicity (log P) of some neutral compounds on the TSK SCX column. These data demonstrate that even for moderately lipophilic compounds, hydrophobic retention is likely to be a major contributor to R_C for polymer and resin-based columns, so these columns may be suitable only for the determination of charge of relatively hydrophilic compounds.

Inorganic cations

Initial validation of the technique was performed by analyses on simple inorganic cations. Unipositive and bipositive ions ($^{24}Na^+$, $^{201}Tl^+$, $^{54}Mn^{2+}$, Co^{2+}) were

Table 3. Observed retention volumes and determined charges for the inorganic cations

	Retention volumes (mL)						
Column	TSK	TSK	TSK	TSK	SCX	SCX	SCX
Cation	Tl-201	Na-24	Mn-54	Co^{2+}	Tl-201	Tl-201	Tl-201
Eluate (A)	1M K^+ aqueous	1M K^+ aqueous	1.1 K^+ aqueous	1M K^+ aqueous	0.1M NH_4^+ aqueous	0.1M NH_4^+ 30% ACN	0.1M NH_4^+ 70% ACN
% A :							
100	24.6	10.6	67.5	36.0	9.0	9.3	7.8
75	34.0	21.0	93.0	54.0	11.1	11.7	9.6
50	58.3	33.0	200.0	100.8	14.4	17.1	14.4
25	-	58.0	-	-	27.0	33.6	28.8
10	-	-	-	-	67.8	80.4	75.0
charge	1.16	1.04	2.18	2.10	0.95	1.02	1.07

investigated using 100% aqueous mobile phases. Co^{2+} was detected by UV absorption (550nm), while the other ions were detected by their γ-emissions. Detection of ^{54}Mn proved difficult, because of the high energy of its γ-photon (840 keV). Results of these studies are shown in table 3. The calculated values of cation charges were in good agreement with the expected values.

To validate the use of acetonitrile as a mobile phase modifier, studies with $^{201}Tl^+$ were extended to include the use of the acetonitrile/water (3:7 and 7:3) mobile phases. These results are shown in table 3. The determined charge is essentially unaffected by the use of the organic modifier, indicating that competing ion activity is unaltered by the use of acetonitrile in the mobile phase. For the remaining studies, an acetonitrile/water ratio of 3:7 was selected. This proportion of organic modifier appeared to be adequate to minimize the contribution of R_C to overall retention for the majority of the cations studied.

Technetium-chelates

Charge determinations were conducted on a series of known "technetium-essential" cations, and cationic derivatives of Tc-PnAO and Tc-DADT complexes. These studies were conducted on the Partisil SCX and TSK-styrene-SCX columns with mobile phases

Table 4 Observed retention volumes and determined charges for the "technetium-essential" cations

	Retention volumes (mL)						
Cation	^{99m}Tc BIN	^{99m}Tc BIN	$^{99}Tc(I)$ DMPE	$^{99}Tc(V)$ DMPE	$^{99m}Tc(V)$ DMPE	$^{99m}Tc(III)$ DMPE	$^{99}Tc(III)$ DMPE
% A:							
100	n/d	n/d	3.6	44	40	7.2	4.0
75	1.8	3.9	5.2	56	56	9.0	8.0
50	6.0	6.0	8.0	80	82	12.6	13.2
25	9.9	10.5	15.6	150	154	22.6	24.8
10	22.2	23.4	39.2	n/d	n/d	48.8	57.2
charge	1.20	0.93	1.08	0.98	1.04	0.90	1.17

In all cases, the column is Partisil SCX, and eluate (A) is 0.1M NH_4OAc in 30% ACN
n/d = not determined.

Table 5. Observed retention volumes and determined charges for the ^{99m}Tc-PnAO and DADT complexes.

	Retention volumes (mL)				
Column	SCX	SCX	SCX	TSK	TSK
Cation	Tc-A35	Tc-Pn110	Tc-Pn110	Tc-Pn116	Tc-Pn127
Eluate (A)	1M K^+	0.07M K^+	0.07M K^+	1M K^+	1M K^+
% A :					
100	3.60	5.40	6.60	2.40	5.70
75	6.00	6.90	7.50	3.00	7.10
50	7.20	9.45	11.40	4.50	10.20
25	12.60	18.00	20.10	8.25	18.30
10	26.40	43.80	49.80	19.35	44.00
charge	0.93	0.96	0.94	0.94	0.92

containing 30% acetonitrile. The results for the technetium-essential cations are given in table 4; those for PnAO and DADT complexes are given in table 5. In general, the calculated charges on all complexes were in good agreement with the expected values.

The ^{99m}Tc PnAO complexes derivatised with either amine or quaternary ammonium substituents provided sharp chromatograms on the silica-based column when eluted with a mobile phase containing NH_4^+. ^{99m}Tc HM-PAO [33], a neutral ^{99m}Tc

PnAO complex was also studied to examine non-specific retention. This complex displayed very slight (approximately 1 mL) retention which was independent of mobile phase competing ion concentration. Thus, this HPLC technique provided no evidence of charge in a metal complex known to be neutral.

Of the technetium-essential cations, only ^{99m}Tc(I) $(dmpe)_3$ demonstrated little non-specific retention. Poor peak shapes were observed for the highly lipophilic cation ^{99m}Tc(I) $(TBI)_6$, indicating either instability or some non-specific interaction. The ^{99m}Tc(V)O_2 $(dmpe)_2$ complex showed considerable non-specific retention. These observations suggest that there is a strong interaction between the TcO_2 metal core and the silanol-based column, as noted previously for this complex [12]. The ^{99m}Tc(III)Cl_2 $(dmpe)_2$ complex displayed intermediate retention, also indicating some interaction between the metal core and free silanol groups. The ^{99}Tc-counterparts of the Tc(V) and Tc(III) dmpe complexes were also examined; the observed retention times for the ^{99}Tc-complexes were similar to the corresponding ^{99m}Tc-complexes, providing additional evidence that the complexes are the same at both concentration levels.

CONCLUSIONS

The absolute charge of cations can be determined readily using a simple HPLC method based on SCX columns. Both the Partisil (silica-based) and TSK (polymer-based) SCX proved to be satisfactory for this purpose, although both columns demonstrated some limitations. The Partisil column should be avoided for test compounds subject to strong interactions with free silanols, while the hydrophobic base of the TSK column may place a limit on its use when examining hydrophobic cations. Through the use of an organic modifier to reduce or eliminate column retention (R_c) due to mechanisms other than ion-exchange, the charge on test compounds could be determined directly from retention data, eliminating the need for an interative approach [8] to correct for R_c. The method confirmed the charge on several "technetium-essential"

cations reported previously, and was used to verify the charge on several new technetium complexes.

ACKNOWLEDGEMENTS

The authors wish to thank Drs. S.A. Cumming, J. Cummins, and L.R. Canning for the syntheses of the TBI and the PnAO ligands, and Dr. D.V. Griffiths for the synthesis of A35.

REFERENCES

1. E. Deutsch, K. A. Glavan, V. J. Sodd, H. Nishiyama, D. L. Ferguson, S. J. Lukes, J. Nucl. Med., 22: 897-907 (1981)
2. D. P. Nowotnik, A. D. Nunn, Drug News & Perspectives, 5: 174-183 (1992)
3. D. P. Nowotnik, "Quantitative structure-distribution relationships (QSDRs) of radiopharmaceuticals," in Radiopharmaceuticals: Using radioactive compounds in Pharmaceutics and Medicine, A. E. Theobald (ed.), Ellis Horwood Ltd., Chichester, 28-56 (1989)
4. G. Subramanian, J. G. McAfee, R. F. Schneider, "Structure/distribution relationship in the design of Tc-99m radiopharmaceuticals," in Safety and efficacy of radiopharmaceuticals, K. Kristensen, E. Norbygaard (eds.), Martinus Nijhoff Publishers, Boston, 5-43 (1984)
5. E. Deutsch, K. Libson, S. Jurisson, L. F. Lindoy, "Technetium chemistry and technetium radiopharmaceuticals," in Progress in Inorganic Chemistry, S. J. Lippard (ed.), J.Wiley & Sons, Inc, New York, 75-139 (1983)
6. J. Steigman, W. C. Eckelman, The Chemistry of Technetium in Medicine, National Academy Press, Washington, D.C., 1992.
7. S. Z. Lever, H. N. Wagner, "The status and future of technetium-99m radiopharmaceuticals," in Technetium and rhenium in chemistry and nuclear medicine 3, M. Nicolini, G. Bandoli, U. Mazzi (eds.), Cortina International, Verona, Italy, 649-659 (1990)
8. D. P. Nowotnik, A. L. M. R. Riley, J. Liq. Chromatogr., 15: 2165-2174 (1992)
9. A. Owunwanne, J. Marinsky, M. Blau, J. Nucl. Med., 18: 1099-1105 (1977)
10. C. D. Russell, R. C. Crittenden, A. G. Cash, J. Nucl. Med., 21: 354-360 (1980)
11. G. M. Wilson, T. C. Pinkerton, Anal. Chem., 57: 246 (1985)

12. E. A. Deutsch, A. R. Ketring, K. Libson, J.-L. Vanderheyden, W. W. Hirth, Nucl. Med. Biol., 16: 191-232 (1989)

13. M. J. Abrams, A. Davison, A. G. Jones, C. E. Costello, H. Pang, Inorg. Chem., 22: 2798-2800 (1983)

14. B. L. Holman, A. G. Jones, J. Lister-James, A. Davison, M. J. Abrams, J. M. Kirshenbaum, S. S. Tumeh, R. J. English, J. Nucl. Med., 25: 1350-1355 (1984)

15. W. A. Volkert, T. J. Hoffman, S. M. Seger, D. E. Troutner, R. A. Holmes, Eur. J. Nucl. Med., 9: 511-516 (1984)

16. H. F. Kung, M. Molnar, J. Billings, R. Wicks, M. Blau, J. Nucl. Med., 25: 326-332 (1984)

17. D. E. Troutner, W. A. Volkert, Eur. Pat. Appl. 84302615.4 (1984)

18. L. R. Canning, D. P. Nowotnik, Eur. Pat. Appl. 179,608 (1984)

19. G. Nechvatal, L. R. Canning, S. A. Cumming, D. P. Nowotnik, R. D. Neirinckx, R. D. Pickett, R. A. Holmes, D. E. Troutner, W. A. Volkert, "New derivatives of Tc-99m PnAO as potential regional cerebral blood flow agents," in Technetium in chemistry and nuclear medicine 2, M. Nicolini, G. Bandoli, U. Mazzi (eds.), Cortina International, Verona, Italy, 193-196 (1987)

20. S. A. Cumming, I. M. Piper, J. F. Burke, B. Higley, A. McQuitty, D. P. Nowotnik, J. Nucl. Med., 29: 934 (1988)

21. D. E. Troutner, W. A. Volkert, T. J. Hoffman, R. A. Holmes, Int. J. Appl. Radiat. Isotop., 35: 467-470 (1984)

22. H. Nishiyama, E. Deutsch, R. J. Adolph, V. J. Sodd, K. Libson, E. L. Saenger, M. C. Gerson, M. Gabel, S. J. Lukes, J.-L. Vanderheyden, D. L. Fortman, K. L. Scholz, L. W. Grossman, C. C. Williams, J. Nucl. Med., 23: 1093-1101 (1982)

23. M. C. Gerson, E. A. Deutsch, K. F. Libson, R. K. Adolph, A. R. Ketring, J.-L. Vanderheyden, C. C. Williams, E. L. Saenger, Eur. J. Nucl. Med., 9: 403-407 (1984)

24. J. L. Vanderheyden, A. R. Ketring, K. Libson, M. J. Heeg, L. Roecker, P. Motz, R. Whittle, R. C. Elder, E. Deutsch, Inorg. Chem., 23: 3184-3191 (1984)

25. D. V. Griffiths, D. J. Tonkinson, J. F. Burke, B. Higley, J. D. Kelly, "Synthesis of complexes of ^{99m}Tc possessing cationic substituents for evaluation as myocardial imaging agents," in Technetium and rhenium in chemistry and nuclear medicine 3, M. Nicolini, G. Bandoli, U. Mazzi (eds.), Cortina International, Verona, Italy, 353-364 (1990)

26. MedChem cLogP Program, v 3.4.2., Day Light Chemical Information Systems, Irvin, CA

27. Handbook of Chemistry and Physics, CRC Press,, 1984-1985.

28. G. Lang, Handbook of Chemistry, McGraw Hill,, 1966.

29. A. E. Theobald, personal communication

30. C. Stylli, A. E. Theobald, Int. J. Appl. Radiat. Isotop., 38: 701-708 (1987)

31. A. Belchalanay, T. Rothlisberger, N. El Tayar, B. Testa, J. Chromatogr., 473: 115-124 (1989)

32. D. P. Nowotnik, T. Feld, A. D. Nunn, J. Chromatogr., 630: 105-115 (1993)

33. R. D. Neirinckx, L. R. Canning, I. M. Piper, D. P. Nowotnik, R. D. Pickett, R. A. Holmes, W. A. Volkert, A. M. Forster, P. S. Weisner, J. A. Marriott, S. B. Chaplin, J. Nucl. Med., 28: 191-207 (1987)

Received: July 13, 1993
Accepted: August 5, 1993

JOURNAL OF LIQUID CHROMATOGRAPHY, 17(3), 549-558 (1994)

EFFECTS OF INJECTION SOLVENTS ON THE SEPARATION OF PORPHYRIN AND METALLOPORPHYRIN IN REVERSED-PHASE LIQUID CHROMATOGRAPHY

JOHN W. HO* AND LEE YUEN FUN CANDY
Department of Applied Biology and Chemical Technology
Hong Kong Polytechnic
Hung Hom
Hong Kong

ABSTRACT

This study reports differences in the chromatographic behavior of protoporphyrin and zinc protoporphyrin in reversed-phase liquid chromatography. The retention parameters of individual porphyrins using different mobile phases and a reversed-phase column were compared. Various solvents were used to dissolve protoporphyrin and zinc protoporphyrin. The solvent effects on the retention characteristics of the porphyrin and metalloporphyrin were studied. The elution order of porphyrins on the reversed-phase column was predictable. In contrast, the elution of zinc protoporphyrin could be significantly changed or reversed with respect to protoporphyrin peak, when a strong base was used as an injection solvent. Also, the retention times of protoporphyrin and zinc protoporphyrin were shifted significantly with different injection solvents. The shifting in retention time of zinc protoporphyrin is more noticeable, and the protoporphyrin peak is remarkably broadened with more basic solvents. The solubility of protoporphyrin and zinc protoporphyrin varies considerably with the injection solvents tested.

INTRODUCTION

Porphyrins are the common tetrapyrrole compounds found in biological materials. Polycarboxylated porphyrins are the intermediary metabolites of heme biosynthesis.

* Corresponding author, visiting H.K. from Utah

Through the continuous decarboxylation of the first uroporphyrinogen III, different porphyrins are formed. Cobyrinic acid, a known precursor of vitamin B_{12} , is biosynthesized from uroporphyrinogen III by a multistep process (1). Protoporphyrinogen IX which is formed by decarboxylation of coproporphyrinogen III. Chelates with iron (II) form heme or hematin if the iron is in the ferric state. Heme and hematin are the most important molecules biochemically. Heme serves as coenzyme for proteins involved in the transfer of oxygen from one site in the organism to another, for enzymes catalyzing a variety of oxidation reactions, and for enzymes catalyzing the cleavage of peroxides. An example includes human hemoglobins, a class of proteins of distinct molecular structure that perform the important function of transporting oxygen from the lungs to various tissues in the body in which oxidative metabolism occurs. Porphyrins also form metal chelates with a variety of metal ions, including those of magnesium, iron, zinc, nickel, cobalt, copper and silver. In such chelates, the metal ion lies in the center of the porphyrin nucleus, four of its ligand sites being occupied by the pyrrole nitrogen atoms. For example, chlorophyll, a magnesium chelate of a substituted porphyrin, is intimately involved in the photosynthetic process. In human lead poisoning and iron-deficiency anemia, protoporphyrin chelates with zinc ions and is present as zinc protoporphyrin in biological tissues (2-3). Analysis of excreted intermediary metabolites of heme biosynthesis and of zinc protoporphyrin is useful as a test for lead poisoning and iron deficiency anemia, and to determine the effect of environmental intoxification on heme biosynthesis.

Determinations of different porphyrins have been reported. In recent years, high performance liquid chromatography (HPLC) has become the preferred technique. In particular, reversed-phase HPLC is more efficient and allows quantitative determination of porphyrins. Three variables characterizing the mobile phase composition, pH, elution

strength and ionic strength for the separation of porphyrins using reversed-phase column, have been studied previously (4-5). The chromatographic behavior of metal-free porphyrins is well characterized. The retention increases as the number of side-chain alkyl substituents increases. Thus, the elution order of porphyrins follows the polarity in reversed-phase liquid chromatography. On the other hand, the chromatographic behavior of metalloporphyrin is not fully understood. Although the determination of metalloporphyrins have been reported previously (6-7), the effects of injection solvents on porphyrins have not been studied.

The present paper describes a reversed-phase HPLC method with a photodiode array UV detector for the study of the chromatography of protoporphyrin and zinc-protoporphyrin. The mobile phase composition and various injection solvents are used to examine the separation performance of protoporphyrin and zinc protoporphyrin.

Experimental

Materials

Protoporphyrin IX and zinc protoporphyrin were purchased from Sigma Chemical Company (St. Louis, MO, USA) and Porphyrin Products, Inc. (Logan, UT), respectively. Tetrahydrofuran and methanol (HPLC quality) were purchased from Sigma Chemicals (MO, USA). All other reagents were of analytical grade.

Apparatus

Experiments were performed on a modular Waters HPLC system equipped with a Rheodyne 7125 injector fitted with a 20-μl sample loop. Separations were made on a Silica gel C18 analytical column (Isco, 4.6 mm x 25 cm). The eluent was monitored with a photodiode array detector (Waters Model 990) with a variable wavelength ranging

from 190 nm to 600 nm equipped with a 8 μl flow cell attachment. All the measurements were recorded and integrated by the Waters 990 data processing system.

Preparation of protoporphyrin IX and zinc protoporphyrin solutions

Protoporphyrin (1.65 μmol) and zinc-protoporphyrin (1.49 μmol) were separately dissolved in 1 ml of each of the following injection solvents : pyridine, NH_4OH (0.5 M), NH_4NO_3, methyl isobutyl ketone, the mobile phases, ethyl acetate, chloroform and sodium hydroxide. The dissolution was made with sonication.

Chromatographic Conditions

Two mobile phases using either acetate or phosphate as buffer were prepared. The first reversed-phase system contained methanol-tetraphydrofuran - 0.1M phosphate buffer (18:30:20, V/V/V), the apparent pH is 5.38, and the second mobile phase system consisted of 22 mM acetate buffer, tetrahydrofuran and methanol (11:15:6, V/V/V), the apparent pH is 6.74. All the pH values were measured by a digital ionalyzer with a pH electrode (Corning, USA). The isocratic method was employed for all the experiments at a flow-rate of 1 ml/min at ambient temperature. The injection volume was 20 μl. The absorbance was monitored at 400 nm during the whole experiment.

Results and discussion

The injection solvent effects on the separation performance of protoporphyrin and zinc protoporphyrin were investigated in the present study. The common variables characterizing the mobile phase composition, pH, elution strength and ionic strength have been studied previously (4). The retention of porphyrins is predictable with respect to the elution order when reversed-phase liquid chromatography is employed for the

separation. Thus, it is known that the retention is governed by the number of carboxyl groups of porphyrins. Protoporphyrin is among the least carboxylated porphyrin. Therefore, it is usually retained for a longer period of time under reversed-phase condition. On the other hand, the retention of metalloporphyrin has not been studied. Much attention is paid to the chemistry and chromatography of other metal-free porphyrins. Zinc protoporphyrin is one of the more important biological molecules and could be used an indicator for clinical test and confirmative diagnosis of porphyrin-related diseases and the abnormality of heme biosynthesis. The previous studies have reported the unusual chromatographic behaviour of zinc protoporphyrin (6-7). However, the retention of metalloporphyrins is not understood.

Zinc protoporphyrin is protoporphyrin chelated with zinc metal ion in the center of the porphyrin nucleus. The retention of zinc protoporphyrin is, therefore, expected to be similar to protoporphyrin chromatographically. However, under reversed-phase condition, metal-free protoporphyrin peak broadening and tailing is noticeable. The elution profile of metallopoorphyrin shows a sharp and symmetrical peak under the same reversed-phase chromatographic conditions (4,6). The smaller particle size (5 μm) of column packings improved the peak shape of protoporphyrin and zinc protoporphyrin. A typical chromatogram is shown in Figure 1. Both mobile phases used in this study, phosphate or acetate buffer, affect the elution profile or peak shape by about the same extent.

While the retention of protoporphyrin can be predicted under a given condition, the retention of metalloporphyrin is not easily followed. The effects of injection solvents on metal-free porphyrins have not been observed, but the retention of metalloporphyrin was significantly changed (6); thus, various solvents were used to prepare protoporphyrin and zinc protoporphyrin solutions for the study. About 20 μl of each of the solutions

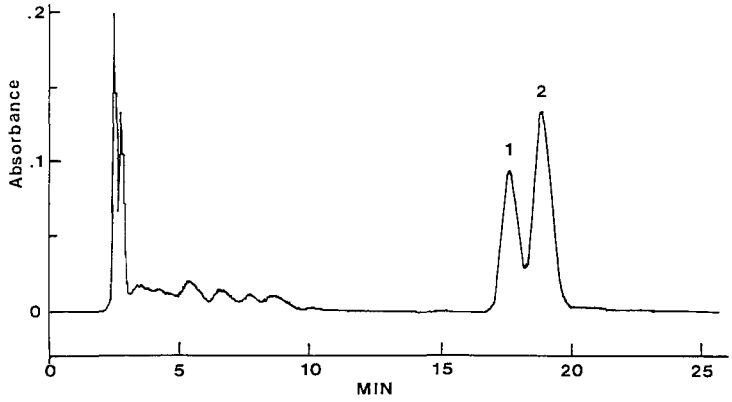

Figure 1 Chromatogram of protoporphyrin (1) and zinc protoporphyrin (2) standards. See chromatographic conditions for experimental details. The injection solvent is pyridine.

were injected onto the HPLC column for analysis. The retention times are summaried in Table I. The solubility of the two compounds varies remarkably. Protoporphyrin is more soluble than zinc protoporphyrin in the various solvents tested. Zinc protoporphyrin was sparingly soluble in ammonium nitrate, methyl isobutyl ketone or ethyl acetate. Hence, there are no retention data available with these solvents.

The influence of ionic strength using sodium phosphate or acetate buffer on retention was studied in the pH range which minimizes the dissociation of zinc protoporphyrin. Two phosphate buffers at different concentrations and one acetate buffer were used to study the retention of protoporphyrin and zinc protoporphyrin. The concentration of the organic modifier, THF, was slightly elevated to facilitate a convenient retention time when 0.1 M phosphate buffer was used. However, the change of THF concentration did not affect the elution order of the compounds. The effects of ionic strength on the retention of protoporphyrin have been reported earlier (6). The retention increases with the ionic strength. The back pressure also increases considerably

Table I

Retention times of protoporphyrin and zinc protoporphyrin

Injection solvents	Retention time (min)					
	phosphate buffer (a)		phosphate buffer (b)		acetate buffer (c)	
	P	Z	P	Z	P	Z
Pyridine	5.60	5.09	16.98	18.18*	6.05	4.68
NH_4OH	5.23	5.86	18.22	19.62	5.60	6.08
NH_4NO_3	6.27	-[e]	17.06	-[e]	6.76	-[e]
Methyl isobutyl Ketone	5.50	-[e]	18.92	-[e]	7.59	-[e]
Ethylacetate	5.71	-[e]	-[e]	-[e]	6.49	-[e]
Chloroform	5.70	5.60	--[f]	--[f]	8.06	5.76
NaOH	4.98	3.67	15.55	18.03	4.44	5.06
Mobile phases[d]	5.90	5.40	16.44	18.56**	7.54	6.64

[a] Eluents : 0.05 M phosphate-methanol-THF (18:30:16).

[b] Eluents : 0.1 M phosphate-methanol-THF (18:30:20).

[c] Eluents : 22 mM acetate-methanol-THF (11:15:6).

[d] The corresponding phosphate or acetate-containing mobile phases

[e] Zinc protoporphyrin is insoluble

[f] not available

P = protoporphyrin

Z = Zinc protoporphyrin

* Pyridine-meOH - 22.51 (Z); 19.36 (P)

** OAc^- - Mobile phase : 16.83 min

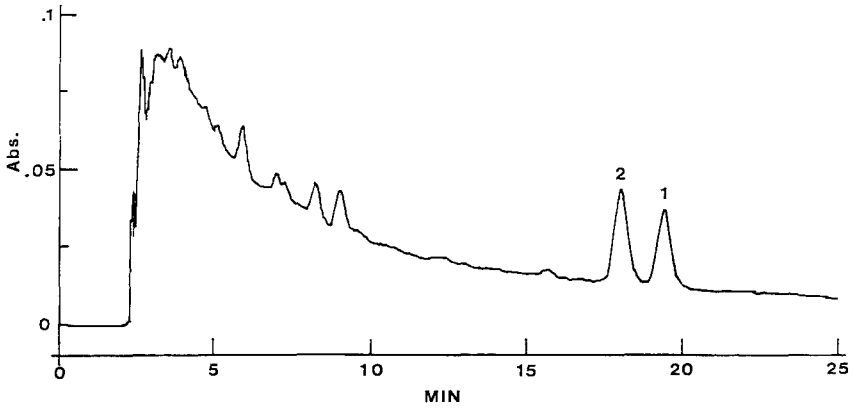

Figure 2 Chromatogram of protoporphyrin (1) and zinc protoporphyrin (2) standards. See chromatographic conditions for experimental details. The injection solvent is NH_4OH.

at higher ionic strength. The protoporphyrin peak is broadened more noticeably than that of zinc protoporphyrin. The result suggests a more efficient partition of zinc protoporyhyrin in the mobile phase. The more pronounced effect of ionic strength is shown on the retention of zinc protoporphyrin.

Among the injection solvents tested, NaOH and NH_4OH show an unusual influence on the retention of zinc protoporphyrin. Essentially, the elution order of zinc protoporphyrin and protoporphyrin was reversed with a strong base as an injection solvent. In contrast, protoporphyrin came off the column first before zinc protoporphyrin with the any other injection solvents tested in the study. Nevertheless, when the ionic strength increases, the shifting in retention of zinc protoporphyrin becomes less affected. Consequently, the elution order of protoporphyrin and zinc protoporphyrin remained the same with phosphate buffer at concentration of about 0.1 M. The reversal of elution

order is only effective at lower ionic strength with buffer concentration < 0.05 M and with NH_4OH or NaOH as the injection solvent. Similarly, the mobile phase with acetate buffer also affects the elution order when a strong base is used as an injection solvent (Table 1). Furthermore, NaOH produced a high background during the elution (Figure 2). Therefore, it is not recommanded as an injection solvent for real sample analysis.

Conclusions

There is a significant effect of injection solvent on the retention of zinc protoporphyrin when a strong base, such as ammonium hydroxide and sodium hydroxide, is used as an injection solvent. Moreover, the ionic strength of a buffer at a lower concentration (< 0.05M) coupled with a strong base as an injection solvent would retain zinc protoporphyrin for a shorter period of time than metal-free protoporphyrin. Consequently, the elution order of protoporphyrin and zinc protoporphyrin appeared to be reversed under this condition. The solvent effect is an important consideration for clinical testing or analysis of metalloporphyrin, which requires an alkaline solvent media for an efficient extraction. Although the mobile phases tested in this study could be used as injection solvents, the solubility of porphyrins is a consideration. Therefore, a weak base (solvent) and an appropriate ionic strength of a buffer solution should be used for the determination of zinc protoporphyrin and protoporphyrin. Also, the retention of metalloporphyrins is worth further study.

Acknowledgements

The financial support of the HK Polytechnic and the University of Utah is gratefully acknowledged. We thank Miss Candy Leung and Miss Carol Tsang for their secretarial assistance.

References

1. Thibaut, D., Debussche, L. and Blanche, F., Proc. Natl. Acad. Sci. USA, 87, 8795-8799, 1990.

2. Piomelli, S., Clin Chem 23, 264-9, 1977

3. Lamola, A.A. and Yamae, T., Science, 186, 936-8, 1974.

4. Ho, J.W., Guthrie, R and Tieckelmann, M., J. Chromatogr., 375, 57-63, 1986.

5. Meyer, H.D., Vogt, W., and Jacob, K., J. Chromatogr., 290, 207-213, 1984.

6. Ho, J.W., LC/GC, 7(4), 348-352, 1989.

7. Tsimidou, M and Macrae, R., J. Chromatogr. Sci., 23, 155-160, 1985.

Received: July 10, 1993
Accepted: August 5, 1993

JOURNAL OF LIQUID CHROMATOGRAPHY, 17(3), 559-577 (1994)

NON-EXCLUSION EFFECTS IN AQUEOUS SEC: BEHAVIOR OF SOME POLYELECTROLYTES USING ON-LINE MASS DETECTORS

GISÈLE VOLET AND JAMES LESEC*
Laboratoire de Physico-Chimie Macromoléculaire
de l'Université Pierre et Marie Curie
(Paris VI) - C.N.R.S. URA n° 278
E.S.P.C.I. - 10 rue Vauquelin - 75231 Paris Cédex 05 - France

ABSTRACT

Aqueous Size Exclusion Chromatography (SEC), coupled with both a home-made viscometer and a low angle laser light scattering detector (LALLS) is a very valuable analytical tool for the characterization of polyelectrolytes. The great interest of this dual mass detection is that molecular weights can be calculated by two different and independent ways. When comparing the two sets of results, it is possible to check whether every chromatographic parameters has been optimized or non exclusion effects occur in addition to the size exclusion mechanism. Two sets of polyelectrolytes were used in this study : a set of sodium polystyrene sulfonate (NaPSS) standards, as anionic polymers and a family of copolymers of acrylamide and N,N,N-trimethylaminoethyl chloride acrylate (AM/CMA) synthetized in our Laboratory as cationic polymers. Important non-exclusion effects, repulsion and adsorption have been encountered in their study. The results are discussed as a function of the ionic strength of the mobile phase and the nature of the salt that was added and interpreted through polymer-packing interactions. The strong influence of the nature of the column, and especially their history is described.

* To whom correspondence should be addressed

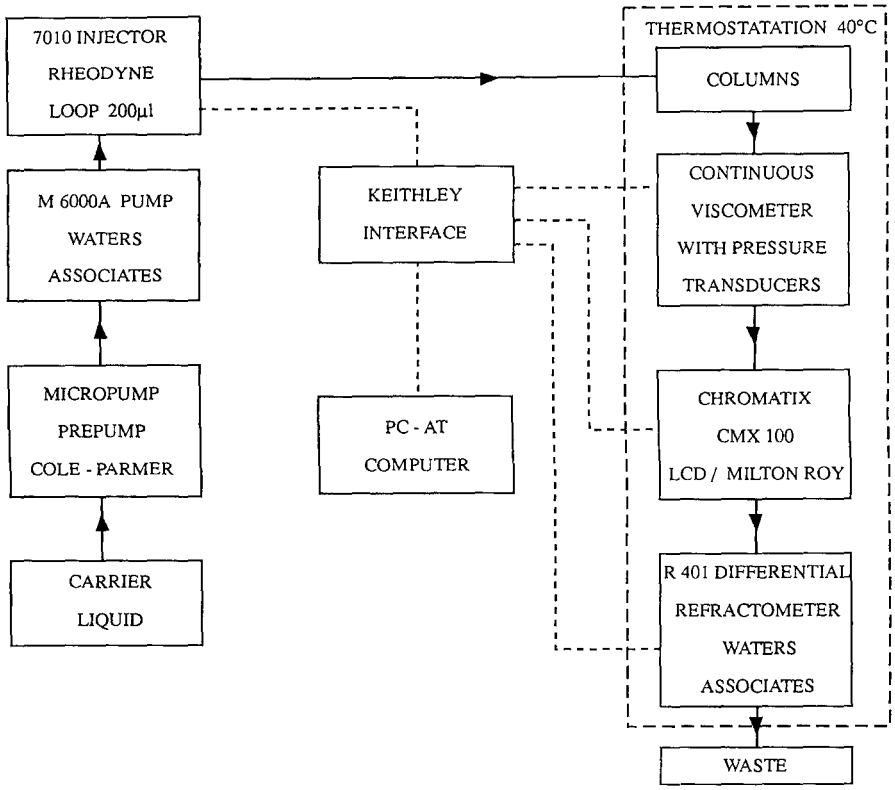

Figure 1 : General scheme of the SEC instrument.

INTRODUCTION

Polyelectrolytes represent a major class of very useful water-soluble polymers. These polymers have ionic groups along their macromolecular chains that involve electrostatic interactions. Then, most applications of polyelectrolytes depend on their viscosity-modifying and surface activity properties. Therefore, polyelectrolytes find uses as viscosity-modifying, gelling or flocculating agents in many areas : water treatment, oil industry, paints, detergents, paper and food industry, etc... Reliable determination of average molecular weights is essential to predict end-use properties of these polymers.

Size Exclusion Chromatography, with a concentration detector and coupled to two on-line mass detectors, appears to be the most efficient method for the determination of molecular weights. This triple coupling allows the calculation of real molecular weights by two different and independent ways. However, the interest of this triple detection is especially important in the case of polyelectrolytes. The presence of ionic groups on the macromolecular chain may induce non-exclusion effects : intramolecular electrostatic interactions and electrostatic interactions between polymer and packing such as ion exclusion (1-2), ion inclusion (3-6) or adsorption (7). The overlay of these non-exclusion effects to the separation mechanism of SEC leads to very erroneous results. Therefore, the possibility of comparing molecular weight values from two different ways becomes of major interest when checking whether the SEC system runs properly with well-controlled parameters or an abnormal behavior of the polymer occurs.

In this paper, we report the behavior of two different families of polyelectrolytes : anionic polymers (sodium polystyrene sulfonate = NaPSS) and cationic copolymers (acrylamide and N,N,N-trimethylaminoethyl chloride acrylate = AM/CMA) chromatographed in mobile phases with increasing ionic strengths. Our experiments were performed with a Waters Associates (Milford, Ma.) modular room temperature instrument equipped with a R 401 refractometer and two mass detectors : a single capillary viscometer and a low angle laser light scattering detector (LALLS) (8). The viscometer allows the determination of intrinsic viscosity versus molecular weight, leading to "universal" molecular weight calculation through universal calibration (9), and gives information on long-chain branching. Simultaneously, the light scattering detector provides absolute molecular weights. The purpose of this work was to investigate the influence of experimental parameters in order to avoid non exclusion effects and to get an accurate characterization of polyelectrolytes using the triple detection.

EXPERIMENTAL

INSTRUMENTATION

The SEC system is described in Figure 1 and is composed of several components described previously (8,9) :

- a micropump prepump (Cole - Parmer, Chicago., Ill.)
- a M 6000A pumping system (Waters Associates, Milford, Ma.)
- a 7010 injector with a 200 µl loop (Rheodyne, Calif.)
- a R 401 differential refractometer (Waters Associates)
- two mass detectors
- and a column set.

Mass detectors

The specific nature of this chromatograph is that both mass detectors are inserted in series between the outlet of the column set and the inlet of the differential refractometer in this sequence : a home-made continuous single capillary viscometer and a light scattering detector. Every component is kept at a well-controlled temperature of 40°C.

Viscometer : This vicometer is made with a 3 meter long Teflon capillary (0.3 mm I.D.) connected to two Sedeme (Paris, France) pressure transducers (CMAC 5 range: 5 bars) at both ends.

LALLS : The light scattering detector is a Chromatix CMX 100 (LDC Analytical). This instrument uses a He - Ne laser (632.8 nm) and measures the scattered light between 5 and 6°.

The great interest of this dual mass detection is that one detector (LALLS) provides absolute molecular weights independent of elution volume. Conversely, molecular weights calculated from universal calibration and viscometry are very dependent on elution volumes since they refer to a calibration curve and may be calculated wrong when elution is disturbed, ie., when non exclusion effects occur.

Column sets

Two sets of columns were used : Ultrahydrogel 500, 1000 and 2000 Å (Waters Associates, Milford, Ma.) and Shodex OH-pak B 803, B 804, B 805 and B 806 (Showa Denko, Tokyo, Japan). Both column sets contain hydrophilic cross-linked gels based on methacrylic copolymers. The real nature of these gels is not described, but according to the suppliers, the gels of these column sets are similar but not identical.

MOBILE PHASES

Mobile phases were water containing various salts ($LiNO_3$, $NaNO_3$ or Na_2SO_4) at various concentrations (0.1 M to 0.75 M). The presence of salt is necessary to screen out the charges on polyelectrolytes in order to avoid polyelectrolyte effects in solution. In every case, 400 ppm of NaN_3 were added to the mobile phase to prevent biological degradation. Every solution was vacuum filtered through 0.45 µm membranes. The flow rate of the mobile phase was 1 cm^3/mn.

DATA ACQUISITION

Injector and detectors were connected to an on-line microcomputer (PC - AT) through a Keithley interface : 199 scanner - multimeter (Cleveland, Ohio). An

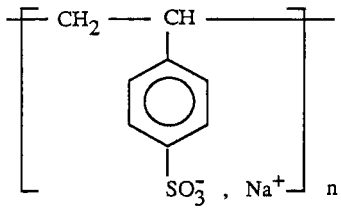

Figure 2 : Sodium polystyrene sulfonate (NaPSS).

Table I : Molecular weights of sodium polystyrene sulfonate standards as quoted by Polymer Laboratories Ltd (Shrosphire, England).

sample number	Nominal molecular weight		Mw / Mn <
	Polystyrene sulfonate ion	Sodium polystyrene sulfonate	
PS 1	31 000	35 000	1.10
PS 2	88 000	100 000	1.10
PS 3	195 000	220 000	1.10
PS 4	354 000	400 000	1.10
PS 5	690 000	780 000	1.10
PS 6	1 060 000	1 200 000	1.10

appropriate personal software "Multidetector GPC Software" (8) allows acquisition and data treatment and leads to reliable interpretations of chromatograms. A detailed description of data acquisition and data handling procedure was reported elsewhere (8).

CALIBRATION

The treatment of viscometric data requires a preliminary calibration of the column set. Two sets of standards were used : polyethylene oxides (20,000 - 850,000) from Toyo Soda (Japan) and pullulan polysaccharides (7,000 - 900,000) from Showa Denko. The universal calibration procedure and all the calibration curves obtained in the different mobile phases are reported in a previous paper (9).

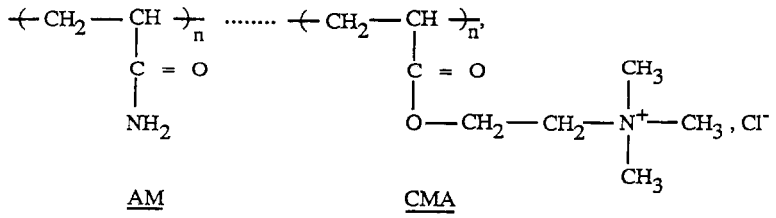

Figure 3 : Copolymer of acrylamide and N,N,N-trimethylaminoethyl chloride acrylate (AM/CMA).

MATERIALS

Two series of polyelectrolytes, representing anionic and cationic polymers, were used in this study (10). Anionic polymers (sodium polystyrene sulfonate standards) are represented in Figure 2. They were obtained from Polymer Laboratories Ltd (Shrosphire, England).

These polymers have a very narrow distribution and contain, a priori, 100% of anionic groups. Their properties, as quoted by the manufacturer, are summarized in Table I.

Cationic copolymers (AM/CMA) were synthetized in our laboratory by radical polymerization (11 - 12) with different degrees of cationic character between 0% and 100% and various molecular weights (Figure 3).

RESULTS AND DISCUSSION

CHARACTERIZATION OF NaPSS

These 100% anionic polymers were studied with both the Ultrahydrogel column set and the Shodex column set. The mobile phases were water containing $LiNO_3$, $NaNO_3$ or Na_2SO_4 with various concentrations between 0.1 M to 0.5 M.

- NaPSS behavior on Ultrahydrogel columns :

NaPSS were completely retained on this packing. Strong interactions occur between anionic polymers and Ultrahydrogel columns, probably due to the presence of charges on the packing surface, opposite to the polyanion.

Table II : Results of sodium polystyrene sulfonates.
$Mw_{univ.}$ and Mw_{LALLS} : average molecular weights calculated from universal calibration and by LALLS detector, respectively.

sample number	Eluent		Ve (cm^3)	[η] ($cm^3.g^{-1}$)	$Mw_{univ.}$	Mw_{LALLS}
PS 1	$NaNO_3$	0.1 M	28.55	18	110 000	42 000
	$LiNO_3$	0.1 M	28.42	19	100 000	40 000
	Na_2SO_4	0.1 M	29.76	16	31 000	40 000
	$LiNO_3$	0.5 M	30.05	12	31 000	36 000
PS 2	$NaNO_3$	0.1 M	27.31	47	160 000	120 000
	$LiNO_3$	0.1 M	27.10	44	190 000	110 000
	Na_2SO_4	0.1 M	28.09	39	90 000	110 000
	$LiNO_3$	0.5 M	28.28	32	90 000	110 000
PS 3	$NaNO_3$	0.1 M	26.16	77	290 000	220 000
	$LiNO_3$	0.1 M	25.69	74	400 000	210 000
	Na_2SO_4	0.1 M	27.02	67	170 000	210 000
	$LiNO_3$	0.5 M	27.31	55	160 000	200 000
PS 4	$NaNO_3$	0.1 M	24.72	150	590 000	470 000
	$LiNO_3$	0.1 M	24.51	150	760 000	500 000
	Na_2SO_4	0.1 M	25.33	130	440 000	440 000
	$LiNO_3$	0.5 M	25.50	87	510 000	410 000
PS 5	$NaNO_3$	0.1 M	24.15	190	650 000	650 000
	$LiNO_3$	0.1 M	24.17	180	850 000	640 000
	Na_2SO_4	0.1 M	24.64	170	570 000	680 000
	$LiNO_3$	0.5 M	24.90	120	510 000	590 000
PS 6	$NaNO_3$	0.1 M	23.11	340	$1.2\ 10^6$	$1.5\ 10^6$
	Na_2SO_4	0.1 M	23.52	280	$1.2\ 10^6$	$1.3\ 10^6$
	$LiNO_3$	0.5 M	23.79	190	$1.1\ 10^6$	$1.1\ 10^6$

- NaPSS behavior on Shodex columns :

On Shodex columns, NaPSS are eluted without any significant adsorption; the results are reported in Table II. Nevertheless, the polyelectrolyte behavior varies with the ionic strength of the mobile phase. The first observation is that the weight average molecular weights Mw_{LALLS} calculated by light scattering are approximately constant and independent of the ionic strength, whatever the molecular weight. The second observation is that elution volumes increase when ionic strength increases, and, at the same time, intrinsic viscosity decreases for every sample. Intrinsic viscosities, which are about the same in $NaNO_3$ and $LiNO_3$ 0.1 M, decrease in Na_2SO_4 0.1 M and decrease again in $LiNO_3$ 0.5 M. The deviation

is about 60% between the sets of values measured in $LiNO_3$ 0.1 M and 0.5 M. This variation may be explained by the presence of salt according to the law (13) :

$$[\eta] = A + \frac{B}{\sqrt{C_s}}$$

where C_s is the salt concentration and A , B are constants. The higher the salt concentration , the more screened out the electrostatic interactions and, therefore, the smaller the hydrodynamic volume. This is qualitatively confirmed by the variations of elution volumes that increase with ionic strength in the order :

$$Ve_{\underset{0.1\ M}{NaNO_3}} = Ve_{\underset{0.1\ M}{LiNO_3}} < Ve_{\underset{0.1\ M}{Na_2SO_4}} \leq Ve_{\underset{0.5\ M}{LiNO_3}}$$

Ionic strength of Na_2SO_4 0.1 M is equivalent to a salt concentration of 0.3 M with a monovalent salt according to the relationship :

$$I = \frac{1}{2} \Sigma\, C_i\, z_i^2$$

where C_i and z_i are the ion concentration in $mol.l^{-1}$ and the number of charge, respectively.

However, the weight average molecular weights $Mw_{univ.}$ calculated using the universal calibration curve are not constant in Table II, but increase when ionic strength decreases; this cannot be explained by the change in hydrodynamic volume since universal calibration takes this effect into account. Accordingly, the decrease of elution volumes is an overlay of two phenomena. When ionic strength decreases, in addition to the increase of hydrodynamic volume and, consequently, the decrease of elution volumes, interactions occur between polyelectrolytes and negatives charges of the packing surface that prevent the polyion from freely diffusing into the pores of the gel matrix. These repulsive interactions between anionic groups on the polyelectrolyte chain and negative charges on the gel surface are more important for low molecular weight compounds (Figure 4). When the ionic strength of the mobile phase is not strong enough to screen out the anionic sites of the packing, these repulsions reduce the effective pore volume available to the polymer. As a result, peaks elute earlier than expected for a neutral polymer with the same size and lead to an overestimation of molecular weights calculated with the universal calibration curve (Table II), especially for low molecular weight polymers that can usually penetrate a larger porous volume, and therefore, a larger specific surface area. In $LiNO_3$ 0.5 M and Na_2SO_4 0.1 M, $Mw_{univ.}$ values are in good agreement with Mw_{LALLS} values that is not the case with mobile phases at 0.1 M salt concentration. $Mw_{univ.}$ are calculated using a universal calibration curve obtained with pullulan standards in the same mobile phase (9).

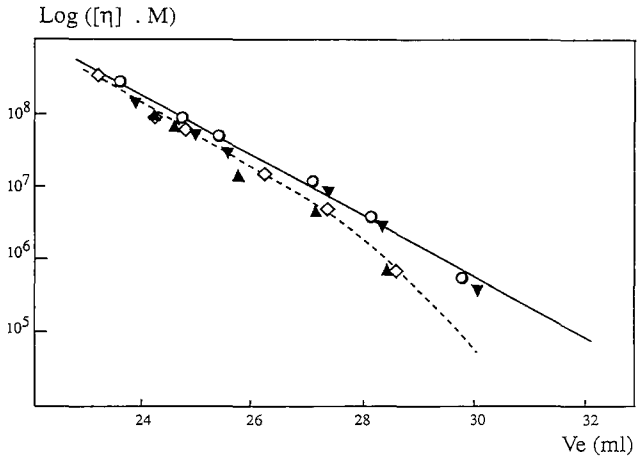

Figure 4 : Universal calibration curves corresponding to NaPSS.
Eluents : (◇) $NaNO_3$ 0.1 M, (▲) $LiNO_3$ 0.1 M, (○) Na_2SO_4 0.1 M, (▼) $LiNO_3$ 0.5 M
(—) pullulan universal calibration curve at 0.5 M,
(---) NaPSS curve at 0.1 M.

As a conclusion of these experiments, an ionic strength corresponding to $LiNO_3$ 0.5 M is required to avoid electrostatic repulsive interactions and to allow an accurate elution of these anionic polymers.

CHARACTERIZATION OF AM/CMA COPOLYMERS

These experiments were performed with the Shodex OH-pak column set. As previously discussed, Shodex packing contains anionic groups on its surface. When a cationic polyelectrolyte, which is oppositely charged, approaches the packing surface, electrostatic attractions may occur, resulting in delayed elution or even, in total adsorption. Therefore, the concentrations of AM/CMA copolymers were measured accurately using the surface area of the refractometric response to prevent erroneous results due to a wrong concentration value. This concentration correction can be made only when the refractive index increment (dn/dc) is known. The variations of dn/dc data are described by the relationship (11) :

$$\left(\frac{dn}{dc}\right)_{\tau} = (1-\tau)\left(\frac{dn}{dc}\right)_{PAM} + \tau\left(\frac{dn}{dc}\right)_{PCMA}$$

where the subscripts PAM, PCMA denote polyacrylamide homopolymer and 100% cationic polymer, respectively, and τ is the cationic rate. The values of specific refractive index increment of PAM and PCMA 0.176 and 0.154 cm^3/g, respectively, were calculated using the refractometer response. The "Multidetector GPC software" allows the correction of every concentration used in every molecular weight calculation ("universal" and LALLS) of the results described later.

For these experiments, we studied AM/CMA copolymers with different levels of cationic character (0 to 100%) and with different molecular weights ranging from 1.2 10^5 to 4.5 10^6 g/mol. The mobile phase was water containing the salt $LiNO_3$ at various concentration from 0.1 M to 0.75 M. With regard to the great number of results, we have chosen to report only a few representative data in Tables III to VIII.

- AM/CMA behavior in terms of cationicity evolution :

For low cationic rates ($\leq$ 5%), the behavior of polyelectrolytes is relatively insensitive to the ionic strength (from 0.1 M to 0.75 M), taking experimental errors into account (Table III). Molecular weights determined from LALLS are constant in the different mobile phases. Molecular weights calculated from viscosity and universal calibration curve are in good agreement with those from LALLS. Moreover, intrinsic viscosities, but also elution volumes, remain constant whatever the salt concentration of the mobile phase. An ionic strength corresponding to $LiNO_3$ 0.1 M is strong enough to allow a good characterization of these polymers.

When the copolymer cationicity is around 6 %, an abnormal elution of the polyelectrolyte is observed in $LiNO_3$ 0.1 M (Table IV). The elution profile is shifted toward high elution volumes (strong increase of elution volume) and molecular weight by LALLS is calculated much smaller than for higher ionic strengths. At the same time, intrinsic viscosity [η] is also calculated too small; this demonstrates the absence of high molecular weight molecules. At this ionic strength, the copolymer is partially adsorbed onto the packing; this is confirmed by the measurement of the surface area of the refractometric profile which is smaller than expected. Moreover, the strong decrease of intrinsic viscosity [η] and Mw by LALLS shows that the highest molecular weight part of the distribution is preferentially adsorbed. Conversely, for this cationicity, ionic strengths of 0.25 M and higher lead to a correct elution of the copolymer.

A similar behavior is observed with 9 to 14% cationicity copolymers (Table V). The results in $LiNO_3$ 0.1 M are not reported since copolymers are totally adsorbed. At 0.25 M, intrinsic viscosities and Mw by LALLS are underestimated, leading to the same interpretation as for the previous copolymers. The increase of solvent ionic strength to 0.5 M and 0.75 M progressively screens out the charges, allowing a normal elution of the copolymer.

Table III : Results of some AM/CMA copolymers with low cationicity rates.
C_{LiNO_3} : $LiNO_3$ salt concentration
$Mw_{univ.}$ and Mw_{LALLS} : average molecular weights calculated from universal calibration and by LALLS detector, respectively.

sample number	% CMA	C_{LiNO_3} (mol.l^{-1})	Ve (cm^3)	[η] (cm^3.g^{-1})	$Mw_{univ.}$	Mw_{LALLS}
12 (PAM)	0	0	23.58	250	980 000	880 000
		0.1	23.76	250	850 000	830 000
		0.25	23.79	270	830 000	860 000
		0.5	23.82	250	820 000	750 000
		0.75	23.70	260	860 000	790 000
23	1	0.1	24.14	190	630 000	570 000
		0.25	24.24	190	610 000	590 000
		0.5	24.26	200	670 000	540 000
		0.75	24.24	200	600 000	580 000
38	3	0.1	23.42	250	1.1 10^6	1.3 10^6
		0.25	23.09	270	1.2 10^6	1.4 10^6
		0.5	23.05	300	1.1 10^6	1.2 10^6
		0.75	23.30	290	1.3 10^6	1.4 10^6
41	5	0.1	24.24	170	510 000	680 000
		0.25	24.39	150	480 000	540 000
		0.5	24.08	180	590 000	590 000
		0.75	24.10	180	630 000	610 000

Table IV : Results of a 6.4% cationic AM/CMA copolymer.
C_{LiNO_3} : $LiNO_3$ salt concentration
$Mw_{univ.}$ and Mw_{LALLS} : average molecular weights calculated from universal calibration and by LALLS detector, respectively
* : partial adsorption of polymer on columns.

sample number	% CMA	C_{LiNO_3} (mol.l^{-1})	Ve (cm^3)	[η] (cm^3.g^{-1})	$Mw_{univ.}$	Mw_{LALLS}
52	6.4	0.1	27.18*	76*	54 000*	200 000*
		0.25	23.84	170	730 000	740 000
		0.5	23.98	180	650 000	730 000
		0.75	23.87	190	840 000	820 000

Table V : Results of some AM/CMA copolymers with medium cationicities.
C_{LiNO_3} : $LiNO_3$ salt concentration
$Mw_{univ.}$ and Mw_{LALLS} : average molecular weights calculated from universal calibration and by LALLS detector, respectively
* : partial adsorption of polymers on columns.

sample number	% CMA	C_{LiNO_3} (mol.l^{-1})	Ve (cm^3)	[η] (cm^3.g^{-1})	$Mw_{univ.}$	Mw_{LALLS}
61	9.5	0.25	24.62	96*	380 000*	470 000*
		0.5	24.41	140	490 000	670 000
		0.75	24.24	140	540 000	610 000
64	13.8	0.25	22.83*	270*	1.6 10^6*	2.1 10^6*
		0.5	21.98	400	3.2 10^6	3.2 10^6
		0.75	21.70	470	3.0 10^6	3.4 10^6

At a cationicity of 24% and above, partial adsorption always occurs, mainly for the highest part of the distribution, even when the salt concentration increases to 0.75 M (Table VI). It is impossible to accurately characterize these polymers. Moreover, at a cationicity of 30% and above, polyelectrolytes are totally retained on the columns at an ionic strength of 0.5 M and are only partially eluted at 0.75 M. For chromatographic reasons, it was not realistic to increase the ionic strength beyond 0.75 M to improve elution of high cationicity copolymers.

- Influence of molecular weight :

The set of AM/CMA copolymers we analyzed was comprised of polymers with different cationicities and various molecular weights ranging from 1.2 10^5 to 4.5 10^6 g/mole. In terms of cationicity, the same behavior was observed whatever the molecular weight (Table VII and VIII). Table VII shows the results of 1% CMA copolymers, similar results are obtained at a salt concentration of 0.1 M and 0.5 M for molecular weights ranging from 100,000 to 4 10^6 g/mole.

In Table VIII, AM/CMA copolymers with cationicity around 7% are compared for three different molecular weights : 300,000 , 800,000 and 2.10^6 g/mole. In every case, results are consistent for ionic strength of 0.25 M and above. Also, a systematic decrease of intrinsic viscosity and Mw by LALLS and an increase of elution volumes are observed when ionic strength decreases to 0.1 M that can be interpreted by the adsorption of the highest molecular weight part of the distribution. Adsorption being a function of molecular weight, it is interesting to point out that Mw_{LALLS} values are systematically calculated around 200,000, whatever the real molecular weight of the copolymer. As Mw_{LALLS} is the weight

Table VI : Results of some AM/CMA copolymers with high cationicities.
C_{LiNO_3} : $LiNO_3$ salt concentration
$Mw_{univ.}$ and Mw_{LALLS} : average molecular weights calculated from universal calibration and by LALLS detector, respectively
χ : amount of eluted polymer (% recovery).

sample number	% CMA	C_{LiNO_3} (mol.l^{-1})	Ve (cm^3)	[η] (cm^3.g^{-1})	$Mw_{univ.}$	Mw_{LALLS}	χ (%)
		0.5	25.58	61	260 000	960 000	65
70	24	0.75	24.68	110	280 000	630 000	75
		0.5		not	possible		
82	32	0.75	24.17	140	510 000	790 000	72
		0.5		not	possible		
92	49.5	0.75	24.23	180	460 000	1.1 10^6	74
		0.5		not	possible		
101	100	0.75	26.51	74	380 000	530 000	78

Table VII : Results of some AM/CMA copolymers with 1% cationicity at various molecular weights.
C_{LiNO_3} : $LiNO_3$ salt concentration
$Mw_{univ.}$ and Mw_{LALLS} : average molecular weights calculated from universal calibration and by LALLS detector, respectively.

sample number	% CMA	C_{LiNO_3} (mol.l^{-1})	Ve (cm^3)	[η] (cm^3.g^{-1})	$Mw_{univ.}$	Mw_{LALLS}
		0.1	27.15	64	120 000	120 000
21	1	0.5	27.17	62	130 000	110 000
		0.1	24.56	160	470 000	460 000
22	1	0.5	24.53	170	490 000	460 000
		0.1	24.14	190	630 000	570 000
23	1	0.5	24.26	200	670 000	540 000
		0.1	21.54	630	3.6 10^6	3.7 10^6
27	1	0.5	21.55	570	3.5 10^6	3.4 10^6

Table VIII : Results of some AM/CMA copolymers with a cationicity about 7% at various molecular weights.
C_{LiNO_3} : $LiNO_3$ salt concentration
$Mw_{univ.}$ and Mw_{LALLS} : average molecular weights calculated from universal calibration and by LALLS detector, respectively
* : partial adsorption of polymer on columns.

sample number	% CMA	C_{LiNO_3} (mol.l^{-1})	Ve (cm^3)	[η] (cm^3.g^{-1})	$Mw_{univ.}$	Mw_{LALLS}
51	7.5	0.10	27.58*	57*	47 000*	150 000*
		0.25	26.65	98	270 000	310 000
		0.50	26.56	93	260 000	270 000
		0.75	26.58	97	280 000	290 000
52	6.4	0.10	27.18*	76*	54 000*	200 000*
		0.25	23.84	170	730 000	740 000
		0.50	23.98	180	650 000	730 000
		0.75	23.87	190	840 000	820 000
53	6.7	0.10	25.07*	160*	270 000*	>270 000*
		0.25	22.71	320	1.6 10^6	1.9 10^6
		0.50	22.93	350	1.8 10^6	1.6 10^6
		0.75	23.02	320	1.5 10^6	1.6 10^6

average of a broad distribution, it can considered that macromolecules with higher molecular weights than 300,000 - 400,000 are completely adsorbed and only smallest macromolecules, having a molecular weight under this limit, are eluted.

- Diagram of AM/CMA copolymers behavior :

All the results are summarized in Figure 5 where we have reported the behavior of polyelectrolytes in terms of copolymer cationicity and ionic strength of the mobile phase. Every experiment is represented by :

○ when the polymer elution is normal, in other words, when molecular weights calculated from universal calibration agree with those measured by LALLS detector,

■ when the polymer is partly retained, in other words, when $Mw_{univ.} < Mw_{LALLS}$ and when most of high molecular weight molecules are adsorbed on the columns,

● when polymers are completely adsorbed on the columns.

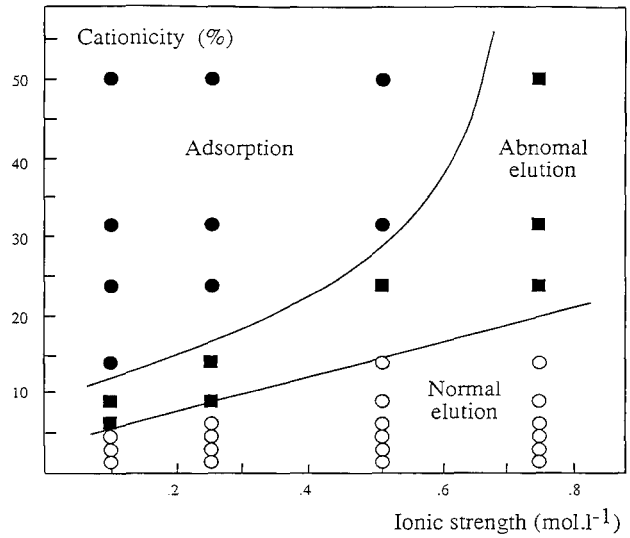

Figure 5 : Diagram of polyelectrolytes AM/CMA behavior versus the ionic strength of the mobile phase.
● total adsorption of polymer on the columns,
■ partial adsorption ($Mw_{univ.} < Mw_{LALLS}$),
○ agreement between $Mw_{univ.}$ and Mw_{LALLS}.

Consequently, the diagram of behavior comprises three areas : normal elution, partial elution and total adsorption. When cationicity increases, it is necessary to increase the ionic strength of the mobile phase to get an accurate characterization of the copolymers. Beyond a cationicity of 20%, it is impossible to characterize these polymers correctly, although the ionic strength value of 0.75 M is above the upper limit of 0.5 M in monovalent salt recommended by the supplier of columns.

It is also very important to note that the diagram shown in Figure 5 corresponds to experiments performed with columns in a given state of use. As an example, beyond 20% of cationicity, the behavior of polymers varies according to the moment when they were injected and elution profiles of the same copolymer may vary. Figure 6 shows the first injection of a 31.5% cationicity copolymer and Figure 7 shows the same copolymer injected some days later. The only difference between the two experiments is that several injections of polymers with the same nature were performed between the two injections. The first profile (Figure 6) could correspond to the profile of a polymer whose highest molecular weights are

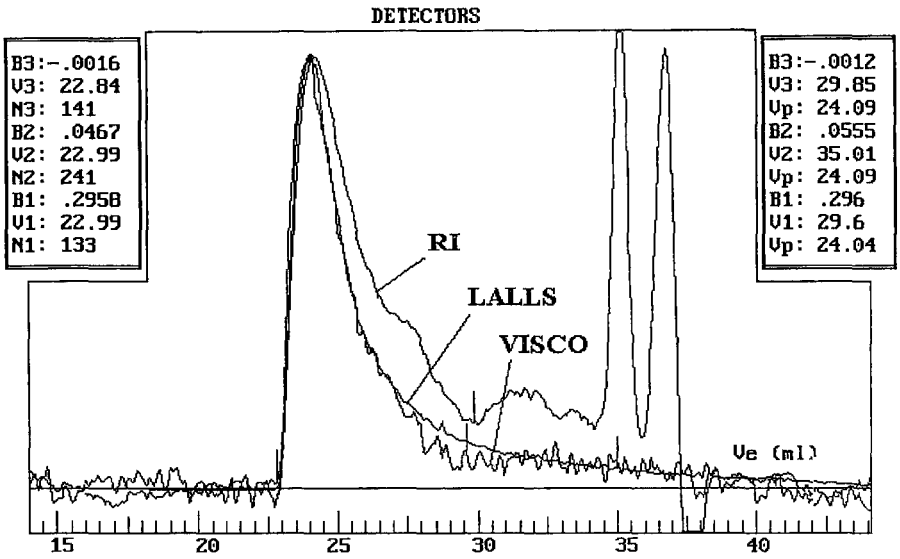

Figure 6 : Chromatograms of a 31.5% cationic copolymer eluted at the beginning of the study.

excluded from the gel because the three profiles (VISCO, LALLS, RI) are beginning in the same time, but the beginning elution volume is 3 cm^3 beyond the exclusion volume of the packing. Therefore, there is no exclusion and this profile corresponds, rather, to a polymer whose highest molecular weights are adsorbed on the columns and other molecular weights eluted later and causing peak tailing.

Moreover, the first profile (Figure 6) corresponds to a percentage of recovery of 36% while the second experiment (Figure 7) with the correct profile corresponds to a recovery of 87%. Obviously, the gradually adsorbed polymers modify the properties of columns by neutralizing the anionic groups on the packing surface. In these experiments, the column performances were drastically improved between the first and the last injection.

This phenomenon, clearly observed for copolymers with cationicity beyond 20%, obviously occurs at lower cationicity but is less important. Therefore, the same experiments, performed on another column set, even with the same nature, could provide a different diagram of behavior, depending on the column history. Before the characterization of such polymers, it could be a good practice to inject some of them until the packing surface becomes stabilized.

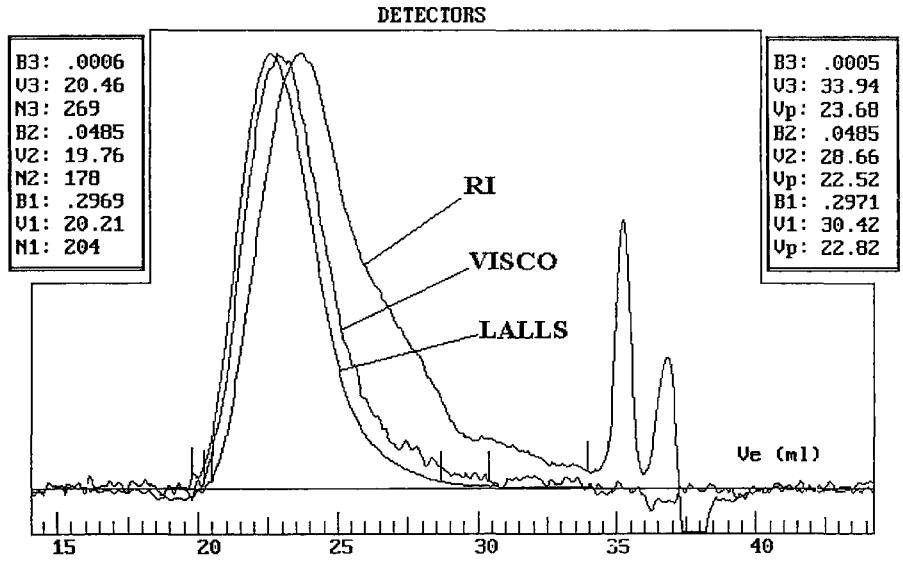

Figure 7 : Chromatograms of a 31.5% cationic copolymer eluted at the end of the study.

CONCLUSION

This study has demonstrated that an accurate characterization of 100% anionic polymers like sodium polystyrene sulfonate can be obtained when a high ionic strength (0.5 M in $LiNO_3$) is used as the mobile phase. This high ionic strength is necessary not simply to avoid the polyelectrolyte effect and to keep NaPSS in a coil-like shape but mainly to screen out repulsive forces between the negative functions of the polyelectrolyte and the negative charges on the packing surface. These forces make a decrease of the available porous volume leading to an apparent decrease of elution volumes, especially in the low molecular weight region, small molecules having access to a larger specific surface.

Conversely, the presence of negative charges on the packing surface disturbs elution of cationic copolymers depending on their cationicity rate. For very low cationicities (around 1%) an ionic strength of 0.1 M in $LiNO_3$ is enough to screen out all the forces and to get a normal elution. For low cationicity (below 6-7%), partial adsorption occurs with mobile phase $LiNO_3$ 0.1 M and it is necessary

to increase the ionic strength to 0.25 M to screen out attractive interactions between the polyelectrolyte and the negative charges on the packing surface, allowing a right elution of the copolymer AM/CMA. When the copolymer cationicity is between 9 and 14%, the same effect occurs but at a higher ionic strength. In that case, $LiNO_3$ 0.5 M is necessary to obtain a right elution of the copolymers. Above a 20% cationicity, partial adsorption always occurs, especially for the highest molecular weights of the distribution, even if the ionic strength of the mobile phase is increased to 0.75 M, that is above the upper limit of salt content for the mobile phase. It has never been possible to run a correct experiment in our conditions and to get the right answer for copolymers with 20% cationicity and above.

Properties of ionic groups of the packing surface of Ultrahydrogel and Shodex columns are different. For example, NaPSS are adsorbed on Ultrahydrogel but elute on Shodex columns.

However, the results obviously depend on experimental conditions : temperature, flow-rate and nature of the mobile phase, nature of columns but also on the age and the history of columns whose packing surface may gradually be modified by adsorption of various solutes.

The conclusions of this sudy on the behavior of some polyelectrolytes in SEC, were possible only because viscometric, light scattering and refractometric detections were used simultaneously. The checkings of refractometric surface area and elution volume, intrinsic viscosity and average molecular weight from LALLS and from universal calibration were essential to understand the behavior of the studied samples.

ACKNOWLEDGEMENTS

We gratefully acknowledge F. Lafuma (Laboratoire de Physico-Chimie Macromoléculaire de l'Université de PARIS VI) who kindly supplied cationic polyelectrolytes. We thank her for helpful communications.

REFERENCES

(1) P.A. Neddermeyer, L.B. Rogers, Anal. Chem., 40, 755 (1968)
(2) M. Rinaudo, J. Desbrieres, Eur. Polym. J., 16, 849 (1980)
(3) C. Tanford, "Physical Chmistry of Macromolecules", Wiley, New - York (1961)
(4) T. Lindstrom, A. De Ruovo, C. Soremark, J. Polym. Sci., a1, 15, 2029 (1977)

(5) P.L. Dubin, I.J. Levy, J. Chromatogr., 235, 377 (1982)
(6) C. Rochas, A. Domard, M. Rinaudo, Eur. Polym. J., 16, 135 (1980)
(7) P.L. Dubin, " Aqueous Size Exclusion Chromatography, Elsevier, New - York (1988)
(8) J. Lesec, G. Volet, J. Appl. Polym. Sci., Appl. Polym. Symp., 45, 177 (1990)
(9) J. Lesec, G. Volet, J. Liq. Chromatogr., 13, 831 (1990)
(10) G. Volet, Thesis, Paris VI (1990)
(11) F. Mabire, R. Audebert, C. Quivoron, Polymer, 25, 1317 (1984)
(12) F. Lafuma, G. Durand, Polymer Bull., 21, 315 (1989)
(13) I. Noda, T. Tsuge, M. Nugasawa, J. Phys. Chem., 74, 710 (1970)

Received: September 13, 1993
Accepted: October 8, 1993

JOURNAL OF LIQUID CHROMATOGRAPHY, 17(3), 579-588 (1994)

HPLC DETERMINATION OF TRACE LEVELS OF ALIPHATIC ALDEHYDES C_1 - C_4 IN RIVER AND TAP WATER USING ON-LINE PRECONCENTRATION

J. LEHOTAY AND K. HROMULAKOVÁ
Department of Analytical Chemistry
Slovak Technical University
Radlinského 9
812 37 Bratislava, Slovakia

ABSTRACT

A simple method has been developed for the separation and quantification of trace amounts of C_1 - C_4 aldehydes in river and tap water. This method utilized the separation of the aldehydes as their 2,4-dinitrophenylhydrazones derivatives by high performance liquid chromatography using on line preconcentration and gradient solvent elution. The reaction of the derivatization was studied on a microscale in water solution at different pH. It was found that aldehydes in spiked sample (at 1 ppb level) are decomposed and unknown compounds are formed. The limits of the detection at a wavelength of 355 nm and a signal/noise ratio of 5 range from 50 ppt for formaldehyde to 200 ppt for butyraldehyde. The mean relative standard deviations for all aldehydes were 10% at 1 ppb level.

INTRODUCTION

Water from polluted rivers is used to feed buffer reservoirs as a first step in the production of drinking water. As the quality of river water is not constant, continuous monitoring is necessary. Aldehydes are important

pollutants of river water, being products of many industrial processes. Aldehydes are known contributors to irritants of the skin, eyes and nasopharyngeal membranes and formaldehyde has been identified as a suspected carcinogen (1,2).

Some HPLC methods for the determination of aliphatic aldehydes after the derivatization have been reported. The commonly used method for aliphatic aldehydes are 2,4- dinitrophenylhydrazine (DNPH) method. In this method, individual aldehydes react with an acidic solution of DNPH to form hydrazone derivatives. The derivatives of aldehydes are diluted in a solvent suitable for gas chromatography (3) or high performance liquid chromatographic analysis (4,5).

HPLC has proved suitable for the separation of certain carbonyl compounds by adsorption chromatography (6 - 8). The use of HPLC has been also published with reversed phase columns (9-12). The application of off-line preconcentration of 2,4-dinitrophenylhydrazones of aldehydes has been described by Kuber at al. (13).

The aim of this paper is to develop a method for the determination of aliphatic aldehydes (C_1- C_4) in which the derivatization reaction is performed directly in a water sample. The quantitative conversion of aldehydes to their corresponding 2,4-dinitrophenylhydrazones on a microscale at room temperature is also studied. To improve the limit of the detection on-line preconcentration has been developed.

EXPERIMENTAL

The LC system for the determination of 2,4-dinitrophenylhydrazones consisted of two Waters pumps (Model 510) and a 150 x 3.2 mm I.D. column packed with 5 μm particles Separon SGX C18 (Tessek, Prague). The preconcentration pump was a Waters pump (Model 501) used at a

flow rate of 1.0 ml/min. Preconcentration was carried out using a 30 x 3.2 mm I.D. precolumn which was packed with Separon C18 (5 μm) (Tessek, Prague). A Waters spectrophotometric detector (Model 484) was used. The analysis was optimized for the determination of 4 dinitrophenylhydrazones (C_1- C_4). Several of these compounds are important for in-time monitoring because they are produced by many technological processes in significant quantities.

The precolumn was washed with 10 ml river or tap water (after derivatization) and subsequent chromatographic separation with gradient elution was done. The mobile phase for the linear gradient was prepared by mixing two solutions : A-: acetonitrile - water 1 : 1

B-: acetonitrile

100% A to 66.7% B over 30 minutes, then to 100% B over 15 minutes.

Prior to use, the water samples were filtered over a 0.45 μm membrane filter. LC gradient - grade acetonitrile was used for the solutions. Water deionized with synthetic resins may contain formaldehyde. All experiments were done at ambient temperature.

RESULTS AND DISCUSSION

Taking advantage of the specific reaction between aldehydes and DNPH we have selected HPLC studies of aldehydes (C_1- C_4) in the tap or river water, to analyze trace levels of aldehydes as 2,4-dinitrophenylhydrazones. A study of the effect of the acid catalyst (hydrochloric acid) concentration on the reaction kinetics was undertaken. Known amount (100 ppb) of propylaldehyde was injected into DNPH solution containing variable amounts of hydrochloric acid catalyst. The reaction mixture was analyzed by reversed phase HPLC at various times after the reaction was initiated . The results indicate that the

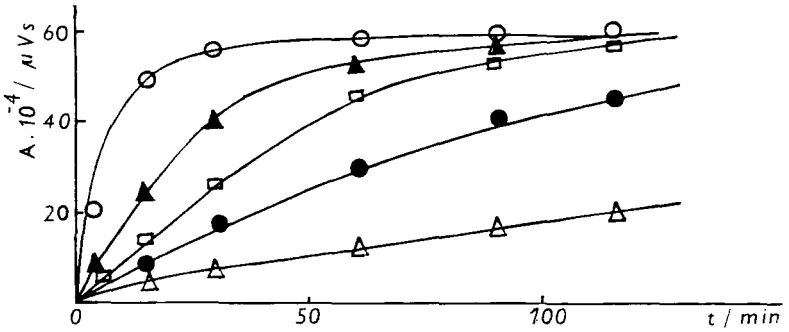

Fig.1. Dependence of reaction yield of 2,4-dinitrophenylhydrazone of propylaldehyde on time at different pH △ - pH=7; ● - pH=4; □ - pH=3; ▲ - pH=2; ○ - pH=1.

reaction proceeds slowly and the best results can be achieved at pH = 1 (Fig. 1).

The reaction between aliphatic aldehydes and DNPH was studied on a microscale at room temperature in water solution at pH = 1. Aldehydes (10 ppb) were added to an excess of DNPH reagent (30 x). The chemical reaction between DNPH and aliphatic aldehydes procceds slowly and the yield depends on the reaction time. Fig. 2 shows that the high yield was achieved during 30 min. for all aldehydes.

A reversed phase C18 packing material for the enrichment column was chosen to conform with the stationary phase used in the analytical column. A high capacity is required for the precolumn, whereas selectivity and efficiency are important for the analytical column. The relationship of sample volume to the adsorbent amount is determined by the substance with the lowest retention. The type and amount of packing material in the precolumn determines the maximum sample volume that can be passed trough the column without sample components breaking through. The break through volume of the phenylhydrazone of formaldehyde was determined

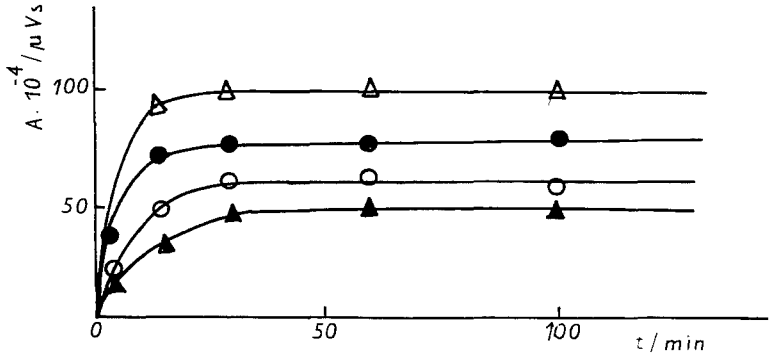

Fig.2. Dependence of reaction yield of 2,4-dinitrophenylhydrazones of C_1- C_4 aldehydes on time.
△ - C_1; ● - C_2; ○ - C_3; ▲ - C_4.

in water at a spiking level 1 ppb by using UV detector at 355 nm. Fig. 3 shows that under the conditions used 2,4-dinitrophenylhydrazone of formaldehyde is quantitatively adsorbed on the 5 μm d_p Separon C18 packing with sample volumes of up to 30 ml. Therefore, when using these conditions quantitative sorption of other derivatives of aldehydes with similar and higher retention can by expected. However, a volume of only 10 ml was used. Compared with a 30 ml sample volume sufficient capacity for sorbent washing is guaranteed.

Filtration of the water sample is a prerequisite for trouble - free operation. Without filtration, the inlet sieve of the enrichment column becomes blocked after a few runs. The pH of the water sample should be between 6 and 7 for the enrichment step and for this reason the tap or river water must be neutralized after the derivatization of aldehydes.

In Figs. 4 and 5 two chromatograms are reproduced to demonstrate blank contribution. Fig.6 shows the chromato-

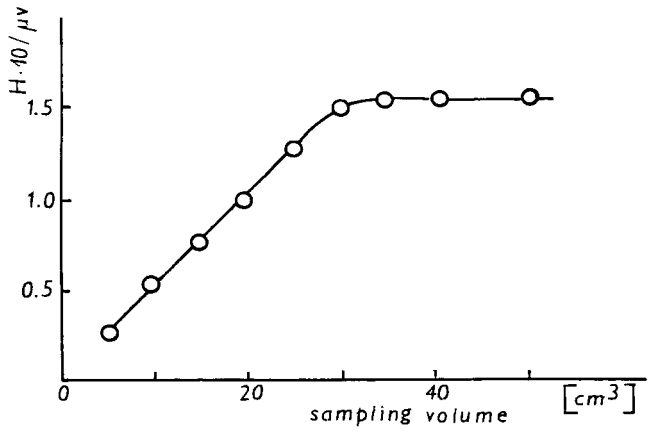

Fig.3. Determination of the break through volume of 2,4-dinitrophenylhydrazone of formaldehyde (1 ppb)
Column Separon C18 (30 x 3.2 mm I.D.)
Flow rate 1.0 ml/min, H - height of the peak

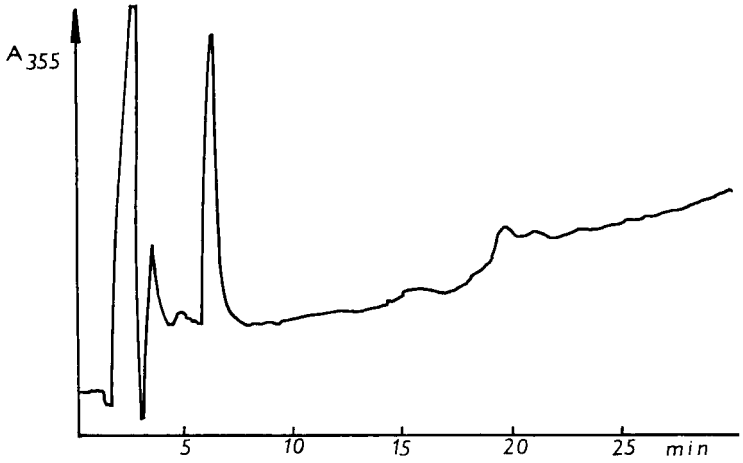

Fig.4.Chromatogram of a blank redistilled water after on-line preconcentration (sampling volume 10 ml, pH = 7)
Chromatographic column Separon SGX C18,
flow rate 0.5 ml/min, mobile phase - see experimental part, UV detection 355 nm.

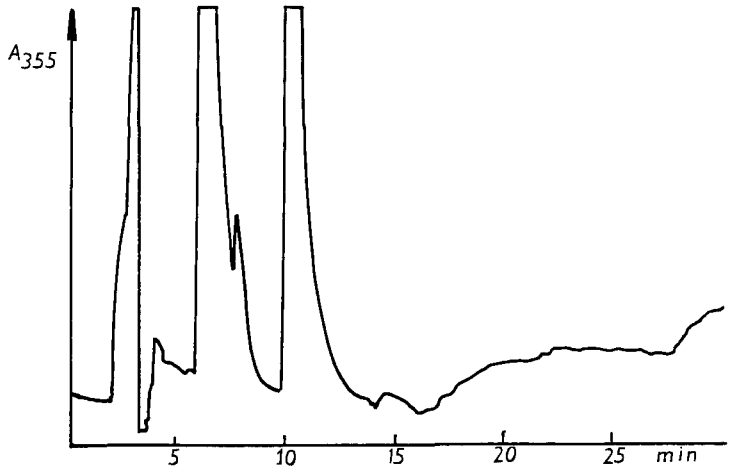

Fig.5.Chromatogram of a blank redistilled water with derivatization reagent after on-line preconcentration (sampling volume 10 ml, pH = 7)
For the chromatographic conditions see Fig. 4.

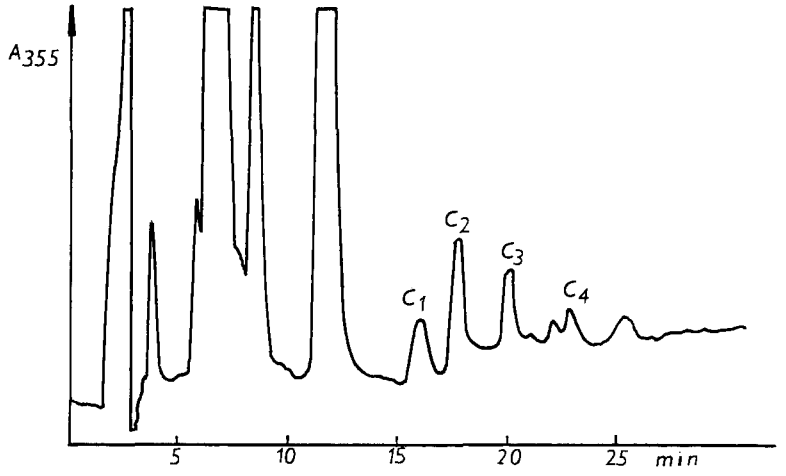

Fig.6.Chromatogram of the spiked redistilled water (1 ppb of aldehydes) after on-line preconcentration (sampling volume 10 ml, pH = 7).
For the chromatographic conditions see Fig. 4.

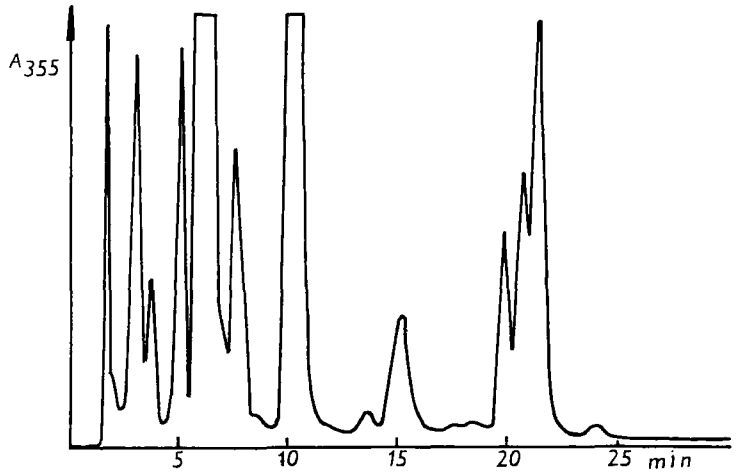

Fig.7.Chromatogram of the river water (Danube) with derivatization reagent after on-line preconcentration. (sampling volume 10 ml, pH = 7.
For the chromatographic conditions see Fig. 4.

gram of spiked redistilled water. A comparison of these chromatograms indicated that 2,4-dinitrophenylhydrazones can be detected in the lower ppb range. Retention times of 2,4-dinitrophenylhydrazones are reproducible with variations usually less than 5%. There is a slight baseline drift associated with the acetonitrile concentration but this does not contribute any additional uncertainties in the quantitative analysis.

Fig. 7 shows the chromatogram of Danube water with derivatization reagent and it is clear that there is no peaks of 2,4-dinitrophenylhydrazones of C_1- C_4 aldehydes. Fig. 8 clearly shows the absence of 2,4- dinitrophenylhydrazones and there can be seen several additional peaks in the spiked sample. This results has led to the conclusion that the additional peaks are the result of reaction

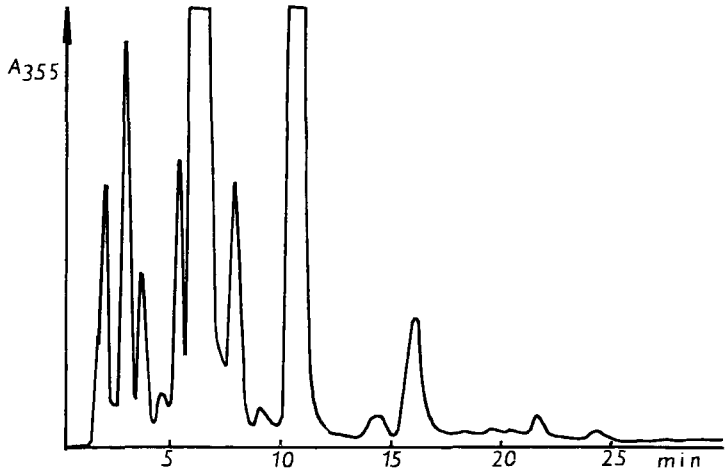

Fig.8.Chromatogram of the spiked river water (1 ppb of aldehydes) after derivatization, on-line preconcentration (sampling volume 10 ml, pH = 7).
For the chromatographic conditions see Fig.4.

products from the reaction of aldehydes with another compounds presented in the river sample. The same conclusion can be done in the case of the tap water where the reaction of aldehydes with chlorine (presented in tap water) can be assumed (at 1 ppb level of aldehydes).

Detection limits afforded by the HPLC method with on line preconcentration are of the order of a nanograms per litre. Lowest limits have been determined using a peak area integrator signal - to - noise ratio of 5. The analytical detection limits range from 50 ppt for formaldehyde to 200 ppt for butyraldehyde In practice, it is obviously extremely difficult to eliminate all impurities in the reagent at levels corresponding to these very low analytical detection limits.

RSD was also determined for quantitative analysis of calibration mixtures and samples prepared in the laborat-

ory. Triplicate injection yielded RSDs of about 10% for all aldehydes at 1 ppb level.

REFERENCES

1. Bailey R.A., Clark H.M., Ferris J.P., Krause S., Strong R.L., Chemistry of the Environment., Academic Pres, New York 1978.
2. Sitting M., Pollution Detection and Monitoring Handbook, Noyes Data Corp., Park Ridge, NJ, 1974.
3. Papa L.J., Turner L.P., J. Chromatogr. Sci., 10, 747 (1972)
4. Selim S., J. Chromatogr. 136, 271 (1977)
5. Kuwata K., Uebori M., Yamasaki Y., J. Chromatogr. Sci., 17, 264 (1979)
6. Carey M.A., Persinger H.E., J. Chromatogr. Sci., 10, 537 (1972)
7. Honed S., Kakehi K., J. Chromatogr. 152, 405 (1978)
8. Heath R.R., Tumlinson J.H., Doolittle R.E., Proveaw A.T., J. Chromatogr. Sci., 13, 380 (1975)
9. Fung.K., Grojean D., Anal. Chem., 53, 168 (1981)
10. Demko P.R., J. Chromatogr., 179, 361 (1979)
11. Nakamura K.I., Asami M., Orita S., Kawada K., J. Chromatogr., 168,221 (1979)
12. Vigh G., Varaga-Pouchy Z., Hlavay J., Petro-Tercza M., Szarfoldi-Salma I., J. Chromatogr., 193, 432 (1980)
13. Kuber R.J., Mopper K., Environ, Sci. Technol., 24, 1477 (1990)

Received: July 29, 1993
Accepted: August 5, 1993

JOURNAL OF LIQUID CHROMATOGRAPHY, 17(3), 589-601 (1994)

ANALYSIS OF METHYL NEODECANAMIDE IN LAKE WATER BY REVERSED-PHASE HIGH PERFORMANCE LIQUID CHROMATOGRAPHY AND GAS CHROMATOGRAPHY-MASS SPECTROMETRY

H. T. RASMUSSEN*, S. K. FRIEDMAN, A. J. MUSTILLI, R. McDONOUGH, AND B. P. McPHERSON
Colgate-Palmolive Company
909 River Road
Piscataway, New Jersey 08855

ABSTRACT

Methyl Neodecanamide (MNDA) has been quantitated in lake water at levels of 0.1 to 1000 ppm. Total recoveries from spiked placebos were 99.8 +/- 2.3% at the 1000 ppm level and 98.3 +/- 4.3% at the 0.1 ppm level (based on 54 determinations at each level). Plots of actual concentrations vs. determined concentrations were linear from 0.07 - 0.13 and 700 - 1300 ppm ($r > 0.999$). Stability of MNDA in lake water was verified by determining the composition by GC/MS immediately after dissolution and after 3 days.

INTRODUCTION

Methyl Neodecanamide (MNDA) is an isomeric distribution of secondary amides with the formula: $C_{11}H_{23}NO$ (Fig. 1). MNDA has

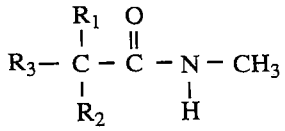

Isomers	R_1	R_2	R_3
	CH_3	CH_3	C_6H_{13}
	CH_3	C_2H_5	C_5H_{11}
	CH_3	C_3H_7	C_4H_9
	C_2H_5	C_2H_5	C_4H_9
	C_2H_5	C_3H_7	C_3H_7

FIGURE 1. Structure of MNDA

shown efficacy as an insect repellent (1) and is for this reason a useful ingredient in household cleaners. To assess ecological toxicity of MNDA, it has been necessary to perform teratology studies on trout, and in support of such studies to quantitate MNDA in lake water at levels of 0.1 - 1000 ppm.

Amides of similar structures to MNDA have previously been separated by GC, either directly (2), or after acylation (3) or alkylation (4). Fatty amides have been separated by normal phase HPLC (5). While each of these methods potentially allow for the analysis of MNDA, reversed-phase HPLC was chosen as the primary method of analysis since it allows for the direct analysis of aqueous samples.

Since ease of operation and the ability to transfer the method to other laboratories were additional requirements, UV detection was used.

MNDA may be monitored at 205 nm, but in order to obtain sub-ppm sensivity, large injection volumes are required, and it is useful to elute MNDA as a single peak to maximize the response. A limitation of eluting MNDA as a single peak is that it is suspected that similar compounds, such as degradation products, may coelute. To ascertain that MNDA composition remained constant, samples were analyzed by GC/MS immediately after dissolution and at the completion of the teratology study (3 days).

EXPERIMENTAL

HPLC

Samples of water used for trout teratology studies and spiked placebos for HPLC analyses were prepared by diluting the appropriate amount of MNDA (synthesized in-house) with lake water (Springborn Laboratories, Switzerland). Samples containing less than 5 ppm of MNDA were diluted to operating concentrations of 0.1 ppm with Milli-Q water (Millipore Corporation, Milford, MA); samples containing from 5 - 1000 ppm MNDA were diluted to operating concentrations of 5 ppm using 50/50 (v/v) Milli-Q water / HPLC Grade methanol (J. T. Baker Inc., Phillipsburg, NJ). Standards were prepared from serial dilution of 100 mg MNDA/100 mL HPLC Grade methanol stock solutions. (Initial solutions were prepared in methanol to expedite dissolution). Stock standards were diluted to an operating concentration of 5 ppm using 50/50 (v/v) Milli-Q

water / HPLC Grade methanol and then in Milli-Q water to an operating concentration of 0.1 ppm.

All HPLC analyses were performed using: a 15 cm x 4.6 mm Dupont Zorbax Rx C8 column (MAC-MOD Analytical, Chadds Ford, PA); a mobile phase consisting of 40/25/35 (v/v/v) acetonitrile (J. T. Baker Inc.)/methanol/water with 10 mM sodium perchlorate (Mallinckrodt Inc., Paris, KY); a Shimadzu Model LC-600 pump (Shimadzu Corporation, Kyoto, Japan) operated at 1 mL/min; and a Shimadzu Model SPD-6A variable wavelength UV detector operated at 205 nm. Samples with operating concentrations of 0.1 ppm were introduced using a Rheodyne Model 7125 injection valve (Rheodyne, Cotati, CA) with a 2 mL loop. Samples with operating concentrations of 5 ppm were introduced using a Waters 712 WISP Autosampler (Waters, Milford, MA) set to inject 200 uL. Chromatograms were monitored using a Kipp and Zonen Model BD 40 strip chart recorder (Baxter, McGaw Park, IL). Quantitation was achieved by manual measurement of the MNDA peak heights.

GC/MS

A 100 mL sample of placebo lake water was extracted with 20 mL of GC/GC/MS Capillary Grade hexane (Baxter, Edison, NJ) to determine if it contained any possible organic contaminants which could coelute with MNDA. The hexane extract was injected into the GC/MS for analysis. A sample of the 1000 ppm MNDA lake water was extracted and analyzed in the same manner. This procedure was run on the first day and third day of the teratology study.

GC/MS was performed using a Finnigan MAT 4605 Gas Chromatograph / Mass Spectrometer (Finnigan, Livingston, NJ). The GC column used for this application was a DB5 FSWCOT, 30 m x 0.25 mm I.D. capillary with a 0.25 um film thickness (J & W Scientific, Folsom, CA). Sample was introduced in the split mode using an injector temperature of 250 °C. Separations were conducted using helium as the carrier gas at a linear velocity of 357 mm/sec. The oven was temperature programmed as follows: Initial temperature = 115°C (hold time = 4 min.); 1st ramp rate = 4.0°C/min. to 170°C; 2nd ramp rate = 40.0°C/min. to 290°C; 3rd ramp rate = 20.0°C/min. to 295°C. Electron Impact (EI) mass spectra (Electron Energy = 70ev) were collected from 28 to 500 AMU using an Ionizer temperature of 130°C and an Electron Multiplier voltage of -1750 V. The Mass Spectrometer was calibrated daily with FC43 ($C_{12}F_{17}N$; MW=671g/mole).

RESULTS AND DISCUSSION

Several constraints were placed on the choice of HPLC operating conditions for the analysis of MNDA at the 0.1 ppm level. To obtain adequate sensitivity a detection wavelength of 205 nm was required along with the use of large (2 mL) injection volumes. Additionally, it was desirable to elute the MNDA isomers as a single peak, resolved from the matrix, to maximize sensitivity.

When large aqueous samples are loaded onto a reversed-phase column, less-polar organics concentrate at the column inlet during the

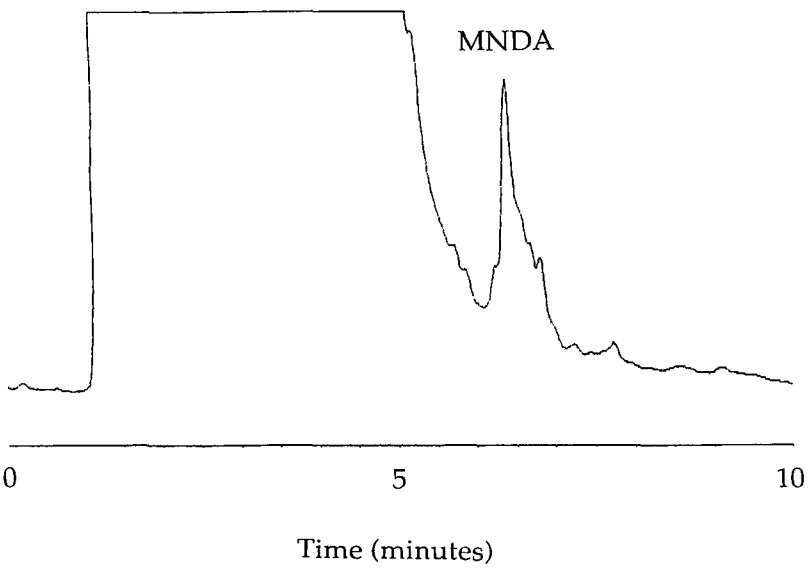

FIGURE 2. Chromatogram of a 0.1 ppm MNDA in Lake water sample. Conditions - Mobile phase: 40/25/35 (v/v/v) acetonitrile / methanol/water with 10 mM sodium perchlorate. Column: 15 cm x 4.6 mm Dupont Zorbax Rx C8 column. Flow rate: 1 mL /min. Detection: UV at 205 nm. Injection volume: 2 mL.

injection and no deleterious volume induced band-broadening is incurred (6). Previous studies have shown that base deactivated column packings such as Zorbax Rx and the addition of perchlorate minimize peak tailing of basic compounds (7-8). Consequently, it was decided to use a Zorbax Rx C8 column and a mobile phase containing 10 mM sodium perchlorate. The use of 205 nm as a detection wavelength limited the choice of solvents to methanol, propanol, acetonitrile and water. A mobile phase consisting of 40/25/35 (v/v/v) acetonitrile / methanol / water with 10 mM sodium perchlorate minimized the separation of MNDA isomers, but provided

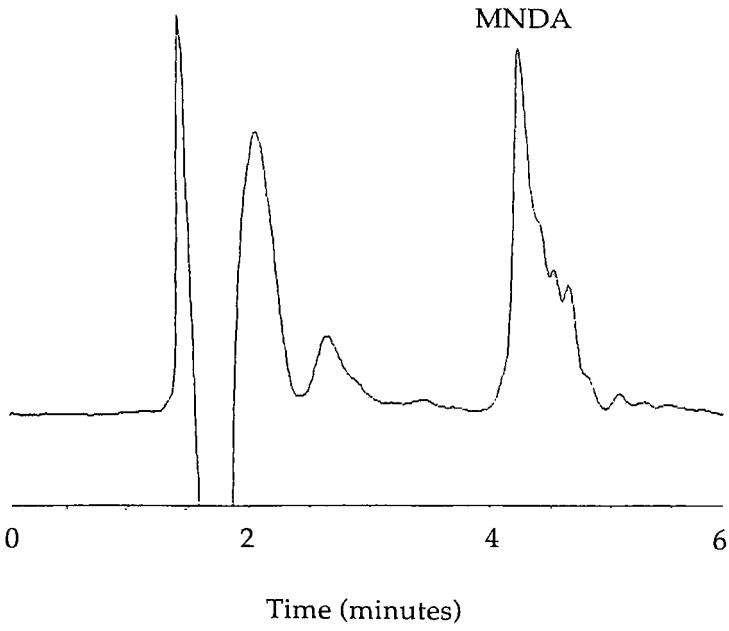

FIGURE 3. Separation of a 1000 ppm MNDA in Lake water sample (Sample was diluted to 5 ppm for analysis). Conditions are as for Fig. 2, except that the injection volume was reduced to 200 uL.

separation from the matrix. A chromatogram of a 0.1 ppm sample is shown in Figure 2.

The method as outlined was used for samples containing up to 5 ppm of MNDA, by diluting the samples to working concentrations of 0.1 ppm. To make the method applicable to the analysis of MNDA at concentrations of up to 1000 ppm, without the need of excessive sample dilution, the method was modified slightly. Samples were diluted to 5 ppm and injected using a 200 uL loop. A chromatogram of a 1000 ppm sample analyzed using the modified method is shown in Figure 3.

To validate the HPLC methods spiked placebos were prepared fresh daily, in triplicate, at concentrations of 0.07, 0.10, 0.13, 700, 1000 and 1300 ppm and analyzed. This procedure was performed by two operators on six non-consecutive days (3 operator days per analyst) for a total of 18 independent analyses at each of the 6 concentrations. To determine recoveries at the 0.1 ppm level the data obtained for 0.07, 0.1 and 0.13 ppm was pooled such that the 0.1 ppm level recovery is based on 54 determinations. (The 1000 ppm data was treated in the same way). The use of 18 determinations at each of the 70, 100, and 130% target concentration has the advantage over analyzing 54 samples at the 100% level of allowing for the determination of linearity.

The results obtained for the validation (Tables I and II) show overall recoveries at the 0.1 and 1000 ppm levels of 98.3 +/- 4.3% and 99.8 +/- 2.3%, respectively. Estimates of variance stemming from analyst-to-analyst , day-to-day and error contibutions were, as shown in the Tables, acceptable at both concentrations. Furthermore, plots of the actual concentration vs. the measured concentration were linear for both levels ($r > 0.999$).

Recoveries for other MNDA concentrations were not determined explicitly. However, it likely that these would not be worse than those reported since the possible sources of variance are maximized for the above levels. For samples containing 0.1 - 5 ppm MNDA, the largest source of variance stems from interference from the lake water matrix; this variance is maximized when the samples are undiluted and the MNDA to matrix concentration is smallest. For samples containing from 5 - 1000

TABLE I

Recoveries for 0.1 ppm MNDA samples.

Operator	Day	Level (% target)	% recovery		
			1	2	3
1	1	70 %	98.9	97.9	99.0
1	1	100 %	101.0	95.1	94.7
1	1	130 %	99.0	100.7	97.5
2	1	70 %	95.5	96.9	102.2
2	1	100 %	90.9	97.8	99.5
2	1	130 %	95.0	93.5	100.5
1	2	70 %	101.0	107.8	106.6
1	2	100 %	99.5	107.1	98.8
1	2	130 %	102.7	100.8	100.2
2	2	70 %	90.2	105.7	105.4
2	2	100 %	93.1	98.3	96.1
2	2	130 %	93.1	102.8	92.1
1	3	70 %	100.3	101.7	105.9
1	3	100 %	92.8	98.8	95.5
1	3	130 %	95.5	96.7	100.2
2	3	70 %	97.3	98.7	100.9
2	3	100 %	98.3	93.6	94.4
2	3	130 %	93.9	93.2	91.5

Overall mean +/- std. dev. = 98.3 +/- 4.3 %
Analyst-to-analyst variance = 1.96 %
Day-to-day variance = 1.46 %
Variance due to error = 3.52 %

TABLE II

Recoveries for 1000 ppm MNDA samples (diluted to 5 ppm).

Operator	Day	Level (% target)	% recovery		
			1	2	3
1	1	70 %	102.0	100.4	100.0
1	1	100 %	100.0	99.2	99.5
1	1	130 %	98.0	97.7	100.6
2	1	70 %	102.8	102.3	99.1
2	1	100 %	101.3	101.0	101.7
2	1	130 %	99.7	100.8	100.7
1	2	70 %	101.8	100.1	101.1
1	2	100 %	101.1	101.8	101.6
1	2	130 %	101.0	99.8	99.7
2	2	70 %	101.6	102.7	101.8
2	2	100 %	99.6	99.8	100.2
2	2	130 %	99.2	99.3	99.1
1	3	70 %	100.0	100.9	97.1
1	3	100 %	99.2	98.3	101.1
1	3	130 %	98.8	98.1	98.6
2	3	70 %	102.1	99.2	100.8
2	3	100 %	88.1	97.2	98.4
2	3	130 %	93.8	97.2	101.8

Overall mean +/- std. dev. = 99.8 +/-2.3 %
Analyst-to-analyst variance = 0 %
Day-to-day variance = 1.27 %
Variance due to error = 1.99 %

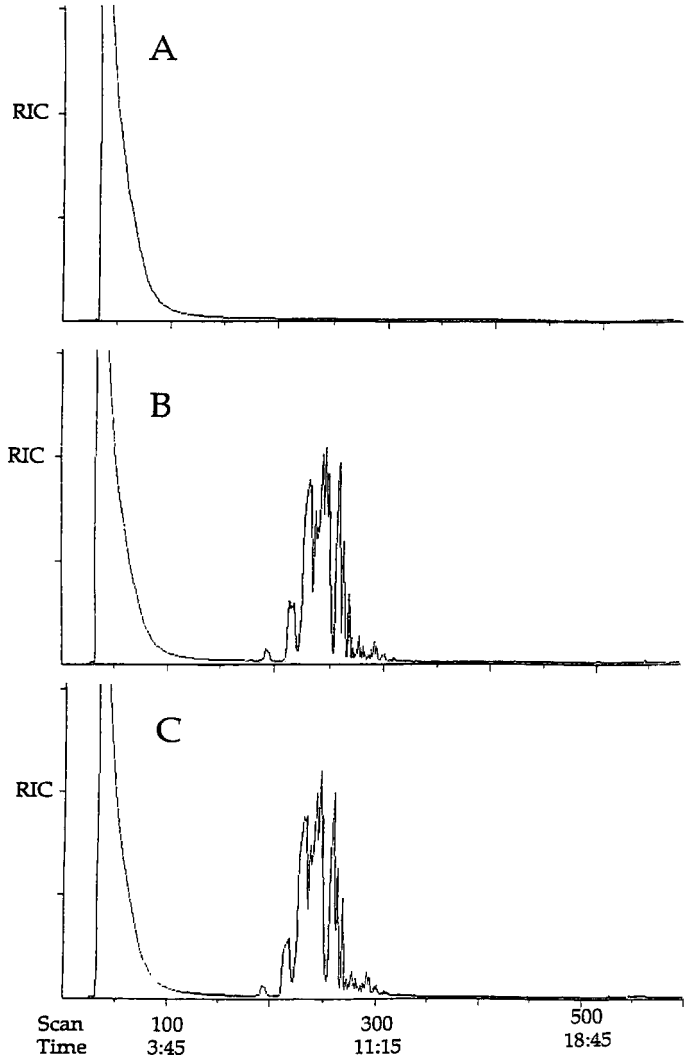

FIGURE 4. RIC Scans of (A) Lake water, (B) Lake water with 1000 ppm MNDA immediately after dissolution, (C) Lake water with 1000 ppm MNDA after 3 days.

ppm MNDA the influence of the matrix is minimal. Consequently, the largest variance is predicted to stem from the dilutions required to reduce the MNDA to the operating concentration of 5 ppm.

On the basis of the reproducibility observed for the HPLC analyses, the method was considered suitable for supporting teratology, providing that any MNDA degradates formed during the study did not coelute with MNDA and thereby provide a higher than actual assay. To verify MNDA stability, GC/MS analyses were performed. The GC/MS data showed no interfering peaks or organic contaminants present in the blank lake water (Figure 4a). The RIC Scans obtained immediately after dissolution and after 3 days for the 1000 ppm MNDA lake water samples are shown in Figures 4b and 4c. The comparison of the RIC Scans and Mass Spectral Data for the 1000 ppm MNDA lake water samples are identical and match exactly what is obtained when MNDA is prepared directly in hexane and analyzed.

CONCLUSIONS

A HPLC method has been developed for the analysis of MNDA in lake water at levels of 0.1 to 1000 ppm. The method has been validated by recoveries from spiked placebo and by GC/MS data which confirms the stability of MNDA in Lake water. The latter data is important since it dismisses the possibility of contributions to the apparent MNDA level by MNDA degradates.

REFERENCES

1. R. J. Steltenkamp, R. L. Hamilton, R. A. Cooper, C. Schal, J. Med. Entomol., 29: 141 (1992)

2. C. N. Wang, L. D. Metcalfe, J. Am. Oil Chem. Soc., 61: 581 (1984)

3. O. Gyllenhaal, H. Ehrsson, J. Chromatogr., 107: 327 (1975)

4. E. Roder, W. Stuthe, Z. Anal. Chem., 266: 358 (1973)

5. J. L. Jasperse, J. Am. Oil Chem. Soc., 65: 1804 (1988)

6. L. R. Snyder, J. J. Kirkland, Introduction to Modern Liquid Chromatography, 2nd ed., Wiley, New York, 1979. p. 565

7. C. B. Huang, J. Liq. Chromatogr., 10: 1103 (1987)

8. R. Gloor, E. L. Johnson, J. Chromatogr. Sci., 15: 413 (1977)

Received: May 12, 1993
Accepted: July 8, 1993

JOURNAL OF LIQUID CHROMATOGRAPHY, 17(3), 603-617 (1994)

HIGH PERFORMANCE LIQUID CHROMATOGRAPHIC DETERMINATION OF 2-FURALDEHYDE AND 5-HYDROXYMETHYL-2-FURALDEHYDE IN PROCESSED CITRUS JUICES

F. LO COCO[1], C. VALENTINI[2], V. NOVELLI[1], AND L. CECCON[3]

[1]*Dipartimento di Scienze e Tecnologie Chimiche*
Università di Udine
Via Cotonificio 108
33100 Udine, Italy

[2]*Laboratorio Chimico delle Dogane di Venezia*
Via Cà Marcello 15
30172 Mestre, Italy

[3]*Dipartimento di Economia e Merceologia*
delle Risorse Naturali e della Produzione
Università di Trieste
Via Valerio 6
34127 Trieste, Italy

ABSTRACT

The occurrence of 2-furaldehyde (F) and 5-hydroxymethyl-2-furaldehyde (HMF) in processed citrus juices is an indication of quality deterioration. A close relationship between flavor changes and F content exists, while HMF can give rise to browning reactions. Both F and HMF are formed during heat processing or storage at improper temperatures. The detection of these compounds becomes more and more important as aseptic processing and packaging of citrus juices are becoming widespread. Aseptic packaging allows higher temperatures during distribution and storage to be employed without microbial spoilage, but off-flavors develop as citrus products are exposed to these conditions.

In this paper a method of determination by high performance liquid chromatography (HPLC) is described. The method is based on the formation of the 2,4-dinitrophenylhydrazones of carbonyl compounds and subsequent reversed-phase separation of these derivatives. Derivatization is carried out by utilizing an acidic solution of 2,4-dinitrophenylhydrazine in acetonitrile. Precipitation of the derivatives of carbonyl compounds is thus avoided, and direct injection of the sample into the HPLC system is allowed. The determination offers a high specificity and a detection limit of the order of 10^{-8} mol/l for both analytes. Recoveries from an orange juice spiked at different levels are quantitative. Reproducibility data are presented.

INTRODUCTION

The occurrence of 2-furaldehyde (F) and 5-hydroxymethyl-2-furaldehyde (HMF) in processed citrus juices is an indication of quality deterioration[1-3]. Citrus juices undergo flavor, taste, color and nutritional changes when stored at warm temperatures and/or for prolonged periods of time[3-7]. Both F and HMF are formed during thermal processing or storage at improper temperatures; for this reason both are useful indicators of temperature abuse in processed citrus juices[3,6,8-11]. In particular, F is virtually absent in fresh citrus juices, whereas large amounts have been found in juices stored at improper temperatures[4,6,10]. A close relationship between flavor changes and F content has been demonstrated; for this reason the F content is useful as an off-flavor indicator[4,6-8]. On the other hand, HMF is correlated with browning reactions[3,8,10-12]. The detection and quantitative determination of these components become more and more important as aseptic processing and packaging of citrus juices assert themselves[6]. Aseptic packaging allows higher temperatures during distribution and storage of the product to be adopted without microbial spoilage, but off-flavors and loss of nutritional value may develop as citrus juices are exposed to these conditions[6].

The classical methods for the quantitative determination of these components in citrus juices are based on colorimetric measurements[1,2,4,6-9,13,14]. These methods I) are time consuming, II) make use of toxic or anyhow hazardous chemicals, III) require a strict control of both reaction time and temperature, since the instability of the colored reaction product may lead to low recoveries and wide statistical variations of the results and IV) no one of the methods is specific[1,2,6,8,9,12-14]. Gas chromatographic procedures have also been proposed for the determination of F and/or HMF not only in citrus juices, but also in other types of food matrices, in particular alcoholic beverages; they offer much higher specificity, sensitivity and speed[5,15-17]. In recent years, high performance liquid chromatographic (HPLC) methods have also been proposed[1-3,6,8,10,18]. These methods are less time consuming, offer improved accuracy, sensitivity and specificity as compared to the colorimetric procedures and utilize less hazardous reagents[3,6,8].

In this paper a HPLC method is described that is based on the formation of the 2,4-dinitrophenylhydrazones (DNPH-ones) of carbonyl compounds. The DNPH-ones obtained are then separated by reversed-phase HPLC and determined with spectrophotometric detection.

MATERIALS

Standards and Reagents

2-Furaldehyde (Prolabo) was doubly distilled and kept in a refrigerator at 0-4°C.

Both 5 hydroxymethyl-2-furaldehyde and 2,4-dinitrophenylhydrazine (Prolabo) were purified by successive crystallizations with HPLC-grade methanol and kept in a refrigerator at 0-4°C.

The Carrez clarification reagent (Carlo Erba) consisted of a 15% (w/v) solution of Carrez I (potassium ferrocianide) and of a 30% (w/v) solution of Carrez II (zinc sulfate).

Perchloric acid (70%) was obtained from Prolabo and acetonitrile (HPLC-grade) from Carlo Erba. Water was distilled, deionized and further purified with a Milli-Q system (Millipore).

2,4-Dinitrophenylhydrazine Solution

A stock reagent solution containing 2.5×10^{-3} mol/l of 2,4-dinitrophenylhydrazine (DNPH) was prepared in acetonitrile. By successive dilutions reagent solutions containing down to 2.5×10^{-6} mol/l of 2,4-dinitrophenylhydrazine were prepared.

2-Furaldehyde and 5-Hydroxymethyl-2-furaldehyde Standard Solutions

A stock standard solution containing 10^{-2} mol/l of both F and HMF was prepared in water. By successive dilutions working standard solutions containing down to 10^{-7} mol/l of both analytes were prepared.

Two aqueous solutions containing 10^{-4} mol/l of F and HMF respectively were also prepared.

METHODS

Calibration Graphs

A 5-ml volume of each working standard solution and 4 ml of a 5 times more concentrated DNPH solution were transferred into a 10-ml glass-stoppered volumetric flask. A few drops of perchloric

acid were added to pH 1 and the volume was made up to the mark with the DNPH solution. The solution was kept on a magnetic stirrer at room temperature for at least 25 min, then 10 μl of the solution were immediately injected into the HPLC system.

Sample Clarification

The procedure described by Lee et al. was adopted with some modifications[1]. 10 ml of juice were pipetted into a 50-ml beaker. 2 ml of Carrez I and 2 ml of Carrez II solution were added slowly with gentle mixing. After standing for 5 min, the mixture was filtered through a Milli-Q system, under suction, into a 25-ml volumetric flask, the filter was washed with distilled water, washings were added to the filtrate and the volume taken up to the mark with distilled water.

Preparation of the Derivatives of Carbonyl Compounds

The same procedure described under **Calibration Graphs** was applied to a 5-ml volume of clarified juice instead of working standard solution.

Determination of Recoveries

To 10 ml of a sample of orange juice was added a 2.5 ml volume of a working standard solution containing from 10^{-2} down to 10^{-6} mol/l of both F and HMF. The sample obtained was processed as described under **Sample Clarification**. A 5-ml volume of the so-obtained clarified juice was subjected to the same procedure described under **Preparation of the Derivatives of Carbonyl Compounds**. Each determination was carried out in triplicate; each solution was injected twice.

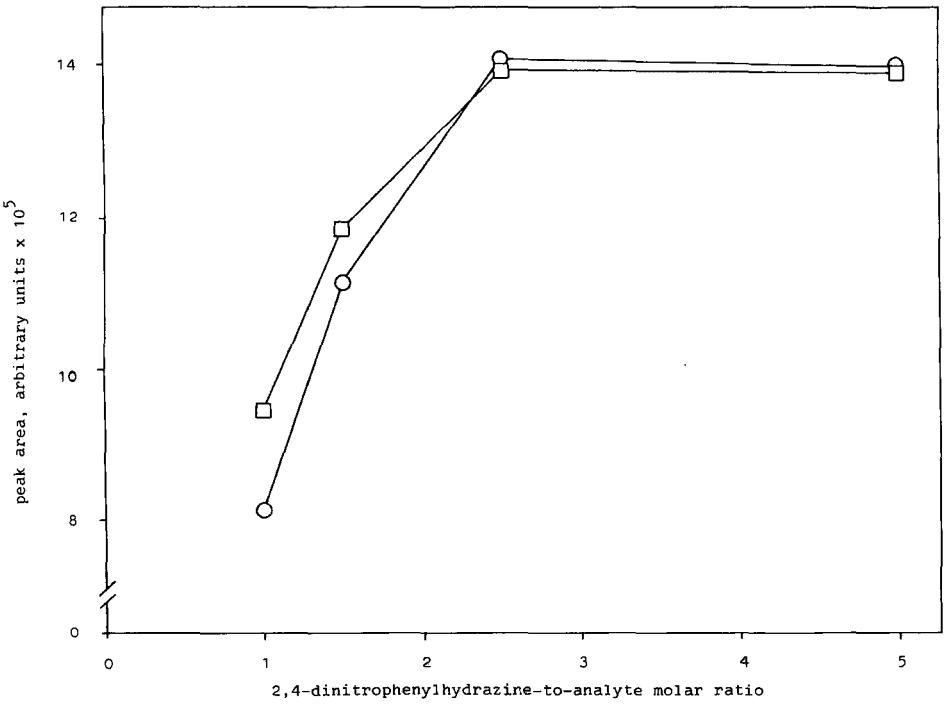

Figure 1. Conversion of 2-furaldehyde (□) and 5-hydroxymethyl-2-furaldehyde (○) to their 2,4-dinitrophenylhydrazones as a function of the 2,4-dinitrophenylhydrazine/2-furaldehyde and 2,4-dinitrophenylhydrazine/5-hydroxymethyl-2-furaldehyde molar ratios. pH of the medium = 1; reaction time = 30 min.

High Performance Liquid Chromatography

A Spectra-Physics Model 8700 high performance liquid chromatograph, equipped with a Knauer Model 8700 variable-wavelength spectrophotometric detector and a 10-μl loop, was used. A Supelcosil LC-18 stainless-steel column (250 x 4.6 mm I.D.; film thickness 5 μm) was employed. Analyses were carried out

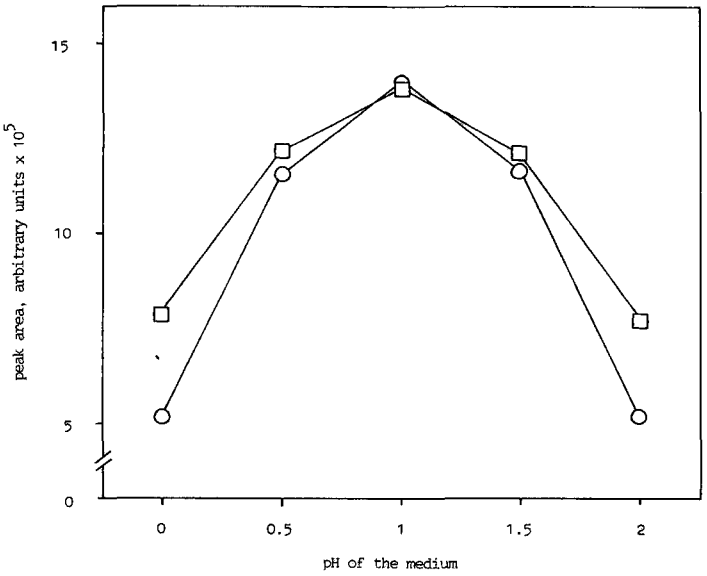

Figure 2. Conversion of 2-furaldehyde (□) and 5-hydroxymethyl-2-furaldehyde (○) to their 2,4-dinitrophenylhydrazones as a function of the acidity of the medium.
2,4-Dinitrophenylhydrazine/2-furaldehyde and 2,4-dinitrophenylhydrazine/5-hydroxymethyl-2-furaldehyde molar ratio = 2.5; reaction time = 30 min.

isocratically at room temperature with acetonitrile-water (55:45, v/v) as the eluent at a flow rate of 1 ml/min. The spectrophotometric detector was set at 385 nm.

Peak areas were determined by means of a Spectra-Physics Model 4270 integrator.

RESULTS

The optimum experimental conditions for obtaining the DNPH-ones of carbonyl compounds present in the sample under

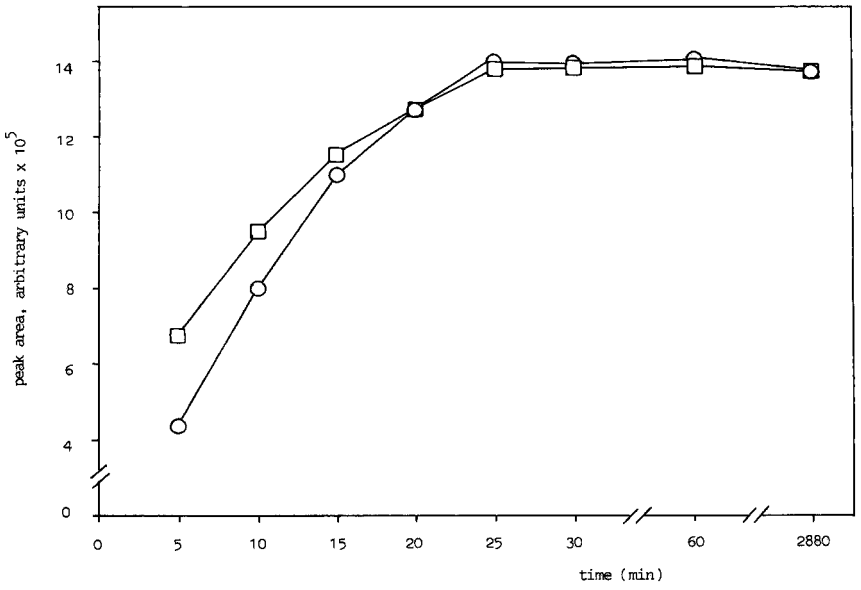

Figure 3. Conversion of 2-furaldehyde (□) and 5-hydroxymethyl-2-furaldehyde (○) to their 2,4-dinitrophenylhydrazones as a function of reaction time.
2,4-Dinitrophenylhydrazine/2-furaldehyde and 2,4-dinitrophenylhydrazine/5-hydroxymethyl-2-furaldehyde molar ratio = 2.5; pH of the medium = 1.

examination were evaluated. We took into account the possible influence of three variables. They are: 1) the DNPH-to-analyte molar ratio, 2) the acidity of the medium and 3) the reaction time. The results obtained are shown in Figures 1-3.

Calibration graphs were obtained for the quantitative determination of both F and HMF, and are shown in Figure 4.

A typical separation of the DNPH-ones of carbonyl compounds from a sample of orange juice is shown in Figure 5.

Recoveries were determined by adding known amounts of both analytes to a sample of orange juice. The amount found in respect

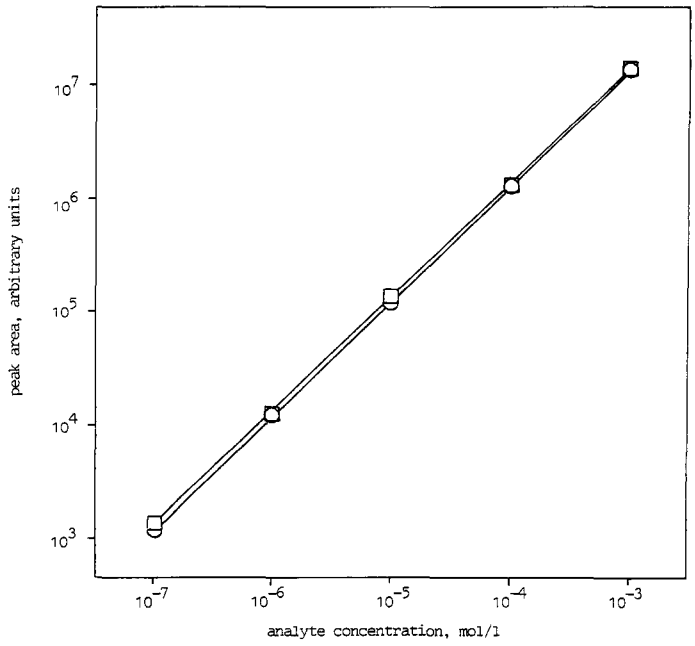

Figure 4. Calibration graph of peak area of the 2,4-dinitrophenylhydrazones of 2-furaldehyde (□) and 5-hydroxymethyl-2-furaldehyde (○) versus concentrations of the analytes. 2,4-Dinitrophenylhydrazine/2-furaldehyde and 2,4-dinitrophenylhydrazine/5-hydroxymethyl-2-furaldehyde molar ratio = 2.5; pH of the medium = 1; reaction time = 30 min.

of the sum between the amount added and that originally present in the sample represents the recovery. The results obtained are shown in Table 1.

Reproducibility was evaluated by carrying out the determination six times on the same commercial sample of orange juice over a period of 48 h; each solution was injected twice.

The procedure was applied to the determination of F and HMF in different samples of commercial citrus juices; each sample was analyzed in duplicate. The results are summarized in Table 2.

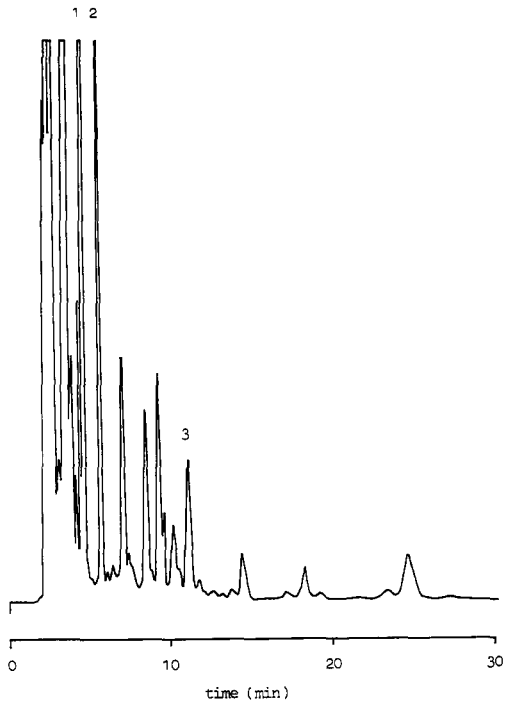

Figure 5. High performance liquid chromatographic separation of the 2,4-dinitrophenylhydrazones of carbonyl compounds from a sample of orange juice. For conditions of analysis see Methods. Peak identification: 1) 2,4-dinitrophenylhydrazine; 2) 2,4-dinitrophenylhydrazone of 5-hydroxymethyl-2-furaldehyde; 3) 2,4-dinitrophenylhydrazone of 2-furaldehyde.

DISCUSSION

Optimization of the Derivatization Step

The key to the determination of F and HMF in citrus juices lies in the sample preparation, since the matrix contains compounds that may interfere with the analytes[1,6]. For this purpose,

TABLE 1

Recoveries of 2-Furaldehyde and 5-Hydroxymethyl-2-furaldehyde Added to Orange Juice*.

Originally present	Added	Found	Recovery (%)
Concentration of 2-furaldehyde (mol/l)			
8.50×10^{-6}	1.0×10^{-7}	$(8.30 \pm 0.26) \times 10^{-6}$	96 ± 3
8.50×10^{-6}	1.0×10^{-6}	$(9.12 \pm 0.29) \times 10^{-6}$	96 ± 3
8.50×10^{-6}	1.0×10^{-5}	$(1.74 \pm 0.04) \times 10^{-5}$	94 ± 2
8.50×10^{-6}	1.0×10^{-4}	$(1.01 \pm 0.03) \times 10^{-4}$	93 ± 3
8.50×10^{-6}	1.0×10^{-3}	$(9.38 \pm 0.03) \times 10^{-4}$	93 ± 3
Concentration of 5-hydroxymethyl-2-furaldehyde (mol/l)			
5.50×10^{-5}	1.0×10^{-6}	$(5.38 \pm 0.22) \times 10^{-5}$	96 ± 4
5.50×10^{-5}	1.0×10^{-5}	$(6.11 \pm 0.20) \times 10^{-5}$	94 ± 3
5.50×10^{-5}	1.0×10^{-4}	$(1.44 \pm 0.05) \times 10^{-4}$	93 ± 3
5.50×10^{-5}	1.0×10^{-3}	$(0.99 \pm 0.04) \times 10^{-3}$	94 ± 4

*Mean of six determinations ± SD

TABLE 2

Concentrations of 2-Furaldehyde and 5-Hydroxymethyl-2-furaldehyde Found in Some Commercial Citrus Juices*

Sample	Concentration of 2-furaldehyde (mol/l)	Concentration of 5-hydroxymethyl-2-furaldehyde (mol/l)
Orange 1**	$(8.50 \pm 0.17) \times 10^{-6}$	$(5.50 \pm 0.11) \times 10^{-5}$
Orange 2	$(1.49 \pm 0.04) \times 10^{-5}$	$(1.19 \pm 0.04) \times 10^{-4}$
Orange 3	$(1.29 \pm 0.05) \times 10^{-5}$	$(1.61 \pm 0.08) \times 10^{-4}$
Grapefruit 1	$(6.51 \pm 0.19) \times 10^{-6}$	$(7.01 \pm 0.28) \times 10^{-5}$
Grapefruit 2	$(1.21 \pm 0.05) \times 10^{-5}$	$(8.51 \pm 0.26) \times 10^{-5}$
Grapefruit 3	$(1.51 \pm 0.04) \times 10^{-5}$	$(1.11 \pm 0.03) \times 10^{-4}$
Lemon 1	$(1.09 \pm 0.02) \times 10^{-5}$	$(5.79 \pm 0.13) \times 10^{-5}$
Lemon 2	$(1.11 \pm 0.03) \times 10^{-5}$	$(5.51 \pm 0.15) \times 10^{-5}$
Tangerine 1	$(1.21 \pm 0.05) \times 10^{-5}$	$(1.21 \pm 0.05) \times 10^{-4}$
Tangerine 2	$(1.29 \pm 0.06) \times 10^{-5}$	$(1.11 \pm 0.04) \times 10^{-4}$

*Mean of six determinations ± SD
**Mean of twelve determinations ± SD

procedures such as distillation[4,6,7,14] or solvent extraction[5,8] or filtration of the juice[2,18] have been developed. However, preliminary distillation allows recovery of only F, yields are low, variable and other volatile components are collected, as well[2,6,7,14]. Solvent extraction is affected by incomplete recoveries and is not specific for the analytes of interest[1]. Filtration is certainly the less troublesome procedure, but at the same time it does not allow the elimination of any of the possibly interfering compounds. A preliminary clean-up procedure that involves juice clarification by means of the Carrez solution, already described by other Authors, allows the elimination of pulp, proteins, fats and carotenoids[1,10,12].

All the HPLC methods so far proposed for the determination of F and/or HMF in citrus juices provide for the injection of the sample without derivatization[1-3,6,8,10,18]. However, we made the clear juice undergo derivatization in order to obtain the DNPH-ones of the carbonyl compounds present. The sensitivity of the method can therefore be improved. This type of derivatization has been already employed by several Authors for the determination of F and/or HMF in other kinds of food matrices[19-21].

The DNPH-ones are usually obtained by employing an excess of DNPH aqueous solution in the presence of hydrochloric acid. Nevertheless, the utilization by us of an acetonitrile DNPH solution offers the advantage of obtaining a solution of the derivatives that may be injected directly into the HPLC system[21]. Long and tedious steps, such as filtration and washing of the derivatives obtained in aqueous solution and preparation of a derivative solution in a suitable solvent before the HPLC determination, may therefore be avoided[21]. The use of perchloric acid instead of hydrochloric acid is due to its higher solubility in acetonitrile[21].

The derivatization step was optimized by us with respect to three parameters: 1) the DNPH-to-analyte molar ratio, 2) the acidity of the medium and 3) the reaction time. For this purpose, the amounts of the derivatives obtained were evaluated on two

aqueous standard solutions containing respectively F and HMF both 10^{-4} mol/l. As can be seen in Figures 1-3, the derivatization reaction is quantitative when the reagent-to-analyte ratio is at least 2.5:1 for both analytes and the acidity of the medium, as evaluated with a pH-meter, is about 1. Under these conditions, both F and HMF are quantitatively converted into their DNPH-ones within 25 min. The derivatives obtained are stable at room temperature for at least 48 h.

Calibration

The calibration graphs were obtained by employing standard solutions of both F and HMF under optimum experimental conditions as described in the preceding section. As may be seen in Figure 4, a straight line was obtained for both analytes over a wide range of examined concentrations, which represent values typically found in real samples. By setting the detector wavelength at the maximum absorbance of the derivatives of both F and HMF, it is possible to determine the detection limit as $3\sigma/S$[22], where S is the sensitivity, which is 1.39×10^{10} for F and 1.26×10^{10} for HMF as obtained from the calibration graphs, and σ is the peak threshold of the integrator, which was set by us at 100. The detection limits are therefore 2.2×10^{-8} mol/l for F and 2.4×10^{-8} mol/l for HMF.

Specificity, Recovery and Reproducibility

The method shows a high specificity because, under the described conditions, the derivatives of both F and HMF are well separated with respect to the other carbonyl compounds present in the sample under examination, as Figure 5 shows.

DNPH must be at least 20 times more concentrated than the analytes to be determined in the analyses of real samples, as an aliquot of the reagent is employed in the derivatization of the

other carbonyl compounds present. In all the samples so far examined, a 1:20 ratio was sufficient, as I) a large peak of the DNPH excess appears in the chromatogram and II) area increments were not obtained for the two analytes of interest by utilizing a 1:50 analyte-to-reagent ratio.

Recoveries of both F and HMF were determined on a fresh orange juice. The juice was selected on the basis of its low content of both F and HMF (8.50×10^{-6} and 5.50×10^{-5} mol/l respectively), two of the lowest levels among those which we found in real samples. As Table 1 shows, recoveries for both analytes ranged from 93 to 96%. Lee et al. have already reported that no loss of both F and HMF was observed during the clarification step of citrus juices by employing the Carrez solution[1].

Reproducibility was good: the average concentration of F was 8.50×10^{-6} mol/l, with a standard deviation of 1.7×10^{-7} mol/l and a relative standard deviation of 2%. The average concentration of HMF was 5.50×10^{-5} mol/l, with a standard deviation of 1.1×10^{-6} mol/l and a relative standard deviation of 2%.

Application

As may be seen in Table 2, in all the samples analyzed the amount of HMF was one order of magnitude greater than the amount of F. The results obtained are in agreement with those already reported by other Authors on processed citrus juices.

REFERENCES

1) H.S. Lee, R.L. Rouseff, S. Nagy, J. Food Sci., 51: 1075-1076 (1986).

2) Z.-F. Li, M. Sawamura, H. Kusunose, Agric. Biol. Chem., 52: 2231-2234 (1988).

3) B. Dauberte, J. Estienne, M. Guerere, N. Guerra, Ann. Falsif. Expert. Chim. Toxicol., 83: 231-253 (1990).

4) S. Nagy, V. Randall, J. Agric. Food Chem., 21: 272-275 (1973).

5) J.H. Tatum, S. Nagy, R.E. Berry, J. Food Sci., 40: 707-709 (1975).

6) J.E. Marcy, R.L. Rouseff, J. Agric. Food Chem., 32: 979-981 (1984).

7) H.L. Dinsmore, S. Nagy, J. Assoc. Off. Anal. Chem., 57: 332-335 (1974).

8) R.M. Mijares, G.L. Park, D.B. Nelson, R.C. McIver, J. Food Sci., 51: 843-844 (1986).

9) D. Tu, S. Xue, C. Meng, A. Espinosa-Mansilla, A. Munoz de la Pena, F. Salinas Lopez, J. Agric. Food Chem., 40: 1022-1025 (1992).

10) H.S. Lee, S. Nagy, J. Food Sci., 53: 168-172,180 (1988).

11) H.S. Lee, S. Nagy, Food Technol., 42, No. 11: 91-94,97 (1988).

12) S. Meydav, Z. Berk, J. Agric. Food Chem., 26: 282-285 (1978).

13) A. Espinosa-Mansilla, F. Salinas, J.J. Berzas Nevado, J. Assoc. Off. Anal. Chem., 75: 678-684 (1992).

14) C.P. Beeman, J. Assoc. Off. Anal. Chem., 70: 601-602 (1987).

15) M. Masuda, M. Yamamoto, Y. Asakura, J. Food Sci., 50: 264-265 (1985).

16) J. Shimizu, M. Watanabe, Agric. Biol. Chem., 43: 1365-1366 (1979).

17) K. MacNamara, J. High Resolut. Chromatogr. Chromatogr. Commun., 7: 641-643 (1984).

18) H.-J. Kim, M. Richardson, J. Chromatogr., 593: 153-156 (1992).

19) E. Puputti, P. Lehtonen, J. Chromatogr., 353: 163-168 (1986).

20) S. Bloeck, A. Kreis, O. Stanek, Alimenta, 25: 23-28 (1986).

21) F. Lo Coco, L. Ceccon, C. Valentini, V. Novelli, J. Chromatogr., 590: 235-240 (1992).

22) D.L. Massart, A. Dijkstra, L. Kaufman, Evaluation and Optimization of Laboratory Methods and Analytical Procedures, Elsevier, Amsterdam, 1978.

Received: March 19, 1993
Accepted: August 10, 1993

JOURNAL OF LIQUID CHROMATOGRAPHY, 17(3), 619-632 (1994)

FLUORIMETRIC DETECTION OF MICROSOMAL LAURIC ACID HYDROXYLATIONS USING HIGH-PERFORMANCE LIQUID CHROMATOGRAPHY AFTER SELECTIVE SOLVENT PARTITIONING AND ESTERIFICATION WITH 1-PYRENYLDIAZOMETHANE

STEVEN R. MASON, LEIGH C. WARD, AND PAUL E. B. REILLY
Department of Biochemistry
Molecular Biosciences Building
University of Queensland
Brisbane, Queensland 4072, Australia

ABSTRACT

A novel and simple method for determining microsomal lauric acid hydroxylase activity is presented. Lauric acid and hydroxy-metabolites are separated using differential acid/base solubilities coupled to solvent partitioning. After esterification with 1-pyrenyldiazomethane, metabolites are quantitated using isocratic high-performance liquid chromatography with fluorimetric detection. Column washing and equilibration between samples is not required. The method was verified by measuring the induction, in rats, of microsomal lauric acid hydroxylase activity by clofibrate. The method has clear advantages over published radiochemical procedures for measuring the formation of hydroxylated metabolites of lauric acid.

INTRODUCTION

High-performance liquid chromatography (HPLC) is an analytical method widely used in the determination of the catalytic activities of cytochrome P450-4A family enzymes towards fatty-acid substrates, especially lauric acid. Such methods employ radiochemical detection [1,2] or complex formation with fluorescent probes such as 9-anthryldiazomethane [3,4] or 4-(bromomethyl)-7-methoxycoumarin [5,6]. These methods have been recently reviewed by Jansen and Fluiter [7]. All these methods detect both the 11- and 12-hydroxy-metabolites of lauric acid. Non-HPLC methods also employ radiochemical detection and use thin layer chromatography [8] or solvent partitioning procedures [9]. These methods are useful for the determination only of total hydroxy-metabolite formation.

In this paper, a novel method is described for determining microsomal lauric acid hydroxylase activities. Similar in principal to the solvent partitioning method described by Giera and VAN Lier [9], selective acid/base solubilities coupled with solvent extraction is used. The method is simple and sensitive and employs the economical use of 1-pyrenyldiazomethane (PDAM). This is a highly fluorescent yet virtually overlooked probe for derivatising organic acids. The derivatised hydroxy-metabolites of lauric acid are quantitated using reverse phase HPLC. The method is flexible and allows for both the rapid determination of total hydroxy-metabolite formation from lauric acid and for the determination separately of the 11- and 12-hydroxy-metabolites. The latter analyses require simple procedural modifications. Application of the method is illustrated by the measurement of the induction of cytochrome P450-4A family enzymes by the hypolipidemic agent, clofibrate, in rats.

EXPERIMENTAL

Chemicals

Clofibrate, lauric acid (sodium salt), 12-hydroxy-lauric acid and 16-hydroxy-palmitic acid were purchased from Sigma (St. Louis, MO, USA); 11-hydroxy-lauric acid was a gift from Dr. S. Imaoka, Osaka City University Medical School, Japan. 1-pyrenyldiazomethane (PDAM) was acquired from Molecular Probes (Eugene, OR, USA). NADP (disodium salt), *d*-glucose-6-phosphate (disodium salt) and glucose-6-phosphate dehydrogenase (yeast enzyme, grade 1) were obtained from Boehringer Mannheim (Sydney, Australia). HPLC-grade ethyl acetate and methanol were purchased from Mallinckrodt (Clayton, Australia). All other chemicals and solvents were of reagent grade and deionised water was further purified using an Milli-Q PLUS ultrapure water system (conductance of 0.07 μS/cm).

Animals and treatment

Random outbred male and female Wistar rats (6 weeks old) were obtained from the Central Animal Breeding Unit, University of Queensland, Australia. Animals were maintained on a commercial rodent diet with water *ad libitum*, and at 24 ± 2°C with a 12-hr light/dark cycle. Test animals were administered clofibrate (200 mg/ml in corn oil) for 7 days by intraperitoneal (I.P.) injection at a dose rate of 200 mg/kg/day. Controls were given an I.P. injection of corn oil. Hepatic microsomal suspensions were prepared separately for each animal [11], frozen in liquid N_2 and stored at -80°C. Cytochrome P450 concentrations were determined [12] and protein concentrations were measured by the method of Lowry *et al.*, [13] using bovine serum albumin as standard.

Enzymatic assays

Lauric acid hydroxylase activities were determined in 200 μl reaction mixtures containing 100 mM Tris-HCl pH 7.4, 125 μM sodium laurate, 2.5 mM glucose-6-phosphate, 1.0 mM NADP, 1.0 IU G6PDH, and 0.10 or 0.25 μM cytochrome P450. Laurate was dispensed (25 μl) into monooxygenase assay tubes (1.5 ml microcentrifuge tubes) from a 1.0 mM methanolic stock solution and the samples were evaporated to dryness at room temperature using a gentle stream of dry filtered air. Laurate was then dissolved by sonication at room temperature for 15 min with a Bransonic 2200 bath sonifier, using an aliquot (150 μl) of the monooxygenase reaction buffer. This procedure ensures the exclusion of solvents from the reaction mixtures. Mixtures containing all components except microsomal suspension were preincubated at 37°C for 5.0 min to allow for temperature equilibration and NADPH generation. Monooxygenase reactions were initiated by the addition of microsomal suspension. After 10 min, reactions were terminated by the addition of 100 μl 1.0 M carbonate buffer pH 10.0, vortex mixed and placed on ice. Laurate was extracted using 1.0 ml of ethyl acetate by thorough vortex mixing and centrifuging for 2.0 min (full speed bench centrifuge) at room temperature. The upper solvent phase was aspirated and discarded. Aliquots (250 μl) of the reaction mixture were transfered to 2.0 ml microcentrifuge tubes, 200 μl of 2.0 M HCl were added, followed by 25 μl of tetrahydrofuran containing internal standard (16-hydroxy-palmitic acid, 80 μM) with vortex mixing at each step. Ethyl acetate (1000 μl) was added and the tubes were shaken for 5.0 min, centrifuged for 2.0 min and 750 μl of the upper solvent phase were transfered to 3.0 ml tapered polypropylene centrifuge tubes. A further 750 μl of ethyl acetate were added to the 2.0 ml tubes which were again shaken and centrifuged with 750 μl of the upper phase removed and added to the

first extract. Combined extracts were evaporated using a gentle stream of dry filtered air at room temperature. Samples were reconstituted for HPLC by the addition of 100 μl of a freshly prepared solution consisting of 50% methanol and 50% ethyl acetate containing 0.25 mg/ml PDAM, with thorough vortex mixing. Samples and PDAM were derivatised overnight at 25°C and then loaded onto a automatic sample injector at 25°C or stored at -20°C for subsequent HPLC analyses.

Preparation of standards

Standard solutions for 11- and 12-hydroxy-laurate metabolites were prepared in methanol and stored in glassware treated with 0.2 g/l cetyltrimethylammonium bromide to minimise adsorption. Separate calibration standards for each metabolite (0.5 to 5 nmole) were prepared by adding aliquots of these methanolic solutions and an appropriate aliquot of methanol containing laurate to 1.5 ml microcentrifuge tubes and evaporating to dryness under a gentle stream of dry air. Monooxygenase assay buffer (200μl) was added to the tubes and the samples were dissolved by sonication at room temperature for 15 min. Carbonate buffer was then added to the tubes which were then treated as described in the enzymatic assays. Optimal excitation and emission wavelengths were determined for PDAM derivatives of laurate and hydroxy-metabolites, after removing excess PDAM using SEP-PAK-C18 cartridges [10], in the HPLC mobile phase using an Aminco SPF500 Spectrophotofluorimeter.

Chromatographic procedure

Hydroxy-laurate metabolites, internal standard and residual laurate were separated chromatographically using a Brownlee Spheri-5 reverse

phase C-18 column (100 x 4.6 mm I.D.). For total hydroxy-metabolite determination, the mobile phase consisted of 87% methanol and 13% buffer (0.02% triethylamine, adjusted to pH 5.0 with 1.0 M orthophosphoric acid). HPLC mobile phase was prefiltered through a 0.22 μm membrane (Durapore; Millipore Corp, Bedford, MA), with additional gas being removed with an inline ERMA model ERC3522 membrane degassing unit. A Shimadzu LC-6A liquid chromatography pump was used to deliver the mobile phase at 2.0 ml/min, and 20 μl aliquots of samples were applied to the column using a Shimadzu SIL-9A automatic injector fitted with a 150 μl loop. PDAM-derivatised fatty-acid samples were detected using a Shimadzu RF-535 variable wavelength monitor (set at low sensitivity) with excitation and emission wavelengths set at 345 nm and 395 nm respectively. Fluorescence data were analysed in terms of peak area ratios with reference to the internal standard using a Shimadzu CR4-A Chromatopac recording integrator.

RESULTS and DISCUSSION

As stated previously, monooxygenase reactions were stopped by the addition of carbonate buffer. In the following ethyl acetate extraction, laurate partitions into the organic solvent phase and the hydroxy-metabolites partition into the aqueous phase. Both of these partitions are highly reproducible removing at least 95% of the lauric acid from the aqueous phase, thus greatly reducing the amount of PDAM required for esterification of the hydroxy-metabolites and internal standard. This also allows for greater substrate concentrations to be used in the assays, without complications associated with the substrate elution profile. For total hydroxy-metabolite determinations, chromatographic run times are reduced to 30 min per run with acceptable resolution of all components using the described

chromatographic conditions. Excess acid is then added to an aliquot of the aqueous phase, after the first ethyl acetate extraction, to render the solutions acidic. The use of an internal standard accounts for any extraction variability of the hydroxy-metabolites from the acidic solution. The monooxygenase assay buffer chosen was 100 mM Tris-HCl pH 7.4. When potassium phosphate buffer (100 mM pH 7.4) was used, the hydroxy-metabolites as well as laurate extracted from the carbonate solution. No such extraction occurred when the carbonate step was omitted using the Tris-HCl buffer. The combination of methanol and triethylamine buffer was the most effective for peak resolution, phosphate buffer (10 mM pH 7.4) was less efficient and addition of either acetonitrile or tetrahydrofuran was not beneficial.

A typical HPLC elution profile for the metabolites of lauric acid obtained using clofibrate-treated male rat liver microsomes is shown in Fig. IC. The elution profile for authentic standards is shown in Fig. IB. The peaks observed near the start of the chromatogram are due to PDAM, as seen in the elution profile for PDAM (Fig. IA). The two hydroxy-metabolites for lauric acid elute as a single peak. Since both derivatised hydroxy-metabolites gave identical fluorescent responses, quantification of the combined peak measures total hydroxy-metabolite formation. Esterification between PDAM and the fatty acids was obtained overnight (approx. 16 h.) at 25°C with no noticeable deterioration of compounds. PDAM is commercially available and inexpensive as used in these assays. PDAM is stable when stored at -20°C in solid form (for up to 5 years [10]) and we found it to be stable at room temperature (<25°) for a few days in 50 % ethyl acetate, 50% methanol, allowing for the use of an automatic sample injector.

A linear relationship was obtained for hydroxy-lauric acid concentration versus the ratio of hydroxy-lauric acid to internal standard

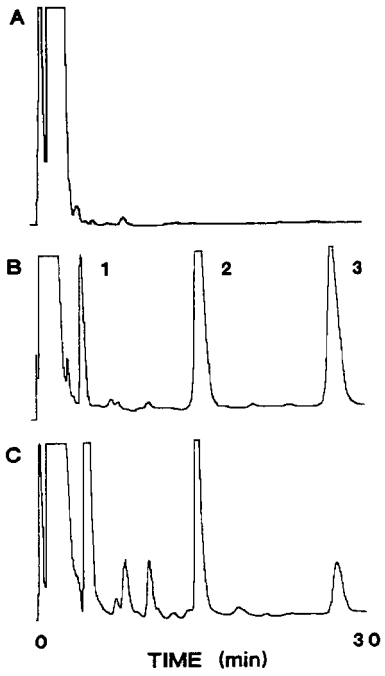

FIGURE 1. Chromatograms obtained with (A) PDAM blank, (B) authentic standards and (C) monooxygenase assays using microsomes prepared from clofibrate treated male Wistar rats. Experimental procedures are described in the text. Peak identities and initial amount are: (1) hydroxylaurate, 0.5 nmol; (2) internal standard, 2.0 nmol and (3) lauric acid, 1.5 nmol. The large peaks associated with the injection front are due to PDAM.

peak areas (Fig. 2), with a coefficient of variation of 0.999. Using the monooxygenase assay conditions described here, total hydroxymetabolite formation was linear up to 0.15 and 0.30 μM cytochrome P450, for microsomes prepared from control and clofibrate treated male Wistar rats respectively (Fig. 3). Percentage liver to body weight ratios

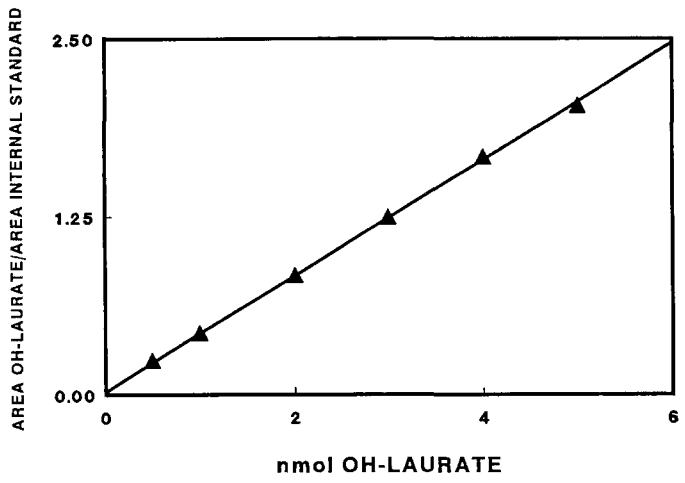

FIGURE 2. Calibration curve for the ratio of peak areas for (11- or 12-) OH-laurate to internal standard (16-OH-palmitate) versus OH-laurate concentration. Experimental procedures are described in the text. Each point represents the mean of 4 values with chromatograms been run over a number of days. Standard deviations are smaller than marker size and less than 3% of the mean in each case. Coefficient of variation is 0.999.

and cytochrome P450 specific contents for clofibrate treated male ($P<0.02$ and $P<0.002$) and female ($P<0.05$ and $P<0.05$) rats were significantly increased compared to the corresponding control animals (Table 1). Monooxygenase activities for lauric acid ω and ω-1 hydroxylases for microsomes prepared from clofibrate treated animals (Table 2) were significantly increased compared to corresponding control animals ($P<0.01$ in each case). These results agree with previously published results [1,2,14] and demonstrate that clofibrate administered by the intraperitoneal route is not as effective as a cytochrome P450 monooxygenase inducer as when given in feed.

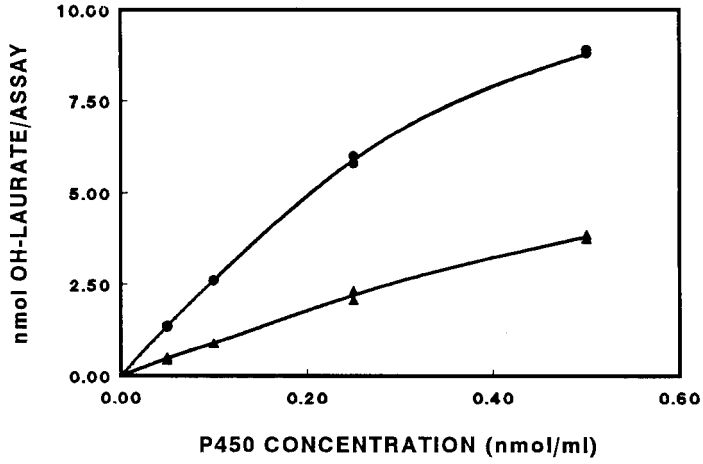

FIGURE 3. Formation of total hydroxylated metabolite from lauric acid using 0.05 to 0.50 μM cytochrome P450. Experimental conditions used are as stated in the text. Duplicate assays for each point are shown. Metabolite formation for microsomes prepared from control and clofibrate treated male Wistar rats were linear up to 0.30 and 0.15 μM cytochrome P450 respectively.

Lauric acid, its hydroxy-metabolites and the internal standard are well separated and resolved with the method described. Chromatograms with low levels of background fluorescence and excellent signal to noise ratios for low metabolite levels were obtained. Quantification of the individual hydroxy-metabolites can be achieved using a recording integrator and the appropriate software. Complete chromatographic separation and quantitation of the lauric acid hydroxy-metabolites requires alternative chromatographic conditions, although run times have to be increased and between run column re-equilibration is needed. With the described method, the following procedural modifications are

TABLE I

EFFECT OF CLOFIBRATE ON LIVER SIZE AND HEPATIC CYTOCHROME P450 SPECIFIC CONTENT IN MALE AND FEMALE WISTAR RATS.
Clofibrate was administered in corn oil for 7 days by I.P. injection at a dose rate of 200 mg/kg/day. Controls received daily I.P. injections of corn oil. Values shown are means ± S.D. (n = 6). Statistical analyses were made with Student's *t*-test.

Animal and treatment	%liver to body weight	P450 specific content nmol/mg protein
male corn oil	3.45 ± 0.24	0.90 ± 0.04
male clofibrate	3.91 ± 0.29[a]	1.05 ± 0.08[b]
female corn oil	3.37 ± 0.29	0.72 ± 0.08
female clofibrate	3.87 ± 0.43[a]	0.83 ± 0.06[a]

a: $P<0.05$ b: $P<0.01$

TABLE 2

EFFECT OF CLOFIBRATE ON HEPATIC MICROSOMAL LAURIC ACID *ω*- AND *ω*-1 HYDROXYLASE ACTIVITIES.
Male and female Wistar rats were administered clofibrate in corn oil for 7 days by I.P. injection at a dose rate of 200 mg/kg/day. Controls received daily I.P. injections of corn oil. Details of analytical procedures are described in the text. Results are expressed as means ± S.D. for triplicate assays of microsomes from 6 animals in each case. Statistical analyses were made with Students *t*-test.

Animal and treatment	Lauric acid hydroxylase activity nmol OH-laurate/min/nmol P450		Total Activity
	11-OH	12-OH	11-OH + 12-OH
male corn oil	2.09 ± 0.13	0.44 ± 0.11	2.53 ± 0.15
male clofibrate	3.40 ± 0.55[c]	4.07 ± 1.38[c]	7.47 ± 1.89[c]
female corn oil	2.47 ± 0.22	0.51 ± 0.09	2.98 ± 0.25
female clofibrate	3.03 ± 0.36[b]	1.24 ± 0.09[c]	4.27 ± 0.43[c]

b: $P<0.01$ c: $P<0.001$

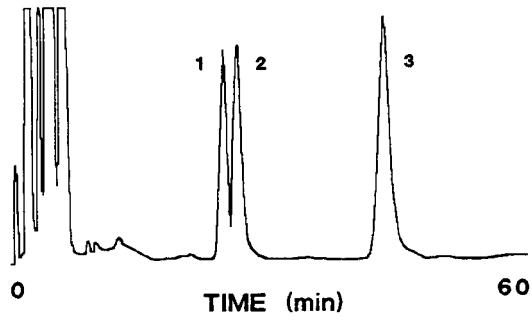

FIGURE 4. Chromatogram obtained for 11- and 12-hydroxy-lauric acids and the internal standard, octanoic acid, using mobile phase consisting of 75% methanol and 25% buffer. Details of analytical procedures are described in the text. Peak identities are : (1) 11-hydroxy-laurate, (2) 12-hydroxy-laurate, and (3) octanoic acid.

required. Octanoic acid is used as an alternative internal standard and is added to the dried residue (from a methanolic stock solution) before the addition of PDAM. The methanol content of the HPLC mobile phase is lowered to 75%. This greatly increases retention times, and after the internal standard has eluted, the column is flushed with HPLC mobile phase (95% methanol) to elute residual laurate, and then equilibrated with the 75% methanol before the next sample is applied to the column. The resultant chromatogram for the 11- and 12-hydroxy-laurate metabolites and octanoic acid is shown in Figure 4.

Although both hydroxy-metabolites of lauric acid may be quantified by this method, it is most suitable for the determination of total hydroxylated metabolite formation due to its simplicity and relatively short chromatographic run times, without the need for radiochemicals, gradient systems, column washing or column equilibration between samples.

REFERENCES

1. T.C. Orton and G.L. Parker, *Drug Metab. Dispos.*, 10: 110-115 (1982).

2. M.N. Milton, C.R. Elcombe and G.G. Gibson, *Biochem. Pharmacol.*, 40: 2727-2732 (1990).

3. S. Imaoka, N. Shimojo, and Y. Funae, *Biochem. Biophys. Res. Commun.*, 152: 680-687 (1988).

4. T. Yoshida, A. Uetake, H. Yamaguchi, N. Nimura and T. Kinoshita, *Anal. Biochem.*, 173: 70-74 (1988).

5. H.A.A.M. Dirven, A.A.G.M. de Bruijn, P.J.M. Sessink and F.J. Jongeneelen, *J. Chromatogr.*, 564: 266-271 (1991).

6. E.H.J.M. Jansen and P. de Fluiter, *J. Liquid Chromatogr.*, 15: 2247-2260 (1992).

7. E.H.J.M. Jansen and P. de Fluiter, *J. Chromatogr. Biomed. Appl.*, 580: 325-346 (1992).

8. G.L. Parker and T.C. Orton,"Induction by oxyisobutyrates of hepatic and kidney microsomal cytochrome P-450 with specificity towards hydroxylation of fatty acids," in *Biochemistry, Biophysics and Regulation of Cytochrome P450*, J.A. Gustaffson, J. Carlstedt-Duke, A. Mode and J. Rafter eds., Elsevier, Amsterdam, 1980, pp 373-377.

9. D.D. Giera and R.B.L. VAN Lier, *Fund. Appl. Toxicol.*, 16: 348-355 (1991).

10. N. Nimura, T. Kinoshita, T. Yoshida, A. Uetake and C. Nakai, *Anal. Chem.*, 60: 2067-2070 (1988).

11. F.P. Guengerich,"Microsomal enzymes involved in toxicology-analysis and separation," in ***Principles and Methods in Toxicology***, A.W. Hayes ed., Raven Press, New York, 1982, pp 609-634.

12. W.R. Estabrook, J. Peterson, J. Baron and A. Hildebrandt,"The spectrophotometric measurement of turbid suspensions of cytochromes associated with drug metabolism," in ***Methods in Pharmacology***, C.F. Chignell ed., Appleton Century Crofts, Meredith Corp., New York, 1972, Vol. 1, 303-350.

13. O.H. Lowry, N.J. Rosebrough, A.L. Farr and R.J. Randall, *J. Biol. Chem.*, **193**: 265-275 (1951).

14. S.K. Bains, S.M. Gardiner, K. Mannweiler, D. Gillett and G.G. Gibson, *Biochem. Pharmacol.*, **34**: 3221-3229 (1985).

Received: June 24, 1993
Accepted: June 30, 1993

JOURNAL OF LIQUID CHROMATOGRAPHY, 17(3), 633-648 (1994)

SEPARATION OF THE MAIN NEUTRAL LIPIDS INTO CLASSES AND SPECIES BY PR-HPLC AND UV DETECTION

SMARAGDI ANTONOPOULOU[1], NIKOLAOS K. ANDRIKOPOULOS[2], AND CONSTANTINOS A. DEMOPOULOS[1]

[1]*University of Athens*
Department of Chemistry
Panepistimioupolis
15771, Athens, Greece
[2]*Harokopio University of Home Economics*
Department of Dietetics
8 Iraklitou Street
10673, Athens, Greece

ABSTRACT

A reversed phase high performance liquid chromatographic method is described that allows separation and estimation of the main neutral lipid classes as well as several species of each class.

By the represented method waxes, hydrocarbons, fatty acids and their methyl esters, sterols and their esters, free glycerylethers, fatty alcohols, vitamin E and mono-, di- and triglycerides are separated into classes and into class species within 55min.

A stepped gradient elution with methanol/water, acetonitrile/methanol, acetonitrile/tetrahydrofuran and isopropanol/acetonitrile was performed onto a reverse phase C18 HPLC column and the effluent was monitored by UV detection at 206 nm.

Application of the method in a plant extract and in a vegetable oil sample is represented.

INTRODUCTION

Both normal (NP-HPLC) and reversed phase (RP-HPLC) high performance liquid chromatographic (HPLC) methods have been used for the separation of neutral and polar lipids from various plants and animal tissues. NP-HPLC is used for the separation of the lipid mixtures into classes while molecular species of each class are usually separated by the RP-HPLC mode.

In the last two decades several NP-HPLC systems have been reported for the separation of neutral lipid classes (1-9) or for both neutral and polar lipid classes (11-19) by using silica based columns of different types. Also, different detection techniques have been applied with the above NP-HPLC systems. For the analyses of mixtures containing the most lipid classes the ultraviolet (UV) detection was usually used in the 205-215nm region, in combination with gradient elution (4, 5, 16) or flow programming and isocratic elution (11), while UV-diode array detection at 190-350nm (9) or 200-400nm (13) was also used with gradient elution. Refractive index (RI) detectors, have been used for the analyses of less number of lipid classes (3,6-8) because they are compatible only with isocratic elution, while infrared (IR) detectors, compatible with gradient elution but requiring compatible solvents, have been rarely employed (2,7).

Lipid mixtures consisted of neutral (1) and phospholipid (19) or both phospholipid and glycolipid (10, 12, 14, 15, 17, 18) classes have been analyzed and quantitated in low concentrations by the flame ionization detection (FID) (1,10, 18) and the light scattering detection (LSD) (12, 14, 15, 17, 19) modes, which considered as "mass" or "universals" without limitations in gradient and solvents.

For the subsequent separation of each individual lipid class into species the reverse phase mode is required. Many RP-HPLC techniques have been developed for the separation of neutral and polar lipid species of an individual class. Such techniques have been separately reported for: waxes (W) (20, 21), long chain hydrocarbons (RH) (22, 23), fatty acids (FA) and their methylesters (FAME) (24, 25), sterols (ST) and their esters (ST.E) (26-33), glycerylether (GE) esters and derivatives (34-38), monoglycerides (MG) and diglycerides (DG) (34-40), fatty alcohols (F.Al.) (41-44) and triglycerides (TG) (33, 45-53).

Vitamin E (VIT. E) species, α-, β-, γ- and δ-tocopherols, have also been analyzed by RP-HPLC systems by UV, at 215 and 280 nm, (53) or fluorometric (FL) (33) detection. The detection of the other referred neutral lipid species analyzed by RP-HPLC was performed by using UV, RI, FL, FID and LSD techniques which are partially reviewed in the Results and Discussion section.

To our knowledge no method has been appeared, till now, describing the simultaneous separation of lipids into classes and species except of an our recent report referred to the separation of synthetic antioxidants, tocopherols and TG in vegetable oils (53) and α-tocopherol, free and esterified cholesterols and TG in human lipoproteins (33) by RP-HPLC and UV/UV-diode array (53) and UV/FL (33) detection.

In the present report a relative easy to run method is described which allows the simultaneous separation of a complex mixture of lipids into classes and species with estimation by UV detection especially useful in preliminary investigation and classification of specific complex natural mixtures and which can be easily applied with no highly sophisticated laboratory equipments.

Several neutral lipid standards as well as a lipid extract from nettle leaves and roots and a soya bean oil sample were analyzed by the represented method. Also, HPLC and detection techniques of the referenced methods are partially reviewed.

EXPERIMENTAL

Materials

All reagents used were of analytical grade purchased from Merck (Darmstadt, G) while HPLC grade solvents were from Fluka (Buchs, CH) and the water was Nanopure grade. Standard lipids were purchased from Sigma (St. Louis, MO, USA), Merck and Serva (Heidelberg, G). The oil sample used was a commercial soyabean oil (Athens, GR). Nettle (Urtica dioica) was collected from countryside (Athens, Attica, GR).

Standard and sample preparation

All standards were prepared as 5% solutions except TG, ST and vitamin E as 1% solutions, in chloroform/methanol (1:1). Soyabean oil was prepared as 5% solution in chloroform/methanol (9:1). Homogenized nettle leaves and roots (approximately 200g) were extracted (54) and neutral lipids were separated from chlorophylles and phospholipids by thin layer chromatography (TLC) using the solvent system petroleum ether/benzene/acetic acid (30:70:2) (55). Neutral lipids as overlapped bands were scrapped off from the TLC plate and extracted according to Bligh-Dyer (54). Counter-current distribution (56) was also used for removing polar lipids traces. The final solution was evaporated in flash evaporator and the remained total neutral lipids were redissolved in a small volume of chloroform/methanol (1:1) which was used for the HPLC.

Chromatography

The liquid chromatographic system consisted of a dual pump Jasco (Tokyo, Japan) model 880-PU HPLC, supplied with a 330µl loop Reodyne (P/N 7125-047) injector, connected to a Jasco model 875-UV detector and a Hewlett-Packard (Avondale, PA,U.S.A.) model HP-3396A integrator-plotter. A Nucleosil-300, C18 column, (7µ, 250x4mm I.D) from Analysentechnik (Mainz, G) was used. The flow rate was 1ml/min and the detection at 206nm (0.4 a.u.f.s) except vitamin E at 280nm (0.4 a.u.f.s). The solvent gradients used are shown in Figs. 1, 2 and 3 with the following eluting solvents: A, methanol/water (80:20); B, acetonitrile/methanol (60:40); C, acetonitrile/tetrahydrofuran (99.5:0.5) and D, isopropanol/acetonitrile (99:1). Volumes 2-200µl of groups of standards were injected each time. Each group contained the species of one lipid class and the 1% or 5% solutions of each group were injected as following:

Vitamin E, 2µl; FA., FAME and ST, 10µl; W, RH, DG, ST.E. and TG, 20µl; GE, 50µl; MG, 150µl and F.Al, 200µl.

RESULTS AND DISCUSSION

The analysis of standards was performed into groups (Fig. 1.). Each group consisted of the species of one (or two) neutral lipid class(es) and the injected amount of each group was the optimum for the UV detection limit of the used instrumentation. Injection of a solution containing the total of the used standards was not used in order to avoid overloading the column.

Before the analysis of each group, each individual standard species was injected separately and the resulted main peak was collected and co-chromatographed on TLC plates with authentic standard in order to con-

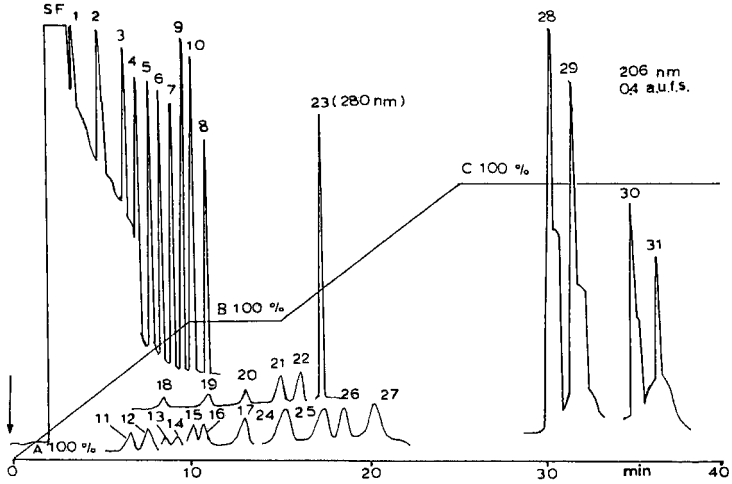

FIGURE 1. HPLC chromatogram(s) of neutral lipid standards. Conditions and solvents A, B and C in Experimental section. Gradient as indicated. Peak identification in Table 1. SF: solvent front.

firm the elution and retention time (RT). The RT's of the separately injected standards are summarized in Table 1.

Several mobil phase combinations were developed to achieve a quite satisfactory separation in a reasonable time. The final chosen solvent systems and gradients resulted in an effective separation within 40min (gradient with solvents A, B and C) or 55min (gradient with solvents A, B, C and D). A linear gradient from solvent A to solvent B in 10min, a hold for 5min in B and then a linear gradient to solvent C in 10min followed by a second hold in C for 15min resulted in a total separation within 40min. By introducing a third linear gradient step from solvent C (decreasing the hold step to 5min), to solvent D in another 10min and holding D for

TABLE 1

RT's of Individual Standards

No	Classes	Species	RT(min)
1	W	Cetiolate	3.50
2	RH	Cycloheptane	5.28
3	RH	Cyclododecane	6.85
4	RH	Cyclodecatriene	7.00
5	FA	Linoleic acid	7.51
6	FA	Palmitoleic acid	7.90
7	FA	Oleic acid	8.44
8	FA	Arachidic acid	10.40
9	FAME	Methylpalmitate	9.14
10	FAME	Methylstearate	9.80
11	MG	α-Monopalmitine	6.73
12	MG	α-Monostearine	8.05
13	F.Al	Cetyl alcohol	8.61
14	F.Al	Behenyl alcohol	9.63
15	GE	Celachyl alcohol	9.74
16	GE	Chimyl alcohol	11.80
17	GE	Batyl alcohol	13.20
18	ST	Desmosterol	8.69
19	ST	Ergosterol	11.30
20	ST	Cholesterol	13.00
21	ST	Stigmasterol	15.00
22	ST	β-Sitosterol	16.34
23	VIT.E	Vitamin E	17.00
24	DG	Diolein	15.62
25	DG	(α,β)-Dipalmitine	17.80
26	DG	(α,γ)-Dipalmitine	18.84
27	DG	(α,β)-Distearine	20.55
28	TG	Trilinolein	30.00
29	TG	Triolein	31.60
30	ST.E	Cholesteryl linoleate	34.80
31	ST.E	Cholesteryl palmitate	36.20

15min, a more distinct separation of TG can be achieved (Fig. 3). The first and the second hold of the gradients are also used for changing the solvent chambers from solvent A to C and from solvent B to D, respectively. These manipulations are required when a two pump delivery HPLC system is used. Tetrahydrofuran and aceto-

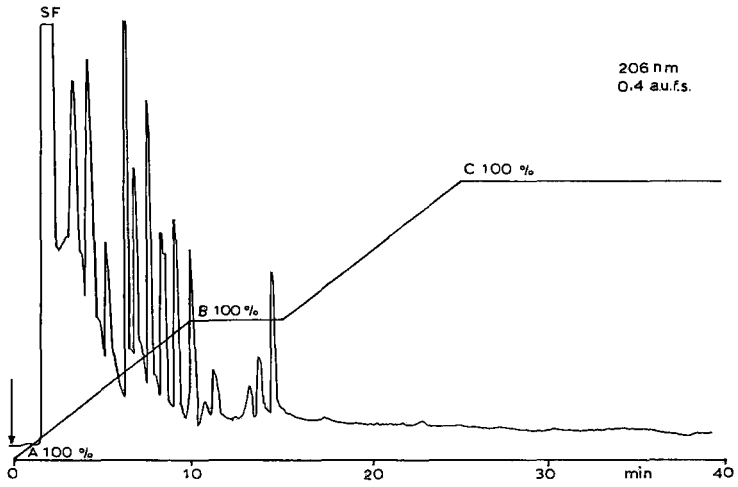

FIGURE 2. HPLC chromatogram of a neutral lipid fraction from nettle (Urtica dioica) leaves and roots extracts. Conditions as in Fig. 1 and in Experimental section. SF:solvent front.

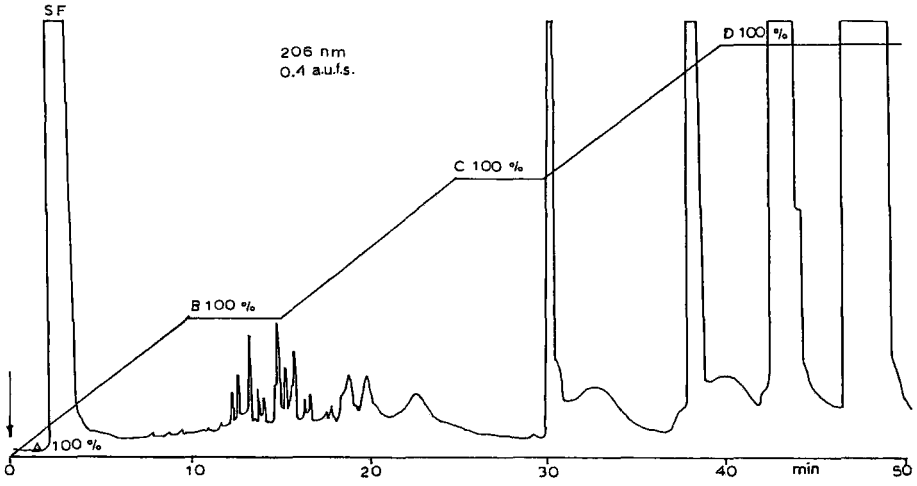

FIGURE 3. HPLC chromatogram of soyabean oil solution (5%). Conditions and solvents A, B, C and D in Experimental section. Gradient as indicated. SF:solvent front.

nitrile were used as minor constituents in solvents C and D, respectively for equilibration of the gradient and keep the baseline in low shift during the chromatographic run. An acid modifier (e. g. phosphoric acid) was not used in solvent A, for sharpening the peaks, because the method is recommended for further examination of the collected peaks in biological experiments (55). For the next injection a 15min equilibration step with solvent A is required. Cyclohexane or n-hexane can also be used for cleaning up the column for the possible nonpolar remained constituents of a natural source chromatographed sample. In the latter case a pre-equilibration step for 5min with solvent D is required.

In Fig. 1 are shown the separations of standard species of W, RH, FA, FAME, F.Al, ST, GE, VIT.E, MG, DG, TG and ST.E classes, which are summarized in Table 1. In the present method the used W and RH species comigrated almost with solvent front and even with low resolution and sensitivity the method offers an alternative choice of analysis, by UV detection, to the previous reported methods. In the previous methods W and RH species are usually quantitated by other techniques than UV detection because of their low absorptivity in the UV region. n-Alkane species have been separated by RP-HPLC using direct (22) or indirect (23) RI detection and wax-ester species have been quantitated by LC-GC coupled systems (20, 21) while RH classes (7, 13) and carotenoids (13) have been analyzed by NP-HPLC and RI (7) or UV-diode array detection (13).

The achieved separation of the used FA and FAME species by the present method, is comparable to the previous reported methods for FA and FAME with UV (24) or FL (25) detection. Free ST species from natural sources (oils and plants) have been separated by RP-HPLC within 30min, at 205 nm UV detection (26-29) with similar pat-

terns to the present method. The simultaneous analyses of cholesteryl esters and TG species have been previously performed by RP-HPLC and UV detection (33) and the individual peaks with good resolution were also represented superimposed. In the present method cholesteryl esters accumulated after the TG fraction but can be collected and further quantitated by other previous reported methods for plant and animal tissues (30, 31) and human plasma (32, 33). VIT.E standard was detected at 280nm and eluted as a single peak with RT similar to the RT of an our previous reported RP-HPLC method (53). Derivatized DG (34-40) and underivatized MG and DG (39) species have been analyzed using UV (35, 36, 38-40), FL (36, 37) or RI (39) detection with elution times comparable to the present method. Underivatized (8) and derivatized (34, 35) GE-ester subclasses have been analyzed by NP-HPLC with RI (8) or UV (34, 35) detection, while derivatized GE-ester species have been separated by RP-HPLC within 30min by UV (35, 36, 38) or FL (36) detection. In the present method is represented an analysis of the underivatized free GE species for the first time. Free F.Al have been previously analyzed by RP-HPLC and direct RI (41, 44) and indirect (42) detection. UV is not usually employed for the detection of F.Al e.g. there is a reference (43) for the effective detection of fatty diols at 200nm. In the present method although relative large amounts of the injected samples were required the detection of free F.Al was realized for the first time at 206nm. MG, DG, GE and F.Al can almost be detected by the used technique with almost appeared peaks even with large amounts of injected sample but the method has the advantage of using underivatized samples in the presence of other components from natural sources. Detailed separations of TG from plants and oils have been reported by RP-HPLC (45, 47, 49-53), silver-

ion HPLC (57-59) and NP-HPLC (60) by using UV (33, 45, 53, 60), RI (47, 50) and LSD or FID detection (49, 51, 52, 57-59). The TG patterns of the present method are comparable to those obtained by a method of semipreparative fractionation of TG, but having longer RT's (47). Finally phospholipids coeluted with solvent front can be collected and separated by HPLC in classes by UV detection (61) and further into class species by FL (62), RI (63) or UV (64) detection.

Applications of the described method are represented in Figs. 2 and 3. A lipid extract from nettle leaves and roots was separated as shown in Fig 2 by using the gradient with the solvents A, B and C. In Fig. 3 soyabean oil was analyzed by using the gradient with the solvents A, B, C and D. By increasing the sensitivity of the detection, several minor constituents of the oil eluted before TG's can be effectively detected. By introducing a fourth gradient step with the solvent D a further separation of TG's was achieved.

In the UV detection mode the detectability and the quantitative determination of each component is referred to its degree of unsaturation and/or to ester and carboxy configuration. These structures are absent or limited (with low extinction coefficients) in the W, RH, F.Al, GE, MG and DG molecules, but the relative large injected amounts shifts the absorptivity over the 200nm, near to the detectable area.

On the other hand UV detection, although requiring non UV-absorbing solvents in the detecting area, is compatible with gradient elution which is necessary for the effective separation of complex lipid mixtures. The recent commercially developed FID and LSD systems overcome the compatibility problems of the other detectors but they still have relative high purchasing, running and maintenance costs. For these reasons UV mode having

relative low cost and easy operation as compared to the resulted detecting informations, remains the most widespread detection technique. Even more UV detection could be the detection of choice when a preliminary separation of a complex natural mixture is required before a further detailed examination. These requirements meet the represented method by which all peaks from quite different in polarity components can be collected for further examination especially when the possible biological activity will be investigated (55).

REFERENCES

1. K., Kiuchi, T., Ohta, H., Ebine, J. Chromatogr. Sci., 13: 461-466 (1975).

2. K., Rayne-Wahl, G.F., Spencer, R., Plattner, R.O., Butterfield, J.Chromatogr., 209: 61-66 (1981).

3. M.D., Greenspan, E.A., Schroeder, Anal. Biochem.,: 127: 441-448 (1982).

4. D.N., Palmer, M.A., Anderson, R.D., Jolly, Anal. Biochem., 140: 316-319 (1984).

5. J.G., Hamilton, K., Comai, J.Lipid Res., 25: 1142-1148 (1984).

6. A.S., Ritchie, M.H., Jee, J.Cromatogr., 329: 273-280 (1985).

7. J.R, Hamilton, S.F., Mitchell, P.A., Sewell, J. Chromatogr., 395: 33-46 (1987).

8. T.A., Foglia, P.D., Vail, T., Iwama, Lipids, 22: 362-365 (1987).

9. M.D., Greenspan, C.Y., Lee Lo, D.P., Hanf, J.B., Yudkovitz, J.Lipid Res., 29: 971-976 (1988).

10. A., Stolyhwo, O.S., Privett, J.Chromatogr. Sci, 11: 20-25 (1973).

11. H.S.G., Fricke, J., Oehlenschlager, J.Chromatogr., 252: 331-334 (1982).

12. W.W., Christie, J.Lipid Res., 26: 507-512 (1985).

13. B.P., Lapin, N.A., Sareva, T.E., Rubtsova, J.Chromatogr., 365: 229-235 (1986).

14. W.W., Christie, J.Chromatogr., 361: 396-399 (1986).

15. A., Stolyhwo, M., Martin, G., Guiochon, J. Liquid Chromatogr., 10: 1237-1253 (1987).

16. J.G., Hamilton, K., Comai, Lipids, 23: 1150-1153 (1988).

17. B.S., Lutzke, J.M., Braughler, J.Lipid Res. 31: 2127-2130 (1990).

18. R.A., Moreau, P.T., Asmann, H.A., Norman, Phytochemistry, 29: 2461-2466 (1990).

19. P.R., Redden, Y.S., Huang, J. Chromatogr., 567: 21-27 (1991).

20. K., Grob, M., Lanfranchi, J.High Res. Chromatogr. 12: 624-627 (1989).

21. K., Grob, M., Lanfranchi, C., Maviani, J. Chromatogr., 471: 397-405 (1990).

22. C.N., Renn, R.E., Synovec, J. Chromatogr., 536: 289-301 (1991).

23. T., Takeuchi, D., Ishil, J.High Res. Chroma togr. Chrom. Commun., 10: 571-573 (1987).

24. C.J., Baker, J.H., Melhuish, J.Chromatogr., 284: 251-256 (1984).

25. J.H., Wolf, J.Korf, J.Chromatogr., 436: 437-445 (1988).

26. R.I., Hunter, K.M., Walden, E., Heftmann, J. Chromatogr., 153: 57-61 (1978).

27. J.M., DiBussolo, W.R., Nes, J. Chromatogr. Sci., 20: 193-202 (1982).

28. B., Holen, J. Am. Oil Chem. Soc., 62: 1344 - 1346 (1985).

29. J.L., Perrin, R., Raoux. Rev. Franc. Corps Gras., 35: 329-333 (1988).

30. H.H., Rees, P.L., Donnahey, T.W., Goodwin,

J. Chromatogr., 116: 281-291 (1976).

31. R.P., Evershed, V.L., Male, J., Goad, J. Chromatogr., 400: 187-205 (1987).

32. X., Faug, S.U., Sheikh, J.C., Touchstone, J.Liquid Chromatogr., 14: 589-598 (1991).

33. K., Seta, H., Nakamura, T., Okuyama, J. Chromatogr., 515: 585-595 (1990).

34. E., Francescangeli, S., Porcellati, L.A., Horrocks, J. Liquid Chromatogr., 10: 2799-2808 (1987).

35. C.S., Ramesha, W.C., Pickett, D.V., Murthy-Krishna, J. Chromatogr., 491: 37-48 (1989).

36. H., Rabe, G., Reichmann, Y., Nakagawa, B., Rustow, D., Kunze, J. Chromatogr., 493: 353-360 (1989).

37. A., Rastegar, A., Rellther, G., Duportail, L., Freysz, C., Leray, J. Chromatogr., 518: 157-165 (1990).

38. T.R., Warne, M., Robinson, J. Am. Oil Chem. Soc., 25: 748-752 (1990).

39. B.G., Sempore, J.A., Bezard, J. Chromatogr., 547: 89-103 (1991).

40. A., Cautafora, R., Masella, J. Chromatogr., 593: 139-146 (1992).

41. F.E., Lockwood, L.J., Matienzo, B., Sprissler, J. Chromatogr., 262: 397-403 (1981).

42. T., Takeuchi, D., Ishii, J. Chromatogr., 393: 419-425 (1987).

43. D., Noel, P., Vangheluwe, J. Chromatogr., 388: 75-80 (1987).

44. S., Husain, G., Pratap, R., Nageswara Rao, J. Chromatogr., 475: 426-431 (1989).

45. V.M., Kapoulas, N.K., Andrikopoulos, J. Chromatogr., 366: 311-320 (1986).

46. L.J., Barron, G., Santa-Maria, J.C., Diez-Masa, J. Liquid Chromatogr., 10: 3193-3212 (1987).

47. M.Jo., Wojtusik, P.R., Brown, J.G., Turcotte, J. Liquid Chromatogr., 11: 2091-2107 (1988).

48. O., Podlaha, B., Toregard, J. Chromatogr., 465: 215-226 (1989).

49. A.J., Palmer, F.J., Palmer, J.Chromatogr., 465: 369-377 (1989).

50. K., Aitzetmuller, J.High Res.Chromatogr., 13: 375 - 377 (1990).

51. T., Rezanka, P., Mares, J.Chromatogr., 542: 145-159 (1991).

52. M.A.M., Zeitoun, W.E., Neff, E.Selke, T.L., Mounts, J.Liquid chromatogr., 14:2685-2698 (1991).

53. N.K., Andrikopoulos, H., Bruschweiler, H., Felber, Ch., Taeschler, J.Am.Oil Chem.Soc., 68: 359-364 (1991).

54. E.G., Bligh, W.J., Dyer, Can.J.Biochem., Physiol., 37:911-917 (1959).

55. S.Antonopoulou, N.K., Andrikopoulos, C.A., Demopoulos, 4th Intern. Congr. on PAF and Related Lipid Mediators, Abs., 61, Snowbird, U.S.A., Sept., 22-25 (1992).

56. D.S., Galanos, V.M., Kapoulas, J.Lipid Res., 3: 134 (1962).

57. W.W., Christie, J.Chromatogr., 454: 273-284 (1988).

58. B., Nikolova-Damyanova, W.W., Christie, B., Hersolf, J.Am.Oil Chem.Soc., 67: 503-507 (1990).

59. P., Laakso, W.W., Christie, J., Pettersen, Lipids, 25: 284-250 (1990).

60. S.H., Rhodes, A.G., Netting, J.Chromatogr., 448: 135-143 (1988).

61. N.K., Andrikopoulos, C.A., Demopoulos, A., Siafaca-Kapadai, J.Chromatogr., 363: 412-417 (1986).

62. A.D., Postle, J.Chromatogr., 415: 241-251 (1987).

63. N.A., Porter, R.A., Wolf, J.R., Nixon, Lipids, 14: 20-24 (1979).

64. S.L., Abidi, T.L., Mounts, J.Liquid Chromatogr., 15: 2487-2502 (1992).

Received: July 27, 1993
Accepted: August 5, 1993

JOURNAL OF LIQUID CHROMATOGRAPHY, 17(3), 649-658 (1994)

SIMPLE AND FAST DETERMINATION OF SOME PHENETHYLAMINES IN ILLICIT TABLETS BY BASE-DEACTIVATED REVERSED PHASE HPLC

MARCO LONGO[1]*, CRISTINA MARTINES[1], LAURA ROLANDI[2], AND ALDO CAVALLARO[1]

[1]*Presidio Multizonale di Igiene e Prevenzione*
Via Juvara, 22 - 20129 Milano - Italy
[2]*Policlinico S. Matteo*
Piazzale Golgi, 2 - 27100 Pavia - Italy

ABSTRACT

A high performance liquid chromatographic (HPLC) method for the simultaneous identification and quantitation of amphetamine, methamphetamine, 3,4-methylenedioxyamphetamine (MDA), N-methyl-3,4-methylenedioxyamphetamine (MDMA), and N-ethyl-3,4-methylenedioxyamphetamine (MDE) in presence of caffeine and ephedrine in illicit tablets is described. A simple and rapid sample preparation procedure was applied in order to allow a high number of samples to be processed per day. The chromatographic separation was performed on a commercially available base-deactivated octadecyl silica column with a gradient system using acetonitrile and 20 mM monobasic potassium phosphate buffer. The flow rate was 1.5 ml/min and peak detection was performed at 220 and 280 nm. Peak identity and homogeneity were determined by mapping of peaks in the 195-370 nm range. Quantitative analysis was performed using external standard method in the concentration range studied. Linearity was evaluated in the range 10-500 µg/ml for the 5 substances in exam and for ephedrine, and in the range 3-100 µg/ml for caffeine. Correlation coefficients ranged from 0.9985 to 0.9999. Good accuracy and between-day precision were achieved.

INTRODUCTION

Amphetamine, methamphetamine, 3,4-methylenedioxyamphetamine (MDA), N-methyl-3,4-methylenedioxyamphetamine (MDMA), and N-ethyl-3,4-methylenedioxyamphetamine (MDE) are drugs of abuse frequently encountered in tablets of illicit provenience.

Psycho-stimulating effect of amphetamines is well known. MDA and its N-alkyl derivatives are reported to act primarily as central nervous system stimulants that may be hallucinogenic in large doses.(1)

Several papers refer to the high performance liquid chromatographic analysis of amphetamines (2-6) and MDAs (6-8) but no method is simple enough to be employed for the routine simultaneous identification and quantitation of the drugs mentioned above.

A major problem associated with the analysis of basic drugs by reversed phase-high performance liquid chromatography (RP-HPLC) is peak tailing caused by ionic interactions between protonated drugs and free silanol groups of the packing material. These interactions may be reduced by using a very acidic mobile phase, modifying ionic strength of the buffer or adding basic modifiers such as tertiary amines.

A second approach, whose application in analytical toxicology has been recently investigated (9,10), is the use of base-deactivated columns in which free silanol groups are masked through various (often not specified) procedures. Analysis performed on such columns show satisfactory peak shape at higher pH values than those required on conventional RP columns. This results in increased column stability and life span.

The utility of photo diode array detection (DAD) in the analysis of illicit drugs has been shown in a number of papers

(6,11-15). Evaluation of peak purity and variation of wavelength during the analysis are two important features of the DAD.

In this paper we describe a simple and fast routine method for the simultaneous identification and quantitation of amphetamine, methamphetamine, MDA, MDMA, and MDE in illicit tablets in presence of ephedrine and caffeine (two common adulterants normally found in "street" samples).

EXPERIMENTAL

Reagents and Chemicals

Ephedrine, amphetamine, methamphetamine, and caffeine were obtained from Sigma Chemical Company (St. Louis, MO, USA). MDA, MDMA, and MDE were obtained from Alltech (Deersfield, IL, USA).

HPLC grade acetonitrile was provided by Carlo Erba (Milan, Italy). Water was obtained from a Milli-Q purification system (Millipore, Bedford, MA, USA).

All other chemicals were analytical grade.

Apparatus

The HPLC system consisted of a Model LC 410 quaternary pump equipped with a Model LC 235 diode array detector, a Model ISS 200 autosampler, a Model 1020D integration system, and a Model GP100 printer-plotter (Perkin Elmer, Norwalk, CT, USA).

Liquid chromatographic conditions

The separation was performed on a 15 cm x 4.6 mm I.D. 5 µm particle size Suplex pKb100 column with a Supelguard precolumn

TABLE 1

Concentration Ranges and Correlation Data for the Compounds examined

COMPOUND	CONCENTRATION RANGES (µg/ml)	CORRELATION COEFFICIENTS (r)
Ephedrine	10-500	0.9985
Amphetamine	10-500	0.9994
Methamphetamine	10-500	0.9996
MDA	10-500	0.9997
MDMA	10-500	0.9997
MDE	10-500	0.9999
Caffeine	3-100	0.9999

containing the same stationary phase (Supelco Inc., Bellefonte, PA, USA) protected by a 3 µm on-line filter unit (Rheodyne, Cotati, CA, USA). A pH 3.8 20 mM phosphate buffer (Solvent A) - acetonitrile (Solvent B) gradient was used. The gradient profile was as follows: 0-3 min, 97% A - 3% B (isocratic); 3-8 min, 85% A - 15% B (linear gradient); 8-12 min, 85% A - 15% B (isocratic). Re-equilibration time of 8 minutes was used. A flow rate of 1.5 ml/min was employed throughout. Eluents were filtered through a 0.45 µm membrane filter (Millipore) and degassed by a constant flow of helium. Detection wavelengths were set as follows: 0-5 min, 220 nm; 5-12 min, 280 nm.

External standard calibration curves

Individual solutions of ephedrine, amphetamine, methamphetamine, MDA, MDMA, MDE, and caffeine in phosphate buffer - acetonitrile (97:3) were prepared at 8 different concentration levels. 20 µl of each standard solution were injected and peak areas obtained were linearly related to

concentration. Concentration ranges and correlation coefficients are reported in Table 1.

Sample preparation

Each tablet was finely powdered and an aliquot of 50 mg was weighed in a 50 ml volumetric flask. A phosphate buffer - acetonitrile mixture (97:3) was added to volume and the solution was sonicated for 5 minutes. Filtration units Millex LCR were used to remove particles greater than 0.5 μm. 20 μl of the filtered solution were injected in duplicate onto the HPLC column.

RESULTS AND DISCUSSION

A base-deactivated column, instead of a conventional RP-HPLC column, was chosen in order to: a) improve peak symmetry and therefore reproducibility; b) shorten elution time; and c) reduce the amount of organic solvents in the mobile phase.

An alternative approach was attempted with a conventional C8 silica column and phosphate buffer/acetonitrile mobile phase, but satisfactory results in terms of peak symmetry and separation were achieved only by using a very acidic mobile phase (pH 2.0), thus shortening column stability. Furthermore, a bigger amount of acetonitrile was required to obtain acceptable elution time.

The Suplex pKb100 is a silica based C18 stationary phase in which residual silanols are electrostatically shielded. Vervoort et al. (10) recently reported that this column gives a very good peak symmetry for basic compounds in a pH range of 2.5-6.0 and that the shielding of free silanols is so effective that addition of basic modifiers is not necessary.

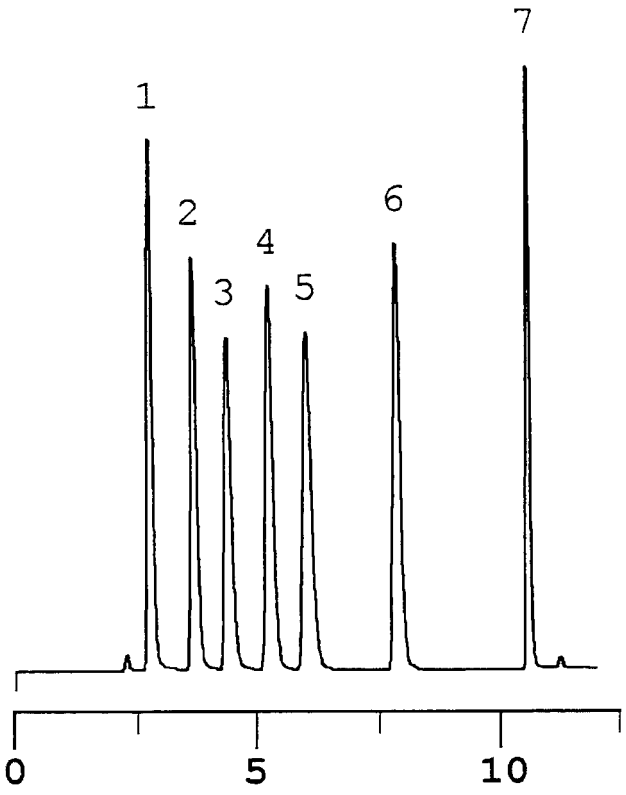

FIGURE 1 : Representative chromatogram showing separation of: (1)ephedrine-102.5 µg/ml; (2)amphetamine-95.7 µg/ml; (3)methamphetamine-100.6 µg/ml; (4)MDA-58.2 µg/ml; (5)MDMA-63.9 µg/ml; (6)MDE-64.2 µg/ml; (7)caffeine-17.5 µg/ml; 20 µl injected; detector sensitivity: 0.2 AUFS.

A representative sample containing the substances of interest was made by mixing accurately weighed amounts of powdered tablets of known composition. This sample was dissolved and injected as previously described. The resulting chromatogram is shown in Figure 1. Retention times (t_R), capacity factors (k'), and asymmetry factors (A_s) are listed in Table 2.

TABLE 2

Chromatographic Characteristics of the Separation

COMPOUND	t_R (min)	k'(*)	A_S (#)
Ephedrine	2.73	1.02	1.84
Amphetamine	3.62	1.68	2.15
Methamphetamine	4.30	2.19	2.37
MDA	5.16	2.82	1.71
MDMA	5.93	3.39	1.83
MDE	7.74	4.73	1.68
Caffeine	10.40	6.70	1.33

(*) dead time for the calculation of k' was determined as first baseline disturbance after injection of methanol;
(#) asimmetry factors (As)were calculated at 10% of the peak height using the ratio of the width of the rear and the front sides of the peak.

TABLE 3

Accuracy and between-day Precision of the Method

COMPOUND	ACTUAL (μg/ml)	EXPERIMENTAL(*) (μg/ml)	RECOVERY (%)	RSD(#) (%)
Ephedrine	102.5	98.4	96.0	0.51
Amphetamine	95.7	92.5	96.7	0.63
Methamphetamine	100.6	97.5	96.9	0.81
MDA	58.2	57.7	99.1	0.64
MDMA	63.9	63.5	99.4	1.05
MDE	64.2	63.7	99.2	0.55
Caffeine	17.5	17.1	97.7	0.76

(*) average values obtained by determination on 5 separate sample weighings
(#) relative standard deviation obtained from 16 replicate measurements of a representative sample solution

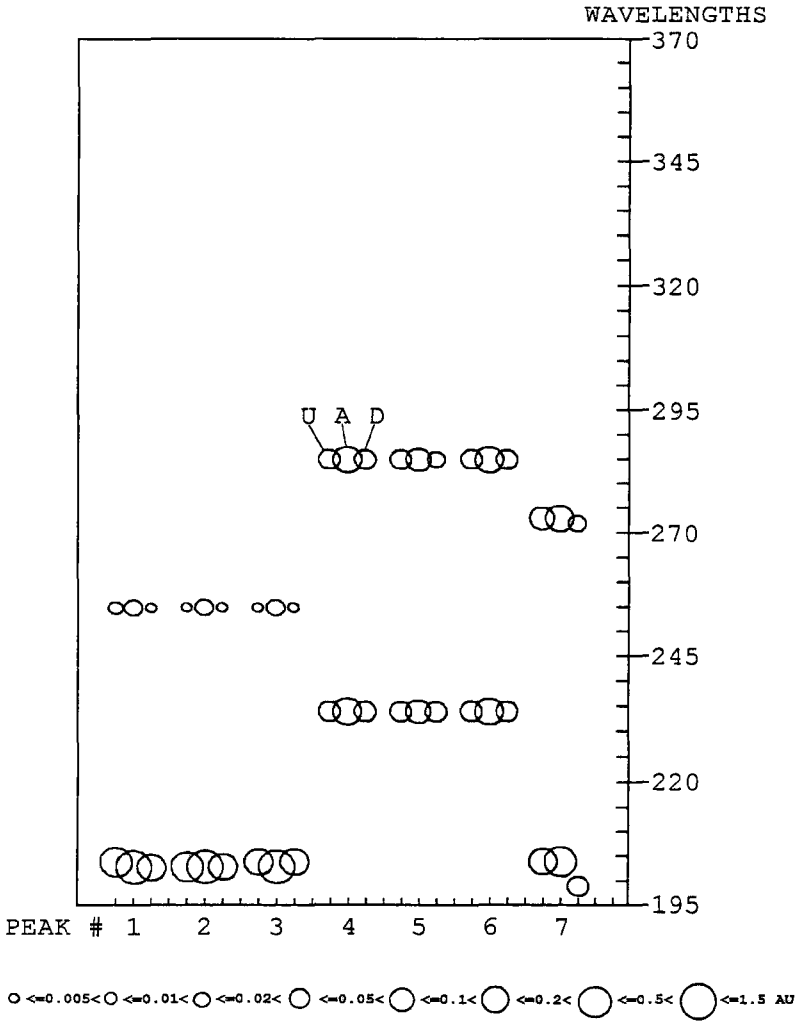

FIGURE 2 : Absorbance profile map of the seven compounds examined: circles represent the intensities of the absorption maxima of the eluting substances. The wavelengths of the absorption maxima at the upslope (U), the apex (A), and the downslope (D) must be coincident for pure peaks.

The between-day precision and accuracy of the proposed method were assessed by the repeated analysis of the representative sample over a period of sixteen days. The results are summarised in Table 3.

A major problem in quantitative analysis is whether a chromatographic peak consists of one or more components, because impurities hidden under the sample compounds falsify results. DAD was used to acquire the UV spectra at the upslope, the apex and at the downslope of each peak. The absorption maxima were plotted peak against wavelength in the spectral absorbance profile map, as it is shown in Figure 2. For pure peaks the wavelengths corresponding to the absorption maxima at the upslope, the apex and at the downslope must be coincident.

A detection wavelength of 280 nm was selected for MDA, MDMA, MDE, and caffeine because of better specificity.

CONCLUSION

The present HPLC method provides a simple, rapid, precise, and accurate means of assay for amphetamines and 3,4-MDAs in tablets of illicit provenience, even in presence of two common adulterants. Hence it appears to be useful in the routine identification and determination of these substances.

REFERENCES

1. F.T. Noggle Jr., C.R. Clark, K.H. Bouhadir, and J. DeRuiter, J. Chromatogr. Sci., 29:78 (1991)

2. I. Jane, J. Chromatogr., 111:227 (1975)

3. T.A. Gough, and P.B. Baker, J. Chromatogr. Sci., 20:289 (1982)

4. F.T. Noggle Jr., J. DeRuiter, and C.R. Clark, J. Chromatogr. Sci., 28:529 (1990)

5. G. Maeder, M. Pelletier, and W. Haerdi, J. Chromatogr., 593:9 (1992)

6. H.J. Helmlin, and R. Brenneisen, J. Chromatogr., 593:87 (1992)

7. F.T. Noggle Jr., J. DeRuiter, C.L. McMillian, and C.R. Clark, J. Liq. Chromatogr., 10:2497 (1987)

8. F.T. Noggle, C.R. Clark, and J. DeRuiter, J. Liq. Chromatogr., 14:1913 (1991)

9. M. Bogusz, M. Erkens, R.D. Maier, and I. Schroeder, J. Liq. Chromatogr., 15:127 (1992)

10. R.J.M. Vervoort, F.A. Maris, and H. Hindriks, J. Chromatogr., 623:207 (1992)

11. R. Brenneisen, K. Mathys, S. Geisshuesler, H.U. Fisch, U. Koelbing, and P. Kalix, J. Liq. Chromatogr., 14:271 (1991)

12. P.A. Hays, and I.S. Lurie, J. Liq. Chromatogr., 14:3513 (1991)

13. H.J. Helmlin, D. Bourquin, and R. Brenneisen, J. Chromatogr., 623:381 (1992)

14. D. Bourquin, and R. Brenneisen, Anal. Chim. Acta, 198:183 (1987)

15. R. Brenneisen, and S. Borner, Pharm. Acta Helv., 60:302 (1985)

Received: March 19, 1993
Accepted: August 2, 1993

JOURNAL OF LIQUID CHROMATOGRAPHY, 17(3), 659-671 (1994)

FLUORESCENCE DETECTION OF MEXILETINE AND ITS *p*-HYDROXYLATED AND HYDROXY-METHYLATED METABOLITES IN HUMAN PLASMA AND URINE BY HIGH-PERFORMANCE LIQUID CHROMATOGRAPHY USING POST-COLUMN DERIVATIZATION WITH *o*-PHTHALALDEHYDE

T. TATEISHI, K. HARADA, AND A. EBIHARA
The Department of Clinical Pharmacology and Therapeutics
Jichi Medical School
Minamikawachi Tochigi 329-04, Japan

ABSTRACT

A liquid chromatographic procedure for the simultaneous determination of mexiletine and two major metabolites, *p*-hydroxymexiletine and hydroxymethylmexiletine, in plasma and urine is described. A reversed-phase ion-pair C_{18} column is used with gradient elution using post-column fluorescence derivatization with *o*-phthalaldehyde. The lower limits of detection are 2 ng/ml for mexiletine and *p*-hydroxymexiletine and 5 ng/ml for hydroxymethylmexiletine. Enzymatic hydrolysis of conjugate forms of oxidative metabolites in urine samples was also performed. The coefficients of variation for replicate assay of spiked samples were uniformly less than 10 % for all the analytes.

INTRODUCTION

Mexiletine (1-(2',6'-dimethylphenoxy)-2-aminoproprane) is a class 1B antiarrhythmic agent used for the control of ventricular arrhythmias (1). Mexiletine is eliminated mainly by hepatic oxidation (2). Among several oxidative metabolites, *p*-hydroxymexiletine and

hydroxymethylmexiletine are considered major metabolites (2,3), and aromatic hydroxylation to *p*-hydroxymexiletine and aliphatic hydroxylation to hydroxymethylmexiletine co-segregates with that of debrisoquine or sparteine (4,5). The oxidation of mexiletine and the formation of its metabolites are quite different between extensive and poor metabolizers of debrisoquine (5) . Although many methods have been reported to detect mexiletine in plasma or serum using HPLC (6,7,8,9,10), a few methods are available to determine mexiletine and *p*-hydroxymexiletine and hydroxymethylmexiletine simultaneously (11,12).

o-Phthalaldehyde (OPTA) has been widely used for the fluorometric analysis of amino acids and biologically active amines (13,14). OPTA easily reacts with primary amines in alkaline medium in the presence of 2-mercaptoethanol, and forms strongly fluorescent isoindolic derivatives. The pre-column method with an OPTA reagent was reported to detect mexiletine and tocainide in plasma (15).

The aim of this study was to develop an HPLC assay for simultaneous determination of mexiletine and its main metabolites, *p*-hydroxymexiletine and hydroxymethylmexiletine, following the formation of a post-column derivative with OPTA in plasma and urine.

MATERIALS and METHODS

Chemical and reagents

Mexiletine, *p*-hydroxymexiletine, hydroxymethyomexiletine and 4-methylmexiletine (internal standard, IS) were generously provided by Nippon Boehringer Ingelheim (Hyo-go, Japan). 1-Octanesulfonic acid sodium salt (HPLC grade) was obtained from Kodak (Rochester, NY, USA). OPTA and mercaptoethanol were purchased from Tokyo

Chemical (Tokyo, Japan) and Wako (Osaka, Japan), respectively. β-Glucuronidase extracted from Helix pomatia (Type H-5) was obtained from Sigma (St.Louis, MO, USA). All other reagents were of analytical-reagent grade. Deionized and distilled water was used throughout this investigation.

Preparation of standards

Stock standard solutions of mexiletine, *p*-hydroxymexiletine, hydroxy-methylmexiletine and 4-methylmexiletine were prepared by dissolving 50 mg of each compound in 50 ml of methanol and stored at 4 °C. Plasma standards for calibration or precision determination in the range 0.01-1.0 μg/ml were prepared by diluting these stock solutions with fresh plasma obtained non-medicated normal volunteers.

Instrumentation and conditions

The chromatographic system consisted of two pumps (880PU, Jasco, Tokyo, Japan), a solvent mixing module (880-31, Jasco, Tokyo, Japan), an automatic injector (855AS, Jasco, Tokyo, Japan), a Wakosil ODS Column (4.6 mm I.D. x 25 cm, Wako, Osaka, Japan) protected with a Wakosil ODS guard column (4.6 mm I.D. x 1 cm, Wako, Osaka, Japan), fluorometer (821FP, Jasco, Tokyo, Japan) and a chart recorder (Chromatocorder12, SIC, Tokyo, Japan). For the post-column method, the column eluate was mixed with OPTA reagent which was delivered by a pump (880PU, Jasco, Tokyo, Japan) through a T-piece (851R, Jasco, Tokyo, Japan). The mixture were allowed to flow successively through 0.5 mm x 5 m long tefzel-tube (865R, Jasco, Tokyo, Japan). The

column with the guard column and tefzel-tube were in a column oven (Oven A-30, Shodex, Tokyo, Japan).

The mobile phase was a mixture of the mobile phase "A" and "B", which consisted of 10 mM H_3PO_4, methanol and 1.4 mM 1-Octanesulfonic acid, the proportions of which were controlled by a gradient program. The mobile phase was delivered at a constant flow rate of 1.0 ml/min. The mobile phase "A" was prepared by mixing 160 ml of methanol, 840 ml of 10 mM H_3PO_4 and 300 mg of 1-Octansulfonic acid sodium salt. The mobile phase "B" was prepared by mixing 800 ml of methanol, 200 ml of 10mM H_3PO_4 and 300 mg of 1-Octansulfonic acid sodium salt. The gradient was 0 to 10 min:65 to 20 % A, 10 to 14 min:20 % A, 14 to 15 min:20 to 65 % A, 15 to 25 min: 65 % A.

The OPTA reagent was prepared everyday by mixing 0.5 ml of mercaptoethanol, 900 ml of 0.2 M borate buffer (PH 10.0) and 100 ml of ethanol dissolved 300 mg of OPTA in advance. This reagent was delivered at a flow-rate of 0.6 ml/min.

The fluorometer was set to an excitation wavelength at 345 nm and an emission wavelength at 445 nm.

Extraction procedure

A 1 ml aliquot of plasma was introduced into a 10ml capped polypropylene centrifuge tube to which 50 ml of the I.S. solution (1 mg), 1 ml of 0.2 M borate buffer (pH 9) and 7 ml of diethyl ether were added. After the mixture was agitated on a reciprocating shaker for 10 min and then centrifuged at 3000 g for 5 min, the sample was frozen in a methanol-dry ice bath. The organic phase was transferred into another polypropylene tube and evaporated to dryness in a stream of nitrogen at 40 °C. The residue was reconstituted with 250 μl of 50:50 mixture of the mobile phase "A" and "B" for a second and 100 μl were injected on to the column.

Enzymatic hydrolysis of conjugate metabolites in urine

A 100 μl aliquot of urine was introduced into a 10ml capped polypropylene centrifuge tube to which 300 μl of 1 M sodium acetate buffer (pH 5.5) and 5.7 mg of Sigma Type H-5 enzyme, containing 440,000 U/g β-glucuronidase (i.e., 2500 U) were added. After vortexing, the tubes were incubated for 1, 2, 3, 4, 6 and 10 hours at 37 °C in a water bath. Following hydrolysis, the samples were mixed with 100 μl of the I.S. solution (2 μg), 1 ml of 0.2 M borate buffer (pH 10) and 7 ml of diethyl ether. Other extraction procedure was same as plasma.

Calibration graph and Recovery

Calibration graphs for mexiletine, *p*-hydroxymexiletine, hydroxymethymexiletine were constructed by the analysis of three standard solutions with the concentrations 0.01, 0.1, 1.0 μg/ml for each compound. Linear calibration plots of mexiletine and its metabolites were generated by least-squares regression of the peak-area ratios of the analyte to the internal standard. The recovery was determined by comparing the peak areas of mexiletine and its metabolites obtained by analyzing a standard plasma sample with the peak areas obtained by direct injection of the standard solution.

Application of the method

Two fully informed healthy subjects received 150 mg of mexiletine orally after overnight fasting. Blood samples were obtained just before and at 0.5, 1, 2, 4, 6, 9, 24, 33 and 48 hours after dosage. Blood samples were mixed with a small amount of heparin

(a)

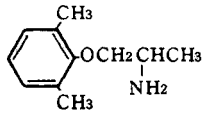

(b)

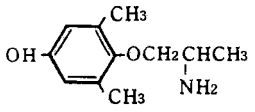

(c)

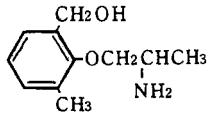

(d)

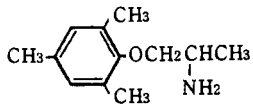

FIGURE 1. Structure of (a) mexiletine, (b) *p*-hydroxymexiletine, (c) hydroxymethylmexiletine, and (d) the internal standard.

and immediately centrifuged at 3000 g, and plasma was stored at - 20 °C until analyzed. Urine was collected for 48 hours and was stored in a refrigerated glass tube at - 20 °C.

RESULTS and DISCUSSION

Recently OPTA has been widely used as a pre-column and post-column derivation reagent for the fluorometric analysis of compounds containing a primary amines. Mexiletine, *p*-hydroxymexiletine, hydroxymethylmexiletine and 4-methylmexiletine contain

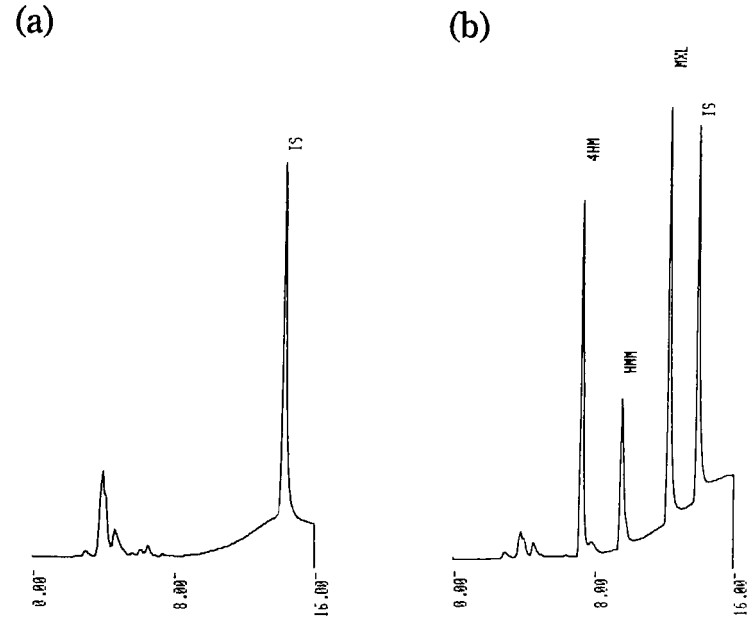

FIGURE 2. Chromatograms obtained from (a) blank plasma containing 1 μg the internal standard, and (b) standard sample containing 1 μg each of *p*-hydroxymexiletine (HM), hydroxymethylmexiletine (HMM), mexiletine (MXL) and the internal standard (IS).

a primary amine group at the β-position of the carbon chain (Figure 1). Although pre-column derivation is convenient for the detection of mexiletine, there were many interfering peaks in a chromatogram of blank plasma and besides, in our experiences, the peaks of *p*-hydroxymexiletine and hydroxymethylmexiletine could not be separated from each other. Therefore, we planned to separate mexiletine and its metabolites by reversed-phase ion-pair HPLC with gradient elution and then to combine them with OPTA.

Typical chromatogram for the extracts of the blank plasma with the I.S. and standard plasma are shown in Figure 2. In post-column derivation, there is no interfering peak to detect mexiletine, its metabolites and the I.S..

TABLE 1.

Coefficients of variation and recovery of *p*-hydroxymexiletine, hydroxymethylmexiletine and mexiletine.

	Intra-assay	Inter-assay	recovery
	n=6	n=7	n=3
p-hydroxymexiletine			
10 ng	6.9 %	9.0 %	96.4 %
100 ng	4.6 %	5.5 %	93.0 %
1000 ng	3.5 %	6.0 %	89.3 %
hydroxymethylmexiletine			
10 ng	7.4 %	9.7 %	73.9 %
100 ng	6.2 %	7.9 %	56.9 %
1000 ng	4.7 %	7.6 %	52.2 %
mexiletine			
10 ng	6.3 %	8.2 %	96.4 %
100 ng	3.4 %	5.6 %	93.1 %
1000 ng	2.9 %	4.4 %	88.6 %

The calibration graphs were obtained by analyzing plasma samples at three concentration of 0.01, 0.1 and 1.0 μg/ml. The ratio of peak areas of mexiletine and its metabolites to the I.S. correlated linearly with their concentrations. The correlation coefficients of the lines constructed were 0.998, 0.997 and 0.998 for p-hydroxymexiletine, hydroxymethylmexiletine and mexiletine, respectively. The limit of detection of the assay

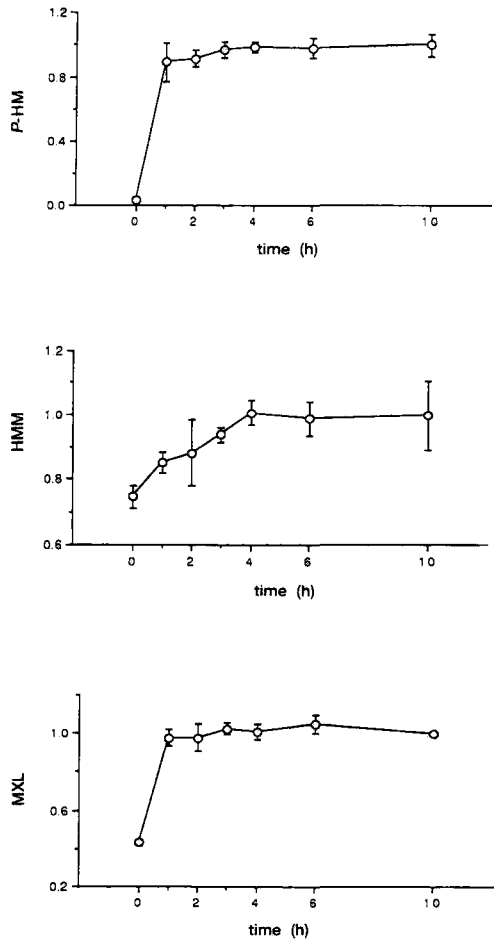

FIGURE 3. Effect of incubation time on the ratio of hydrolysis of *p*-hydroxymexiletine, hydroxymethylmexiletine, and mexiletine in a 100 µl of No 1 subject urine with 2500 U of β-glucuronidase. n=6, mean ± SD.

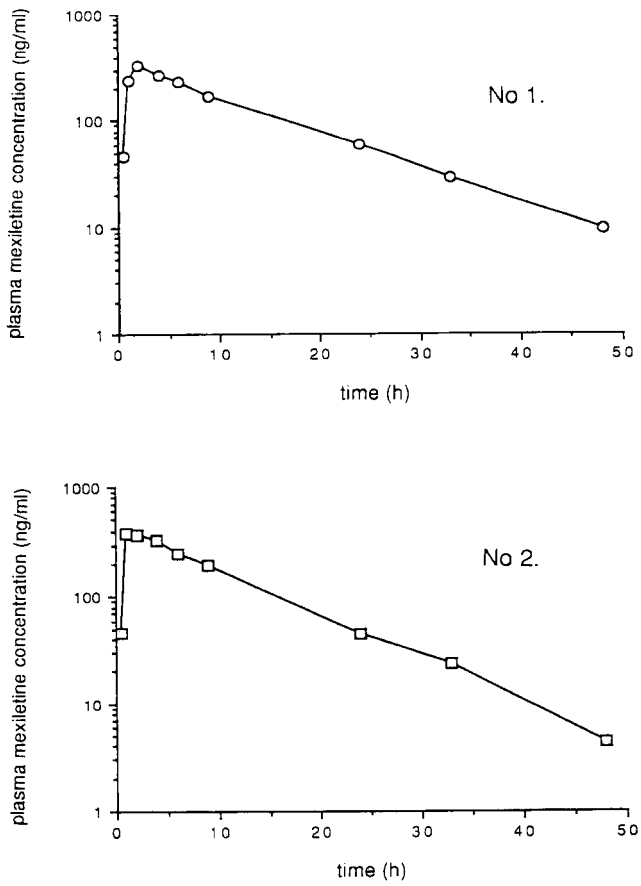

FIGURE 4. Plasma concentration time curve for mexiletine in two healthy volunteer after oral administration of 150 mg mexiletine hydrochloride.

determined in extracted plasma samples was 2, 5, and 2 ng/ml for *p*-hydroxymexiletine, hydroxymethylmexiletine and mexiletine, respectively. Table 1 shows the coefficient of variations of mexiletine and its metabolites for intra-assay and inter-assay and their recoveries. Diethyl ether extraction yielded an satisfactory extraction for *p*-hydroxymexiletine and mexiletine, whereas the recovery of hydroxymethylmexiletine

TABLE 2.

Pharmacokinetics and urinary recovery for 48 hours of mexiletine and its metabolites after a single oral administration of 150 mg mexiletine hydrochloride in two healthy subjects.

		No 1	No 2
Pharmacokinetics			
	Cmax (ng/ml)	327.2	377.9
	tmax (h)	2	1
	AUC (ng×h/ml)	4448.7	4690.0
	t1/2 (h)	9.3	7.3
	CLtot (L/h)	28.0	26.6
	CLren (L/h)	5.8	3.2
	CLhep (L/h)	22.2	23.3
Urinary recovery			
	mexiletine (%)	8.9	3.7
	p-HM (%)	22.0	20.1
	HMM (%)	19.9	26.1
	n-HM (%)	9.3	12.8

Cmax:maximum concentration, tmax:time of Cmax, AUC:area under the concentration -time curve from 0 to infinity. t1/2:terminal half-life, CLtot: apparent total clearance, CLren:renal clearance, CLhep:hepatic clearance (CLtot-CLren).
Values in urinary recovery are expressed as % of the administrated dose.
p-HM:*p*-hydroxymexiletine, HMM:hydroxymethylmexiletine, n-HM:*n*-hydroxymexiletine.

was insufficient. Since the coefficient of variation of hydroxymethylmexiletine was small, this extraction procedure was applied.

p-Hydroxymexiletine and hydroxymethylmexiletine are eliminated in urine unchanged and as glucuronide conjugates. *n*-Hydroxymexiletine is also eliminated in urine as a glucuronide conjugate. But this conjugate is reported to be changed to mexiletine after hydrolysis(5). To determine the incubation time, the concentrations of *p*-hydroxymexiletine, hydroxymethylmexiletine and mexiletine from a 100 μl of urine collected for 48 hrs from No. 1 subject were measured after incubation for 1, 2, 3, 4, 6 and 10 hours with 2500 U of β-glucuronidase. Incubations were carried out at 37 °C. Figure 3 shows that the percent of concentrations of three compounds after incubation for each period, compared with the concentrations after incubation for 10 hours. Maximal yield of the hydrolyzed metabolites and mexiletine were attained within 4 hours. The coefficients of variation of intra-day assay after enzymatic hydrolysis of urine samples (n=10) were 3.6 %, 3.5 % and 2.7 % for *p*-hydroxymexiletine, hydroxymethylmexiletine and mexiletine (*n*-hydroxymexiletine), respectively. Table 2 shows the pharmacokinetic parameters of mexiletine and the fractionary recovery of its metabolites from two subjects after the oral administration of 150 mg mexiletine.

In conclusion, the present post-column detection method shows good reproducibility and sensitivity for the determination of mexiletine and its metabolites in plasma and urine. This assay method can be recommended for pharmacokinetic study, especially in determining metabolic clearance.

ACKNOWLEDGEMENTS

We gratefully acknowledge the technical assistance provided by Ms. T. Kawaguchi. We are also indebted Nippon Boehringer Ingelheim Co., Ltd for kindly supplying mexiletine, *p*-hydroxymexiletine, hydroxymethylmexiletine and 4-methylmexiletine.

REFERENCES

1. R.L. Woosley, T. Wang, W. Stone, L. Sidoway, K. Thompson, H.J. Duff, I. Cerkus, D. Roden, Am. Heart J., 107:1058-1070(1984).
2. A.H. Beckett and E.C. Chidomere, Postgrad. med. J., 53(Suppl.I) :60-66(1977).
3. K.N. Scott, M.W. Cohgh, B.J.Wilder, C.M. Williams, Drug Metab. Dispos. 1:506-515(1973).
4. F. Broly, N. Vandamme, C. Libersa, M. Lhermitte, Br. J. clin. Pharmac., 32:459-466(1991).
5. J. Turgeon, C. Fiset, R. Giguere, M. Gilbert, K. Moerike, J.R. Rouleau, H.K. Kroemer, M. Eichelbaum, O. Grech-Belanger, P.M. Belanger, J. Pharmacol. Exp. Ther., 259:789-798(1991).
6. R.K. Bhamra, R.J. Flanagan, D.W. Holt, J. Chromatogr., 307:439-444(1984).
7. H. Breihaupt and M. Wilfling, J. Chromatogr., 230:97-105 (1982).
8. L.J. Dusci and L.P. Hackett, J. Anal. Toxicol., 9:67-70(1985).
9. O. Grech-Belanger, J. Turgeon, M. Gilbert, J. Chromatogr. Sci., 22:490-492(1984).
10. N. Shibata, M. Akabane, T, Minouchi, T, Ono, H, Shimakawa, J. Chromatogr., 566:187-194(1991).
11. B.K. Kramer, K.M. Ress, F. Mayer, V. Kuhlkamp, H.M. Liebich, T. Risler, L. Seipel, J. Chromatogr., 493:414-420 (1989)
12. D. Paczkowski, M. Filipek, Z. Mielniczuk, J. Andrzejczak, W. Poplawska, D. Sitkiewicz, J. Chromatogr., 573:235-246 (1992).
13. M.H. Joseph and P. Davies, J. Chromatogr., 277:125-136 (1983).
14. T.P. Davis, C.W. Gehrke, C.W. Gehrke, Jr., T.D. Cunningham, K.C. Kudo, K.O. Gerhardt, H.D. Johnson C.H. Williams, J. Chromatogr., 162:293-310(1979).
15. R.N. Gupta and M. Lew. J. Chromatogr., 344:221-230(1985).

Received: July 20, 1993
Accepted: August 5, 1993

JOURNAL OF LIQUID CHROMATOGRAPHY, 17(3), 673-683 (1994)

ANALYSIS OF TRACE LEVELS OF DEOXYNIVALENOL IN COW'S MILK BY HIGH PRESSURE LIQUID CHROMATOGRAPHY

D. K. VUDATHALA*, D. B. PRELUSKY, AND H. L. TRENHOLM
Centre for Food and Animal Research
Agriculture Canada
Central Experimental Farm
Ottawa, Ontario, Canada K1A 0C6

ABSTRACT

An HPLC method using UV detection for the analysis of trace levels of the mycotoxin deoxynivalenol (DON) in milk is described. For a small sample size of 3.0 ml, the cleanup method included precipitation of milk protein with acetic acid, followed by the additional removal of protein and fat by filtration. The resulting filtrate was eluted through an Extrelut column, followed by a second elution through a charcoal-alumina column. HPLC separation of the eluent was accomplished on a C18 reversed phase column and 4% acetonitrile (ACN) in water as the mobile phase. Acceptable detection limit of 5 ng/ml milk and very consistent recoveries of 57.1±1.2% were obtained with milk spiked in the range 25-200 ng/ml. This method is superior to the existing methods that are tedious and/or required expensive GC/MS instrumentation.

INTRODUCTION

Deoxynivalenol (DON, vomitoxin) is a fungal metabolite, produced by various species of Fusarium, most commonly present in cereals and feed (Vesonder et al. 1973). In swine exposure of feed contaminated with DON has been reported to cause feed refusal, reduced weight gain and in case of acute exposure, emesis (Forsyth

et al. 1977, Friend et al. 1982 & 1983, Schuch et al. 1982, Trenholm et al. 1984, Vesonder 1980/81). However, dairy cattle, sheep and poultry do not display any apparent sign of toxicity on exposure to DON at the levels typically found in naturally contaminated grain and feedstuffs (Trenholm et al. 1984, Hamilton et al. 1985). While dairy cows have been shown to transmit negligible levels of DON or its metabolites (Cote et al. 1986) into milk on exposure to DON after a single dose (Prelusky et al. 1984), exposure over an extended period of five days to three cows at a very high dose of DON led to noticeable quantity of DOM-1, a metabolite of DON, in one cow. However the exposure of DON contaminated feed over a longer period and to a larger number of cows needed to be carried out to fully evaluate the accumulation of DON or DOM-1 into its milk in free form and/or as glucronide conjugate. For this type of study a simple method was required that could be applied to a large number of samples at the same time.

Although there are several methods reported in the literature for the analysis of DON in cereal grain and mixed feed (e.g., Bennett et al. 1983, Chang et al. 1984, Cohen and Lapointe 1982, Ehrlich et al. 1983, Scott et al. 1981, Visconti and Bottalico 1983), the methods reported for its analysis in milk are limited. Swanson et al. (1986) used 40 ml of milk and the procedure is tedious and time consuming. The method described by Prelusky et al. (1984) although comparably simple required the selectivity of GC-selective ion monitoring (SIM)/MS. The purpose of the present study was not only to develop a method that was relatively simple, rapid and sensitive but also that used small sample size and did not require GC/MS instrumentation.

EXPERIMENTAL

Chemicals and Materials

Sterile 0.45 μm Millex-HA filters were purchased from Millipore Products Division, Bedford, MA, USA. Extrelut columns, 3 ml capacity, manufactured by EM Science (A division of EM Industries Inc., Gibbstown, NJ, USA) were used for liquid/liquid extraction. The charcoal/alumina (1.5 g/1.4 g) columns used were packed in-house by using 10 ml (8 mm id) borosilicate glass pipets (Fisher Scientific, Pittsburgh, PA, USA), activated charcoal (Darco G-60, Baker Chemical co., Phillipsburg, NJ, USA), neutral alumina (70-230 mesh, Merck M 01077-36, BDH Chemicals, Toronto, ON, Canada) and glass wool, according to the method reported by Trenholm et al.(1985). Water used was of NANOpure quality and all the solvents were of HPLC grade (BDH Chemicals). ß-Glucuronidase (500,000 units in 4.0 ml) and deoxynivalenol were purchased from Sigma Chemical Company, St. Louis, MO, USA.

Standard Solutions

DON was dissolved in 4% acetonitrile (ACN) in water to give a stock concentration of 1 μg/ml. Recoveries were calculated by comparing peak-heights of DON from milk extracts with standards. Clean milk was obtained from cows fed with standard feeding ration and housed at the CFAR green-belt farm, Nepean, Ontario. Milk samples were stored frozen prior to use.

Sample Preparation

Three ml milk samples, spiked with DON (0-200 ng/ml), were incubated at 50°C for 15 min with 300 μl of 5% acetic acid to

precipitate protein, followed by centrifugation at 3500 rpm for 10 min. The supernatant was filtered through a 0.45 μm millipore filter to remove any remaining protein and fat. The filtrate was made basic (pH 7-8) with the addition of solid sodium bicarbonate (100 mg), which was then transferred to the Extrelut column. The sample was allowed to be absorbed on the column matrix over a period of 15 minutes. DON was then eluted from the column with 7 x 3 ml of 6% methanol in ethyl acetate and the eluent (approximately 20 ml) collected in a 25 ml glass tube. The eluent was evaporated to dryness under a stream of nitrogen at 50°C, redissolved in 4 ml of ACN:water (21:4), and loaded onto a charcoal/alumina column that was pre-washed with 15 ml of ACN:water (21:4). The sample tube was washed with 4+2 ml of ACN:water (21:4) and the washings were added on to the charcoal/alumina column. The column was eluted with an additional 20 ml of ACN:water (21:4). All eluted fractions (~30 ml) from the charcoal/alumina column were collected, evaporated to dryness (N_2, 50°C) and redissolved in 600 μl of 4% ACN in water. A sample of 100 μl (equivalent to 0.5 ml milk) was then injected onto HPLC for analysis.

Instrumentation

The HPLC analysis of DON was performed with a Spectra-Physics SP 8800 autosampler, SP 8810 pump, SP 4400 integrator and 783 A programmable absorbance detector from Applied Biosystems Inc. A reversed-phase 25 X 0.46 cm column packed with C18 packing material of 5 μm particle size (CSC-Nucl. 120A/ODS, Chromatographic Sciences Company Inc., Montreal, QC, Canada) was used. The guard column used was ADSORBOSPHERE C18 with 5 μm packing (Alltech Associates Inc., Applied Sciences Labs, Deerfield, Il, USA).

The mobile phase consisted of 4% ACN in water, pumped at a flow rate of 1.0 ml/min. The UV detector was set at a wavelength of 220 nm, range 0.001 AUF and rise time of 5 sec; and integrator was used at attenuation of 8-32 and chart speed of 0.25 cm/min. A 100 µl sample solution was injected on full-loop injection mode in the sequence: standard, 2 samples and standard.

Enzymatic Hydrolysis

A 3 ml milk sample was incubated with 1.5 ml of 0.1 M phosphate buffer (pH 6.8) containing 3000 units of ß-glucuronidase (0.4 ml of ß-glucuronidase was dissolved in phosphate buffer to give a total volume of 25 ml; 2000 units/ml) for 16 h at 37°C. Following hydrolysis milk contents were then prepared for HPLC analysis as described under sample preparation.

RESULT AND DISCUSSION

Due to the complexity of the milk matrix with components of a wide range of polarity, it was challenging to get extracts purified sufficiently to be analyzed for trace levels of DON at an UV-wavelength of 220 nm by HPLC. To achieve this, it was necessary that the interfering fat and proteins present in milk be adequately removed. Attempted initially was the addition of ammonium sulfate solid to precipitate out the protein, but the resulting product obtained after cleanup remained unsuitable for analysis. Subsequently, a weak acid such as 5% acetic acid was found to be a better choice to precipitate the protein. Although protein and fat tend to aggregate on addition of acid to warm milk (50°C), filtration was done with 0.45 µm filter to get a clear

filtrate from the whey. This process removed most of the fat globules that have diameter of 1-8 μm (Mulder and Walstra 1974). Increasing the pH of the filtrate with sodium bicarbonate to 7-8 was necessary to obtain a sufficiently clean chromatogram. Without this step the extract was not suitable for analysis of DON due to interfering compounds carried over during the cleanup.

Because the Extrelut columns supplied by the company were found to introduce contaminants into the analyses, it was necessary that columns were washed with 3 x 5 ml of ethyl acetate and dried overnight under vacuum prior to use. The alkaline filtrate (equivalent to 3 ml of milk) was loaded onto these pre-cleaned Extrelut columns. For elution, 7 x 3 ml of 6% methanol in ethyl acetate was found to be appropriate for optimum recovery of DON. At any higher proportion of methanol, although recoveries may have improved slightly, the columns bled unwanted contaminants. The eluent was dried at 50°C under a stream of nitrogen. The residue, however, was found not suitable at this point for direct analysis on HPLC and required further cleanup.

Standard charcoal/alumina columns (0.75 g/0.7 g) were tried as a second step of cleanup, but did not give sufficiently clean extracts. However, samples obtained by using twice the amount of charcoal and alumina (i.e., 1.5 g of charcoal and 1.4 g of alumina) were found to be suitable for analysis. Chromatograms of milk extracts did not show any interfering peaks at the retention time of DON, when sample extracts equivalent to 0.5 ml of milk were injected.

The hydrolysis with ß-glucronidase was carried out to free any DON or DOM-1 glucronide conjugate that may be present in the milk of cows fed contaminated feed. It was done to ensure that the

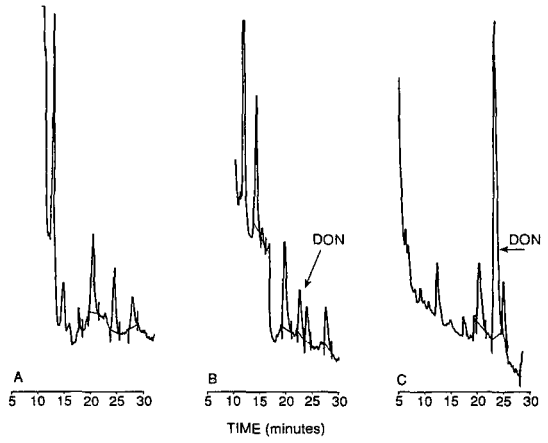

Figure 1: High pressure liquid chromatograms of (a) extract of clean milk; (b) milk spiked with 10 ng/ml of DON; and (c) milk spiked with 100 ng/ml of DON. Equivalent of 0.5 ml milk was injected for each of these chromatograms.

addition and hydrolysis of spiked samples with ß-glucronidase does not introduce any interference with the DON analysis.

Recoveries of DON from Milk

Three ml of clean milk, free of DON, was spiked with various amounts of DON to determine the recoveries and limit of detection. To establish the detection limit milk spiked with 5, 10, 15, 20 and 25 ng/ml of DON was used and for recoveries milk spiked at 25, 50, 75, 100, 125, 150, 175 and 200 ng/ml of DON was used. The recoveries for 25-200 ng/ml were consistently in the range of 55-59% regardless of concentration (shown in Table 1).

A number of factors might have contributed to the lower recovery of DON from milk. First, the concentration of DON used

Table 1: Recoveries of DON from Milk

Conc. of DON (ng/ml of milk)	% Recovery[1]
25	57.2±6.4
50	56.3±9.7
75	56.2±5.6
100	58.4±9.1
125	57.9±4.3
150	55.4±8.2
175	58.7±3.4
200	56.3±4.6

1. average ± standard deviation (n=6)

was very low. The precipitation of protein followed by filtration to remove protein and fat could be the major factor. It is very difficult to get all the liquid from the protein precipitate by filtration. The residual liquid in the protein precipitate and the protein itself might have retained some DON. The two sequential cleanups through Extrelut column and charcoal/alumina column could also have made some contribution to the lower recovery.

Linearity and Sensitivity

The relationship between the peak height and concentration of DON was linear over the range of 25-200 ng/ml of milk (r^2=0.98). Although DON could be detected in spiked milk at a minimal concentration of 5 ng/ml (based on 3 X baseline noise), the response varied below 25 ng/ml. It could be quantified readily over the range of 25-200 ng/ml.

Precision

Since equivalent to 0.5 ml of milk was injected on column, the system precision of the assay was determined by making multiple injections from a set of standard solutions with known DON contents of 10-100 ng on column. System precision, using the equipment described here, was 2.3% relative standard deviation (RSD) at 10 ng on column (n=6) and 1.6% at 100 ng on column (n=6).

CONCLUSIONS

A novel HPLC method for the analysis of trace levels (5-200 ng/ml) of DON in small milk volumes is described. This method is well suited to monitor trace residues of DON in milk after exposure to DON contaminated feed. Although recovery of DON was less than ideal, it remained very consistent (57.1±1.2%) in the 25-200 ng/ml range.

BIBLIOGRAPHY

BENNETT, G.A.; STUBBLEFIELD, R.D.; SHANNON, G.M.; SHOTWELL, O.M. Gas chromatographic determination of deoxynivalenol in wheat. J. Assoc. Off. Anal. Chem.; 66: 1479-1480 (1983).

CHANG, H.L.; DE VRIES, J.W.; LARSON, P.A.; PATEL. H.H. Rapid determination of deoxynivalenol (vomitoxin) by liquid chromatography using modified Romer column cleanup. J. Assoc. Off. Anal. Chem.; 67: 52-54 (1984).

COHEN, H.; LAPOINTE, M. Capillary gas-liquid chromatographic determination of vomitoxin in cereal grains. J. Assoc. Off. Anal. Chem.; 65(6): 1429-1434 (1982).

COTE, L. M.; DAHLEM, T.; YOSHIZAWA, T.; SWANSON, S. P.;BUCK, W. B. Excretion of deoxynivalenol and its metabolite, DOM-1, in milk, urine, and feces of lactating dairy cows. J. Dairy Sci.; 2416-2423 (1986).

EHRLICH, K.C.; LEE, L.S.; CIEGLER, A. A simple, sensitive method for detection of vomitoxin (deoxynivalenol) using reversed phase, high performance liquid chromatography. J. Liq. Chromatogr.; 6: 833-843 (1983).

FORSYTH, D.M.; YOSHIZAWA, T.; MOROOKA, N.; TUITE, J. Emetic and refusal activity of deoxynivalenol to swine. Appl. Environ. Microbiol.; 34(5): 547-552 (1977).

FRIEND, D.W.; TRENHOLM, H.L.; ELLIOT, J.I.; THOMPSON, B.K.; HARTIN, K.E. Effect of feeding vomitoxin-contaminated wheat to pigs. Canadian Journal of Animal Science; 62: 1211-1222 (1982).

FRIEND, D.W.; TRENHOLM, H.L.; FISER, P.S.; THOMPSON, B.K.; HARTIN, K.E. Effect on dam performance and fetal development of deoxynivalenol (vomitoxin) contaminated wheat in the diet of pregnant gilts. Canadian Journal of Animal Science; 63: 689-698 (1983).

HAMILTON, R.M.G.; TRENHOLM, H.L.; THOMPSON, B.K.; GREENHALGH, R. The tolerance of white leghorn and broiler chicks, and turkey poults to diets that contained deoxynivalenol-contaminated wheat. Poultry Sci.; 273-286 (1985).

MULDER, H.; WALSTRA P. The milk fat globule emulsion science as applied to milk products and comparable foods. Commonwealth Agr. Publ. Document, Wageningen, The Netherlands, 1974, pp. 210-227 .

PRELUSKY, D.B.; TRENHOLM, H.L.; LAWRENCE, G.A.; SCOTT, P.M. Nontransmission of deoxynivalenol (vomitoxin) to milk following oral administration to dairy cows. J. Environ. Sci. Health; B19: 593-609 (1984).

SCHUH, M.; LEIBETSEDER, J.; GLAWISCHNIG,E. Chronic effects of different levels of deoxynivalenol on weight gain, feed consumption, blood parameters, pathological as well as histopathological changes in fattening pigs. Fifth International IUPAC Symposium on Mycotoxins and Phycotoxins: 273-276 (1982).

SCOTT, P.M.; LAU, P-Y.; KANHERE, S.R. Gas Chromatography with electron capture and mass spectrometric detection of deoxynivalenol in wheat and other grains. J. Assoc. Off. Anal. Chem.; 64(6): 1364-1371 (1981).

SWANSON, S.P.; DAHLEM, A.M.; ROOD, H.D., Jr.; COTE, L.-M.; BUCK, W.B.; YOSHIZAWA, T. Gas chromatographic analysis of milk for deoxynivalenol and its metabolite DOM-1. J. Assoc. Off. Anal. Chem.; 69: 41-43 (1986).

TRENHOLM, H.L.; HAMILTON, R.M.G.; FRIEND, D.W.; THOMPSON, B.K.; HARTIN, K.E. Feeding trials with vomitoxin (deoxynivalenol)-contaminated wheat: Effects on swine, poultry, and dairy cattle. Journal of the American Veterinary Medical Association; 185(5): 527-531 (1984).

TRENHOLM, H.L.; WARNER, R.M.; PRELUSKY, D.B. Assessment of extraction procedures in the analysis of naturally contaminated grain products for deoxynivalenol (vomitoxin). J. Assoc. Off. Anal. Chem.; 68: 645-649 (1985).

VESONDER, R.F.; CIEGLER, A.; JENSEN, A.H. Isolation of the emetic principle from Fusarium-infected corn. Appl. Microbiol.; 26: 1008-1010 (1973).

VESONDER, R.F.; HESSELTINE, C.W. Vomitoxin: natural occurrence on cereal grains and significance as a refusal and emetic factor to swine. Process. Biochem; 12-44 (1980/81; Dec./Jan.).

VISCONTI, A.; BOTTALICO, A. Detection of Fusarium trichothecenes (nivalenol, deoxynivalenol, fusarenone and 3-acetyldeoxynivalenol) by high-performance liquid chromatography. Chromatographia; 17: 97-100 (1983).

Received: July 18, 1993
Accepted: August 5, 1993

JOURNAL OF LIQUID CHROMATOGRAPHY, 17(3), 685-705 (1994)

SIMULTANEOUS MEASUREMENT OF MONOAMINE, AMINO ACID, AND DRUG LEVELS, USING HIGH PERFORMANCE LIQUID CHROMATOGRAPHY AND COULOMETRIC ARRAY TECHNOLOGY: APPLICATION TO *IN VIVO* MICRODIALYSIS PERFUSATE ANALYSIS

IAN N. ACWORTH[1,2], JIAN YU[1], ELIZABETH RYAN[2], KATHLEEN COX GARIEPY[1,2], PAUL GAMACHE[2], KEITH HULL[1], AND TIMOTHY MAHER[1]

[1]*Department of Pharmacology*
Massachusetts College of Pharmacy
179 Longwood Avenue
Boston, Massachusetts 02115
[2]*ESA, Inc.*
45 Wiggins Avenue
Bedford, Massachusetts 01730

ABSTRACT

An automated HPLC coulometric array-ECD method is described for the simultaneous analysis of monoamines, their metabolites, derivatized amino acids, and pharmacological agents. This method has been used with in vivo microdialysis in urethane-anesthetized animals to examine extracellular fluid levels of endogenous and exogenous analytes after the peripheral administration of drugs. An aliquot of dialysate was initially analyzed for the monoamines, their metabolites and drugs by isocratic elution and detection on eight serial coulometric electrodes (0 to 490 mV; 70 mV increment). The remaining sample was then derivatized, pre-column, with OPA/ßME and, after column switching, was analyzed on a parallel isocratic system with detection on four electrodes (set at 250, 450, 550 and 650 mV respectively). Compounds were identified by their retention time and electrochemical profile across the arrays. This method had a limit of detection of 0.125 pg/µl for the monoamines and 0.75 pg/µl for amino acids (both with a signal to noise (S/N) ratio of 3:1). The detector response was linear over several orders of magnitude (0.25 to 20 pg/µl) for monoamines, their metabolites and the amino acids. The analysis was completed within 25 min.

A variety of drugs were also measured including: apomorphine (Apo), hydralazine (H), isoproterenol (Iso), methoxamine (Mx), morphine sulfate (M) and its metabolite morphine-3-glucuronide (M3G), and phenylephrine (Phe). The limit of detection for these compounds varied from 0.215 to 10.65 pg/µl (Phe

and M3G respectively) with a S/N ratio of 3:1. The detector response was linear from 0.5-500 pg/µl and the linear regression correlation coefficient (r) varied from 0.9969 to 0.9998 (H and M3G respectively).

The peripheral administration of H (10 mg/kg i.v.) produced a 40% decrease in blood pressure (BP) and caused an almost immediate 220 fold increase in striatal dopamine (DA) levels. Levels of DOPAC and HVA decreased by 80-90% and those of the amino acids glutamate (GLU), aspartate (ASP), taurine (TAU) and gamma amino-butyric acid (GABA) increased 30-120 fold. Striatal levels of H reached a maximum of 9 pg/µl (405 pg/collection) 40 min after its administration. Nitroprusside (NPr) infusion (0.06-0.3 mg/min/kg i.v.) also decreased BP by 30%, increased striatal DA levels by 100 fold, and decreased levels of DOPAC and HVA by 40-50%. Although the amino acids were also affected, their levels began to increase only 140 min after the start of drug administration. NPr could not be detected using this method. In a separate experiment, hippocampal perfusate levels of M were found to reach a maximum of 12.6 pg/µl (567 pg/collection), 40min after its peripheral administration (10 mg/kg i.p.). Although M decreased hippocampal ECF levels of GABA and GLY, it appeared to have little effect on the other analytes measured.

This method not only makes it possible to study the interaction between different neurotransmitter pathways but also offers a more detailed inspection of the mechanism of drug action, a direct measure as to whether drugs pass through the blood-brain barrier (BBB) as well as direct acquisition of pharmacokinetic data.

INTRODUCTION

The central efficacy of a drug may ultimately depend upon its level within the brain. Levels, in turn, are dependent upon several other factors including: dosage, route of administration, clearance (catabolism, metabolic conversion, excretion), tissue distribution and most importantly on its ability to pass the BBB. In the past, the central level of a drug was usually determined by examination of tissue homogenates with the inherent loss of compartmentalization, cellular distribution and the necessary use of large numbers of animals (for dose-response and temporal studies). Only recently have techniques become available with the potential for such studies to be done in vivo [for reviews see 1,2,3]. One such method, microdialysis, overcomes many of the above disadvantages and allows for continuous monitoring of the changes in a drug's level within discrete brain regions in a single animal [4-8]. Microdialysis has now become a routine sampling technique [9,10] which allows examination of the chemical microenvironment within the extracellular space of a variety of tissues including blood, adipose, liver and muscle. Most commonly used in nervous tissue, microdialysis is often coupled to HPLC analysis for examination of neurotransmitter release and metabolism in neurochemical, pharmacological, physiological or behavioral studies [see 11].

The central mechanism of drug action is often not exclusive to one particular neurotransmitter pathway but the drug may exert its effect via a dynamic interplay between various neurotransmitter systems which are involved at a primary, secondary or even tertiary level. The simultaneous measurement of the release and metabolism of different neurotransmitter systems should afford a better

understanding of a drug's action. Concurrent measurement of dialysate levels of the drug affecting neurotransmitter release is not often practical [12] but extremely desirable.

We report here an HPLC array-ECD method capable of measuring monoamines, their metabolites, amino acids and drug levels concurrently in microdialysis perfusates. We have used this technique to examine the effects of drug-induced hypotension on striatal neurotransmitter release and drug levels in perfusates obtained from the urethane anesthetized rat. This technique has also been used to examine the passage of morphine through the BBB and its effect on various neurotransmitter pathways. Finally, we have used this technique to resolve a variety of centrally acting drugs and metabolites.

METHODS

Materials

HPLC grade ultra-pure water (Milli-Q, Millipore, Bedford, USA) >18 megaohm/cm^3 was further purified by passing through C18 solid phase extraction columns (Millipore Sep-Pak C18) to remove residual trace organics, and was used for preparation of all mobile phases and other solutions. o-Phthalaldehyde (OPA), beta-mercaptoethanol (ßME) and external standards were obtained from Sigma (St. Louis, MO, USA). Drugs utilized were either obtained from Sigma or RBI (Natick, MA, USA). All chemicals used in the HPLC analysis were of the highest grade available from either Sigma or Fluka (Buchs, Switzerland). Solvents were HPLC grade and were obtained from EM Science (Gibbstown, NJ, USA). Salts used in the artificial cerebro-spinal fluid (aCSF) perfusion medium were Microselect grade from Fluka.

Microdialysis

Male Sprague-Dawley rats (275-325 g) were anesthetized with urethane (2 g/kg i.p. with additional doses as necessary). Animals had both their carotid artery (connected to a Stathm pressure transducer and a Grass 79D polygraph for BP and heart-rate monitoring) and jugular vein (for drug administration) cannulated with heparinized PE50 tubing. After placement in a stereotaxic frame, the cranial skin was incised and the periosteum resected. A hole was drilled through the cranium above the right striatum

using a 1.8 mm trephine. A pre-calibrated 3 mm loop-design regenerated cellulose microdialysis probe (ESA, Inc., Bedford, MA, USA) was placed within the striatum using the following coordinates from Bregma (flat-skull): AP +0.7 mm; LR 2.7 mm; DV -7.5 mm from dura. Animals had their temperature monitored by rectal thermistor and were maintained at 37±0.5 ^{o}C using a heating pad. aCSF (based on the composition developed by Moghaddam and Bunney [13] but lacking ascorbic acid) was perfused through the probe at 1.5 µl/min using a Model 22 microperfusion pump (ESA, Inc.). Samples were collected every 20 min into 10 µl of 0.2 M perchloric acid (PCA) in order to minimize monoamine degradation.

For the experiments examining the passage of M through the BBB the above protocol was modified as follows: the animals were not vascularly cannulated; the probe was placed in the right hippocampus (from Bregma: AP -5.8 mm; LR 4.8 mm; DV -7.5 mm from dura); and M was administered intraperitoneally.

Experimental Design

After placement of the probe within the specified brain region and after a 90-120 min period of injury-mediated monoamine release, samples were continuously collected and analyzed every 20 min. Following attainment of baseline (a steady-state situation defined as the period when levels of DA varied by less than 10% in at least three consecutive samples), the drug was administered. After a further 2-3 hr period, animals were euthanised by anesthetic overdose.

Drug Administration

Animals received either H (10 mg/kg bolus i.v., in physiological saline) or NPr (i.v. infusion; 0.06-0.3 mg/min/kg in saline, to decrease BP by 30%) or M (10 mg/kg i.p. in saline).

Probe Pre-calibration

The in vitro recovery of each probe was determined by perfusion of the probe with aCSF while placing the probe in a mixture of either external standards (1-3 µM) or drugs (1 mg/ml) dissolved in

acidified (0.1 M PCA) aCSF. After a period of 30 min (to achieve steady-state), 2-3 samples were collected every 20 min, at a flow rate of 1.5 µl/min and at a temperature of 24 ^{o}C. External standards were analyzed directly (drugs were analyzed after further dilution) as described below. The average probe recovery (with minimal inter-probe variability) was 30% for the monoamines, 40% for the amino acids and typically 15-18% for the various drugs studied. The same probe was able to be used in more than ten animals before decreased recovery compromised the analytical sensitivity. The in vitro recovery was only used to measure individual probe performance and inter-probe variability and not used to estimate extracellular fluid concentrations (this would be misleading as the diffusion kinetics in vivo are known to differ from those in vitro [14,15]).

HPLC Coulometric Electrode Array Analysis

Samples were analyzed with a Coulochem Electrode Array System (CEAS, Model 5500, ESA Inc.) in dual isocratic mode consisting of a Model 465 autoinjector, two Model 420 dual piston pumps, a ten port switching valve and three coulometric array cell modules (each with four graphite working electrodes). The flow diagram for the analysis of monoamines, metabolites and drugs as well as derivatized amino acids has previously been described [16]. Briefly, analytes were separated on two stainless steel 150 x 4.6 mm NBS columns containing 5 µ M.S. Gel C18 (ODS particles having 120A pore size; distributed by ESA Inc.). Two detector arrays were used. Monoamines, metabolites and drugs were measured on eight electrodes (0 to 490 mV, 70 mV increments; vs. palladium reference); the OPA/ßME amino acid derivatives were measured using four electrodes set at 250, 450, 550 and 650 mV, respectively. The columns, pulse dampeners and electrode arrays were housed in a temperature regulated compartment maintained at 33±0.1 ^{o}C. System control, data acquisition and analysis were performed with the CEAS software on an Epson 386 computer. Two twenty microliter aliquots of diluted perfusate were analyzed for each sample [16].

Derivatization Protocol.

Samples were derivatized automatically on the autosampler. The method was based on that of Donzanti and Yamamoto [17], modified by the addition of 10 µM EDTA to the borate buffer diluent. Fresh OPA stock solutions were prepared weekly (27 mg OPA was dissolved in 1 ml methanol; after the

addition of 5 µl of ßME, this solution was diluted to 10 ml with a borate/EDTA solution (0.1 M sodium tetraborate, pH 9.3; 10 µM EDTA)). The stock solution was stored at 4 ^{o}C and was protected from light. The OPA working solution was prepared daily by dilution of the OPA stock solution with borate/EDTA 1:3 (v/v). The working solution was placed in amber vials in the refrigerated autosampler (4 ^{o}C).

Mobile Phases

Monoamines, metabolites and drugs were eluted using mobile phase A, consisting of: 0.054 M monobasic sodium phosphate containing 1.24 mM heptane sulfonic acid (sodium salt)/methanol 92:8 (v/v), adjusted to pH 3.0 with HPLC grade phosphoric acid. Amino acid derivatives were eluted using mobile phase B, consisting of: 0.139 M dibasic sodium phosphate/ acetronitrile/ methanol - 71.9:3.1:25 (v/v/v), adjusted to pH 6.8 with HPLC grade phosphoric acid. A flow rate of 1.2 ml/min was used for both mobile phases.

Standards

Individual monoamine and metabolite standard stock solutions (0.1 to 1.0 mg/ml) were prepared in 0.1 M PCA containing 10 µg/ml ascorbic acid and 10% methanol (v/v). Each solution was purged with nitrogen and stored at -80 ^{o}C (stable for several months). Amino acid stock solutions (1 mg/ml) were prepared in 50% methanol (v/v) and stored at -4 ^{o}C. An external standard mixture was used for the perfusate analysis containing the monoamine and metabolites at 5 pg/µl and the amino acids at 500 pg/µl prepared in acidified (0.1 M PCA) aCSF.

Individual drug standards (1 mg/ml) were prepared in water and stored at 4^{o}C with the exception of apomorphine and hydralazine which were dissolved in 50% methanol v/v containing 10 µg/ml ascorbic acid and were prepared on the day of analysis (also stored at 4 ^{o}C). Drug mixtures for analysis were prepared at final concentrations ranging from 10-100 pg/µl in 10 µg/ml ascorbic acid.

Data Analysis

Data were acquired and analyzed using the CEAS software version 4.0 (ESA, Inc.). Data manipulation was performed using LOTUS 1-2-3 (Lotus Corp., Cambridge, MA, USA) and GBSTAT (Dynamic Microsystems, Inc., Silver Spring, MD, USA) software.

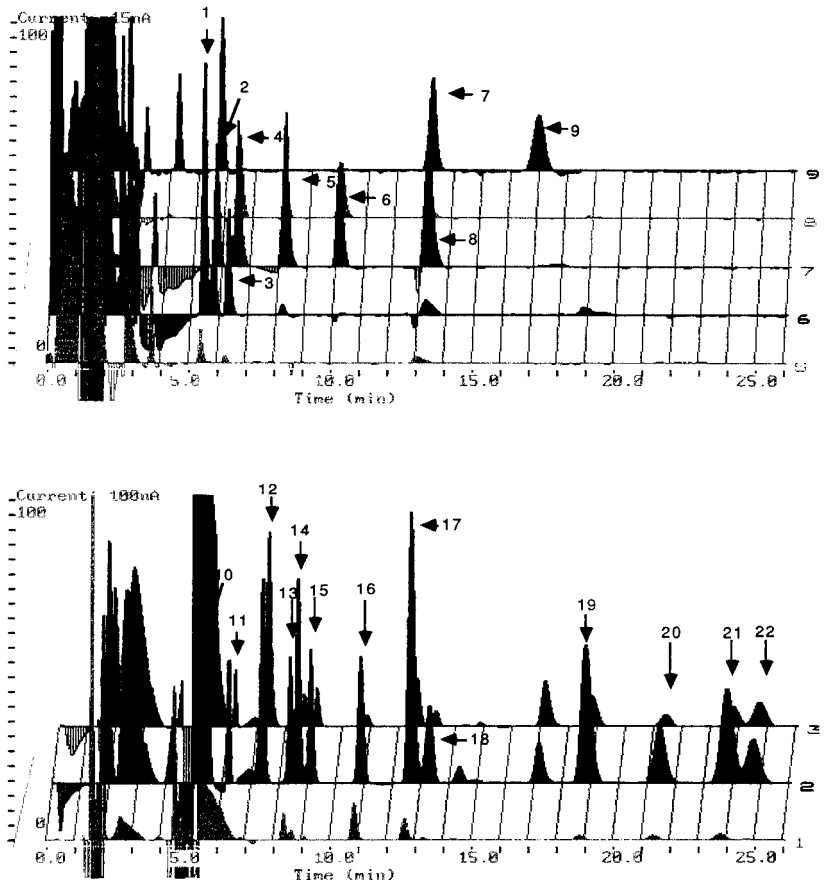

FIGURE I

Three dimensional chromatogram of the external standard mixture illustrating chromatographic and voltammetric resolution of each compound. The upper figure illustrates resolution of the monoamines and metabolites (100 pg on column) on electrodes 5 to 9 (0 to 280 mV; 70 mV increments) at a sensitivity of 15 nA full scale. The lower figure illustrates the resolution of derivatized amino acids (10 ng on column) on electrodes 1 to 3 (250, 450 and 550 mV respectively) at a sensitivity of 100 nA full scale. 1 - DA; 2 - 3-hydroxykynurenine; 3 - DOPAC; 4 - 5-hydroxytryptophan; 5 - 5HTOL; 6 - 5HIAA; 7 - 3MT; 8 - 5HT; 9 - HVA; 10 - ASP; 11 - GLU; 12 - ASN; 13 - HIS; 14 - SER; 15 - GLN; 16 - ARG; 17 - GLY; 18 - THR; 19 - TAU; 20 - ALA; 21 - GABA; 22 - TYR.

TABLE I
Abbreviations, Approximate Retention Times And Oxidation Potenials For Analytes Discussed In Text

MONOAMINES AND METABOLITES	ABBREVIATIONS	APPROXIMATE R.T. (min)	OXIDATION POTENTIAL (mV)
3-Methoxytyramine	3MT	14.12	280
5-Hydroxyindole-acetic acid	5HIAA	10.78	140
5-Hydroxytryptamine	5HT	14.13	140
5-Hydroxytryptophan	5HTP	6.60	140
5-Hydroxytryptophol	5HTOL	8.75	140
Dopamine	DA	5.57	70
3,4-Dihydroxyphenyl-acetic acid	DOPAC	6.34	70
Homovanillic Acid	HVA	17.58	280
Norepinephrine	NE	2.51	70
AMINO ACIDS			
Alanine	ALA	21.69	450
Arginine	ARG	10.70	450
Asparagine	ASN	7.50	450
Aspartic acid	ASP	5.56	450
GABA	GABA	24.12	450
Glutamine	GLN	9.22	450
Glutamic acid	GLU	6.28	450
Glycine	GLY	12.75	450
Histidine	HIS	8.48	450
Serine	SER	8.76	450
Taurine	TAU	18.99	450
Threonine	THR	13.40	450
Tyrosine	TYR	25.02	450
DRUGS			
Apomorphine	APO	4.50	0
Hydralazine	H	12.50	0
Isoproterenol	ISO	8.90	70
Methoxamine	Mx	5.00	900
Morphine	M	11.10	280
Morphine-3-glucuronide	M3G	4.00	900
Phenylephrine	Phe	7.60	700

RESULTS

External Standard Analysis

Two, three-dimensional chromatograms obtained from the analysis of the 18 component external standard are shown in Figure I. The abbreviation, retention time and oxidation potential for each compound are summarized in Table I. A representative chromatogram showing the resolution of the drug

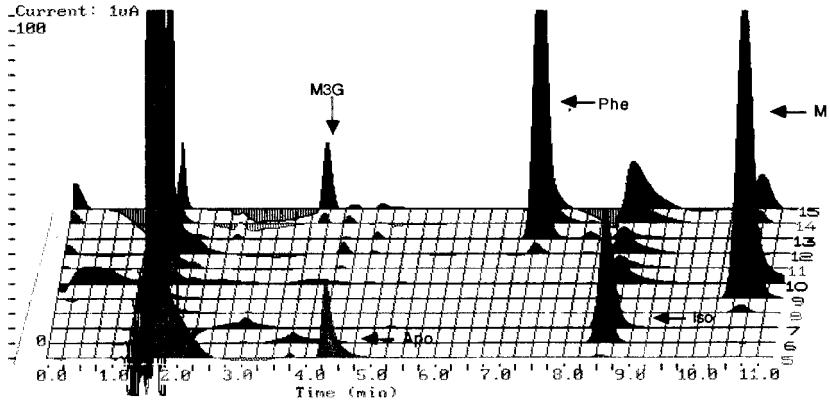

FIGURE II

Three dimensional chromatogram showing resolution of external standard drug mixture (1 ng/ul). An extended monoamine electrode array (twelve electrodes spanning 0 to 950 mV) was initially used to better examine each drug's electrochemical behavior. Output from electrodes 5 (0 mV) through 15 (800 mV) are shown at a gain of 1 μA. Analytical conditions are as described above.

standard mixture is shown in Figure II. Analysis of aCSF did not show any contaminant peaks capable of interfering with measured analytes (data not shown). The assay was completed within 25 min.

Linearity And Limit Of Detection

Regression analysis of the peak height versus concentration of the monoamines, metabolites and amino acids demonstrated linear response over the range 0.25-20 pg/μl (correlation coefficient values (r) for 5HT, 5HIAA, DA and GABA were 0.9989, 0.9969, 0.9999 and 0.9975 respectively). Similarly, the drugs analyzed showed linear response over a concentration range of 0.5-500 pg/μl with r values for H, Iso, M, M3G and Phe of 0.9969, 0.9998, 0.9998, 0.9998 and 0.9998 respectively. Drug linearity (each point represents an n of 3) is presented in Figure III.

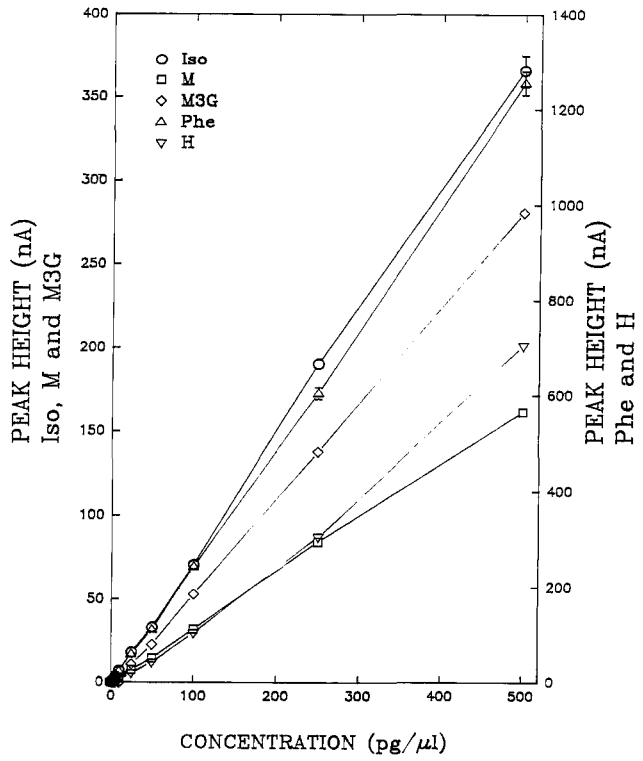

FIGURE III

Linearity of drug standards shown as peak height response (nA) over a concentration range of 0-500 pg/μl. Data presented as mean±SEM, n=3 for each data point.

The limit of detection (S/N ratio of 3:1) estimated from external standards for microdialysis perfusates was approximately 0.125 pg/μl for the monoamines and 0.75 pg/μl for the amino acids. The limit of detection (pg/μl) for H, Iso, M, M3G and Phe were: 0.65, 0.28, 1.25, 10.65 and 0.215 respectively.

Endogenous Metabolite Levels

The basal levels (in pg/collection, presented as mean±SEM) and ratio accuracies of monoamines, metabolites and amino acids in both striatal (n=3-6) and hippocampal (n=3) microdialysate samples are

TABLE II
Basal Striatal and Hippocampal ECF Analyte Levels

Monoamines and Metabolites	Basal Striatal Levels: pg/Collection Mean ± SEM (n = 3-6)	Basal Striatal Levels: Typical "Ratio Accuracy"	Basal Hippocampal Levels: pg/Collection Mean ± SEM (n = 3)	Basal Hippocampal Levels: Typical "Ratio Accuracy"
3MT	54 ± 8.6	0.98	ND	–
5HIAA	2880 ± 585	0.99	1530 ± 63	0.99
5HT	ND	–	19.4 ± 11	0
5HTOL	ND	–	ND	–
DA	51.8 ± 6.8	0.99	6.3 ± 0.5	0.96
DOPAC	12645 ± 1485	0.70	259 ± 47	0.95
HVA	13905 ± 225	0.79	117 ± 14	0.95
NE	ND	–	ND	–
Amino Acids				
ALA	13095 ± 450	0.95	7695 ± 1215	0.98
ARG	14355 ± 1305	0.94	10170 ± 675	0.93
ASN	3420 ± 225	0	3510 ± 90	0
ASP	2835 ± 585	0	3730 ± 90	0.23
GABA	383 ± 32	0	293 ± 45	0
GLN	318195 ± 22860	0.91	21105 ± 4680	0.62
GLU	12870 ± 540	0.93	4860 ± 270	0.94
GLY	16425 ± 4590	0.93	5850 ± 765	0.75
HIS	11115 ± 495	0.91	ND	0.60
SER	21105 ± 1980	0.99	10395 ± 225	0.96
TAU	12501 ± 945	0.94	8973 ± 270	0.77
THR	21780 ± 3555	0.96	16470 ± 405	0.99
TYR	1800 ± 45	0.98	5625 ± 270	0.98

ND = Not detectable

corrected 3 Oct 94/AP

TABLE II
Basal Striatal and Hippocampal ECF Analyte Levels

	Basal Striatal Levels		Basal Hippocampal Levels	
Monoamines and Metabolites	pg/Collection Mean ± SEM (n = 3-6)	Typical "Ratio Accuracy"	pg/Collection Mean ± SEM (n = 3)	Typical "Ratio Accuracy"
3MT	54 ± 8.6	0.98	ND	--
5HIAA	2880 ± 585	0.99	1530 ± 63	0.99
5HT	ND	--	19.4 ± 11	0
5HTOL	ND	--	ND	--
DA	51.8 ± 6.8	0.99	63. ± 0.5	0.96
DOPAC	12645 ± 1485	0.70	259 ± 47	0.95
HVA	13905 ± 225	0.79	117 ± 14	0.95
NE	ND	--	ND	--
Amino Acids				
ALA	13095 ± 450	0.95	7695 ± 1215	0.98
ARG	14355 ± 1305	0.94	10170 ± 675	0.93
ASN	3420 ± 225	0	3510 ± 90	0
ASP	2835 ± 585	0	8730 ± 90	0.23
GABA	383 ± 32	0	293 ± 45	0
GLN	318195 ± 22860	0.91	21105 ± 4680	0.62
GLU	12870 ± 540	0.93	4860 ± 270	0.94
GLY	16425 ± 4590	0.93	5850 ± 765	0.75
HIS	11115 ± 495	0.91	ND	0.60
SER	21105 ± 1980	0.99	10395 ± 225	0.96
TAU	12501 ± 945	0.94	8973 ± 270	0.77
THR	21780 ± 3555	0.96	16470 ± 405	0.99
TYR	1800 ± 45	0.98	5625 ± 270	0.98

ND = Not detectable

presented in Table II. More than 50-70 additional peaks were found in the microdialysis samples but could not be identified or quantitated due to the lack of appropriate external standards.

The effects of infusion with either H or NPr on striatal analyte levels calculated as percent of baseline (mean of three consecutive basal samples) at 20 and at 180 min are summarized in Table III. As shown in Figure IV, H caused an almost immediate 40% decrease in BP while increasing ECF DA levels 220 fold and decreasing those of DOPAC and HVA 80-90% (upper graph); there was also a rapid 30-120 fold increase in amino acid levels (lower graph). Although NPr also stimulated DA release by approximately 100 fold, decreased DOPAC and HVA levels 40-50% and decreased BP 30% (Figure V, upper graph), the effect of NPr on amino acid levels (Figure V, lower graph) was markedly different to that of H. The passage of H through the BBB reached a maximum of 9 pg/µl (405 pg/collection; uncorrected for in vitro

TABLE III
Effects of Hydralazine Or Nitroprusside On Striatal Analyte Levels

Monoamines and Metabolites	Hydralazine % Of Baseline At 20 min	Hydralazine % Of Baseline At 180 min	Nitroprusside % Of Baseline At 20 min	Nitroprusside % Of Baseline At 180 min
3MT	(8.2)	(15.62)	203	262
5HIAA	93	17	99	41
5HT	ND	ND	ND	(1.11)
5HTOL	ND	(1.2)	ND	ND
DA	22374	3427	1394	10350
DOPAC	101	20	108	51
HVA	77	12	95	31
NE	ND	ND	ND	ND
Amino Acids				
ALA	257	647	105	509
ARG	89	100	84	75
ASN	130	241	91	163
ASP	651	1929	95	1029
GABA	3468	25796	133	6044
GLN	83	71	78	50
GLU	472	3466	102	2030
GLY	217	915	78	249
HIS	91	131	84	104
SER	200	255	80	102
TAU	525	3398	77	1432
THR	139	172	87	139
TYR	114	248	111	260

ND = Not detectable

The numbers in paranthesis are given in pg/µl (not as a percentage change of baseline) as basal striatal levels of 3MT and 5HTOL, and basal hippocampal levels of 5HT were below the detection limit.

recovery) 40 min after its peripheral administration and is presented in Figure VI. NPr could not be detected using this method. Infusion of saline (i.v.) had no effect on any of the measured analytes (data not shown).

The peripheral administration of M had little effect on hippocampal metabolite levels with the exception of GABA and GLY which showed marked decreases (presented as % change of baseline at 20min and 80 min. See Table IV). The passage of M through the BBB reached a maximum of 12.6 pg/µl (567 pg/collection; uncorrected for in vitro recovery) 40 min after its i.p. administration and is shown in Figure VII. M3G could not be measured centrally after peripheral administration of M. Administration of saline (i.p.) had no effect on any of the measured analytes (data not shown).

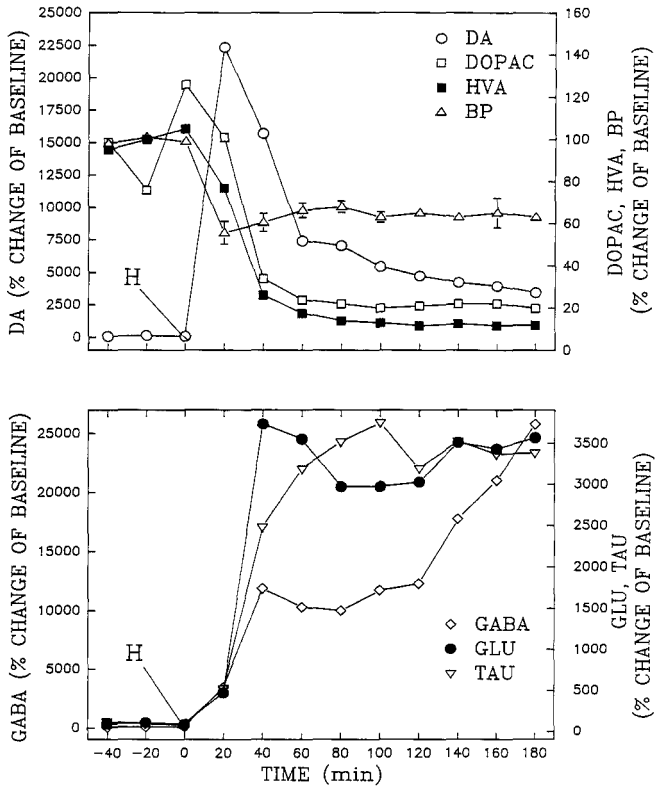

FIGURE IV

The effects of H (10 mg/kg i.v. given as bolus at t=0 min) on striatal ECF levels of analytes and blood pressure in the urethane anesthetized rat. Data are presented as % change of basal levels (100%) vs. time (min). The upper figure shows the response of DA (left vertical axis) and of DOPAC, HVA and BP (right vertical axis) to H infusion. The lower figure shows the response of GABA (left vertical axis) and of GLU and TAU (right vertical axis) to H infusion.

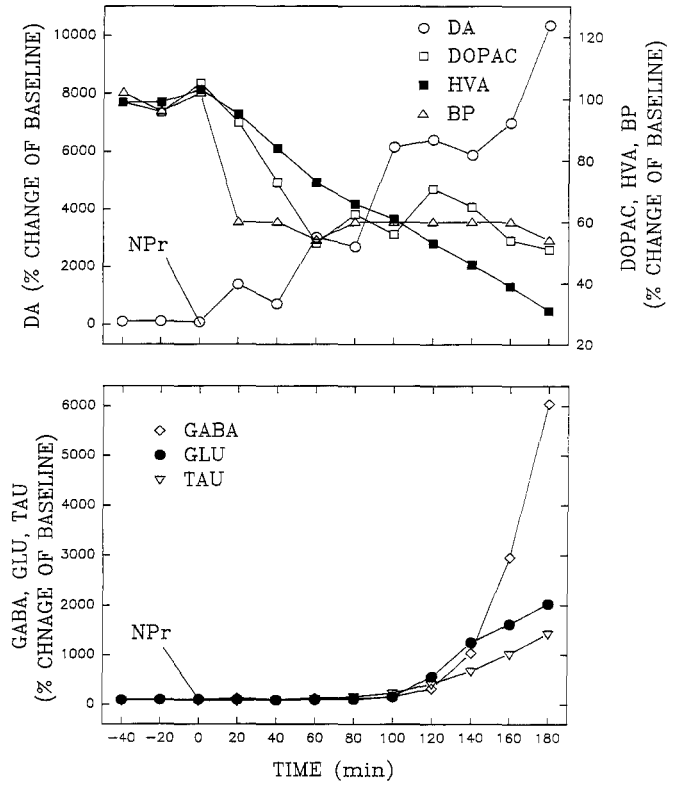

FIGURE V

The effects of NPr (0.06-0.3 mg/min/kg i.v.; infusion started at t=0 min) on striatal ECF levels of analytes and blood pressure in the urethane anesthetized rat. Data are presented as % change of basal levels (100%) vs. time (min). The upper figure shows the response of DA (left vertical axis) and of DOPAC, HVA and BP (right vertical axis) to NPr infusion. The lower figure shows the response of GABA, GLU and TAU to NPr infusion.

TABLE IV
Effects Of Morphine On Hippocampal ECF Analyte Levels

Monoamines and Metabolites	% Of Baseline 20 min	80 min	Amino Acids	% Of Baseline 20 min	80 min
3MT	ND	ND	ALA	67	63
5HIAA	85	97	ARG	81	81
5HT	98	30	ASN	94	105
5HTOL	ND	ND	ASP	ND	ND
DA	150	121	GABA	78	52
DOPAC	103	133	GLN	57	56
HVA	97	41	GLU	110	91
NE	ND	ND	GLY	66	16
			HIS	85	87
			SER	80	78
			TAU	86	96
			THR	80	75
			TYR	88	73

ND = Not detectable

DISCUSSION

The results presented here indicate that this method may be used for the routine measurement of a variety of analytes in microdialysis samples. Multiple analyte measurement in a single analytical run should minimize experimental error induced by excessive sample handling, sample instability, as well as differences in extraction efficiency and instrument calibration. Additionally, data is obtained from a single animal overcoming potential errors caused by inter-animal variability. The coulometric array also allows for on-line resolution of co-eluting peaks (e.g. 5HT and 3MT). Since resolution is obtained in two dimensions (chromatographic and voltammetric), many components may be selectively determined within a single run. Response "ratio accuracies" (a simple mathematical comparison of the respective hydrodynamic voltammograms obtained from the external standard and the sample unknown [18,19]) provide an objective index of peak purity and confirmation of peak identity. The closer this number is to unity the greater the certainty of peak purity. A response "ratio accuracy" of zero represents a situation where there is only sufficient signal to quantitate on the highest responding electrode.

Our method is also capable of measuring a variety of drugs and can be used to examine their passage through the BBB. This is the first report of the direct measurement of the passage of H into the brain. Penetration is unlikely the result of H's unrestricted access through damaged areas of the BBB caused by probe insertion as the BBB is known to rapidly reseal after the initial trauma [14,20].

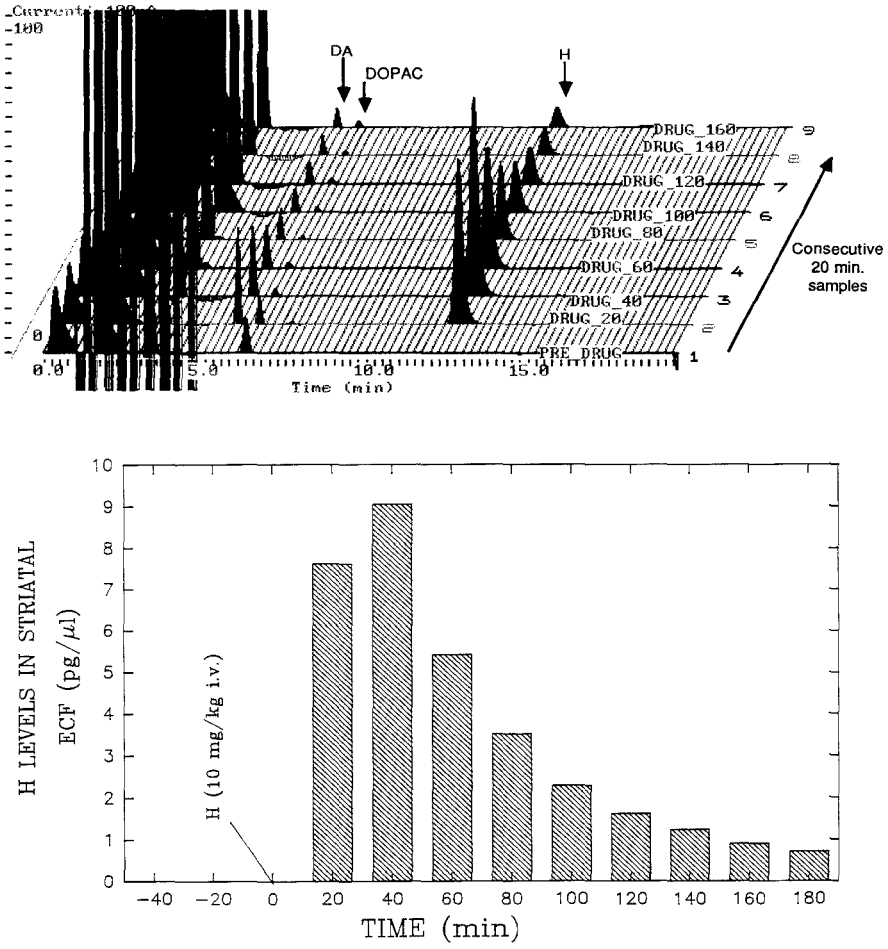

FIGURE VI

The simultaneous measurement of the passage of H through the BBB and its effect on striatal DA and DOPAC levels is illustrated in the upper figure. The response of electrode 5 (0 mV; 100 nA sensitivity full scale) is shown for consecutive 20 min samples, before and after H infusion (10 mg/kg i.v. given as a bolus at "Pre Drug"; #1). Striatal levels of H reached a maximum of 9 pg/μl 40 min after its administration - lower figure.

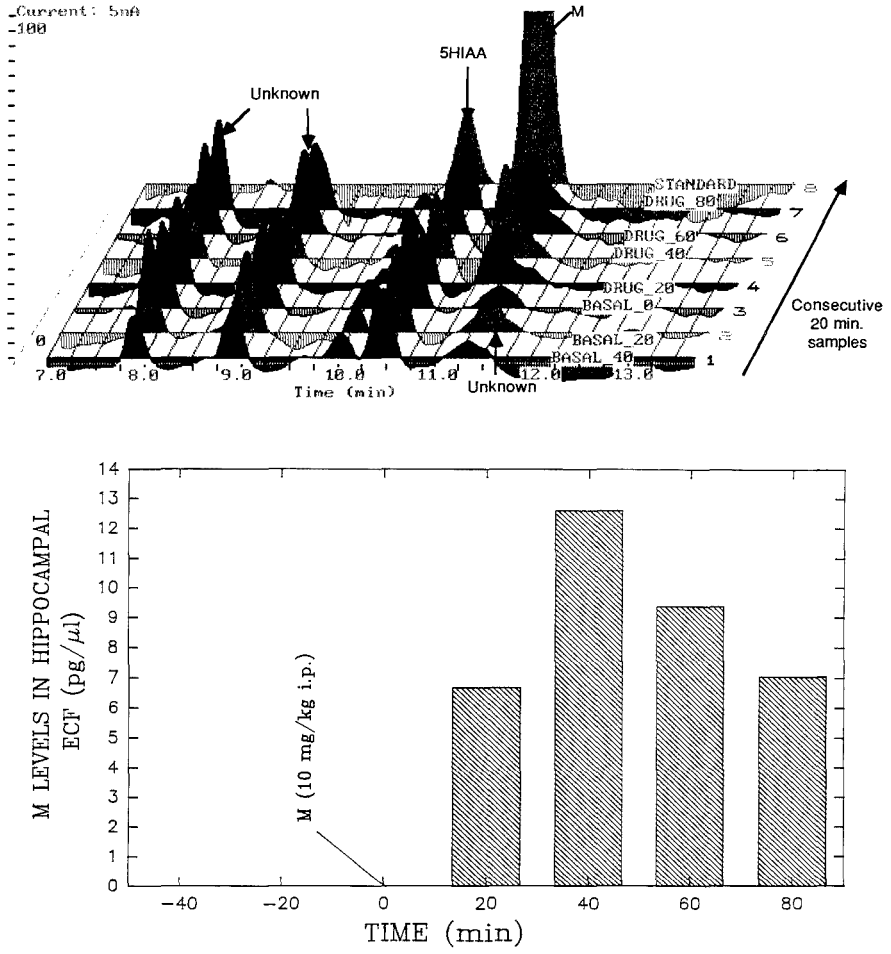

FIGURE VII

The simultaneous measurement of the passage of M through the BBB and its effect on hippocampal levels of 5HIAA and unknowns is illustrated in the upper figure. The response of electrode 9 (280 mV; 5 nA sensitivity full scale) is shown for consecutive 20 min samples, before and after M infusion (10 mg/kg i.p. given as a bolus at "Basal - 0") as well as for M external standard (100 ng/ml; #8). An unknown endogenous analyte eluted just after the M peak, but did not interfere with M quantification. Hippocampal levels of M reached a maximum of 12.6 pg/μl 40 min after its administration - lower figure.

Drugs used in this study were chosen due to their use in ongoing research. Of all the drugs measured the assay was least sensitive for measurement of M3G. This low M3G sensitivity may be due to the fact that its oxidation occurred at +900 mV, a potential with more noise and at which potential many endogenous compounds also oxidize. Apo was the most difficult compound to measure reliably due to its inherent instability and tendency to auto-oxidize. The inclusion of ascorbic acid in the diluent solution and EDTA (1 μM) in the mobile phase improved Apo's stability to some degree. Problems caused by system heavy metal catalyzed oxidation [21] were diminished by replacing the majority of stainless steel in contact with the fluid path with inert PEEK components wherever possible. Several other drugs were also examined including clonidine, MPP^+, quinpirole and SKF-38393. However, these could not be measured using the current system and their detection awaits further method development.

Basal analyte levels were generally in good agreement with values previously published for both the striatum [13, 22-24] and the hippocampus [22,25-27] when differences in probe membrane surface area, perfusion flow-rate, anesthetic and animal model are taken into consideration. Although tissue levels of NE can be easily quantitated using this method, due to the proximity of the NE peak to the void disturbance and low NE levels typically found in hippocampal microdialysis samples (ca. 1-10 pg/collection [26,28] accurate measurement of NE levels in these samples is difficult. The elution of NE can be delayed by reducing the methanol concentration of mobile phase A to 4% which then enables NE to be quantitated without void interference. Although 5HT is thought to act as a neurotransmitter in both the striatum [27] and hippocampus [29], over-estimation of its ECF level can easily occur as a result of simultaneous release from lysed platelets when surrounding tissue is damaged [30]. A more appropriate experiment would use the awake-animal model. This would permit at least 12 hrs between the time of probe insertion and the start of ECF analysis by which time neurotransmitter levels should more closely reflect basal conditions [31-33]. DA has previously been reported to be released from hippocampal synaptosomes [34] and has been recently measured in hippocampal ECF using microdialysis [35]. However, whether it acts as a neurotransmitter per se, or represents a precursor pool which is co-released with NE is presently being addressed [36].

Our data supports previous reports that drug induced hypotension can markedly increase striatal DA release while decreasing its catabolism [37]. Although both the antihypertensive H and NPr promote DA release to the same extent, the differences in the time course of DA release and the patterns of amino acids detected argues against a common mechanism of action. It is unlikely that H's effect can be

entirely explained through its weak monoamine oxidase inhibitor ability (administration of pargyline elevated ECF DA levels to a much lesser extent) or to ischemia. Ischemia would be expected to elevate 5HT to detectable levels [38,39] and to promote monoamine release in other brain regions. H has previously been reported to elevate DA and NE by only 2-3 fold in the hippocampus and has been shown to have no significant effect on their ECF levels in the pre-frontal cortex [40]. It is also doubtful that H is acting through a non-specific toxic mechanism as its effects on both DA and BP levels can be blocked by the co-administration of the alpha$_1$ adrenergic agonist Mx (a situation which would not be expected to interfere with the passage of H through the BBB) [37].

In a previous report F. Matos and colleagues [12] examined levels of M and its effect on 5HT, 5HIAA and HVA in the ECF from several brain regions as well as in CSF. Our data complement their findings and our method permits a more detailed examination of the effects of M on a variety of other compounds including several amino acids. Although M had some effect on most of the amino acids it markedly decreased the levels of the inhibitory amino acids, GABA and GLY, by 48 and 84% respectively. Interestingly, although M has previously been reported to act at opioidergic receptors in the substantia nigra and striatum and to involve interactions with both dopaminergic and GABA-ergic neurons [41], no reports of its action on hippocampal ECF levels of GABA could be found. Similarly, the peripheral administration of M has also been shown to decrease GLY levels in mouse brain homogenates [42] but its effect on ECF levels of GLY has not been previously demonstrated. In humans, M3G is the principal catabolite and potent morphine antagonist (M6G is only a minor metabolite) [43]. Hippocampal ECF levels of M3G could not be measured after peripheral M administration, suggesting either that formation of this conjugate is not the major route of catabolism in rat brain or, that if formed in the periphery, does not pass through the BBB.

In conclusion, our results demonstrate the potential of coupling microdialysis to HPLC array-ECD analysis for measuring drug levels in the ECF obtained from discrete brain areas with simultaneous determination of monoamines, metabolites and amino acids. The use of the awake, freely-moving animal will allow for the study of drug-induced changes in behavior concomitantly with the continuous monitoring of drug levels in discrete brain regions. It is hoped that different methods can be similarly linked using the switching valve so that different analytes may be measured simultaneously in the same sample (e.g. amino acids and derivatized drugs).

ACKNOWLEDGMENTS

The authors would like to thank Sheri Cottreau for help with preparation of the figures.

REFERENCES

1. F. Moroni, G. Pepeu, (1984) "The Cortical Cup Technique," in Measurement of Neurotransmitter Release In Vivo, C.A. Marsden, ed., John Wiley, Chicester, 1984, pp. 63-79.

2. A. Philippu, (1984) "Use of Push-pull Cannulae to Determine Release of Endogenous Neurotransmitters in Distinct Brain Areas of Anesthetized and Freely Moving Animals," in Measurement of Neurotransmitter Release In Vivo, C.A. Marsden ed., John Wiley, Chicester, 1984, pp. 3-37.

3. T.L. Yaksh, "Spinal Superfusion in Rat and Cat," in Measurement of Neurotransmitter Release In Vivo, C.A. Marsden ed., John Wiley, Chicester, 1984, pp. 107-124.

4. Y.L. Hurd, J. Kehr, U. Ungerstedt U. J. Neurochem., 51: 1314-1316 (1988)

5. K. Sabol, C. Freed, J. Neurosci. Methods, 24: 163-168 (1988)

6. L. Stahle, S. Segersvard, U. Ungerstedt, Eur. J. Pharmacol., 185: 187-193 (1990)

7. E.P. Wala, W.R. ., Martin, J.W. Sloan, Psychopharmacol. Berl., 105: 535-540 (1991).

8. W. Maruyama, D. Nakahara, M. Ota, T. Takahashi, A. Takahashi, T. Nagatsu, T. and M. Naoi, J. Neurochem., 59: 395-400 (1992)

9. U. Ungerstedt, "Measurement of Neurotransmitter Release by Intracranial Dialysis," in Measurement of Neurotransmitter Release In Vivo, C.A. Marsden ed., John Wiley, Chicester, 1984, pp. 81-105.

10. U. Ungerstedt, "Introduction to Microdialysis," in Microdialysis in The Neurosciences. Techniques in The Behavioral and Neural Sciences, Vol. 7. T.E Robinson and J.B. Justice Jr. eds., Elsevier, London, 1991, pp. 3-22.

11. H. Rollema, B.H.C. Westerink, W.J. Drijfhout, Monitoring Molecules in Neuroscience, Krips Repro, Meppel, The Netherlands, 1991.

12. F.F. Matos, H. Rollema, A.I. Basbaum, J. Neurochem., 58, 1773-1781 (1992)

13. B. Moghaddam, B. S. Bunney, J. Neurochem., 53, 652-654 (1989)

14. H. Benveniste, A.J. Hansen, "Practical Aspects of Using Microdialysis for Determination of Brain Interstitial Concentrations" in Microdialysis in The Neurosciences. Techniques in The Behavioral and Neural Sciences, T.E Robinson and J.B. Justice Jr., eds., Vol. 7. Elsevier, London, 1991, pp. 81-100

15. P.F. Morrison, P.M. Bungay, J.K. Hsiao, I.N. Mefford, K.H. Dykstra, R.L. Dedrick, "Quantitative Microdialysis," in Microdialysis in The Neurosciences. Techniques in The Behavioral and Neural Sciences, T.E Robinson, J.B. Justice Jr. eds., Vol. 7. Elsevier, London, 1991, pp. 47-80.

16. P. Gamache, E. Ryan, C. Svendsen, K. Murayama, I.N. Acworth, J. Chromatog., 614, 213-220 (1993)

17. B.A. Donzanti, B.K. Yamamoto, Life Sci., 43: 913-922 (1988)

18. W.R. Matson, P. Langlais, L. Volicer, P.G. Gamache, E. Bird, K.A. Mark, Clin. Chem., 30: 1477-1488 (1984)

19. J.A. Wolff, L.J. Fisher, L. Xu, H.A. Jinnah, P.J. Langlais, P.M. Luvone, K.L. O'Malley, M.B Rosenberg, S. Shimohama, T. Friedmann, F.H. Gage, Proc. Natl. Acad. Sci., 86: 9011-9014 (1989)

20. U. Tossman, U. Ungerstedt, Acta Physiol. Scand., 128: 9-14 (1986)

21. J. X-. Huang, J.D. Stuart, W.R. Melander, C. Horvath, J. Chromatog., 316: 151-161 (1984)

22. U. Tossman, G. Jonsson, U. Ungerstedt, Acta Physiol. Scand., 127: 533-545 (1986)

23. I.N. Acworth, M.J. During, R.J. Wurtman, Brain Res. Bull., 21: 473-477 (1988)

24. J. Kehr, U. Ungerstedt, J. Neurochem., 51: 1308-1310 (1988)

25. A. Hamberger, B. Nystrom, Neurochem. Res., 9: 1181-1191 (1984)

26. E.D. Abercrombie, J.M. Finlay, "Monitoring Extracellular Norepinephrine in Brain Using In Vivo Microdialysis and HPLC-EC," in Microdialysis in The Neurosciences. Techniques in The Behavioral and Neural Sciences, T.E Robinson and J.B. Justice Jr., eds. ,Vol. 7. Elsevier, London, 1991, pp. 253-274.

27. A. Adell, A. Carceller, F. Artigas, J. Neurochem., 56: 709-712 (1991)

28. E.D. Abercrombie, M.J. Zigmond, J. Neurosci., 9: 4062-4067 (1989)

29. P. Kalen, R.E. Strecker, E. Rosengren, A. Bjorklund, J. Neurochem., 51, 1422-1435 (1988)

30. J.R. Fozard, The Peripheral Actions of 5-Hydroxytryptamine, Oxford University Press, New York 1989.

31. B.H.C. Westerink, M.H.J. Tuinte, J. Neurochem., 46: 181-185 (1986)

32. B.H.C. Westerink, J.B. De Vries, J. Neurochem., 51: 683-687 (1988)

33. D.M. Camp, T.E. Robinson, J. Neurochem., 58: 1706-1715 (1992)

34. M. Verhage, W.E.J.M. Ghijsen, F. Boomsma, F.H Lopes da Silva, J. Neurochem., 59: 881-887 (1992)

35. C.S. Biggs, B.R. Pearce, L.J. Fowler, P.S. Whitton, J. Neurochem., 59: 1702-1708 (1992)

36. K.C. Gariepy, B.A. Bailey, J. Yu, T.J. Maher, I.N. Acworth, J. Chromatog., (submitted).

37. J. Yu, K. Gariepy, I.N. Acworth, T.J. Maher, Poster #197.10, pp. 460. Society for Neuroscience, Anaheim, California, 1992.

38. G. Damsma, D.P. Boisvert, L.A. Mudrick, D. Wenkstern, H.C. Fibiger, J. Neurochem., 54, 801-808 (1990)

39. G.S. Sarna, T.P. Obrenovitch, T. Matsumoto, L. Symon, G. Curzon, J. Neurochem., 55: 937-940 (1990)

40. J. Yu, I.N. Acworth, K. Gariepy, T.J. Maher, T. The Federation of American Societies for Experimental Biology, New Orleans, 1993.

41. K. Kamato, Japan J. Pharmacol., 45, 439-447 (1987)

42. P. Stern, S. Catovic, N. Filipovic, Pharmacol., 10: 97-108 (1973)

43. G.J. Mulder, Annu. Rev. Pharmacol. Toxicol., 32: 25-49 (1992)

Received: June 6, 1993
Accepted: August 2, 1993

JOURNAL OF LIQUID CHROMATOGRAPHY, 17(3), 707-719 (1994)

RETENTION VALUES OF SULPHONIC ACIDS AS A FUNCTION OF THE NATURE AND CONCENTRATION OF INORGANIC SALT IN REVERSED-PHASE ION-PAIR LIQUID CHROMATOGRAPHY

HANFA ZOU*, YUKUI ZHANG, MINGFANG HONG, AND PEICHANG LU
National Chromatographic R & A Center
Dalian Institute of Chemical Physics
Academia Sinica
Dalian 116011, People's Republic of China

ABSTRACT

The capacity factors of phenylamine and naphthylamine sulphonic acids in reversed-phase ion-pair liquid chromatography (RP-IPC) with different concentration of inorganic anions were measured. The capacity factors of ionic solutes decreases in the order NaF > NaBr >= $NaNO_3$ > Na_2SO_4, which is the same as their order of anion retention values in anion ion chromatography. The good linear relationship between logarithm of capacity factors at different inorganic salt eluents were observed. The effect of salt concentration (C_s) on retention follows an equation based on the Gouy-Chapman model:

$$\ln k' = A - R(Z_A/Z_I) \ln C_s$$

The absolute value of slopes in RP-IPC is much smaller than the ratio of solute charge to eluent ion charge in ion chromtagraphy, and increases with the ionic solute charges as well as the retention value of the eluent ions in ion chromatography, but decreses with charge of eluent ions. The value of intercepts are also related with physico-chemical behaviors of the ionic solute and eluent ions. The combined effects of salt concentration and salt nature on retention values can be described by

$$\ln k' = a + b/n_e \ln C_s + c \ln t'_s + d\, n_e$$

The salt concentration C_s and adjusted retention value of salt in ion chromatography ($\ln t'_s$) makes the negative, but the negative

charges of sulphonic acids does a positive contribution to retention values in RP-IPC.

INTRODUCTION

Theoretical models which describe the manner in which solute retention varies with changing eluent composition in reversed-phase ion-pair liquid chromatography (RP-IPC) are of fundamental importance to the understanding of solute retention mechanisms. Moreover, valid models provide an essential basis for selection of the best eluent composition to effect a desired separation, whether this selection be performed on a trial-and-error basis, or with the aid of a computer optimization procedure. Since the inception of RP-IPC, a great number of models of RP-IPC have been published[1-7] and the excellent reviews of them have appeared[1, 8].A majority of the proposed models,including the ion-pair model [1] and dynamic ion-exchange model[1,5,6] are stoichiometeric, i.e., they construct a reaction scheme and the corresponding equilibrium constants express the interaction between the oppositely charged ion-pair reagent and the analyte ions in the system. By combining these constants with the Langumir isotherm equations are obtained for capacity factors as a function of different variables. On the other hand, the non-stoichiometeric models include the ion-interaction mechanism[1,3] and electrostatic model in which the Gouy-Chapman theory is applied to ion-pair liquid chromatography[9-13]. However, the study of effect of inorganic salts on retention has been much more limited than that of organic modifiers[13-15] and ion-pair reagents[16]. In this paper, the retention behavior of aromatic sulphonic acids at different inorganic salt eluents in RP-IPC has been studied. A quantitative correlation of solute retention vs. the salt concentration and nature has been observed.

Table 1 Name of Sulphonic Acids and Their Code as Well as Negative Charge (n_e).

Code	Solute Name	n_e
1	1-Aminobenzene-3-sulphonic acid	1
2	1-Amino-4-methoxybenzene-2-sulphonic acid	1
3	1-Amino-4-chlorobenzene-3-sulphonic acid	1
4	1-Amino-4-methylbenzene-3-sulphonic acid	1
5	1-Aminonaphthalene-5-sulphonic acid	1
6	2-Aminonaphthalene-5-sulphonic acid	1
7	1-Aminobenzene-2,4-disulphonic acid	2
8	1,3-Diaminobenzene-4,6-disulphonic acid	2
9	2-Aminonaphthalene-4,8-disulphonic acid	2
10	2-Aminonapthatlene-3,6-disulphonic acid	2
11	2-Aminonaphthalene-4,7-disulphonic acid	2
12	2-Aminonaphthalene-4,6,8-trisulphonic acid	3

EXPERIMENTAL

Materials

The phenylamine and naphthylamine sulphonic acids analysed (listed in Table 1) were from the Dyestuff Lab., Chemical Enginerring Department, Dalian University of Sciences and Technology. Standard solutions were prepared in water. Double-distilled water was used throughout. The methanol, tetrabutyl-ammonium iodide (TBAI), NaH_2PO_4, NaOH, HCl and the eluent inorganics salts NaF, NaBr, $NaNO_3$ and Na_2SO_4 used were analytical grades.

Apparatus

RP-IPC experiments were on a stainless-steel column (150X4.6 mm I.D.) packed with Nucleosil-C_{18}, 7 μm, (Macherey-Nagel, Duren, Germany). The column was packed by the National Chromatographic R & A Center, Dalian, China. The mobile phases were different concentration of inorganic salts in the eluents, keeping constant the ratio of methanol to water at 25/75, the concentration of ion-pair reagent TBAI at 6 mmol/l, the NaH_2PO_4 at 10 mmol/l, pH 7.02 respectively. The eluent delivery was by a Waters-510 pump (Waters Assoc., Milford, MA, USA). Eluates were detected by a BT-3000 UV detector set at 254 nm (Biotronik, Tubingen, Germany). Sample was loaded by a U6K syringe loading sample injector. Eluent pH was measured on a SA-720 pH meter (Orion Res. Inc., Chicago, IL, USA). The flowrate was 1.0 ml/min. All experimental data were processed by a computer.

RESULTS AND DISCUSSION

The retention times of sulphonic acids with different inorganic salt concentration were measured. The capacity factors of test solutes calculated from retention times are in Tables 2 and 3 respectively.It can been observed that the capacity factors in RP-IPC decrease in the order NaF > NaBr >= $NaNO_3$ > Na_2SO_4, which is the same as their order of anion retention values in ion chromatography with XAD-1 as the stationary phase[19], Table 4 gives the adjusted retention time of these four anions in IC. The linear regression analysis of logarithm of the capacity factors at different kinds of inorganic salts with concentration 15 mmol/l has been carried out, and the obtained results are given in Figures 1, 2 and 3 respectively. It can be seen that there is a good linear relationship of the logarithm of capacity factors

Table 2 Capacity Factors of Phenyl and Naphthylamine Sulphonic Acids at Different NaF and NaBr Concentration in RP-IPC. Other Experimental Conditions See Text.

Code	NaF				NaBr			
	0.015	0.025	0.05	0.10	0.015	0.025	0.05	0.01
1	1.12	0.560	0.347	0.380	0.947	0.613	0.433	0.240
2	2.25	1.71	1.39	1.03	1.86	1.31	1.04	0.700
3	3.91	2.98	2.46	1.81	3.14	2.30	1.87	1.28
4	2.17	1.70	1.45	1.01	1.83	1.35	0.993	0.667
5	3.09	2.46	2.07	1.61	2.64	2.02	1.56	1.11
6	7.18	6.21	5.05	4.09	6.17	4.52	3.92	2.82
7	2.09	1.36	0.900	0.467	1.71	0.928	0.560	0.313
8	1.71	1.01	0.647	0.293	1.40	0.751	0.347	0.113
9	4.68	3.48	2.27	1.51	3.95	2.41	1.48	0.727
10	6.55	4.75	3.41	2.26	5.43	3.63	2.18	1.12
11	5.31	3.71	2.64	1.68	4.35	2.48	1.67	0.847
12	11.30	6.57	4.10	1.93	9.05	4.57	2.09	0.747

at different kinds of inorganic salts under the same concentration as the eluent salts, and the values of slope are very close an unity. Therefore, the relative capacity factors are independent on the kinds of eluent inorganic salts in our RP-IPC experimental conditions.

In order to express the effect of eluent inorganic salt concentration on the retention in RP-IPC, the following equation has been derived based on the Gouy-Chapman theory[15]

$$\ln k' = A - R(Z_A/Z_I) \ln C_s \qquad (1)$$

Table 3 Capacity Factors of Phenylamine and Naphthylamine Sulphonic Acids at Different $NaNO_3$ and Na_2SO_4 Concentration in RP-IPC. Other Experimental Conditions See Text.

Code	$NaNO_3$				Na_2SO_4			
	0.015	0.025	0.05	0.50	0.015	0.025	0.05	0.01
1	0.993	0.573	0.420	0.220	0.807	0.633	0.413	0.327
2	1.87	1.30	0.940	0.520	1.67	1.41	1.08	0.907
3	3.16	2.35	1.70	1.13	2.85	2.57	2.19	1.63
4	1.93	1.27	0.953	0.567	1.63	1.39	1.03	0.793
5	2.75	1.95	1.51	1.03	2.39	2.06	1.68	1.33
6	6.48	4.85	3.85	2.90	5.85	5.30	4.17	3.38
7	1.67	0.980	0.433	0.520	1.27	0.873	0.487	0.227
8	1.38	0.787	0.307	0.093	1.03	0.633	0.353	0.140
9	3.67	2.43	1.33	0.620	3.07	2.29	1.57	1.17
10	5.55	3.61	1.96	0.940	4.41	3.43	2.31	1.66
11	4.31	2.63	1.50	0.680	3.24	2.34	1.88	1.17
12	9.02	4.70	1.90	0.487	6.20	3.75	1.97	1.07

Table 4 Adjusted Retention Time of Anions in IC with XAD-1 (0.007 mequiv./g) as the Stationary Phase and 0.1 mmol/l Phthalate Solution (pH 6.25) as the Eluent. Other Experimental Conditions See Ref.19.

Anion	Adjusted Retention Time (min)
F^-	1.40
Br^-	1.88
NO_3^-	1.90
SO_4^{2-}	7.64

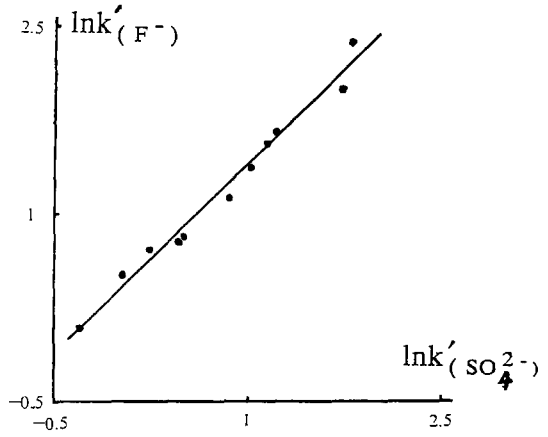

Figure 1 Linear relationship of ln $k'_{(F^-)}$ with 15 mmol/l NaF as the eluent ion versus ln $k'_{(Br^-)}$ with 15 mmol/l NaBr as the eluent ion.

ln $k'_{(F^-)}$ = 0.180 + 1.006 ln $k'_{(Br^-)}$, r = 0.9994, n = 12

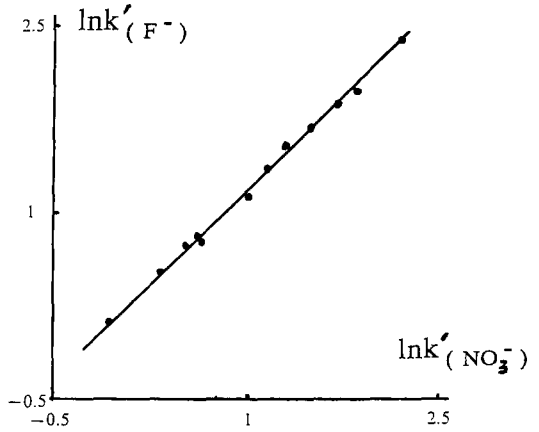

Figure 2 Linear relationship of ln $k'_{(F^-)}$ with 15 mmol/l NaF as the eluent ion versus ln $k'_{(NO_3^-)}$ with 15 mmol/l NaNO as the eluent ion.

ln $k'_{(F^-)}$ = 0.167 + 1.010 ln $k'_{(NO_3^-)}$, r = 0.9972, n = 12

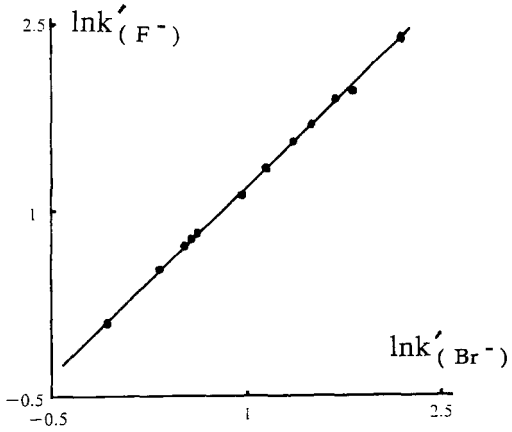

Figure 3 Linear relationship of ln $k'_{(F^-)}$ with 15 mmol/l NaF as the eluent ion versus ln $k'_{(SO_4^{2-})}$ with 15 mmol/l Na_2SO_4 as the eluent ion.

ln $k'_{(F^-)}$ = 0.377 + 1.008 ln $k'_{(SO_4^{2-})}$, r = 0.9840, n = 12

where the parameter A is mainly determined by the electrostatic and hydrophobic interactions, Z_A and Z_I are the ionic charges of the analyte and eluent salt respectively, R is a constant related with the physico-chemical behavior of the analyte and eluent ions and smaller than 1.0. Therefore, the value of slope in eqn.(1) in RP-IPC should be much smaller than that in ion chromatography. The results of linear regression analysis of the experimental data in Tables 2 and 3 according to eqn.(1) were given in Tables 5 and 6. It can be seen that the linear regression coefficient from eqn.(1) in most cases is greater than 0.99, which strongly supports the validity of eqn.(1).

Table 5 Intercept A and Slopes of Plots of lnk' vs. Logarithm of F^- and Br^- Concentration for the Experimental Data Shown in Table 2.

Code	F^-			Br^-		
	A	slope	r	A	slope	r
1	-2.483	-0.564	0.8745	-3.003	-0.698	0.9947
2	-0.879	-0.396	0.9950	-1.481	-0.493	0.9925
3	-0.298	-0.390	0.9938	-0.778	-0.452	0.9923
4	-0.680	-0.341	0.9923	-1.596	-0.522	0.9985
5	-0.282	-0.331	0.9950	-0.917	-0.447	0.9982
6	0.728	-0.297	0.9999	0.156	-0.387	0.9844
7	-2.491	-0.769	0.9960	-3.192	-0.871	0.9952
8	-3.241	-0.898	0.9940	-5.107	-1.307	0.9962
9	-0.968	-0.599	0.9999	-2.282	-0.870	0.9967
10	-0.446	-0.551	0.9988	-1.746	-0.823	0.9981
11	-0.836	-0.593	0.9980	-2.046	-0.827	0.9935
12	-1.383	-0.903	0.9959	-3.229	-1.295	0.9985

Analysing the data shown in Tables 5 and 6, following conclusions can be made: (1) The absolute value of slopes differ markedly between analyte ions, and increases with charge number of a solute, this implies that the charges of solute make an important contribution to the value of slope and the retention in RP-IPC. (2) The absolute value of slopes for the solutes with the same charge, e.g. for the monovalent and divalent solutes, decreases with increasing of the retention value in RP-IPC, which means that the effect of electrostatic interaction on retention

Table 6 Intercept A and Slopes of Plots of lnk' vs. Logarithm of NO_3^- and SO_4^{2-} Concentration for the Experimental Data Shown in Table 3.

Code	NO_3^-			SO_4^{2-}		
	A	slope	r	A	slope	r
1	-3.218	-0.753	0.9891	-2.285	-0.490	0.9934
2	-2.108	-0.653	0.9932	-0.872	-0.328	0.9964
3	-1.095	-0.534	0.9989	-0.778	-0.452	0.9923
4	-1.968	-0.618	0.9928	-1.121	-0.387	0.9986
5	-1.115	-0.499	0.9948	-0.415	-0.308	0.9993
6	0.109	-0.411	0.9951	0.540	-0.297	0.9959
7	-4.194	-1.124	0.9994	-3.508	-0.905	0.9960
8	-5.506	-1.397	0.9964	-2.111	-0.934	0.9999
9	-2.578	-0.933	0.9974	-1.044	-0.511	0.9978
10	-2.172	-0.933	0.9985	-0.703	-0.521	0.9994
11	-2.543	-0.957	0.9975	-0.974	-0.509	0.9901
12	-4.097	-1.521	0.9939	-3.980	-0.957	0.9815

decreases with increasing of the solute hydrophobicity. (3) The absolute value of slopes increases in the order NaBr >= $NaNO_3$ > NaF for the monovalent eluent ions, which is the same as their order of retention in ion chromatography. But the absolute value of slopes with the divalent anion SO_4^{2-} as the eluent ion is much lower than that with anions Br^- and NO_3^- as the eluent ions, however, the retention of SO_4^{2-} in ion chromatography is much larger than that of Br^- and NO_3^-. This behavior can be

Table 7 Value of Parameters a, b, c And d in Eqn.(2); r Is Regression Coefficient,n Is the Data Number Used For Correlation.

Code	a	b	c	d	r	n
1	-4.505	-0.781	0.164	1.108	0.981	15
2	-3.455	-0.525	-1.101	2.529	0.971	16
3	-2.506	-0.468	-0.990	2.282	0.985	16
4	-3.390	-0.528	-1.077	2.432	0.973	16
5	-2.361	-0.440	-0.880	2.011	0.981	16
6	-1.170	-0.383	-0.860	1.902	0.977	16
7	-5.578	-0.906	-1.256	3.056	0.955	16
8	-8.507	-1.275	-1.837	4.641	0.968	16
9	-4.774	-0.818	-1.542	3.600	0.981	16
10	-4.163	-0.791	-1.451	3.413	0.979	16
11	-4.601	-0.810	-1.562	3.572	0.979	16
12	-6.921	-1.287	-2.034	4.954	0.972	16

attributed to the difference in the charge of eluent anions. (4) The value of parameter A differ markedly between analyte ions, and decreases in the order NaF > NaBr > $NaNO_3$ for the monovalent eluent salts, which qualitatively agree with the order of anion retention values in ion chromatography.But with divalent anion SO_4^{2-} as the eluent ion, such a phenomenon can not be observed, which also showes the important role of the charge of eluent ion. The linear regression analysis of the parameter A at different eluent inorganic salts has been carried out, and the obtained results are follows

$$A_{(F^-)} = 0.494 + 0.761\ A_{(Br^-)} \quad , \quad r=0.9427,\ n=12$$

$$A_{(F^-)} = 0.618 + 0.678\ A_{(NO_3^-)} \quad , \quad r=0.9308,\ n=12$$

$$A_{(F^-)} = -0.171 + 0.649\ A_{(SO_4^{2-})} \quad , \quad r=0.7520,\ n=12$$

It can be seen that there is a linear relationship between the parameter A and the monovalent eluent ions, but no such a linear relationship between the monovalent and divalent eluent ions.

The retention values of ionic solute as a function of the concentration of eluent anions and nature can be expressed by

$$\ln k' = a + b/n_e \ln C_s + c \ln t'_s + d\ n_e \qquad (2)$$

where a, b, c and d are the constants for a given solute, t'_s the adjusted retention time of eluent anions and n_e the negative charge of solutes, respectively. The results of quantitative correlation of experimental data shown in Tables 1, 2, 3 and 4 according to eqn.(2) are given in Table 7. It can be seen that the regression coefficients is higher than 0.97 at the most cases, which supports the validity of eqn.(2). The value of parameter b and c are negative, but the parameter d is positive, which means that the contribution of eluent anion and the adjusted retention time make a negative, but the negative charges of sulphonic acids does a positive contribution to retention value in RP-IPC

ACKNOWLEDGMENT

The financial support from the Natural Science Foundation of China is gratefully acknowledged.

REFERENCES

1. B.A.Bidlingmeyer, J. Chromatogr. Sci., 18, 525(1980)
2. A.Tilly-Melin, Y-Askemark, K.G.Wahlund, G.Schill, Anal. Chem., 51, 976(1979)

3. B.A.Bidlingmeyer, S.N.Deming, W.P.Price Jr., B.Sachok, M.Petrusek, J. Chromatogr., 186, 419(1979)
4. C.T.Huang, R.B.Taylor, J. Chromatogr., 202, 333(1980)
5. P.T.Kissinger, Anal. Chem., 49, 883(1977)
6. J.H.Knox, R.A.Hartwick, J. Chromatogr., 204, 3(1981)
7. S.Afrashtehfer, F.F.Cantwell, Anal. Chem., 54, 2422(1982)
8. Cs.Horvath and W.R.Melander, "Ion-Pair Chromatography-Theory and Biological and Pharmaceutical Application" (edited by M.T.W.Hearn), p.27, Marcel Dekker, New York, 1985
9. J.Stahlberg, J. Chromatogr., 356, 231(1986)
10. A.Bartha, Gy.Vigh, J.Stahlberg, J. Chromatogr., 506, 85(1990)
11. H.Liu, F.F.Cantwell, Anal. Chem., 63, 2032(1990)
12. P.C.Lu, H.F.Zou, Y.K.Zhang, Mikrochimica Acta, III, 35(1990)
13. H.F.Zou, Y.K.Zhang, P.C.Lu, J. Chromatogr., 545, 59(1990)
14. Hong Mingfang, Zou Hanfa, Zhang Yukui, Lu Peichang, Acta Chimica Sinica (in Chinese), 51, 178(1993)
15. Y.K.Zhang, H.F.Zou, M.F.Hong, P.C.Lu, Chromatographia, 32, 538(1991)
16. H.F.Zou, Y.K.Zhang, M.F.Hong, P.C.Lu, Chromatographia, 35, 390(1993)
17. H.F.Zou, Y.K.Zhang, M.F.Hong, P.C.Lu, Chromatographia, 32, 329(1991)
18. H.F.Zou, Y.K.Zhang, M.F.Hong, P.C.Lu, J. Chromatogr., 625, 169(1992)
19. J.S.Fritz, D.T.Gjerde and C.Pohlandt, "Ion Chromatography", A.H.Verlag, Heidelberg, Germany, 1982, p.106.

Received: July 24, 1993
Accepted: August 5, 1993

JOURNAL OF LIQUID CHROMATOGRAPHY, 17(3), 721-724 (1994)

THE BOOK CORNER

CAPILLARY ELECTROPHORESIS TECHNOLOGY, Edited by N. A. Guzman, Volume 64, Chromatographic Science Series, J. Cazes Series Editor, Marcel Dekker, Inc., New York, 880 pages, 1993. Price: $165.00.

This book, which was published in August 1993, was just received by The Journal. A full review will be published at a later date. However, a few comments are in order. This, Volume 64 of the Chromatographic Science Series, edited by J. Cazes, is an impressive book of 880 pages, over 1200 up-to-date references and a generous number of tables, figures and equations. The book is written by people who represent the "Who's Who in Capillary Electrophoresis." We quote here from the Foreword, written by Professor James Jorgenson:

"The book before you is a large and impressive volume written by experts in the field of capillary electrophoresis. It is a thorough treatment of the field as it exists, and offers many insights into where the field is heading. The book covers all important aspects of capillary electrophoresis, from the basics of the electrophoretic process through the various operational modes of capillary electrophoresis, details of hardware and instrumentation, and, finally, a generous treatment of applications."

Table of Contents:

4. **The Buffer in Capillary Zone Electrophoresis**, G. M. Janini and H. J. Issaq, (119).

5. **Organic Solvents in Capillary Electrophoresis**, E. Kenndler, (161).

6. **Controlling Migration Behavior in Capillary Electrophoresis: Optimization Strategies for Method Development**, M. G. Khaledi, R. S. Sahota, J. K. Strasters, C. Quang and S. C. Smith, (187).

7. **Dynamic Changes of Electrolyte Systems in Zone Electrophoresis**, P. Bocek and P. Gebauer, (261).

8. **Chemical Derivatization of Fused Silica Capillaries**, F. E. Regnier and D. Wu, (287).

9. **Technology of Separation Capillaries for Capillary Zone Electrophoresis and Capillary Gel Electrophoresis: The Chemistry of Surface Modification and Formation of Gels**, G. Schomburg, (311).

10. **Capillary Electrophoresis with Coated Capillaries**, J. Kohr and H. Engelhardt, (357).

11. **Capillary Zone Electrophoresis of Biopolymers with Hydrophilic Fused-Silica Capillaries**, Z. El Rassi and W. Nashabeh, (383).

12. **Covalent Surface Modification for Capillary Electrophoresis: Characterization and Effect of Nonionic Bondings on Separations in Capillary Electrophoresis**, A. M. Dougherty and M. R. Schure, (435).

13. **Direct Control of Electroosmotic Flow in Capillary Electrophoresis by Using an External Electric Field**, P. Tsai and C. S. Lee, (475).

14. **Semipreparative Capillary Electrophoresis and Its Advantages**, T. Tsuda, (489).

15. **Micropreparative Capillary Electrophoresis**, C. Fujimoto and K. Jinno, (509).

16. **Mass Spectrometric Detection for Capillary Electrophoresis**, R. D. Smith and H. R. Udseth, (525).

17. **Capillary Zone Electrophoresis-Mass Spectrometry: Continuous Flow Fast-Atom Bombardment and Electrospray Ionization**, K. B. Tomer, (569).

18. **Optical Detection Schemes for Capillary Electrophoresis**, E. S. Yeung, (587).

19. **Laser-Induced Fluorescence Detection for Capillary Electrophoresis: A Powerful Analytical Tool for the Separation and Detection of Trace Amounts of Analytes**, L. Hernandez, N. Joshi, P. Verdeguer and N. A. Guzman, (605).

20. **Chiral Separation by Capillary Electrophoresis and Electrokinetic Chromatography**, K. Otsuka and S. Terabe, (617).

21. **The Sheath-Flow Cuvette in DNA Sequencing by Capillary Gel Electrophoresis and Two-Spectral-Channel, Laser-Induced Fluorescence Detection**, J. Zhang, D. Y. Chen, H. R. Harke and N. Dovichi, (631).

22. **The Use of Capillary Electrophoresis in Clinical Diagnosis**, N. A. Guzman, C. L. Gonzalez, L. Hernandez, C. M. Berck, M. A. Trebilcock and J. P. Advis, (643).

23. **The Utility of Capillary Electrophoresis in Forensic Science**, D. M. Northrop, (673).

24. **Capillary Electrophoresis and Electrokinetic Capillary Chromatography of Drugs in Body Fluids**, W. Thormann, (693).

25. **Quantitative Analysis with Capillary Zone Electrophoresis**, A. M. Hoyt, Jr., (705).

26. **Capillary Polyacrylamide Gel Electrophoresis**, A. Guttman, (715).

27. **Use of Cyclodextrins in Capillary Electrophoresis**, S. Fanali, (731).

28. **Prospects for the Use of Capillary Electrophoresis in Neuroscience**, M. A. Hayes, S. D. Gilman and A. G. Ewing, (753).

29. **Capillary Isoelectric Focusing of Peptides, Proteins and Antibodies**, J. R. Mazzeo and I. S. Krull, (795).

30. **Behavior of Recin on Untreated and Treated Capillary Electrophoresis Columns**, H. B. Hines and E. E. Brueggemann, (819).

MICROSCOPIC AND SPECTROSCOPIC IMAGING OF THE CHEMICAL STATE, Edited by M. D. Morris, Practical Spectroscopy Series, Volume 16, Marcel Dekker, Inc., New York, 512 pages, 1993. Price: $175.00.

This volume, which is written for practicing chemists familiar with modern spectroscopies, but providing helpful tutorial materials on basic imaging processes for contemporary chemists with little background in the field, Microscopic and Spectroscopic Imaging of the Chemical State summarizes underlying spectroscopic theory and the principles of light microscopy and scanned probe microscopy. It includes practical introductory information on instrumentation, computer-based image enhancement, and image processing; details imaging techniques based on electronic and vibrational spectroscopy, nuclear magnetic and electron paramagnetic resonance, x-ray absorption and fluorescence, and mass spectrometry; analyzes scanning tunneling, atomic force, near-field optical, and thermal wave microscopies, and more.

Containing nearly 300 drawings, photographs, and micrographs that help readers judge the quality of images obtainable by each technique, Microscopic and Spectroscopic Imaging

of the Chemical State is an essential resource for analytical and physical chemists, chemical engineers, biochemists, spectroscopists, materials and polymer scientists, and graduate students in the above disciplines.

Table of Contents:

JOURNAL OF LIQUID CHROMATOGRAPHY, 17(3), 725-730 (1994)

LIQUID CHROMATOGRAPHY CALENDAR

1994

JANUARY 10 - 14: Supercritical Fluid Chromatography and Extraction, Hyatt Regency Hotel on the Inner Harbor, Baltimore, Maryland. Contact: Larry T. Taylor, Dept of Chemistry, Virginia Polytechnic Institute & State University, Blacksburg, VA 24061, USA.

JANUARY 16 - 20: 19th IUPAC Symposium on the Chemistry of Natural Products, Karachi, Pakistan. Contact: Prof. Atta-Ur-Rahman, Director H. E. J. Research Institute of Chemistry, University of Karachi, Karachi-75270, Pakistan.

FEBRUARY 2 - 3: AOAC Southeast Section Meeting, Ramada Hotel & Convention Center, Atlanta, GA. Contact: Doug Hite, Technical Services, P. O. Box 40627, Melrose Station, Nashville, TN 37204, USA.

FEBRUARY 28 - MARCH 4: PittCon'94: Pittsburgh Conference on Analytical Chemistry & Applied Spectroscopy, Chicago, Illinois. Contact: Pittsburgh Conference, Suite 332, 300 Penn Center Blvd, Pittsburgh, PA 15235-9962, USA

MARCH 22 - 24: PrepTech '94, A New Conference on Industrial Bioseparations, Meadowlands Hilton Hotel, S3ecaucus, New Jersey. Contact: Symposium Manager, PrepTech '94, ISC, Inc., 30 Controls Drive, Shelton, CT 06484, USA.

APRIL 10 - 15: 207th ACS National Meeting, San Diego, Calif. Contact: ACS Meetings, ACS, 1155 16th Street, NW, Washington, DC 20036, USA.

APRIL 19 - 22: Rubber Division ACS, 145th Spring Technical Meeting, Palmer House Hotel, Chicago, Illinois. Contact: C. Morrison, Rubber Division, P.O. Box 499, Akron, OH 44309-0499, USA.

MAY 8 - 13: HPLC '94: Eighteenth International Symposium on High Performance Liquid Chromatography, Minneapolis Convention Center, Minneapolis, Minnesota. Contact: Mrs. Janet Cunningham, Barr Enterprises, P.O. Box 279, Walkersville, MD 21793, USA.

JUNE 1 - 3: Joint 26th Central Regional/27th Great Lakes Regional Meeting, ACS, Kalamazoo and Huron Valley Sections. Contact: H. Griffin, Univ of Michigan, Ann Arbor, MI 48109, USA.

JUNE 1 - 3: International Symposium on Hormone & Veterinary Drug Residue Analysis, Congress Centre Oud Sint-Jan, Brugge, Belgium. Contact: Prof. C. Van Peteghem, University of Ghent, L:aboratory of Food Analysis, Harelbekestraat 72, B-9000 Ghent, Belgium.

JUNE 5 - 7: VIth International Symposium on Luminescence Spectrometry in Biomedical Analysis - Detection Techniques & Applications in Chromatography and Capillary Electrophoresis, Congress Centre Oud Sint-Jan, Brugge, Belgium. Contact: Prof. Dr. Willy R. G. Baeyens, University of Ghent, Pharmaceutical Institute, Dept. of Pharmaceutical Analysis, Harelbekestraat 72, B-9000 Ghent, Belgium.

JUNE 12 - 15: 1994 Prep Symposium & Exhibit, sponsored by the Washington Chromatography Discussion Group, at the Georgetown University Conference Center by Marriott, Washington, DC. Contact: Janet E. Cunningham, Barr Enterprises, P. O. Box 279, Walkersville, MD 21793, USA.

JUNE 13 - 15: Fourth International Symposium on Field-Flow Fractionation (FFF'94), Lund, Sweden. Contact: Dr. Agneta Sjogren, The Swedish Chemical Society, Wallingatan 24, 2 tr, S-111 24 Stockholm, Sweden.

JUNE 19 - 23: 24th National Medicinal Chem. Symposium, Little America Hotel & Towers, Salt Lake City, Utah. Contact: M. A. Jensen & A. D. Broom, Dept. of Medicinal Chem, 308 Skaggs Hall, Univ of Utah, Salt Lake City, UT 84112, USA.

JUNE 19 - 24: 20th International Symposium on Chromatography, Bournemouth International Centre, Bournemouth, UK. Contact: Mrs. Jennifer A. Challis, The Chromatography Society, Suite 4, Clarendon Chambers, 32 Clarendon Street, Nottingham, NG1 5JD, UK.

JUNE 24 - 27: BOC Priestly Conference, Bucknell University, Lewisburg, PA, co-sponsored with the Royal Soc of Chem. Contact: ACS Meetings, 1155 16th Street, NW, Washington, DC 20036-4899, USA.

JULY 31 - AUGUST 5: American Society of Pharmacognosy Annual Meeting, International Research Congress on Natural Products, joint meeting with the Assoc. Français pour l'Enseignement et la Recherche en Pharmacognosie, and the Gesellschaft fur Arzneipflanzenforschung, and the Phytochemical Society of Europe, Halifax, Nova Scotia, Canada. Contact: D. J. Slatkin, P. O. Box 13145, Pittsburgh, PA 15243, USA.

AUGUST 21 - 26: 208th ACS National Meeting, Washington, DC. Contact: ACS Meetings, ACS, 1155 16th Street, NW, Washington, DC 20036-4899, USA.

SEPTEMBER 5 - 7: 25th International Symposium on Essential Oils, Grasse, France. Contact: Assoc. des Ingenieurs et Techniques de la Parfumerie (A.I.T.P.), 48 ave. Riou-Blanquet, 06130 Grasse, France.

OCTOBER 16 - 19: 46th Southeastern regional Meeting, ACS, Birmingham, Alabama. Contact: L. Kispert, Chem Dept, Univ of Alabama, Box 870336, Tuscaloosa, AL 35115, USA.

NOVEMBER 2 - 5: 29th Midwestern Regional Meeting, ACS, Kansas City, Kansas. Contact: M. Wickham-St. Germain, Midwest Res. Inst, 425 Volker Blvd, Kansas City, MO 64110, USA.

NOVEMBER 13 - 16: 50th Southwest Regional Meeting, ACS, Fort Worth, Texas. Contact: H. C. Kelly, Texas Christian Univ, Chem Dept, Ft. Worth, TX 76129, USA.

DECEMBER 4 - 6: IBEX'94, International Biotechnology Expo & Scientific Conference, Moscone Center, San Francisco, California. Contact: Cartlidge & Associates, Inc., 1070 Sixth Avenue, Suite 307, Belmont, CA 94002, USA.

1995

MARCH 6 - 10: PittCon'95: Pittsburgh Conference on Analytical Chemistry & Applied Spectroscopy, New Orleans, Louisiana. Contact: Pittsburgh Conference, Suite 332, 300 Penn Center Blvd., Pittsburgh, PA 15235-9962, USA.

APRIL 2 - 7: 209th ACS National Meeting, Anaheim, Calif. Contact: ACS Meetings, ACS, 1155 16th Street, NW, Washington, DC 20036-4899, USA.

MAY 31 - JUNE 2: 27th Central regional Meeting, ACS, Akron Section. Contact: J. Visintainer, Goodyear Research, D415A, 142 Goodyear Blvd, Akron, OH 44236, USA.

JUNE 15 - 17: 50th Northwest/12th Rocky Mountain Regional Meeting, ACS, Park City, Utah. Contact: J. Boerio-Goates, Chem Dept, 139C-ESC, Brigham Young Univ, Provo, UT 84602, USA.

JULY 9 - 15: SAC'95, The University of Hull, UK, sponsored by the Analytical Division, The Royal Society of Chemistry. Contact: The Royal Society of Chemistry, Burlington House, Picadilly, London W1V 0BN, UK.

AUGUST 20 - 25: 210th ACS National Meeting, Chicago, Illinois. Contact: ACS Meetings, ACS, 1155 16th Street, NW, Washington, DC 20036-4899, USA.

OCTOBER 18 - 21: 31st Western Regional Meeting, ACS, San Diego, Calif. Contact: S Blackburn, General Dynamics, P. O. Box 179094, San Diego, CA 92177-2094, USA.

OCTOBER 22 - 25: 25th Northeastern Regional Meeting, ACS, Rochester, New York. Contact: T. Smith, Xerox Corp, Webster Res Center, M/S 0128-28E, 800 Phillips Rd, Webster, NY 14580, USA.

NOVEMBER 5 - 7: 30th Midwestern Regional Meeting, ACS, Joplin, Missouri. Contact: J. H. Adams, 1519 Washington Dr, Miami, OK 74354, USA.

NOVEMBER 29 - DECEMBER 1: Joint 51st Southwestern/47th Southeastern Regional Meeting, ACS, Peabody Hotel, Memphis, Tenn. Contact: P.K. Bridson, Chem Dept, Memphis State Univ, Memphis, TN 38152, USA.

DECEMBER 17 - 22: 1995 International Chemical Congress of Pacific Basin Societies, Honolulu, Hawaii. Contact: ACS Meetings, 1155 16th Street, NW, Washington, DC 20036-4899, USA.

1996

FEBRUARY 26 - MARCH 1: PittCon'96: Pittsburgh Conference on Analytical Chemistry & Applied Spectroscopy, Chicago, Illinois. Contact: Pittsburgh Conference, Suite 332, 300 Penn Center Blvd., Pittsburgh, PA 15235-9962, USA.

MARCH 24 - 29: 211th ACS National Meeting, New Orleans, LA. Contact: ACS Meetings, ACS, 1155 16th Street, NW, Washington, DC 20036-4899, USA.

JUNE 16 - 21: "HPLC '96: Twentieth International Symposium on High Performance Liquid Chromatography," San Francisco Marriott Hotel, San Francisco, California. Contact: Mrs. Janet Cunningham, Barr Enterprises, P. O. Box 279, Walkersville, MD 21793, USA.

AUGUST 18 - 23: 212th ACS National Meeting, Boston, Mass. Contact: ACS Meetings, 1155 16th Street, NW, Washington, DC 20036-4899, USA.

OCTOBER 24 - 26: 52nd Southwestern Regional Meeting, ACS, Houston, Texas. Contact: J. W. Hightower, Chem Eng Dept, Rice Univ, Houston, TX 77251, USA.

NOVEMBER 6 - 8: 31st Midwestern Regional Meeting, ACS, Sioux Falls, South Dakota. Contact: J. Rice, Chem Dept, S. Dakota State Univ, Shepard Hall Box 2202, Brookings, SD 57007-2202, USA.

1997

APRIL 6 - 11: 213th ACS National Meeting, San Antonio, Texas. Contact: ACS Meetings, ACS, 1155 16th Street, NW, Washington, DC 20036-4899, USA.

SEPTEMBER 7 - 12: 214th ACS National Meeting, Las Vegas, Nevada. Contact: ACS Meetings, 1155 16th Street, NW, Washington, DC 20036-4899, USA.

1998

MARCH 29 - APRIL 3: 215th ACS National Meeting, St. Louis, Missouri. Contact: ACS Meetings, 1155 16th Street, NW, Washington, DC 20036-4899, USA.

AUGUST 23 - 28: 216th ACS National Meeting, Orlando, Florida. Contact: ACS Meetings, 1155 16th Street, NW, Washington, DC 20036-4899, USA.

1999

MARCH 21 - 26: 217th ACS National Meeting, Anaheim, Calif. Contact: ACS Meetings, 1155 16th Street, NW, Washington, DC 20036-4899, USA.

AUGUST 22 - 27: 218th ACS National Meeting, New Orleans, Louisiana. Contact: ACS Meetings, 1155 16th Street, NW, Washington, DC 20036-4899, USA.

2000

MARCH 26 - 31: 219th ACS National Meeting, Las Vegas, Nevada. Contact: ACS Meetings, 1155 16th Street, NW, Washington, DC 20036-4899, USA.

AUGUST 20 - 25: 220th ACS National Meeting, Washington, DC. Contact: ACS Meetings, 1155 16th Street, NW, Washington, DC 20036-4899, USA.

2001

APRIL 1 - 6: 221st ACS National Meeting, San Francisco, Calif. Contact: ACS Meetings, 1155 16th Street, NW, Washington, DC 20036-4899, USA.

AUGUST 19 - 24: 222nd ACS National Meeting, Chicago, Illinois. Contact: ACS Meetings, 1155 16th Street, NW, Washington, DC 20036-4899, USA.

2002

APRIL 7 - 12: 223rd ACS National Meeting, Orlando, Florida. Contact: ACS Meetings, 1155 16th Street, NW, Washington, DC 20036-4899, USA.

SEPTEMBER 8 - 13: 224th ACS National Meeting, Boston, Mass. Contact: ACS Meetings, 1155 16th Street, NW, Washington, DC 20036-4899, USA.

The Journal of Liquid Chromatography will publish, **at no charge**, announcements of interest to liquid chromatographers in every issue of the Journal. To be listed in the LC Calendar, we will need to know: Name of the meeting or symposium, sponsoring organization, when and where it will be held, and whom to contact for additional details. Incomplete information will not be published. You are invited to send announcements to **Dr. Jack Cazes, Editor, Journal of Liquid Chromatography, P.O. Box 2180, Cherry Hill, NJ 08034-0162, USA.**

Fullerene Science and Technology

An International and Interdisciplinary Journal

CONTENTS

(Volume 1, Number 1, 1993)

ISSN: 1064—122X

Choose the best chromatographic technique and obtain optimum results analyzing lipids of biological origin with...

Contains contributions from over 20 internationally acclaimed experts in the field!

Lipid Chromatographic Analysis

(Chromatographic Science Series/65)

edited by

TAKAYUKI SHIBAMOTO

University of California, Davis

December, 1993
424 pages, illustrated
$135.00

Focusing on **state-of-the-art** gas chromatography (GC) and high-performance liquid chromatography, this **practical** reference discusses the theories behind and applications of the latest developments in chromatographic techniques—assessing the strengths and limitations of each methodology.

Presenting many detection methods **for the first time**, ***Lipid Chromatographic Analysis***

- provides a comprehensive review of conventional column and thin-layer chromatography
- outlines supercritical fluid chromatography for lipids
- examines a **new** GC technique to detect plasmalogen phospholipids
- details the first systematic description of a microanalytical procedure for cholesterol and related compounds
- explains a GC analysis of lipid breakdown products for monitoring biological processes such as aging, carcinogenesis, and mutagenesis
- describes techniques that allow for the simultaneous analysis of nonpolar and polar lipids
- elucidates applications of gas chromatography-mass spectroscopic detection for lipids analysis
- and more!

Furnishing more than 220 helpful tables, drawings, and equations, ***Lipid Chromatographic Analysis*** is an essential resource for analytical, lipid, petroleum, food, and flavor chemists; biochemists; biologists; microbiologists; physiologists; pharmacologists; toxicologists; and upper-level undergraduate and graduate students in these disciplines.

Contents

ISBN: 0—8247—8941—5

This book is printed on acid-free paper

Marcel Dekker, Inc.

270 Madison Avenue, New York, NY 10016
(212) 696-9000

Hutgasse 4, Postfach 812, CH-4001 Basel, Switzerland
Tel 061-261-8482

Understand one of the fastest growing analytical techniques in the field of separation science and learn its many applications with...

Furnishes more than **1200** up-to-date references and nearly **670** helpful tables, equations, drawings, and photographs!

Capillary Electrophoresis Technology

(Chromatographic Science Series/64)

edited by **NORBERTO A. GUZMAN**
The R. W. Johnson Pharmaceutical Research Institute, Raritan, New Jersey

August, 1993 / 880 pages, illustrated / $165.00

From the Foreword...

"...[this book] is a large and impressive volume....It is a thorough treatment of the field as it exists and offers many insights into where the field is heading.... the authors...have produced a marvelous, up-to-date, and well-organized guide."

—James W. Jorgenson
Department of Chemistry
University of North Carolina at Chapel Hill

Tracing the sequence of new observations that has led to current understanding in the field, this **outstanding** reference presents the basic concepts, instrumentation, and applications of capillary electrophoresis—examining its many **unique** features such as high-power resolution, high-mass sensitivity, overall sensitivity, and low-sample volume requirements.

Highlights the use of capillary electrophoresis for the identification, separation, detection, and characterization of substances *on the molecular counting level!*

Illustrating the major technical maneuvers for common operations and applications, ***Capillary Electrophoresis Technology***

- outlines the theoretical concepts and mathematical expressions of capillary electrophoresis
- describes advances in instrumentation hardware and detection systems
- explains the advantages and limitations of the different variants of capillary electrophoresis
- provides **special coverage** of areas in which capillary electrophoresis has grown increasingly popular, including the identification and characterization of small molecules and macromolecules
- and much more!

Written by **over 50** experts from universities, laboratories, and industrial and research centers throughout the U.S. and abroad, ***Capillary Electrophoresis Technology*** is an essential reference for analytical and clinical chemists and biochemists, chemical engineers, biologists, pharmacists, biotechnologists, and upper-level undergraduate and graduate students in these disciplines.

Contents

ISBN: 0—8247—9042—1

This book is printed on acid-free paper

Marcel Dekker, Inc.
270 Madison Avenue
New York, NY 10016
(212) 696-9000
Hutgasse 4, Postfach 812
CH-4001 Basel, Switzerland
Tel 061-261-8482

Use a selective solid phase for any given bioorganic mixture effectively *with...*

Handbook of Affinity Chromatography

Contains over 200 helpful tables, figures, and equations!

(Chromatographic Science Series/63)

edited by

TONI KLINE, *Bristol-Myers Squibb Pharmaceutical Research Institute, Princeton, New Jersey*

June, 1993
344 pages, illustrated
$135.00

Outlining the fundamental principles by which all interactions occur, this practical reference focuses on harnessing the biochemistry of bioorganic compounds in order to separate them—presenting new techniques and applications that affect the planning of research strategies.

Written by international experts in the field, the ***Handbook of Affinity Chromatography***

- discusses how to create a customized separation system without having to invent a whole new technology to support it
- details current purification methods for several classes of proteins
- introduces surface plasma resonance detection and weak affinity chromatography
- documents successful laboratory experiences relevant to future purifications
- explores research on affinity chromatography as a topic in its own right within the field of biorecognition
- and more!

Providing more than 1200 literature citations to allow for in-depth study of specific topics, the ***Handbook of Affinity Chromatography*** is an invaluable resource for analytical and protein chemists; research biochemists; molecular biologists; immunologists; pharmacologists; separation scientists; bioprocess technologists; design, chemical/biochemical, and research and development engineers; process development managers; and upper-level undergraduate and graduate students in these disciplines.

Marcel Dekker, Inc.
270 Madison Avenue, New York, NY 10016
■ (212) 696-9000
Hutgasse 4, Postfach 812, CH-4001 Basel, Switzerland
■ Tel. 061-261-8482

CONTENTS

ISBN: 0—8247—8939—3

This book is printed on acid-free paper

ELECTRONIC MANUSCRIPT SUBMISSION

Effective immediately, manuscripts will be accepted on computer diskettes. A printed manuscript must accompany the diskette. For approximately one year, the diskettes will be used, on an experimental basis, to produce typeset-quality papers for publication in the Journal of Liquid Chromatography. Diskettes must be in an IBM-compatible format with MS-DOS Version 3.0 or greater. The following word processing formats can be accommodated:

ASCII	DisplayWrite Native
EBCDIC	Enable 1.0, 2.0, 2.15
Framework III 1.0, 1.1	IBM Writing Assistant
Microsoft Word 3.0, 3.1, 4.0, 5.0	Multimate 3.3
Multimate Advantage 3.6	Multimate Advantage II 3.7
Navy DIF	Office Writer 4.0, 5.0, 6.0, 6.1
PeachText 5000 2.12	PFS:First Choice 1.0, 2.0
PFS:Write Ver C	Professional Write 1.0, 2.0, 2.1
Q&A Write 3.0	RapidFile (Memo Writer) 1.2
Samna Word IV & IV+ 1.0, 2.0	Total Word 1.2, 1.3
Volkswriter 3, 4	Volkswriter Deluxe 2.2
Wang PC Ver 3	WordPerfect 4.1, 4.2, 5.0, 5.1*
WordStar 3.3, 3.31, 3.45, 4.0, 5.0, 5.5, 6.0	XyWrite III
	XyWrite III+

* The **preferred** word processor is **WordPerfect 5.1.**

Manuscripts and diskettes should be prepared in accordance with the **Instructions for Authors** given at the back of this issue of the Journal. They should be sent to the Editor:

Dr. Jack Cazes
Journal of Liquid Chromatography
P. O. Box 2180
Cherry Hill, NJ 08034

INSTRUCTIONS TO AUTHORS

Journal of Liquid Chromatography is published in the English language for the rapid communication of research in liquid chromatography and its related sciences and technologies.

Directions for Submission

One typewritten manuscript, suitable for direct reproduction, and two (2) clear copies with figures must be submitted. Since the Journal is produced by direct photography of the manuscripts, typing and format instructions must be strictly followed. Non-compliance will result in return of the manuscript to the author and will delay its publication. To avoid creasing, manuscripts should be placed between heavy cardboards before mailing.

Manuscripts may also be submitted on **computer diskettes**. A printed manuscript must also be submitted with diskettes because, at the present time, we are experimenting with manuscripts on diskettes. Diskettes must be readable with an IBM-compatible computer (Macintosh or other type not acceptable) and must be formatted with MS-DOS 3.1 or greater. Be sure to indicate the word processing software that was used to prepare the manuscript diskette.

Manuscripts and computer diskettes should be mailed to the Editor:

Dr. Jack Cazes
Journal of Liquid Chromatography
P. O. Box 2180
Cherry Hill, NJ 08034

Reprints

Due to the short production time for papers in this journal, it is essential to order reprints immediately upon receiving notification of acceptance of the manuscript. A reprint order form will be sent to the author with the letter of acceptance for the manuscript. Reprints are available in quantities of 100 and multiples thereof. Twenty (20) free reprints will be included with orders of 100 or more reprints.

Format of the Manuscript

1. The general format of the manuscript should be:
   Title
   Author(s)' names and full addresses
   Abstract
   Text Discussion
   References

2. **Title & Authors:** The entire title should be in capital letters and centered within the width of the typing area, located at least 2 inches (5.1 cm) from the top of the page. This should be followed by 3 lines of space, then by the names and addresses of the authors, also centered, in the following manner:

A SEMI-AUTOMATIC TECHNIQUE FOR THE SEPARATION AND DETERMINATION OF BARIUM AND STRONTIUM IN WATER BY ION EXCHANGE CHROMATOGRAPHY AND ATOMIC EMISSION SPECTROMETRY

F. D. Pierce and H. R. Brown
Utah Biomedical Test Laboratory
520 Wakara Way
Salt Lake City, Utah 84108

3. **Abstract:** The title **ABSTRACT** should be typed, capitalized and centered, 3 lines below the addresses. This should be followed by a **single-spaced**, concise abstract. Allow 3 lines of space below the abstract before beginning the text of the manuscript.

4. **Text Discussion:** Whenever possible, the text discussion should be divided into major sections such as

INTRODUCTION
MATERIALS
METHODS
RESULTS
DISCUSSION
ACKNOWLEDGEMENTS
REFERENCES

These **major headings** should be separated from the text by two lines of space above and one line of space below. Each major heading should be typed in capital letters, centered and underlined.

Secondary headings, if any, should be placed flush with the left margin, underlined and have the first letter of main words capitalized. Leave two lines of space above and one line of space below secondary headings.

5. The first word of each **paragraph** within the body of the text should be indented five spaces.

6. **Acknowledgements**, sources of research funds and address changes for authors should be listed in a separate section at the end of the manuscript, immediately preceding the references.

7. **References** should be numbered consecutively and placed in a separate section at the end of the manuscript. They should be typed single-spaced, with one line space between each reference. Each reference should contain names of all authors (with initials of their first and middle names); do not use *et al.* for a list of authors. Abbreviations of journal titles will follow the American Chemical Society's Chemical Abstracts List of Periodicals. The word **REFERENCES** should be capitalized and centered above the reference list.

Following are acceptable reference formats:

Journal:

1. D. K. Morgan, N. D. Danielson, J. E. Katon, Anal. Lett., 18: 1979-1998 (1985)

Book:

1. L. R. Snyder, J. J. Kirkland, Introduction to Modern Liquid Chromatography, John Wiley & Sons, Inc., New York, 1979.

2. C. T. Mant, R. S. Hodges, "HPLC of Peptides," in HPLC of Biological Macromolecules, K. M.

Gooding, F. E. Regnier, eds., Marcel Dekker, Inc., New York, 1990, pp. 301-332.

8. Each page of manuscript should be numbered lightly, with a light blue pencil, at the bottom of the page.

9. Only standard symbols and nomenclature, approved by the International Union of Pure and Applied Chemistry (IUPAC) should be used.

10. Material that cannot be typed, such as Greek symbols, script letters and structural formulae, should be drawn carefully with dark black India ink. Do not use any other color ink.

Additional Typing Instructions

1. The manuscript must be prepared on good quality **white bond paper**, measuring approximately 8½ x 11 inches (21.6 cm x 27.9 cm). The typing area of the first page, including the title and authors, should be 5½ inches wide by 7 inches high (14 cm x 18 cm). The typing area of all other pages should be no more than 5½ inches wide by 8½ inches high (14 cm x 21.6 cm).

2. The **title, abstract, tables and references** are typed single-spaced. All other text should be typed 1½-line spaced or double line spaced.

3. It is essential to use **dark black** typewriter or printer ribbon so that clean, clear, **solid characters** are produced. Characters produced with a dot/matrix printer are not acceptable, even if they are "near letter quality" or "letter quality." Erasure marks, smudges, hand-drawn corrections and creases are not acceptable.

4. **Tables** should be typed on separate pages, one table to a page. A table may not be longer than one page. If a table is larger than one page, it should be divided into more than one table. The word **TABLE** (capitalized and followed by an Arabic number) should precede the table and should be centered above the table. The title of the table should have the first letters of all main words in capitals. Table titles should be typed single line spaced, across the full width of the table.

5. **Figures (drawings, graphs, etc.)** should be professionally drawn in **black** India ink on separate sheets of **white** paper, and should be placed at the end of the text. They should not be inserted in the body of the text. They should not be reduced to a small size. Preferred size for figures is from 5 inches x 7 inches (12.7 cm x 17.8 cm) to 8½ inches by 11 inches (21.6 cm x 27.9 cm). **Photographs** should be professionally prepared *glossy* prints. A typewriter or lettering set should be used for all labels on the figures or photographs; they may not be hand drawn.

Captions for figures should be typed single-spaced on a separate sheet of white paper, along the full width of the type page, and should be preceded with the word FIGURE and an Arabic numeral. All figures and lettering must be of a size that will remain legible after a 20% reduction from the original size. Figure numbers, name of senior author and an arrow indicating "top" should be written in light blue pencil on the back of the figure. Indicate the approximate placement for each figure in the text with a note written with a light blue pencil in the margin of the manuscript page.

6. The **reference list** should be typed single-spaced. A single line space should be inserted after each reference. The format for references should be as given above.